UNCLASSIFIED

APAE-2

REACTORS—POWER

UNITED STATES ATOMIC ENERGY COMMISSION

HAZARDS SUMMARY REPORT FOR THE ARMY PACKAGE POWER REACTOR

July 27, 1955

Alco Products, Inc.
Schenectady, New York

Technical Information Service Extension, Oak Ridge, Tenn.

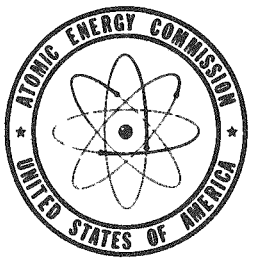

UNCLASSIFIED

DISCLAIMER

This report was prepared as an account of work sponsored by an agency of the United States Government. Neither the United States Government nor any agency Thereof, nor any of their employees, makes any warranty, express or implied, or assumes any legal liability or responsibility for the accuracy, completeness, or usefulness of any information, apparatus, product, or process disclosed, or represents that its use would not infringe privately owned rights. Reference herein to any specific commercial product, process, or service by trade name, trademark, manufacturer, or otherwise does not necessarily constitute or imply its endorsement, recommendation, or favoring by the United States Government or any agency thereof. The views and opinions of authors expressed herein do not necessarily state or reflect those of the United States Government or any agency thereof.

DISCLAIMER

Portions of this document may be illegible in electronic image products. Images are produced from the best available original document.

Date Declassified: April 12, 1957.

LEGAL NOTICE

This report was prepared as an account of Government sponsored work. Neither the United States, nor the Commission, nor any person acting on behalf of the Commission:

A. Makes any warranty or representation, express or implied, with respect to the accuracy, completeness, or usefulness of the information contained in this report, or that the use of any information, apparatus, method, or process disclosed in this report may not infringe privately owned rights; or

B. Assumes any liabilities with respect to the use of, or for damages resulting from the use of any information, apparatus, method, or process disclosed in this report.

As used in the above, "person acting on behalf of the Commission" includes any employee or contractor of the Commission to the extent that such employee or contractor prepares, handles or distributes, or provides access to, any information pursuant to his employment or contract with the Commission.

This report has been reproduced directly from the best available copy.

Issuance of this document does not constitute authority for declassification of classified material of the same or similar content and title by the same authors.

Since nontechnical and nonessential prefatory material has been deleted, the first page of the report is page 5.

Printed in USA. Price $6.00. Available from the Office of Technical Services, Department of Commerce, Washington 25, D. C.

AEC Technical Information Service Extension
Oak Ridge, Tennessee

APAE-2

HAZARDS SUMMARY REPORT

for the

ARMY PACKAGE POWER REACTOR

JULY 27, 1955

ALCO PRODUCTS, INCORPORATED

POST OFFICE BOX 414

SCHENECTADY, NEW YORK

CONTRACT NO. AT (11-1) - 318

SUMMARY

The APPR-1 is described and the various hazards are reviewed. Because of the reactor's location near the nation's Capitol, containment is of the utmost importance. The maximum energy release in any possible accident is 7.4 million BTU's which is completely contained within a 7/8 inch thick steel cylindrical shell which hemispherical ends. The vapor container is 60 feet high and 32 feet in diameter and is lined on the inside with 2 feet of reinforced concrete which provides missile protection and is part of the secondary shield.

All possible nuclear excursions are reviewed and the energy from any of these is insignificant compared to the stored energy in the water.

The maximum credible accident is caused by the reactor running constantly at its maximum power of 10 megawatts and through an extremely unlikely sequence of failures, causing the temperature of the water in the primary and secondary systems to rise to saturation; whereupon a rupture occurs releasing the stored energy of 7.4 million BTU's into the vapor container. If the reactor core melts during the incident, a maximum of 10^8 curies of activity is released.

While it appears impossible for a rupture of the vapor container to occur except by sabotage or bombing, the hazards to the surrounding area are discussed in the event of such a rupture occurring simultaneously with the maximum credible accident.

ACKNOWLEDGMENTS

While the primary responsibility for reviewing the hazards associated with the APPR-1 has rested with ALCO, the outside contributions to this report have been of immense value. Design calculations have been carried out in close co-operation with Stone and Webster, particularly in the case of the vapor container. ALCO has used much of the information developed in the original ORNL conceptual design, and is further indebted to ORNL for the reactor simulator tests.

Many of the calculations on nuclear excursions were done with assistance from the Reactor Physics Section of Battelle Memorial Institute. The Army Reactor Branch of the A.E.C. did considerable work in collecting data on the site, as well as offering many helpful suggestions in the general preparation of the report.

The chapter on hazards to the surrounding area in the event of a catastrophe and the appendix on meterology and climatology were prepared with the aid of the Scientific Services Division of the U.S. Weather Bureau. The information contained in the appendix on geology and hydrology was obtained from a report prepared by the Water Resources Division of the U.S. Geological Survey.

In evaluating the requirements for missile protection, valuable assistance was given by the Department of Docks, U.S. Navy in Boston and by Army Ordnance at Aberdeen.

HAZARDS SUMMARY REPORT
for the
ARMY PACKAGE POWER REACTOR

Table of Contents

CHAPTER

CHAPTER I - INTRODUCTION

A. General

The Army Package Power Reactor will be designed, constructed and operated for the first six months by ALCO PRODUCTS, INC. on contract with the Army Reactors Branch of the A.E.C. (Contract No. AT (11-1)-318). The APPR-1 is a prototype of a reactor designed to meet the requirements and site conditions of a remote military base. Since the prototype reactor is to be constructed at a site in the United States, some of the design requirements were changed to meet these needs. In particular containment of the maximum credible accident is provided. The reactor is to be used as a training facility for troops and specialists who might eventually be required to operate and service remote plants. The requirement that all components be transportable by air still exists even though the site is not remote.

B. Description

The APPR-1 is a 10,000 kilowatt pressurized water reactor delivering 1825 net kilowatts of electricity with 2.5 inches of mercury back pressure (85^{o} F. condenser cooling water). Where lower temperature condenser water is available, back pressure can be reduced, permitting delivery of 1925 net kilowatts at 1.5 inches of mercury back pressure. The fuel elements are similar to those in the MTR but are made of stainless steel rather than aluminum, and in addition to the fissionable material contain a burnout poison in the form of boron.

The reactor operates at a pressure of 1200 psia and outlet temperature of 450^{o}F. at full power. Two primary coolant pumps in parallel are provided either of which will provide the design flow rate of 4000 gpm. The water flows from the

reactor to a steam generator, where heat is transferred to the secondary (steam) system from the generator and back through the pump to the reactor inlet. This entire primary loop is installed inside a vapor container 32 feet in diameter and 60 feet high as shown in the cutaway view in Fig I-1. The enclosure will contain the energy released from all of the steam generated by flashing of the superheated primary and secondary system water volumes when the maximum amount of heat has been stored in these volumes.

The turbine generator room is shown in Fig. I-1 just outside the vapor container with the control room on the second floor behind it. To the left of the vapor container may be seen the spent fuel pit where used fuel elements are stored. The rest of the building contains offices, laboratories, shops, etc.

C. Site

The reactor is to be built at Fort Belvoir, Virginia within the bounds of the Engineering Research and Development Laboratory, and bordering on Gunston Cove, as shown in Fig I-2. The nearest living quarters are 3000 feet from the site and house government personnel living on the Fort. A summary of the wind velocities and direction may be seen tabulated in the Figure.

The location of Fort Belvoir with respect to Washington and surrounding area is shown in Fig. I-3. Metropolitan Washington has a population of 1,460,000, practically all of which lies within a 20 mile radius of the site. Needless to say, the most important activities in the nation are centered within the 20 mile radius shown. The tremendous importance of complete containment of the APPR-1 in the event of an accident is recognized.

The meteorology, climatology, geology, and hydrology of the site are summarized in Appendix "A".

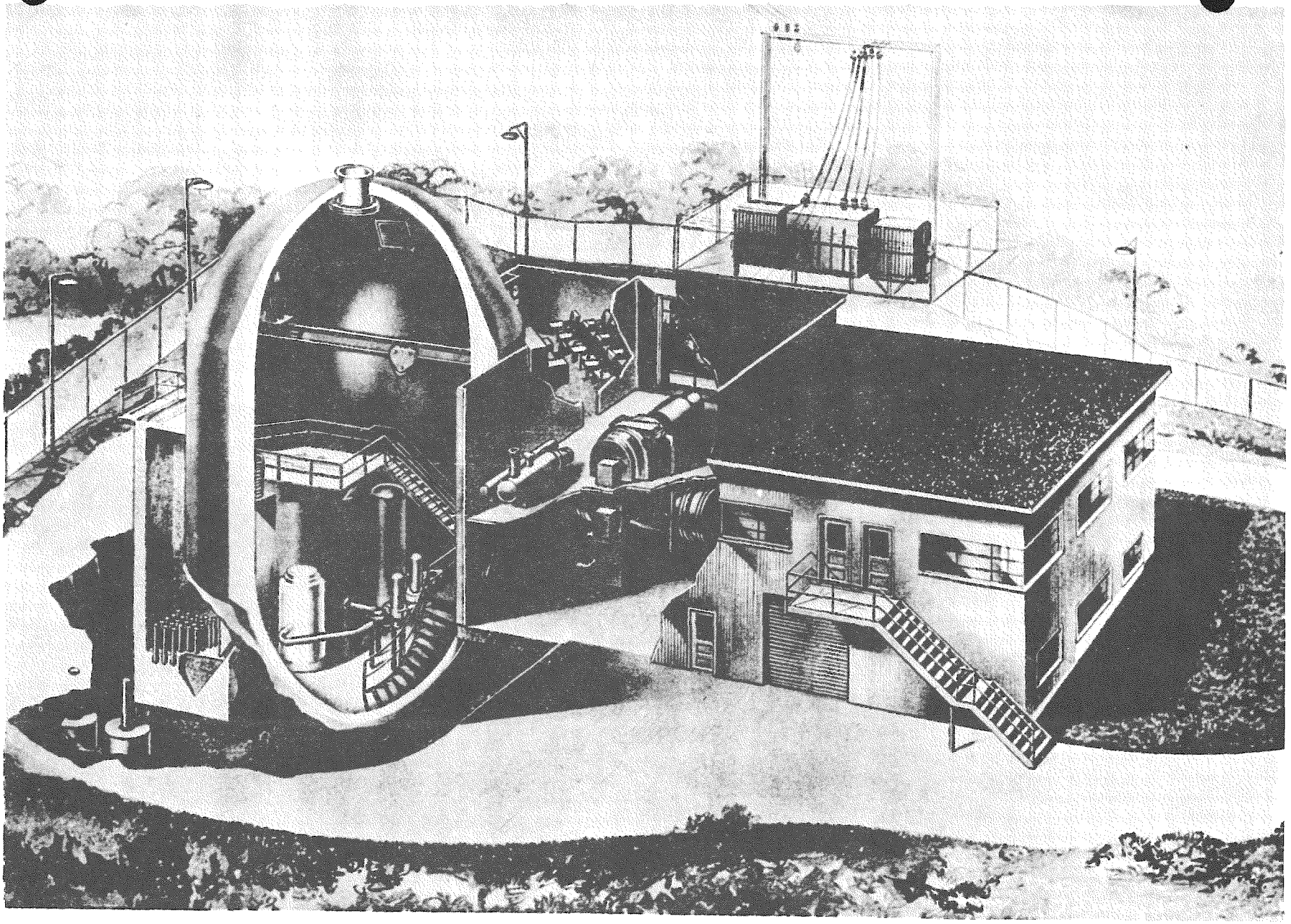

FIG. I-1 CUTAWAY VIEW OF THE APPR-1

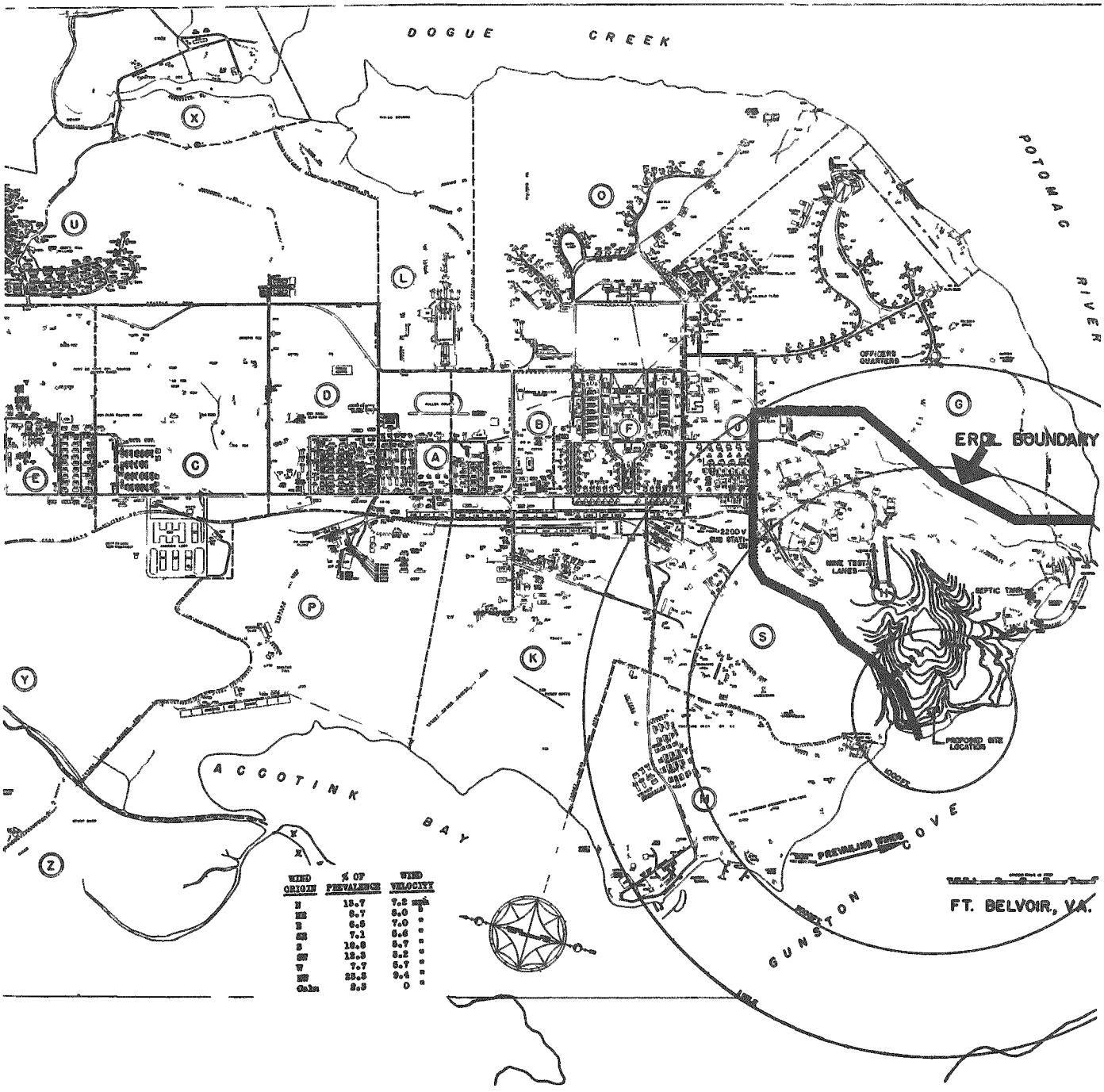

FIG. I-2 MAP OF THE FT. BELVOIR AREA

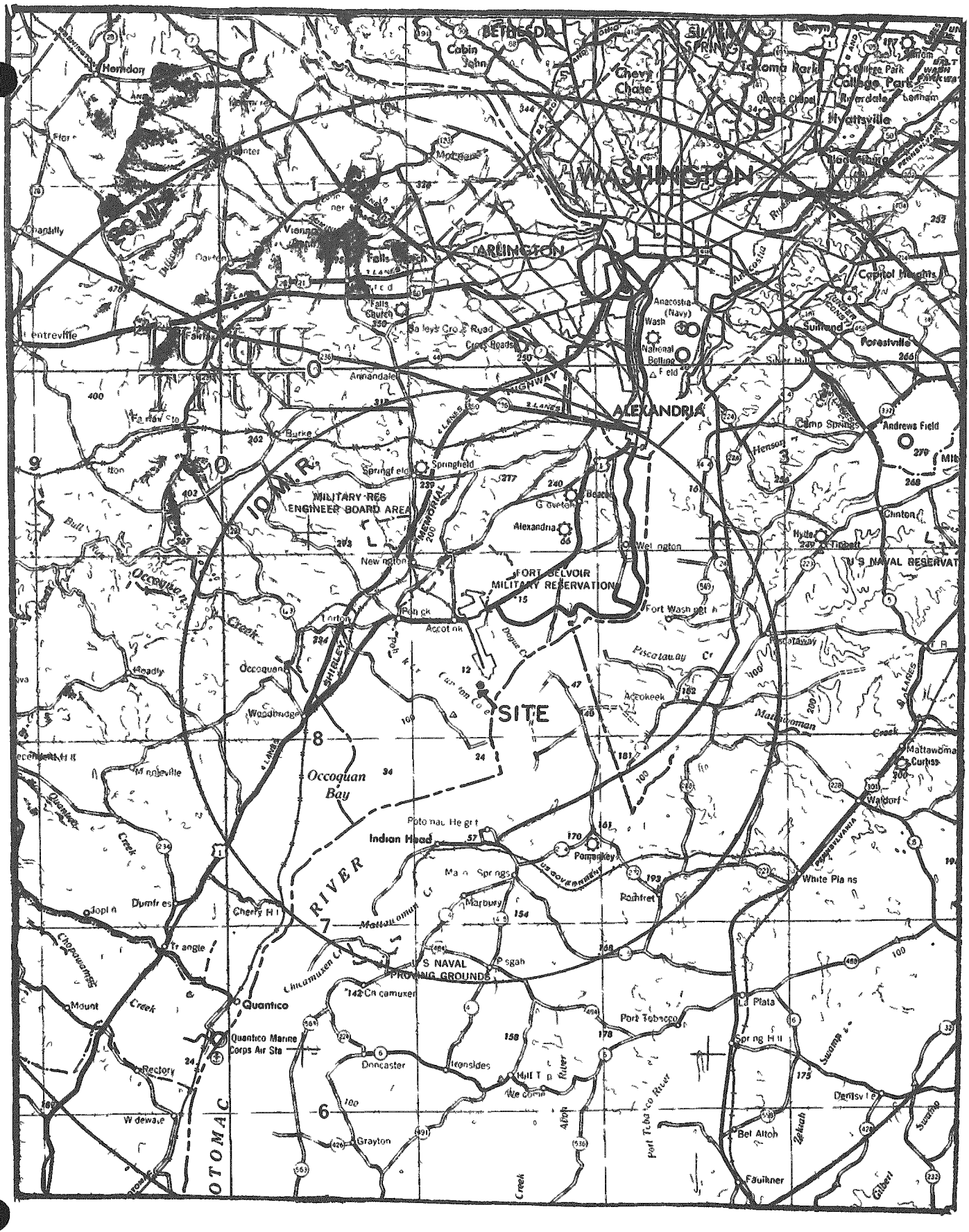

FIG. I-3 MAP OF THE AREA INCLUDING WASHINGTON, D.C.

D. Design Data

The following is a summary of design data on the APPR-1. More complete descriptions of the individual components listed here may be found in subsequent sections of the report, along with some of the design considerations involved.

1. Overall Plant Performance

Thermal power developed in reactor	kw BTU/hr	10,000 34.1×10^6
Electric power generated	kw (1.5 in. Hg) (2.5 in. Hg)	2105 2005
Net electric power delivered	kw (1.5 in. Hg) (2.5 in. Hg)	1925 1825
Power required for auxiliaries	kw	180
Thermal efficiency of net electric power generation	% (1.5 in. Hg) (2.5 in. Hg)	19.25 18.25
Power density of reactor core	kw/liter	71.7
Core life before refueling	Mw-yr	15

2. Reactor Data

Core

Average Diameter	in.	22.2
Height	in.	22.0
Volume of core	liters cu. in.	139.5 8513
Uranium content of new core	kg U 235	17.7
Critical mass after 15 Mw-years	kg U 235	10.2
Stainless steel content excluding matrix	kg	110.06

Core (Cont.)

Stainless steel content in matrix	kg	98.04
Poison content, natural boron	kg	0.172
B_4C content	kg	0.220
UO_2 content (1.136 kg/kg U)	kg	21.47
Water content at 0.83 g/cm^3 (450°F)	liters kg	111.1 92.2
Metal-to-water ratio		0.256
Excess k, (Multiplication) new, cold clean core	%	10
Maximum Excess k during operating period, hot cold	% %	7 16
Neutron flux, average, thermal, at end of 15 Mw-yr cycle	n/cm^2-sec.	2.7×10^{13}

Fuel Plates

Type of plates: rectangular, flat UO_2-ss-B_4C core, clad in 304L stainless steel.

Geometry of plates		Fuel Core	Overall
Thickness	in.	0.020	0.030
Width	in.	2.500	2.760
Length	in.	22.0	23.0

Stainless steel cladding

Thickness	in.	0.005
Spacing between plates	in.	0.134

Composition of fuel section of plates

UO_2	wt %	17.94
ss	wt %	81.88
B_4C	wt %	0.18

Fuel Plates (Cont.)

Geometry of ss side plates		Overall
Thickness	in.	0.050
Width	in.	2.912
Length	in.	23.0
Atom ratios in reactor core		
U 235	atoms	1
H_2O	molecules	68
Fe, Ni, Cr	atoms	48.4
B	atoms	0.212
Fuel plates per fuel assembly		18
Number of fuel assemblies		40
Fuel Plates per control rod assembly		16
Number of control rod assemblies		5
Total number of fuel plates		800
Dimensions of fuel assembly (overall)		
Thickness	in.	2.912
Width	in.	2.800
Length	in.	35.25

Control Rods

Type - Modified square "basket" to fit fuel space in lattice; upper section contains absorber material - lower section contains fuel sub-assembly. Actuating rack rigidly attached to bottom of basket.

Composition - Upper section: 16.3% B_4C in Copper, 3/8 inch thick; clad with 304 stainless steel, 1/32 inch thick, formed into square to fit basket. Lower Section: Similar to active fuel element except has 16 fuel plates and is adapted to fit inside basket.

Overall length including rack	in.	95
Number		5
Travel	in.	22

Control Rods (Cont)		
Weight of rod	lb.	75
Acceleration of rod after release	ft/sec^2	24.4
Maximum distance for rod to drop	in.	22
Thermal Data of Reactor at Full Power		
Operating pressure in reactor	psia	1200
Coolant inlet temperature at reactor	^oF	431.6
Coolant outlet temperature at reactor	^oF	450
Properties of Coolant		
Density at 450^oF at 431.6^oF	lb/ft^3 lb/ft^3	51.75 52.60
Change in density per ^oF	lb/ft^3-^oF	0.046
Viscosity at 445^oF	lb/ft-hr	0.295
Thermal conductivity	$BTU/hr-ft^2-^oF/ft$	0.39
Specific heat	$BTU/^oF-lb$	1.115
Coolant flow through core	gpm lb/hr	4000 1.66×10^6
Number of flow passes through reactor		1
Flow area in core	ft^2	2.083
Velocity in core passages	fps	4.3
Design heat output	BTU/hr	34.1×10^6
Heat transfer area	ft^2	611.1
Average heat flux	$BTU/hr-ft^2$	55,900
Peak-to-average heat flux ratio used for design (assumed)*		4:1

*Actual peak-to-average flux ratio not available at this time.

Thermal Data of Reactor at Full Power (Cont.)

Ratio of maximum to average heat flux in any one channel (cosine distribution)		1.31 1
Ratio of heat absorbed in hottest channel to average channel (4.0 1.31)		3.05 1
Maximum bulk water temperature, hottest channel	°F	487.6
Reynolds number in core		58,400
Film coefficient of heat transfer	BTU/hr-ft^2-°F	2,570
Maximum surface temperature	°F	554
Boiling temperature at 1200 psia	°F	567.2
Heat transfer coefficient of scale (assuming 0 010 in scale at k = 1.0 BTU/hr-ft^2-°F/ft)	BTU hr-ft^2-°F	1200
Maximum metal temperature		
with assumed scale	°F	742
with no scale	°F	565.7

3. Primary System Equipment

Pressure Vessel, ASTM-A-212, Grade B, clad with 304 stainless steel

Inside diameter	in.	48
Wall thickness	in.	2.5
Thickness of cladding, min.	in.	0.125
Design stress (ASME Code)	psi	17,500
Overall length of vessel	in.	138
Thickness of head	in.	2.5
Diameter of head	in.	38
Diameter of opening at top of vessel	in.	26
Inside diameter of thermal shield	in.	34.875

Pressure Vessel (Cont.)		
Thickness of thermal shield	in	2
Length of thermal shield	in	68
Insulation thickness	in.	4
Primary Coolant Pumps, centrifugal, canned rotor		
Operating head of pump	ft	28
Operating temperature at suction	^{o}F	431.6
Hydraulic horsepower at 4000 gpm, hot	hp	23.5
cold	hp	28.4
Number of pumps normally operated		1
Number of pumps installed		2

Steam Generator, vertical, double pass, U tubes

Tube side fluid; primary coolant.

Shell side fluid: boiling water and steam.

Materials: Tubes, partition, shrouds and baffle: 304 stainless steel.

Shell, tube sheet, nozzles: Type A-212 carbon steel clad with type 304 stainless steel.

Design Pressure		
Tube Side	psi	1500
Shell side	psi	450
Design temperatures		
Tube side	^{o}F	650
Shell side	^{o}F	650
Operating pressures		
Tube side	psia	1200
Shell side	psia	200-422

Steam Generator (Cont.)		
Full load heat transfer	BTU/hr	3.41×10^7
Heat transfer surface		
Steam generating region	ft^2	938
Superheat region	ft^2	214
Number of tubes		
Steam generating region		326
Superheat region		44
Diameter of tubes, O.D.	in.	0.75
Tube wall thickness	in.	0.065
Velocity in tubes	fps	11.5
Reynolds number in tubes		933,000
Overall heat transfer coefficient	$BTU/hr\text{-}ft^2\text{-}^oF$	495
Total head loss on tube side	ft of hot fluid	16.7
Full load steam flow	lb/hr	34,200
Feedwater temperature	^oF	250
Steam quality at entrance to superheater	%	99.7
Superheat	^oF	25
Steam pressure at full load	psia	200
Insulation thickness	in.	4
Pressurizer, SA 212 carbon steel clad with 304 stainless steel		1
Length	in.	102
Diameter, ID	in.	45
Wall thickness	in.	1
Heaters (two)	kw	50

Pressurizer (Cont)		
Insulation thickness	in	4
Design pressure	psi	1500
Design temperature	^{o}F	650
Pipe size, schedule 80	in.	4
Primary Coolant Piping, 304L stainless steel		
Pipe size, Schedule 80	in.	12
Diameter, OD	in.	12.75
Wall thickness	in.	0.687
Diameter, ID	in.	11.376
Maximum allowable internal pressure (ASA B31.1-1951)	psi	1500
Insulation thickness	in.	4
4. Control Rod Drive Mechanism		
Total Travel	in.	22
Rod Speed - either direction	in./min	3
Rod Accel. during scram	ft/sec^2	24.4
Fineness of position control	in.	0.062
Motor - 1/6 HP with integral brake 115 v. 3 ph. 60 cy. 1750 rpm		
Clutch - Warner 400 size Power supplied from AC line through rectifier		
Capacity - 0 rpm	ft-lb	20
Time to release	millisec.	53
Clutch located on low speed shaft just out-board of seal and position indicator		

Reduction gearing - totally enclosed, multistage planetary integral with motor - ratio		3200:1
Seal: Spindle type rotary (Kuchler-Huhn)		
Maximum leakage	lb/hr	10
Operating friction	in.-lb	1.4
Maximum break-away friction	in.-lb	12
Rack and Pinion (16 Pitch)		
Material 440 C SS		
Face width	in.	0.750
Back-up Roller - Stellite - 3		
Position Indicator		
Helipot type		AN
Total Turns		approx. 9

5. Primary Make Up System

Water Purification System, single column, mixed bed		
Capacity	gph	200
Effluent impurities	ppm	less than 1
Overall dimensions	in.	24 x 36 x 120
Approximate weight	lb	700
Chemical regenerants required per cycle (30 days)		
Cation, acid	lb	1.5
Anion, caustic	lb	4
Primary Coolant Feed Pump, Duplex		
Capacity	gpm	1
Discharge pressure	psia	1250

Primary Coolant Feed Pump, Duplex (Cont.)		
Motor size	hp	3
Number required for operation		1
Number to be installed		2
Control-Rod Seal Water Return Pumps		
Capacity	gph	20
Discharge pressure	psia	20
Motor size	hp	1/2
Number required for operation		1
Number to be installed		2

6. Shield Design

Primary Shield

Shield tank		
Inner radius	in.	32
Outer radius	in.	80.4
Height	in.	202
Inner Wall - steel thickness (below top shield disc)	in.	2
7 Shield rings - steel thickness of each ring	in.	2
Spacing between rings	in.	1
Height (inner ring)	ft	9
Water - Specific Gravity (minimum)		0.97
Top shield		
Water thickness	in.	100

Primary Shield (Cont.)		
Water specific gravity (minimum)		0.97
Steel thickness	in.	2
Secondary Shield		
Vapor Container		
Steel wall, thickness	in.	0.875
Concrete		
Thickness	in.	24
Specific gravity		2.3
Additional radial shielding-concrete		
Thickness	in.	36
Height (above basement floor)	ft	27
Specific gravity		2.3
Fuel Element Shielding		
Height of water above fuel element transfer tube opening	ft	12
Dose Rate		
Tolerance dose rate for 40-hr. week	mr/hr	7.5
Design dose rate		
Control room reactor operation	mr/hr	1.5
Above vapor container, reactor operation	mr/hr	150
Outside primary shield, 24 hours after shutdown	mr/hr	1.0
Adjacent to primary piping or to steam generator 24 hours after shutdown	mr/hr	22

7. Steam System

Turbine Generator- Condensing Turbine, Gear Driven Generator		1
Steam to throttle	psia	190
Exhaust pressure, abs	in. Hg	1.5
Rating, at 0.8 power factor	kw	2105
Voltage	volts	4160
Frequency	cps	60
Exciter - direct-connected		
Generator - open-air cooled		
Extraction nozzle, at 4680 lb/hr	psia	35
Steam to throttle, full load	lb/hr	32,325
Turbine efficiency, full load	%	65.5
Generator efficiency, full load	%	96
Gear, bearings and windage efficiency	%	98.5
Automatic controls: frequency, voltage		
Safety devices: overspeed, low vacuum, vacuum breaker.		
Exhaust quality, full load	%	90.5
Condenser, horizontal, shell and tube, two-pass		1
Heat transfer	BTU/hr	28.5×10^6
Steam flow, max.	lb/hr	29,000
Hot well depression, max.	^oF	10
Coolant temperature, in, max.	^oF	85
Effective surface	ft^2	2840
Velocity in tubes	fps	7.0

Condenser (Cont.)		
Quality of steam	%	90
Tubes (18 gage), diameter, OD	in	0.75
Design pressure - Tube side	psi	60
Shell side		Full Vacuum
Air removal equipment Twin jet steam ejectors with intercooler and aftercooler.		
Closed Feedwater Heater		
Storage tank capacity	gal	5000
Supply at full load	min	67
Outflow rate	lb/hr	34,400
Operating pressure	psia	200
Outflow temperature	^{o}F	250
Controls: float, high and low level alarm, relief, gage glass		
Evaporator, bent-tube, self-de-scaling with preheater		1
Raw water inflow	lb/hr	1884
Storage tank capacity	gal	5000
Supply at full load	hr	22
Evaporator blowdown	lb/hr	134
Steam supply pressure, saturated	psia	190
Heating steam requirement, 190 psia	lb/hr	2350
Purity	ppm	1
O_2 content, maximum	cc/1	0.005

Boiler Feed Pumps (With Hot-Well) two stage centrifugal		2
Number running at full load		1
Speed	rpm	3550
Capacity, each	gpm	75
Head, at 75 gpm	ft	630
Water temperature	^{o}F	109
Estimated efficiency	%	66
Rated power, each	hp	20
Coolant Circulating Water Pump, Vertical, single stage		2
Number running at full load		1
Speed	rpm	1760
Capacity, each	gpm	4500
Head	ft	50
Fluid temperature	^{o}F	35-85
Estimated Efficiency	%	82
Drive motor size, each	hp	75
Reactor Shutdown Cooling Pump, steam turbine drive		1
Speed	rpm	3550
Capacity	gpm	75
Head	ft	630
Water temperature	^{o}F	109

8. Power Plant Building

Overall dimension, main part of building	ft	27 x 68 x 47
Dimensions of control room and storage wing	ft	18 x 22 x 35

Total floor area	ft^2	6550
Total volume of building	ft^3	105,000
Bridge crane span	ft	22
Crane load capacity	tons	10

CHAPTER II - REACTOR

A. Core

The ALCO design of the APPR-1 reactor core is essentially unchanged from that proposed by the Oak Ridge National Laboratory (1). The fuel elements are arranged in a 7 x 7 array with the corners missing and with 5 of the 45 positions occupied by the control rods as shown in Figure II-1.

The reactor uses uranium, fully enriched in the U-235 isotope. The core contains 17.7 kg of U-235, for 15 MW years loading. The fuel, in the form of uranium dioxide, is incorporated into flat-plate-type fuel assemblies which are similar in design to the fuel elements employed in the MTR and STR. The metal to water ratio in the active section of the reactor is 0.256.

The rectangular fuel plates consist essentially of UO_2 particles uniformly dispersed and imbedded in a matrix of stainless steel which is clad on all sides with wrought 304L (low-carbon) stainless steel. A small quantity of poison B_4C is added to the fuel mixture to facilitate reactor control.

The core of a fuel plate, is composed of 17.94 wt % UO_2, 0.18 wt % B_4C, and a matrix of 81.88 wt % stainless steel. This core measures approximately 22.00 in. long, 2.50 in. wide, and 0.020 in. thick in the finished plate. The cores are jacketed by the picture-frame technique which seals the uranium from exposure to the cooling water and also retains the fission products. The hot working operation results in a good metallurgical bond between cladding and core. The cladding-core-cladding thickness in mils is 5-20-5.

(1) List of references included at end of this report.

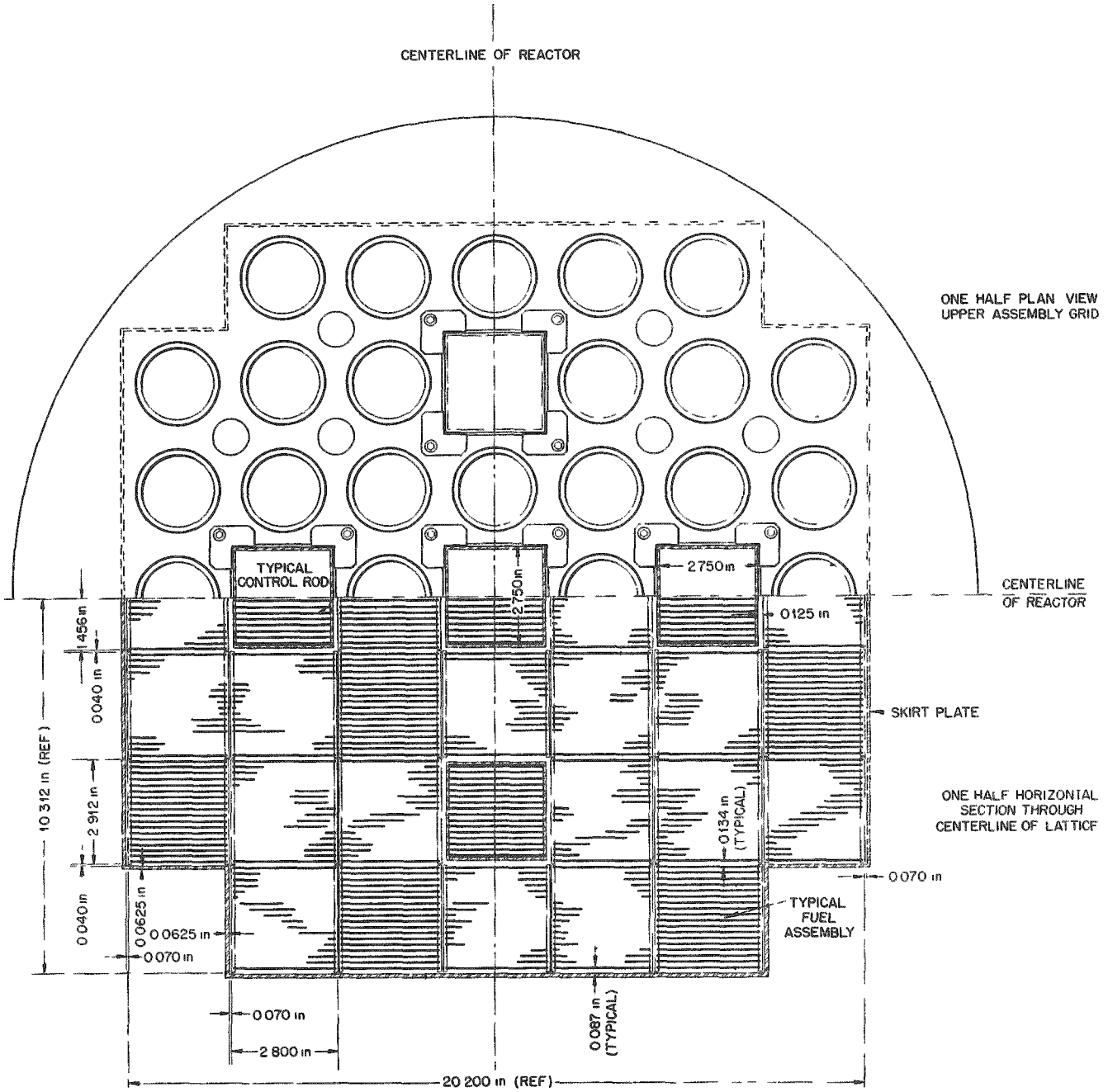

FIG. II-1 REACTOR CORE CROSS SECTION

Eighteen of these composite plates, each 2.76 in. wide by 23.00 in. long, overall dimensions, are assembled into a single unit which is designated as a fuel element. The plates with a nominal 0.134 in. water gap space between them are brazed into a pair of stainless steel side plates of 0.050 in. thickness.

The brazed assembly is then equipped on each end with stainless steel end boxes by plug welding. The end boxes adapt the unit to the supporting grids which in turn firmly fix the position of the element in the reactor core. Each fuel element contains 398 grams of U 235 and 3.82 grams of boron.

The fuel plates are designed to be used in both the fuel assembly and, with slight size differences, the fuel section of the shim rod assembly. Making all active sections to one specification simplifies fabrication. The number of fuel plates in both the fuel elements and control rods in the reactor core totals 800.

The reactivity of the reactor is lowered when the control rods are inserted to the "in" position, i.e., resting on their shock absorbers. The five control rods in the loading are identical. The rods are constructed in two segments. The upper segment contains B_4C in a copper matrix clad with stainless steel [2]. This section resides in the lattice when the rod rests in the shock absorbers. The lower segment, containing a fuel element with 16 fuel plates, is raised into the lattice when the control rod is up.

The function of the grid and support structure is to position and support the fuel and control assemblies, Fig. II-2. The structure consists of the skirt support plate, the upper assembly grid, the skirt, the lower assembly grid, the shock absorbers and the control pinion supports. Except for the upper grid, these components are assembled as a unit and lowered into the pressure vessel before the

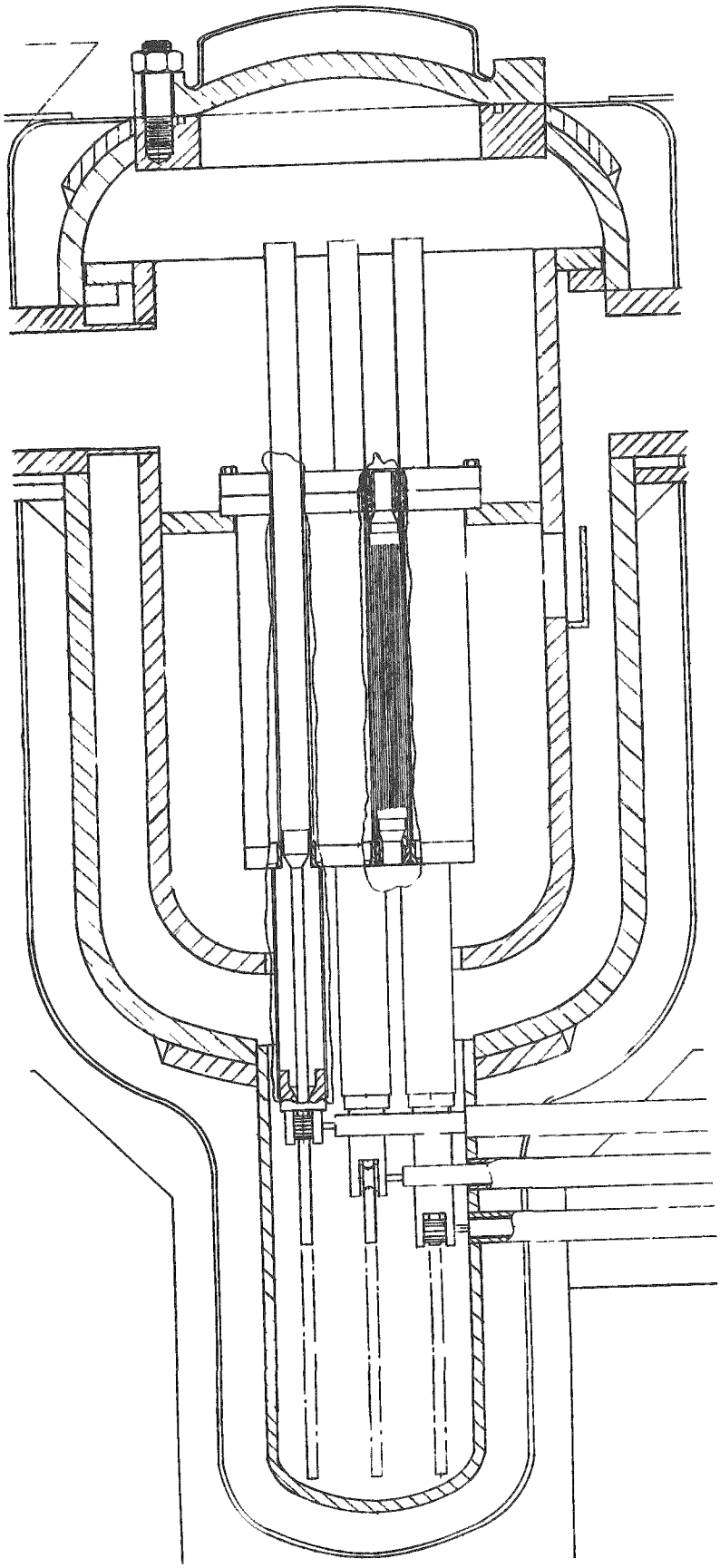

FIG. II-2 REACTOR CORE AND PRESSURE VESSEL

upper section of the vessel is welded into place. The fuel elements are fixed in place by the upper and lower grids. The upper grid is held down by bolt latches compressing the assembly springs.

The skirt, which serves the purpose of connecting the upper and lower grids, is made of 1/16 in. stainless steel sheet. In cross section the skirt is a square with each corner formed in an internal right angle to give added rigidity. The skirt also helps to direct the flow of cooling water through the core.

B. Pressure Vessel

The reactor core, including control rods and control rod extensions, is enclosed within a pressure vessel, Fig. II-2. This pressure vessel consists of a cylinder 48 in. I.D. by 64 in. long having ASME ellipsoidal heads at each end. It is constructed of carbon steel type SA 212 Grade B. All joints are welded, radiographed, and stress relieved. All internal surfaces in contact with the primary water are clad with stainless steel Type 304, 0.125 in. thick.

The main shell is penetrated at four points. A dished cover is attached at the top by means of 18 alloy steel studs, 2-1/2 inches in diameter, threaded into a reinforcing ring which is welded into a circular opening cut into the upper head. An additional reinforcing ring is attached to the head at this point. Inlet and outlet pipes are welded to the cylindrical shell on opposite ends of a diameter 10 inches below the upper end of the cylindrical section. An enclosure for the control rods and associated drive mechanism is welded into the bottom head. This extension is cylindrical, 18 inches I.D. by 32 inches long, and is closed at the bottom by an ASME ellipsoidal head.

It is welded into a circular opening in the lower head and is reinforced by a ring in a manner similar to that used at the upper end. The control rod en-

closure is further penetrated by five tubular members which house the control rod drive shafts and extend outward approximately 4 feet under the primary shield surrounding the pressure vessel.

Structural support for the pressure vessel is by means of a ring attached to the outside diameter of the cylindrical section just below the inlet and outlet pipes. This ring rests on a support ring welded to the inner steel shielding ring which in turn rests on a concrete structure in the bottom of the vapor container.

The pressure shell and control rod extension is surrounded by thermal insulation 4 inches thick, which in turn is contained in a water-tight steel shell. Additional insulation is applied to the removable cover at the top of the pressure shell. Necessary provisions are made inside the pressure shell for support of the core structure and thermal shield which also serves as an internal baffle to control cooling water flow to the core.

The pressure shell is designed and fabricated in accordance with applicable sections of ASME code, section VIII, covering Unfired Pressure Vessels, edition of 1952. The design conditions are based on a maximum temperature of 650°F. and a maximum allowable working pressure of 1600 psig. The temperature and pressure chosen are somewhat higher than actual design conditions for the APPR-1, but it is felt desirable to design the major structural elements on a conservative basis, partly for safety reasons and partly to permit a margin for variations in operating conditions in order to make the first unit as versatile as possible within reasonable structural and economic limitations. These design conditions result in wall thickness of the main pressure shell of 2-1/2 inches exclusive of cladding and 1 inch in the control rod enclosure.

C. Control Rod Drives

The control rod drives have been modified extensively over those proposed by ORNL. It was considered desirable to simplify the control rod drives and to provide as positive a mechanism as possible. To attain this end the control rods have been inverted and the drive moved to the bottom of the pressure shell. The sense of control motion of the control rods is unchanged in that they are raised to increase activity and lowered to reduce reactor output. Thus gravity can be used as the major motivating force for emergency insertion of the control rods to scram the reactor. Control rod travel under motor control is at 3 inches per minute.

The drive train, Fig. II-3, consists of a rack attached to the bottom of each control rod, a pinion meshing with this rack and a drive shaft attached to each pinion extending outward through enclosing tubes where connection is made through a Warner electric clutch to a motor and reduction gear drive.

Penetration of the pinion shaft through the pressure-containing wall is by means of a metallic sealing unit manufactured by the Kuchler-Huhn Company of Philadelphia, Pa. This unit consists of a series of floating rings surrounding the shaft to be sealed, which rings provide a very close-clearance annular leakage path from the pressure volume to the outside. There is a small controlled amount of leakage as a result of this close clearance. The construction of the unit is such that virtually no rubbing occurs between the sealing elements, so that wear is extremely small.

Make-up water for the primary system is introduced at the high pressure end of the seal. This arrangement reduces the problem of disposal of such seal leakage as does occur, since this leakage is largely confined to uncontaminated

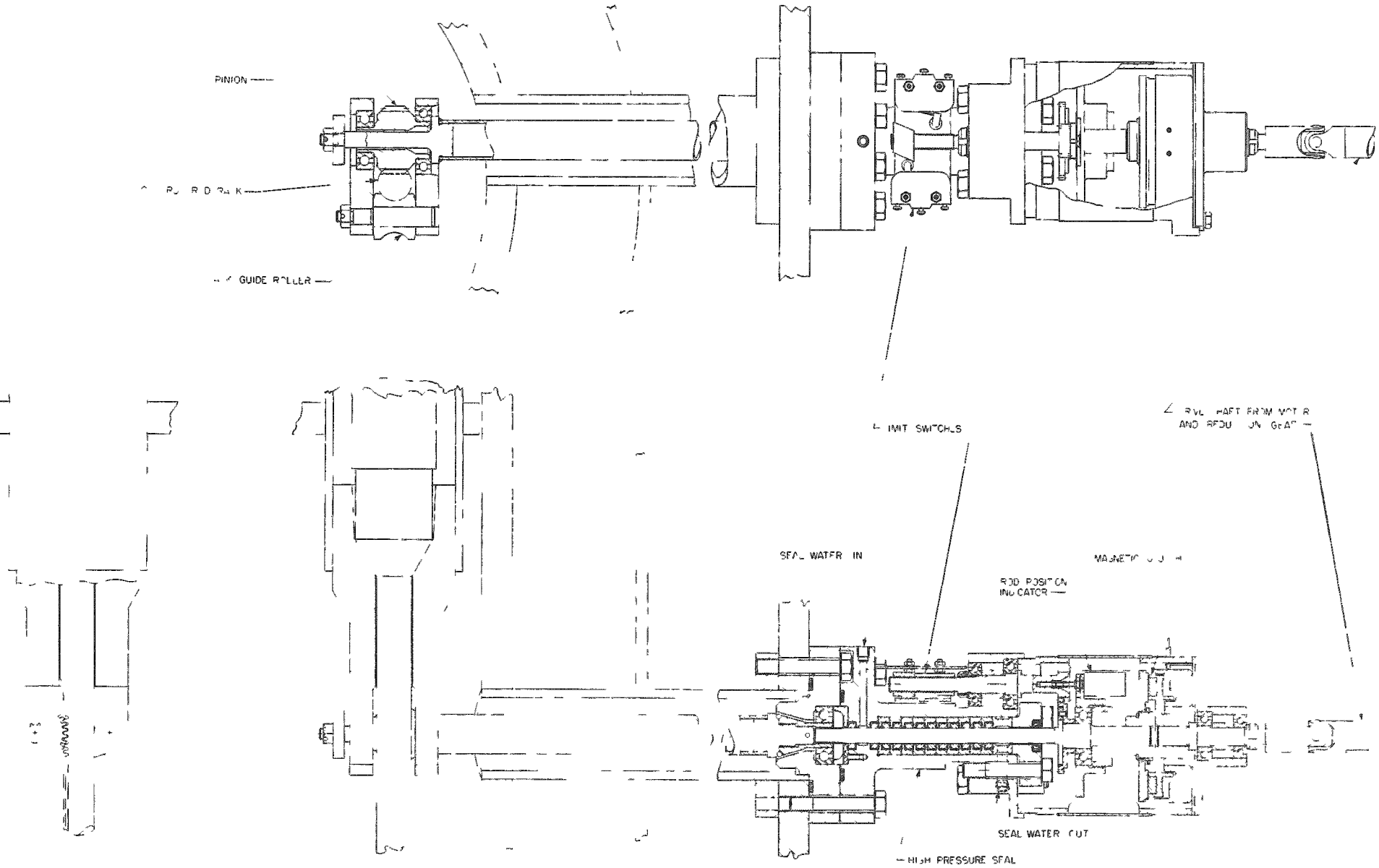

FIG. II-3 CONTROL ROD DRIVE MECHANISM

water, which is then disposed of along with the primary system waste.

Provision is made in the design to remove and replace the complete seal unit without draining the primary system, thus minimizing the hazards associated with handling this large quantity of contaminated water, and making this replacement a simple, routine maintenance procedure. Working area in which this operation and other maintenance operations on drive motors, etc., are performed is shielded for adequate protection of maintenance personnel.

The actuating mechanism comprises two major assemblies for each control rod. One of these, consisting of the rack and pinion and associated bearings, operates in the primary system water and is inside the pressure vessel. The other, connected to the first through the seal discussed above, includes the 3 phase, 60 cycle driving motor with integral brake and reduction gear box, scram clutch, rod position indicator and limit switches. These units are outside the pressure vessel, but within the vapor container. They are of conventional design and are conventionally lubricated, inspected and maintained.

Since the rack and pinion, bearings, etc., immersed in the pressure vessel are not readily available for maintenance, utmost reliability and service life are primary factors in their design. These characteristics are achieved through careful attention to design details such as tooth loading, bearing loading, selection of materials, etc. Experience gained from STR operation and other sources has been made available and used. An exhaustive test program will be run using actual components, and taking into consideration all such pertinent factors as thermal distortion, material wear, corrosion, etc.

The control rod structure itself, Fig. II-4, consists of a stainless steel

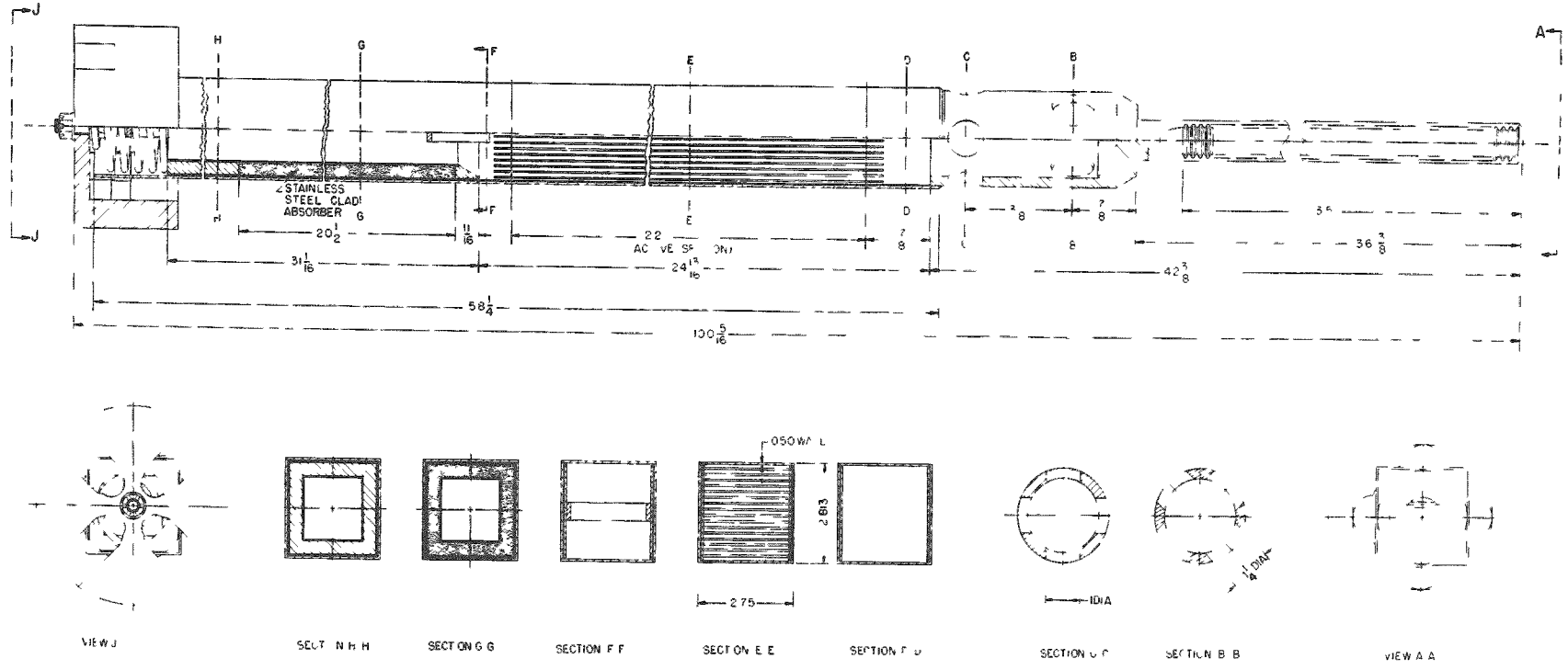

FIG. II-4 CONTROL ROD DETAIL

square tubular member running vertically through the core and having a rack rigidly attached to its lower end The absorber and fuel sections are inserted in this container from the top and retained by spring means The absorber section is on top. Suitable openings are provided to permit coolant to flow through both fuel and absorber sections at the same rate as it flows through the active fuel elements. The control rod is supported at the top by recirculating ball bearing elements and at the rack end by the pinion and a back-up roller. No intermediate support is used. External clearances except at the two support points are great enough to prevent danger of binding due to thermal distortion, foreign matter, etc.

Emergency insertion of the control rods is performed by de-energizing the electric scram clutch. This unit is a standard commercial item manufactured by the Warner Electric Clutch and Brake Company, and has a torque rating approximately three times that necessary to operate the rods. Release time of the clutch is 0.053 seconds maximum. Effective weight of the control rod assembly is approximately 61 lbs. (including flotation effect with the reactor cold). Inertia mass of the rod assembly is 2.18 slugs, and inertia of all connected rotating parts referred to the rod is 0.145 slugs.

Friction data on radial ball bearings in pure water under the loading conditions that exist is almost entirely lacking. It appears, however, that a coefficient of friction of 0.2 is highly conservative. During a scram, the only load on the bearings is the weight of the rotating parts, plus a slight increment due to angular acceleration from the pinion as it is driven by the rack. This load is approximately 8 pounds. Taking into account the radii of the bearings, this gives an equivalent friction force at the rack of approximately 0.5 pound.

Seal friction extrapolated from tests of a somewhat larger unit is approximately 1.4 pounds at the rack, and rod guide friction is assumed to be negligible. To provide for contingencies, an overall friction force of 4 pounds is assumed. Seal break-away friction is approximately 12 pounds equivalent at the rack, but decreases to the above figure as soon as any motion occurs.

The net drop force available is thus 57 pounds and total effective mass to be accelerated is 2.33 slugs, giving acceleration of 0.76 g. The drop time vs. travel is shown in Fig. II-5. The rods are decelerated during the final 3 inches of drop by a dash pot shock absorber.

Control rod position is continuously indicated by means of a Helipot and meter, the Helipot being mechanically driven by the pinion drive shaft between the scram clutch and the seal. Limit switches are also provided at this point to prevent overtravel of the rods. Accuracy of rod positioning and indication is plus or minus .062 inches or better.

D. Primary Shield

Figure II-6 is an elevation drawing of the reactor and primary shield with a plan view in Fig. II-7. Outside of the pressure vessel are four inches of insulation held in place by a 3/8 inch shell of steel. After a small air gap there is the inner wall of the shielding vessel which is a two inch thick steel cylinder. This inner wall of the shield tank also supports the pressure vessel below the inlet and outlet pipes. The shield tank is forty-six inches thick and is filled with water. Seven steel cylinders two inches thick are arranged concentrically around the inner wall of the tank, with one inch of water between adjacent cylinders. These seven layers of steel, plus the two inch inner wall of the tank, give a total of sixteen inches of steel radially

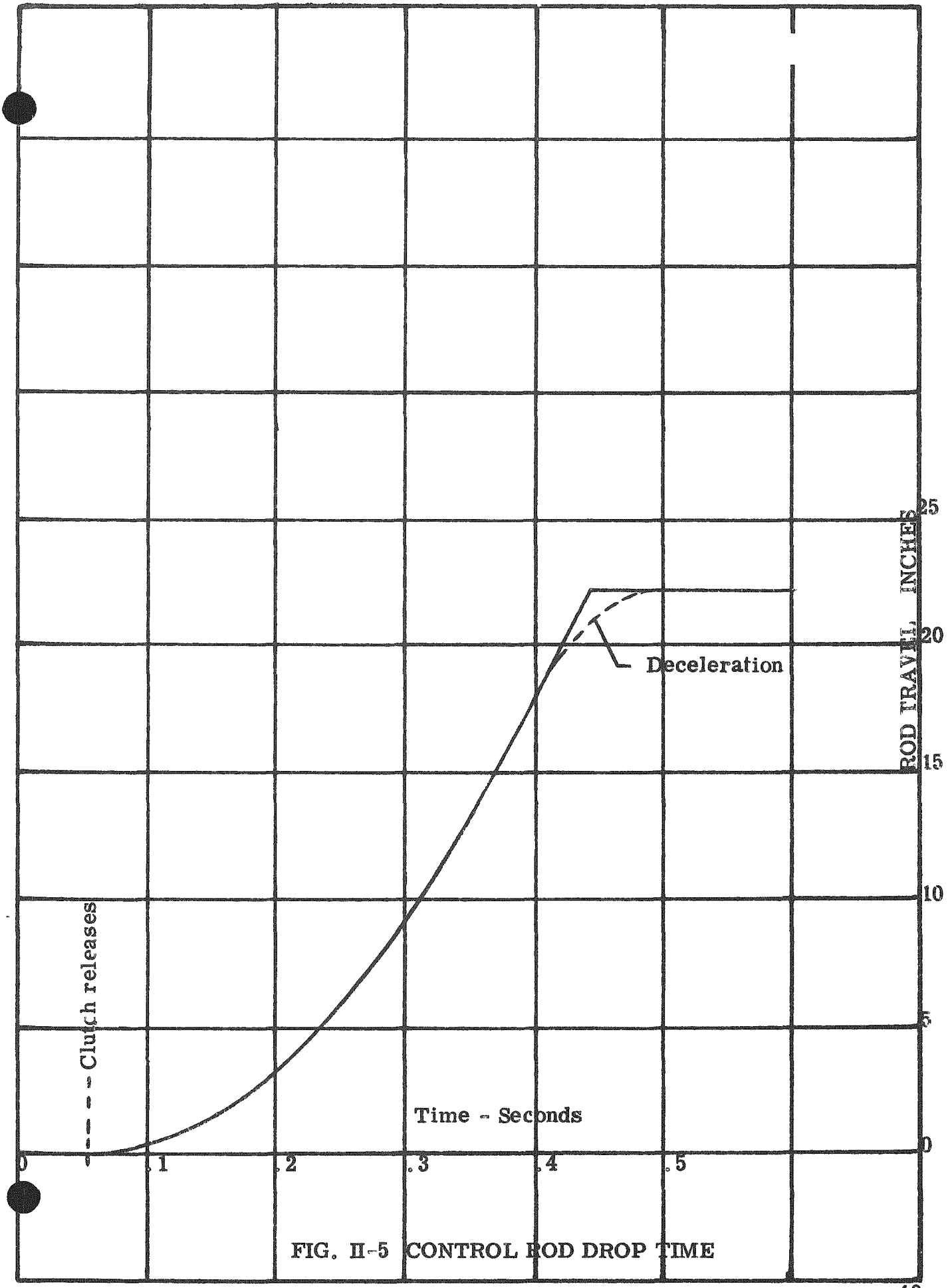

FIG. II-5 CONTROL ROD DROP TIME

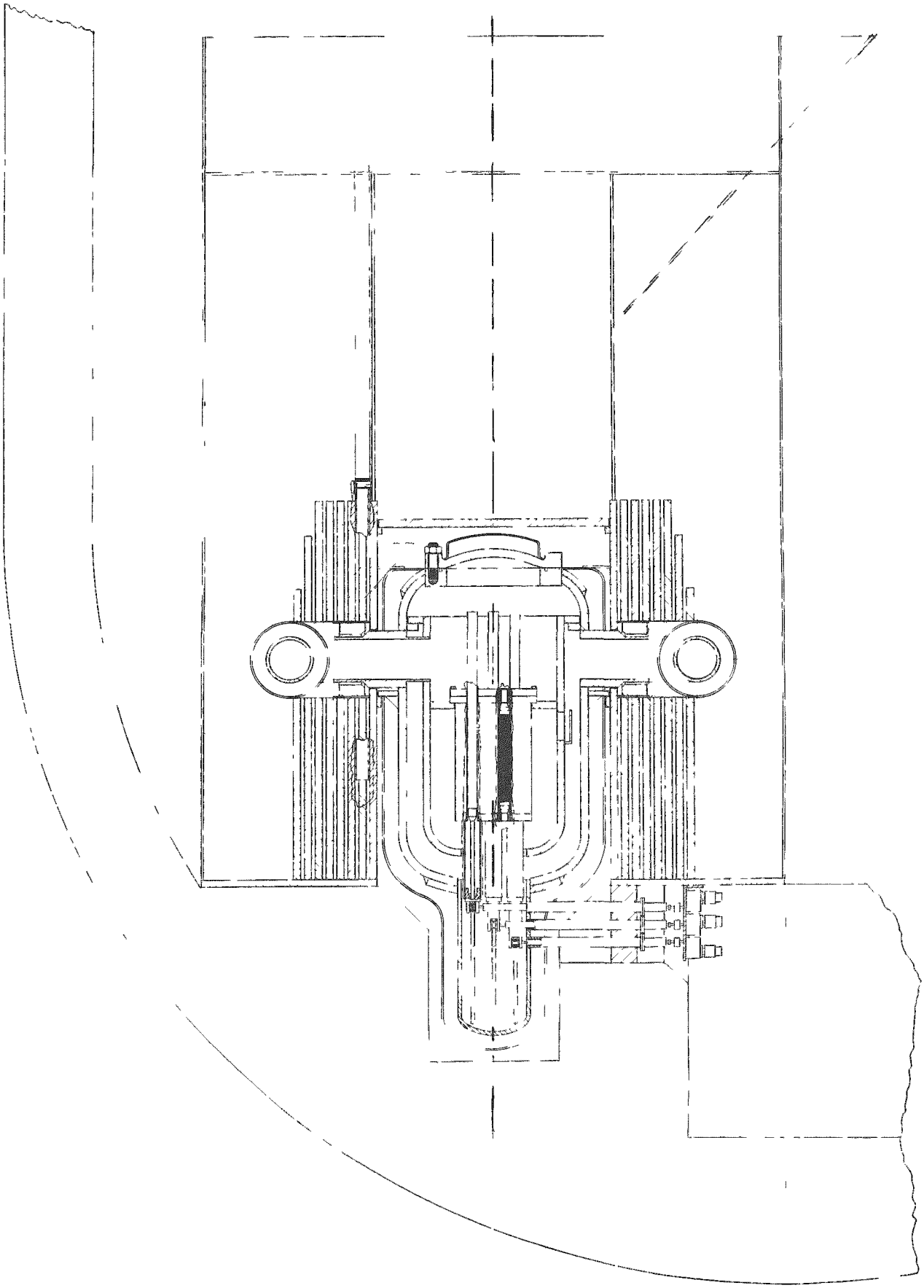

FIG. II-6 PRIMARY SHIELD - ELEVATION

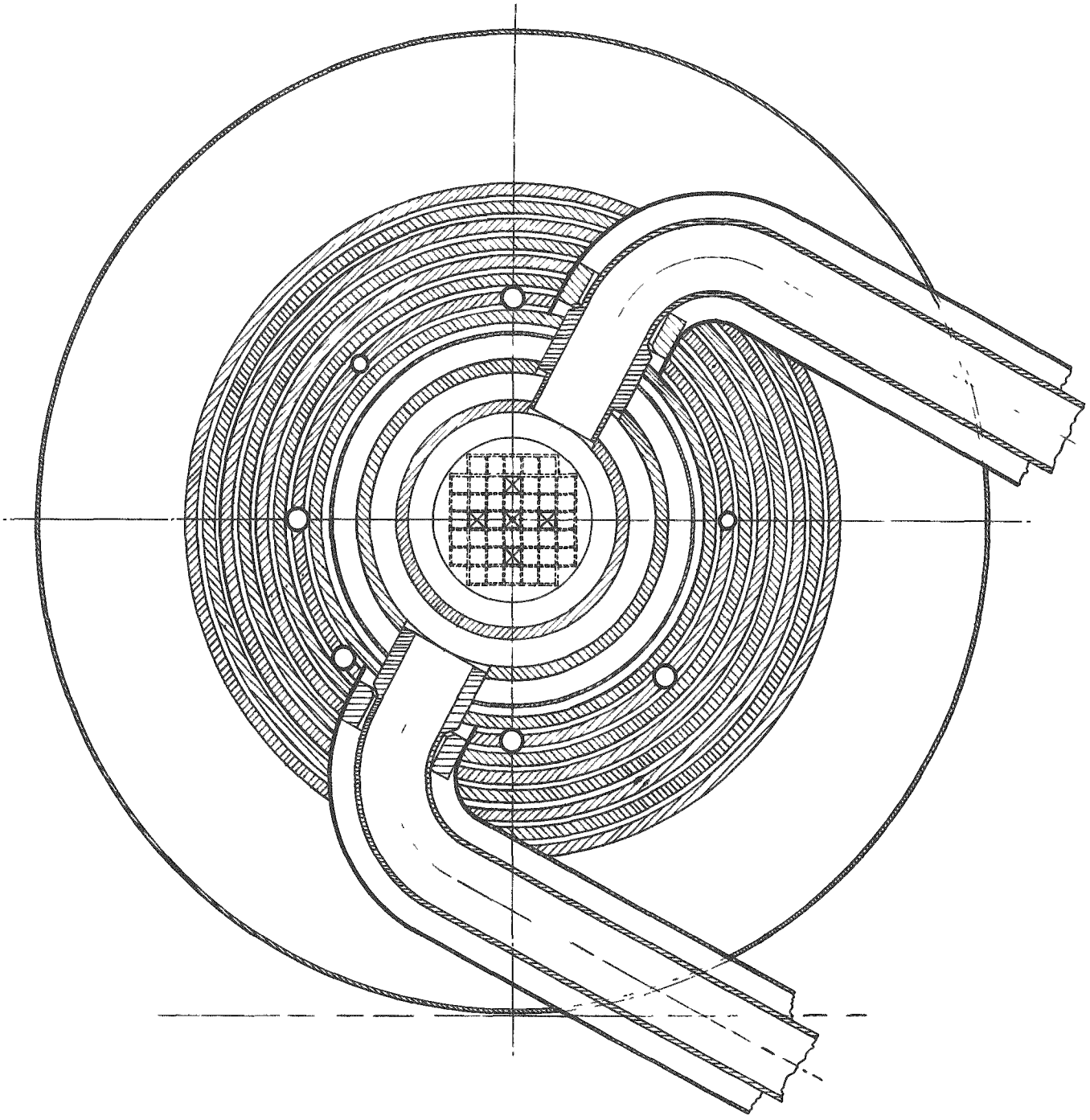

FIG. II-7 PRIMARY SHIELD - PLAN

around the reactor outside of the pressure vessel and constitute the primary gamma shield.

Above the pressure vessel, the inner wall of the shield tank forms a well, nine feet deep, which is filled with water. A removable iron disc, two inches thick, is mounted close above the pressure vessel for additional gamma shielding. Around the inlet and outlet pipes to the reactor pressure vessel there is four inches of insulation which is a void in the shield. Since the pipes are located above the core and turn at right angles within the shield tank, direct streaming of radiation through the annular voids cannot occur. To prevent scattered radiation from penetrating the shield a ring of steel seven inches thick is located around the pipe close to the pressure vessel as shown in Figure II-6.

E. Reactor Instruments

Five ionization chambers and two BF_3 counters are used on the APPR-1. The chambers are mounted next to the inner wall of the shield tank as shown in Figure II-6. For the critical experiment neutron counters will be mounted temporarily within the pressure vessel next to the core.

There are three PCP ionization chambers which serve to actuate the safety level scram system, and a compensated ionization chamber is connected to the log N and period meters. The fifth ionization chamber provides the signal to a micro-micro-ammeter as well as to the servo control at low flux levels.

The control and safety circuity is described in greater detail in Chapter VI.

CHAPTER III - POWER PLANT

The power plant is composed essentially of two systems - the primary or pressurized water and the secondary or steam, together with auxiliaries required to insure proper functioning of the two systems as an integrated plant to produce power. The fundamental flow diagram is shown on Figure III-1, and the heat balance on Figure III-2. The primary system equipment such as reactor, steam generator, cooling water circulating pumps and pressurizer in the vapor container are shown in Figure III-3 Elevation and Figure III-4 Plan.

A. Primary System

The primary system includes the reactor with control rods, two coolant circulating pumps, piping, the tube portion of the steam generator, a pressurizer with 100 KW of electric heaters, water purification and make-up equipment.

The water is circulated through the reactor at a rate of 4000 gpm by one pump with a duplicate pump in reserve (100% standby), a check valve being provided to preclude counterflow through the inactive pump. The circulating pumps are centrifugal type with "canned" motors to eliminate leakage. Motor windings are water cooled. Sufficient back circulation is provided in the check valve to keep the dormant "leg" and inactive pump hot. The water in the system is maintained at 1200 psia to preclude boiling (saturation temperature 568°F.) in the reactor. This water enters the reactor at about 431°F. and leaves at 450°F. when operating at full load. The electric heaters in the pressurizer vessel maintain pressure at 1200 psia. Over-pressure protection is provided by a relief valve set at 1500 psi at the pressurizer vessel. The water level in the pressurizer is automatically

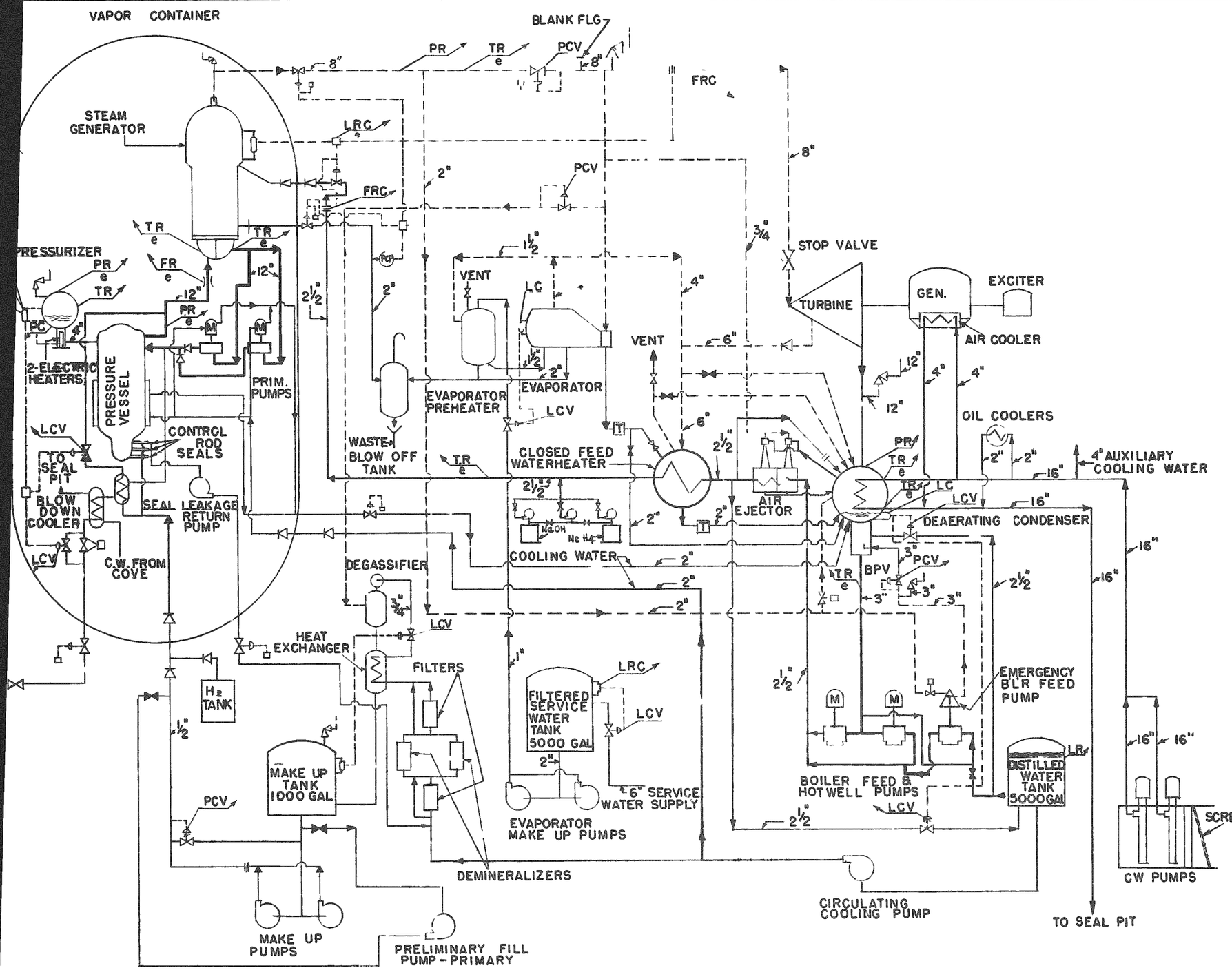

-LEGEND-

- STEAM
- WATER
- CONTROL
- NORMALLY CLOSED
- SAFETY VALVE
- TRAP
- ORIFICE
- ION CHAMBER
- VALVE IN OUTGOING LINE FROM VAPOR CONTAINER AUTOMATICALLY CLOSES ON PRESSURE RISE
- TRIP VALVE
- CONTROL BOARD MOUNTED INSTR.
- LOCALLY MOUNTED INSTRUMENT
- BOARD MOUNTED INSTRUMENT ELECTRIC TRANSMISSION INDICATING PRESSURE GAGES & THERMOMETERS NOT SHOWN
- MOTOR OPERATED VALVE
- PCV. PRESSURE CONTROL VALVE
- LCV. LEVEL CONTROL VALVE
- HLA. HIGH LEVEL ALARM
- LLA. LOW LEVEL ALARM
- BPV. BACK PRESSURE VALVE
- FRC. FLOW RECORD'G CONTR.
- LRC. LEVEL RECORD'G CONTROL
- TR. TEMPERATURE RECORDER
- LC. LEVEL CONTROLLER
- PC. PRESSURE CONTROLLER
- FR. FLOW RECORDER
- FI. FLOW INDICATOR
- PR. PRESSURE RECORDER

FIG. III-1 FUNDAMENTAL FLOW DIAGRAM

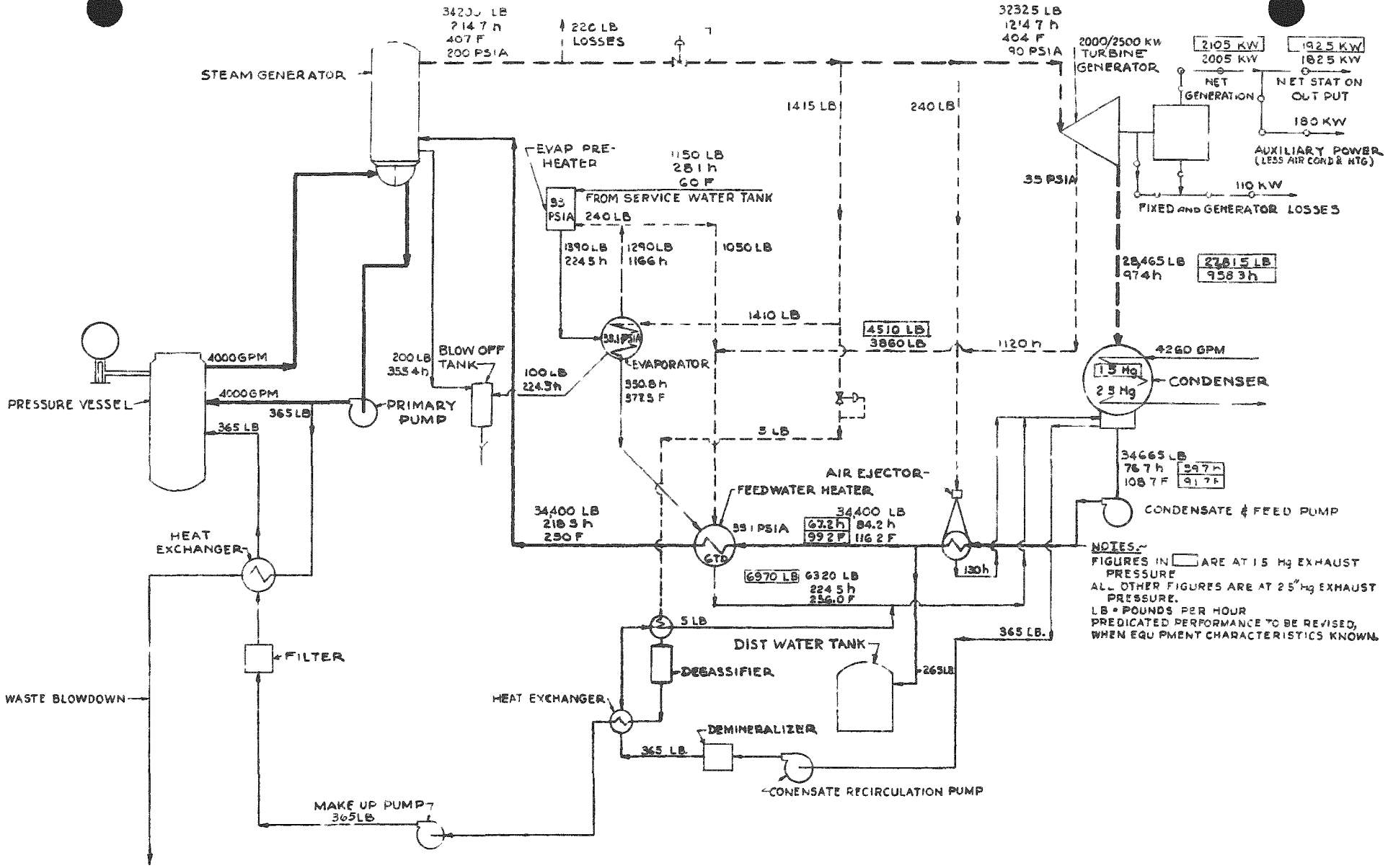

FIG. III-2 PREDICTED PERFORMANCE - HEAT BALANCE DIAGRAM

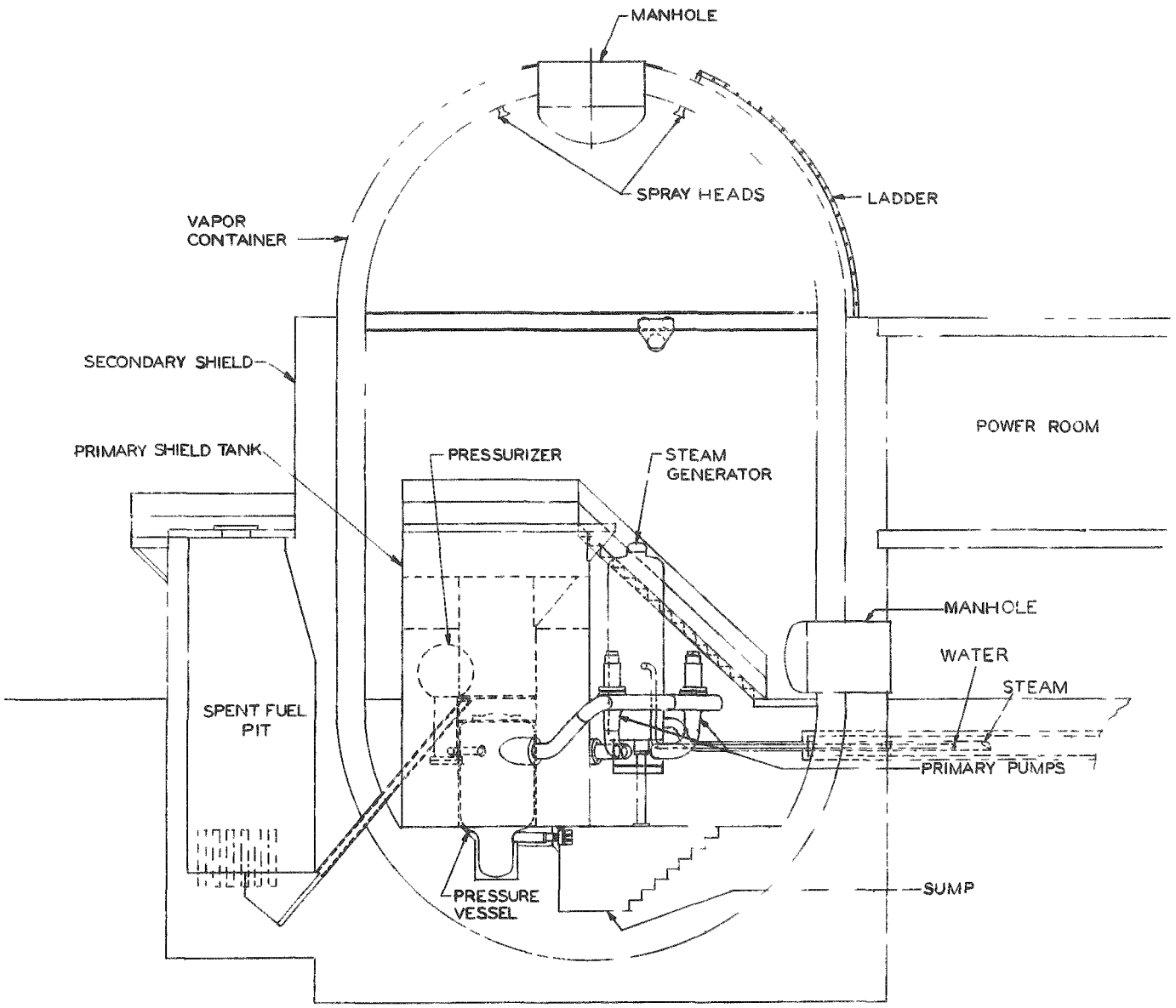

FIG. III-3 EQUIPMENT ARRANGEMENT IN VAPOR CONTAINER ELEVATION

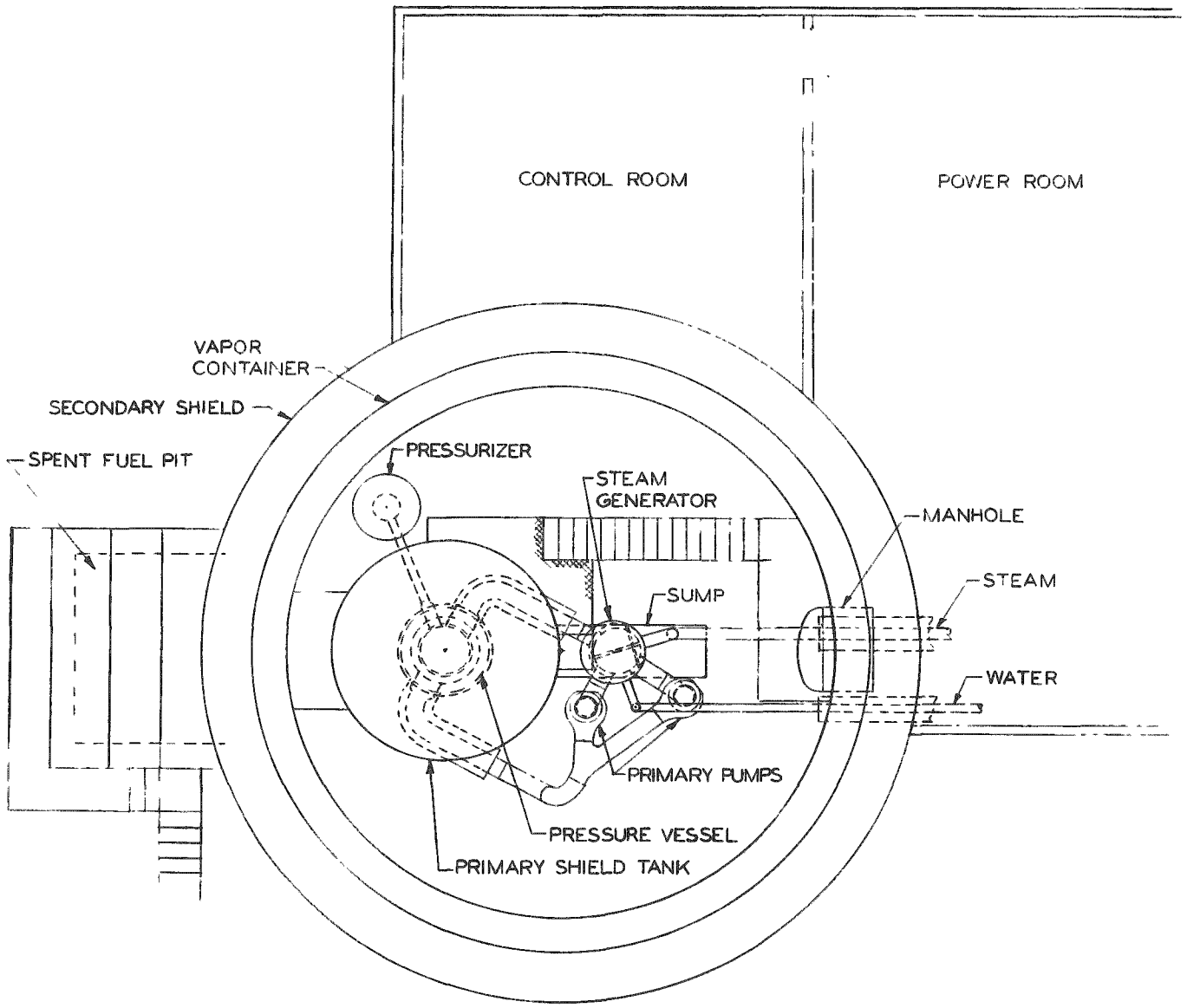

FIG. III-4 EQUIPMENT ARRANGEMENT IN VAPOR CONTAINER - PLAN

maintained by means of a level controller valve in the make-up water line. The signal to the valve comes from the level control indicator at the pressurizer.

A control valve remotely operated from the control room permits venting noncondensible gases from the system. High and low water alarm with control board mounted instruments and level, pressure and temperature recorders are provided to record conditions in the pressurizer vessel. A flow recorder indicating circulating water flow through the reactor is provided. Pressure in the primary line as it leaves the reactor and water temperature entering and leaving reactor are also recorded.

All incoming steam and water lines penetrating the vapor container are equipped with check valves both inside and outside the container; outgoing lines are equipped with differential pressure valves outside the container to provide seal protection in the event of damage to piping.

B. Pressurizer

The pressurizer is fabricated from carbon steel plate clad with stainless steel. Two 50 KW electric heaters with elements covered by stainless sheath welded to the mounting flange are used.

The pressurizer is designed so as to provide sufficient system pressure, even with the temperature changes accompanying rapid load changes. With a negative temperature coefficient, a sudden drop in load causes a momentary (60-90 sec) rise in system temperature of as much as $16^{\circ}F$, while with increase of load the reverse is true. These temperature changes result in volume changes in the primary coolant, with corresponding fluctuation in level within the pressurizer. With sudden drops in system temperature, the decrease in coolant volume is com-

pensated for by reduction in pressure and flashing into steam of some of the water in the pressurizer. With sudden increases in temperature, however, the system is not so simple in its response.

Evaluation of the capability of the pressurizer to accommodate sudden increases in temperature involves principally the two independent variables of (a) the degree of mixing between the water being expelled from the primary system into the pressurizer and (b) the volume of steam in the pressurizer.

To define these pressurizer design parameters, the system has been analyzed for the pressure-temperature (of primary system) relationship for two sizes of steam dome (25 and 35 cu. ft. respectively) and two conditions of mixing - (1) complete instantaneous mixing and (2) no mixing, i.e., complete stratification. The first condition is closely approximated by a spray in the vapor space, such that water entering into the pressurizer does so only through the spray. The second case is achieved by a diffuser in the entrance passage so that the incoming water is slowed to very low velocity by the time it meets the bulk of the water in the pressurizer.

The results of this analysis are shown in Figure III-5. It will be seen that the pressure variation with sudden drop of temperature is relatively insensitive to vapor volume and can occur only adiabatically, i.e., case (2) above. For increases of temperature, the pressure is quite responsive to vapor volume and is dependent upon the degree of mixing. The two limiting conditions assumed above produce markedly different response. For complete mixing, the pressure drops at first as water enters from the primary system. The temperature of the primary coolant being considerably below the saturation temperature at system pressure of 1200 psi

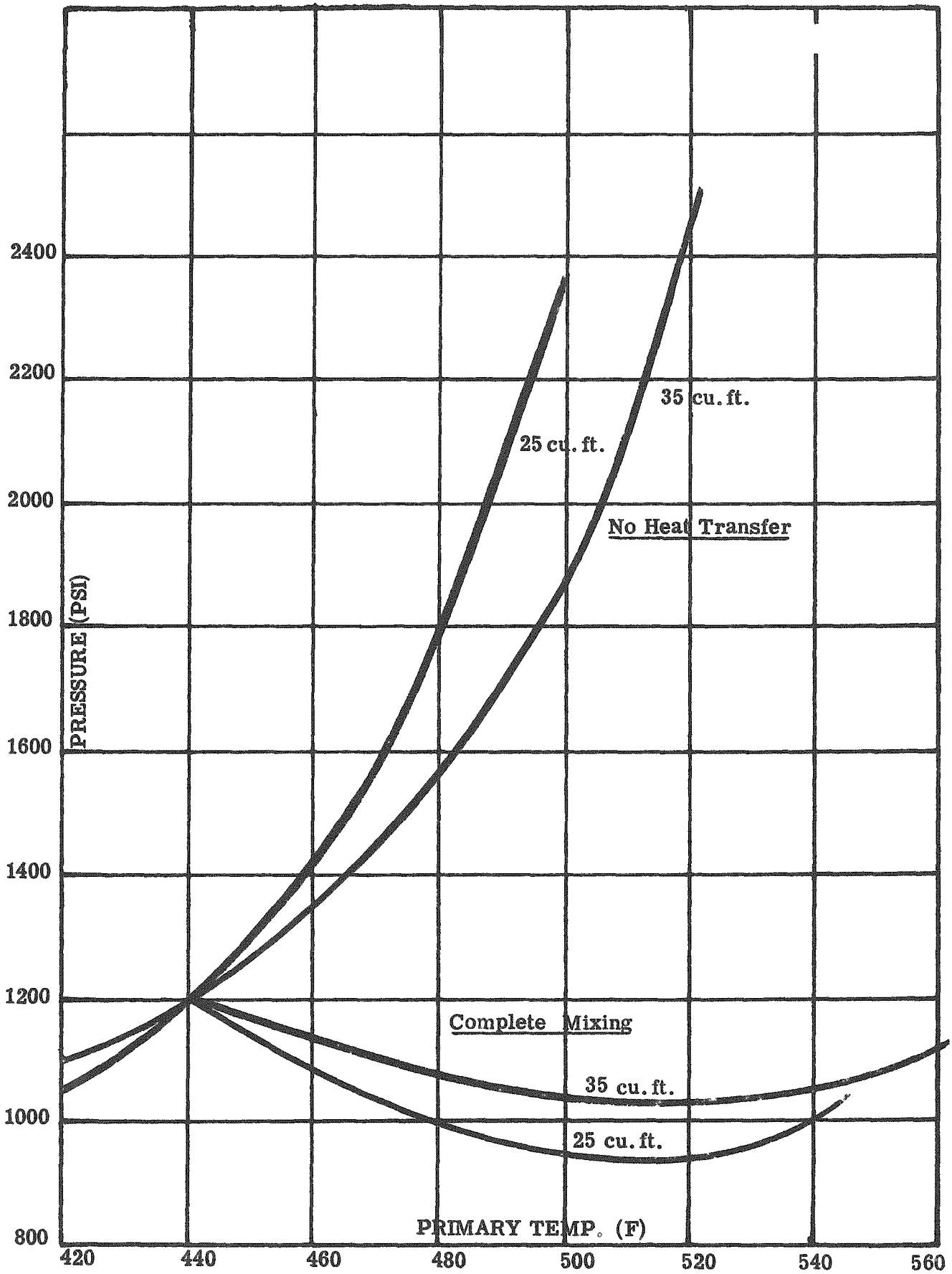

FIG. III-5 PRESSURE VS SYSTEM TEMPERATURE

causes condensation to occur in the steam dome. If the primary system temperature rise continues for a long enough time, the pressure rises again due to the fact that the incoming water is approaching the saturation temperature. With complete stratification of the water, the effect of water expansion from the primary system into the pressurizer is simply compression of the steam in the vapor volume. In a well insulated pressurizer, the heat leakage is trivial in the time interval involved, so that the compression may be considered as adiabatic.

In view of the foregoing, the pressurizer design selected for the APPR-1 is the 25 cu.ft. non-mixing design. It has adequate capacity to absorb fluctuations in temperature due to changes in load, since the maximum temperature change of $16^{\circ}F$ produces a pressure variation of 150 psi or less. The lack of nozzles to achieve mixing simplifies the design (particularly since the spray system implies some kind of orificing or check valve to force water through the nozzle).

C. Primary Make-up and Blowdown

The make-up water for the primary system, as well as the secondary system, is drawn from the service water supply at Fort Belvoir. The water has the following approximate analysis:

	PPM		PPM
SiO_2	10.0	HCO_3	26.0
Fe	9.2	SO_4	27.0
Ca	16.0	Cl	8.5
Mg	1.2	F	0.1
Na	8.1	NO_3	1.0

Total solids approximate 85 PPM

This service water is first treated to produce make-up feed for the secondary system. The controlling impurities are chloride and dissolved oxygen. An evaporator with a deaerating preheater which is very effective in reducing these impurities is used. The condensate contains a maximum of 1 ppm total dissolved solids with a maximum oxygen content of 0.005 cc/liter. The chloride content based on 1 ppm total solids is approximately 0.1 ppm. This treated water for the primary and secondary systems is held in a 5000 gallon stainless steel tank. A portion of this water is pumped through a mixed bed demineralizer and a tray type deaerator then stored in a 1000 gallon stainless steel tank. A filter is installed in this line just upstream of the demineralizer. The effluent from the demineralizer and deaerator will contain less than 0.5 ppm solids and 0.1 ppm oxygen. A solids content not exceeding 2 ppm is maintained by blowdown of the system. This blowdown is 365 pounds per hour. The 1000 gallons of primary water is approximately one day's supply which would be available in emergencies in event of failure in the treatment of the service supply.

This blowdown from the primary system is considered waste. It is placed in a hold-up tank for 24 hours to reduce radioactivity within tolerance limits set for drinking water. After this hold-up it is discharged to the Potomac River by dilution with the condenser cooling water. Both the make-up and blowdown are metered continuously to determine conductivity. Daily chemical analysis of the water will be made until such time as the curves are established. All water that might be radioactive is monitored and must meet proper tolerances prior to final disposition.

Hydrogen gas dissolved in the water at approximately 50 cc/liter is used as the corrosion inhibitor. The hydrogen is introduced into the make-up water line

between the two check valves in the make-up water line penetration through the vapor container. The hydrogen is supplied from 220 cu. ft. bottles. These cylinders can only be used down to a pressure of approximately 1250 psi which utilizes 82 cu. ft. of gas per cylinder. Thus, 32 cylinders of gas are required per year.

D. Secondary System

The feedwater for the steam generator is obtained from the condenser hot well and is circulated by the condensate hot well pump through a closed type feedwater heater which raises the temperature to 250°F. by steam bled from the turbine at approximately 35 psia. A unique three element regulating valve is provided in the feedwater connection to the steam generator. Measurement of both steam and feedwater flow provide anticipatory action on the basic control from the steam generator water level, thus insuring close regulation. Feedwater and steam flow are recorded. An adjustable blowdown into a blowdown tank is provided to maintain proper conditions in the steam generator and the system.

At full load, steam is generated at 200 psia. A superheat of 25 degrees to 407°F. to provide improved steam conditions is obtained by novel design of the steam generator. This steam passes through a pressure control valve set at 250 psi to preclude over-pressure reaching the turbine. Safety valves are provided in the line before and after the pressure reducing valve to protect both the steam generator and turbine from over-pressure.

Temperature and pressure recorders are installed between the steam generator and the control valve and a steam flow recorder is installed between the control valve and the turbine. A stop valve is applied at the turbine throttle.

A 2 inch bypass line for feeding the turbine-driven hot well pump is located

ahead of the pressure control valve. This pump is provided for emergency circulation in the event of electrical failure resulting in stoppage of the electrically-driven pumps. A 2 inch line is located between the pressure reducing valve and the turbine to supply steam to the evaporator and the air ejectors at partial loads. At full load, 35 psig steam will be used for evaporation.

Steam at 190 psia (includes line losses of 10 psi) enters the turbine and is discharged into the deaerating condenser.

At decreasing loads with a primary coolant inlet temperature to the steam generator of 450°F., the temperature on the secondary steam side will approach 450°F. At no load, steam will be generated at 423 psia.

The origin and part of the treatment procedure of the secondary water supply was described in connection with the primary water treatment. The secondary water is continuously degassified in the deaerating type of main condenser to maintain a maximum of 0.01 ppm oxygen in the condensate. Chemical treatment by an amine is used to reduce the free oxygen to practically zero and to increase the pH to 8.5 to reduce corrosion to a very low value.

Continuous blowdown of the secondary at 350 lbs. per hour maintains the water in proper condition. This blowdown leads through a blowdown tank to disposal. The steam leaving the steam generator and the blowdown is monitored continuously for activity as a check on any leakage of the primary water into the secondary system.

The steam generator feedwater pumps are of unique design in order to match the varying steam demands and pressure. At full flow of 75 gpm the head at the discharge nozzle is 596 ft.; at 5 gpm this head is 1116 ft.

E. Auxiliaries

The usual auxiliaries incident to steam power plant operation will be provided.

A chlorinating system to treat the river water supply to be used for condenser circulation, electric generator cooling, bearing oil coolers and vapor container cooling will be installed.

The condenser circulating water pumps will be duplicates of 4500 gpm capacity either of which will provide sufficient cooling water for operation of the plant at 100% capacity.

CHAPTER IV - VAPOR CONTAINER

A. Structure

The vapor container is a combination steel and concrete structure 32 feet inside diameter and 60 feet in height as shown in Figure IV-1. It consists of a 7/8 inch thick steel cylindrical outer shell with spherical ends. Inside this shell are two feet of reinforced concrete to provide stiffness. It also provides a rupture-proof container which will contain missiles that might result from some failure to the high pressure primary system. The interior surface of the concrete is lined with light steel plate to facilitate cleaning and to serve as a form when pouring the concrete. The outer shell is subject to a very small thermal expansion (1/2 inch on the circumference) which permits burial in the ground without resulting difficulties. The outer shell, including access openings, pipe and conduit penetrations, will be completely fabricated, erected and tested prior to installation of concrete and inner lining.

A manhole with a 6.5-foot clear opening is provided in the top of the container through which the major pieces of apparatus are lowered. After the equipment is completely installed, the manhole door, made of 2-1/2 inch steel plate, will be bolted closed and seal welded to insure air tightness. There is a double door access opening at the lower plant floor level, designed for quick access for refueling and maintenance. Both the inner and the outer door, each made of 2-1/2-inch steel, are bolted closed and equipped with special seal gaskets. The space between the inner and outer doors is filled with water which together with the two doors gives the equivalent shield protection provided by the total thickness of five feet of concrete. A water level gauge glass provided with a low water alarm is

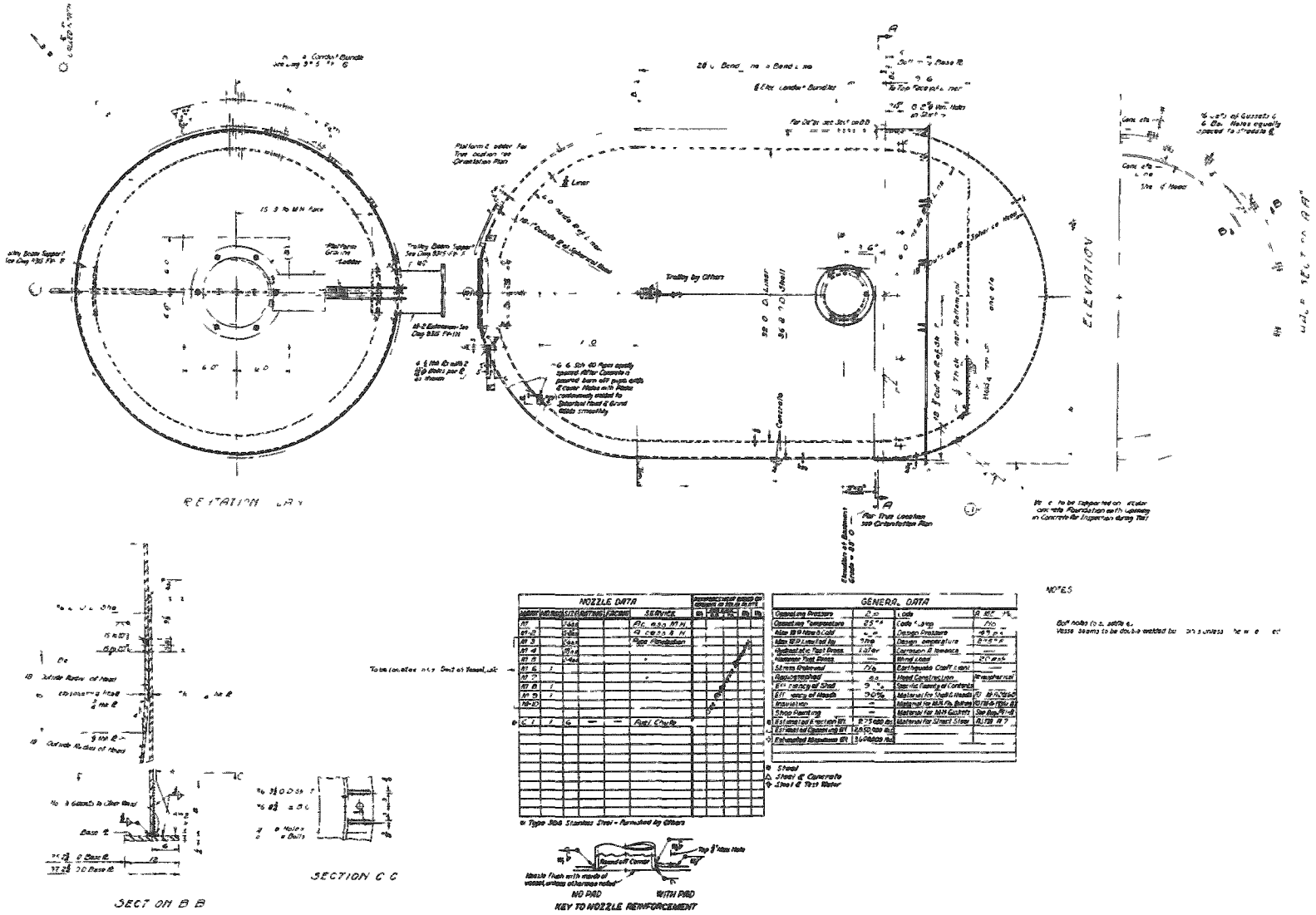

FIG. IV-1 VAPOR CONTAINER

provided. Details of the top access opening and the lower access opening are shown in Figures IV-2 and IV-3.

The construction proposed permits a stable vapor container structure in which equipment can be mounted, and which is not seriously affected by the high temperatures that might occur in the event of a rupture of the primary or secondary systems. There is insufficient heat in the coolant system to raise the temperature of the concrete more than 15°F. Therefore, the temperature of the outer steel shell will not be affected significantly even in case of such rupture.

B. Leak Testing

Prior to the hydrostatic and leakage tests a detergent soap bubble test with air at 15 psig will be made. Any leaks found during this test will be repaired before conducting the hydrostatic tests. The structure will be given hydrostatic-proof test to 75 psig. It will also be given a water leakage test at a pressure of 75 psig, as outlined in Appendix B-1. The leakage is not to exceed 4 cubic feet in 24 hours.

C. Penetrations

Penetration openings for various pipes and wiring conduit are designed to preclude radiation streaming, provide adequate shielding and maintain design stress integrity.

The details of penetrations are shown in Figures IV-4, IV-5 and IV-6.

D. Cooling & Ventilation

It is necessary to provide cooling for the interior of the vapor container at all times when the reactor is in operation. It has been estimated that the heat loss from the equipment is approximately 50,000 BTU per hour when the reactor is running

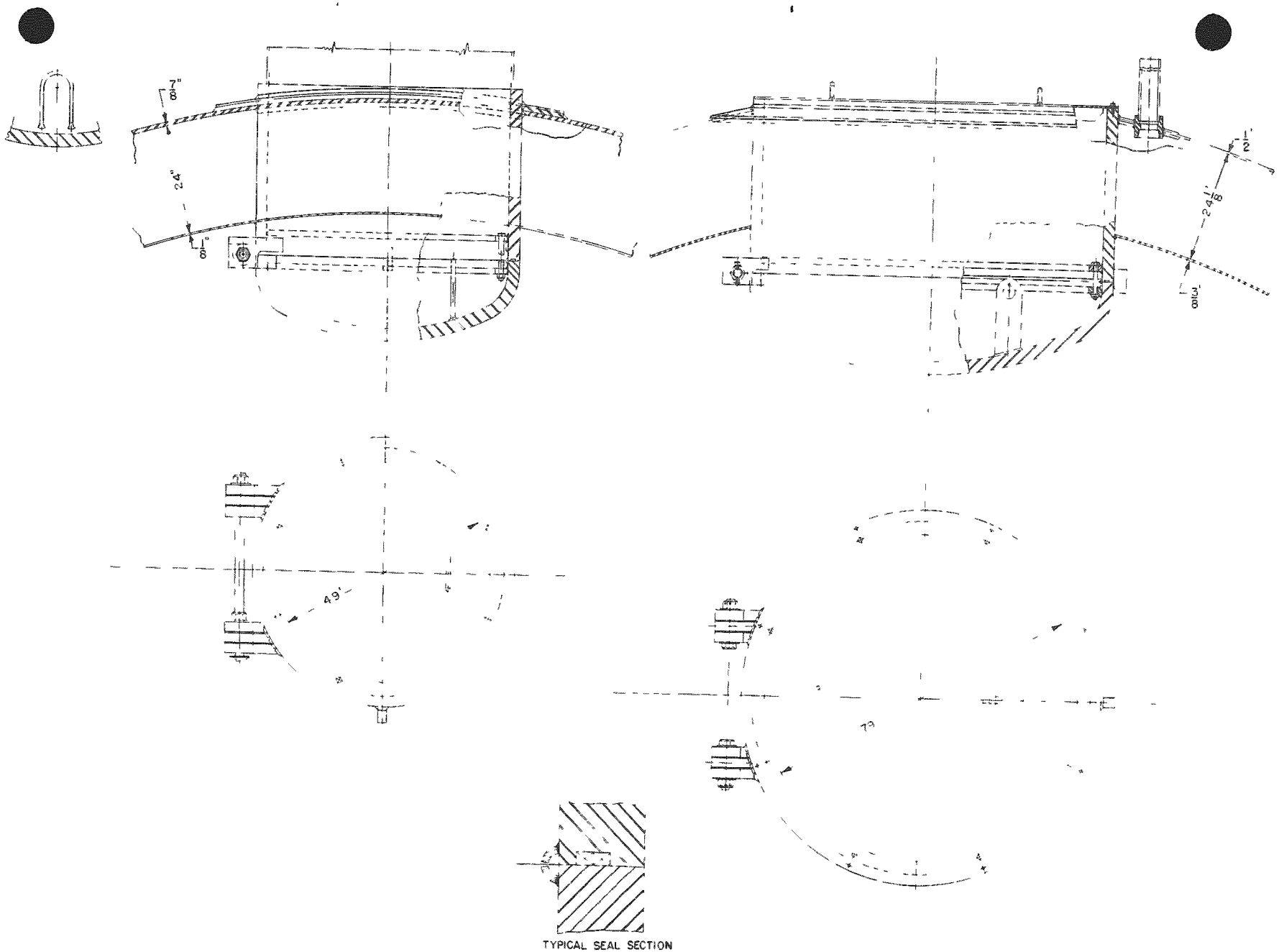

FIG. IV-2 VAPOR CONTAINER MANHOLE DETAILS

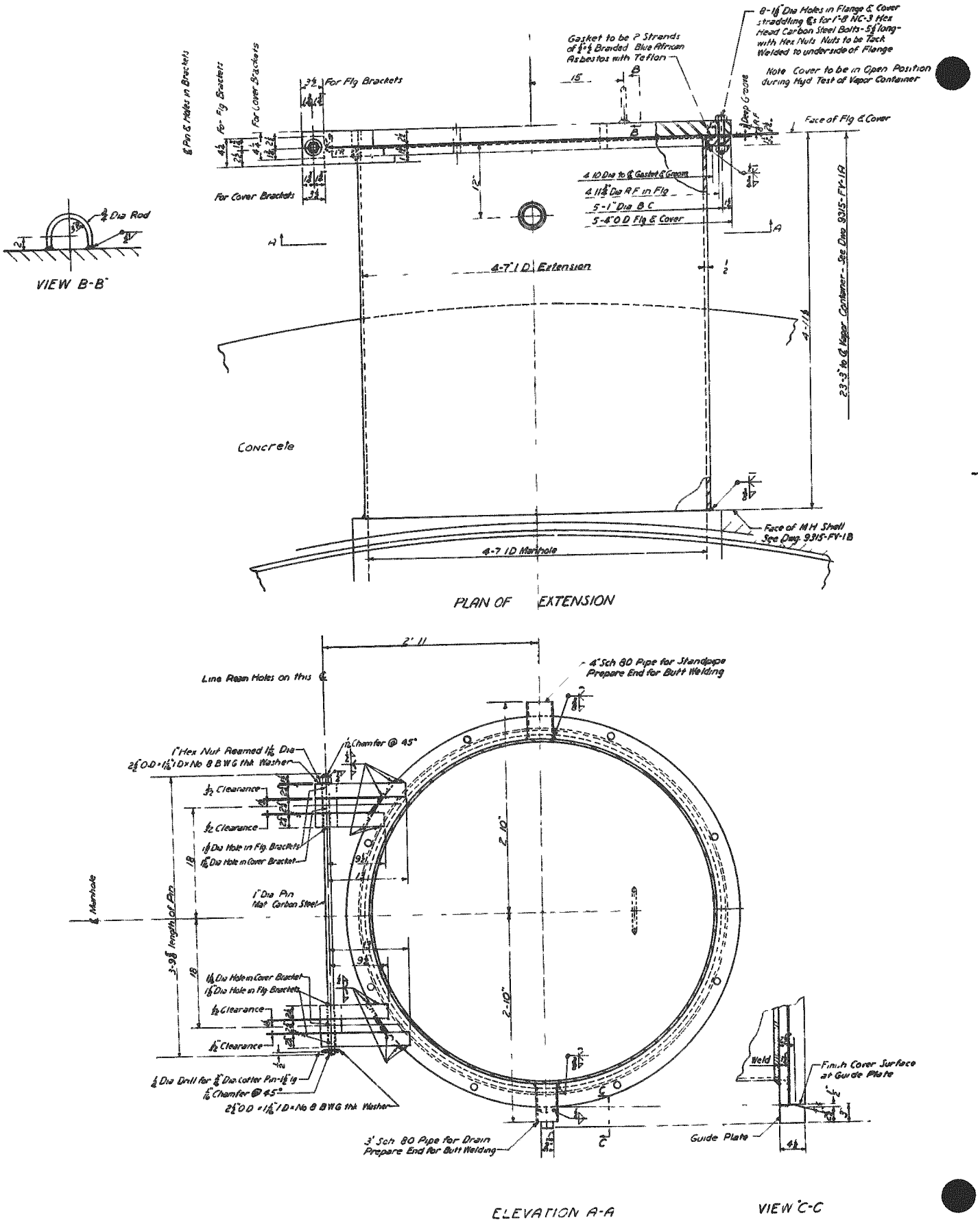

FIG. IV-3 VAPOR CONTAINER BOTTOM MANHOLE EXTENSION

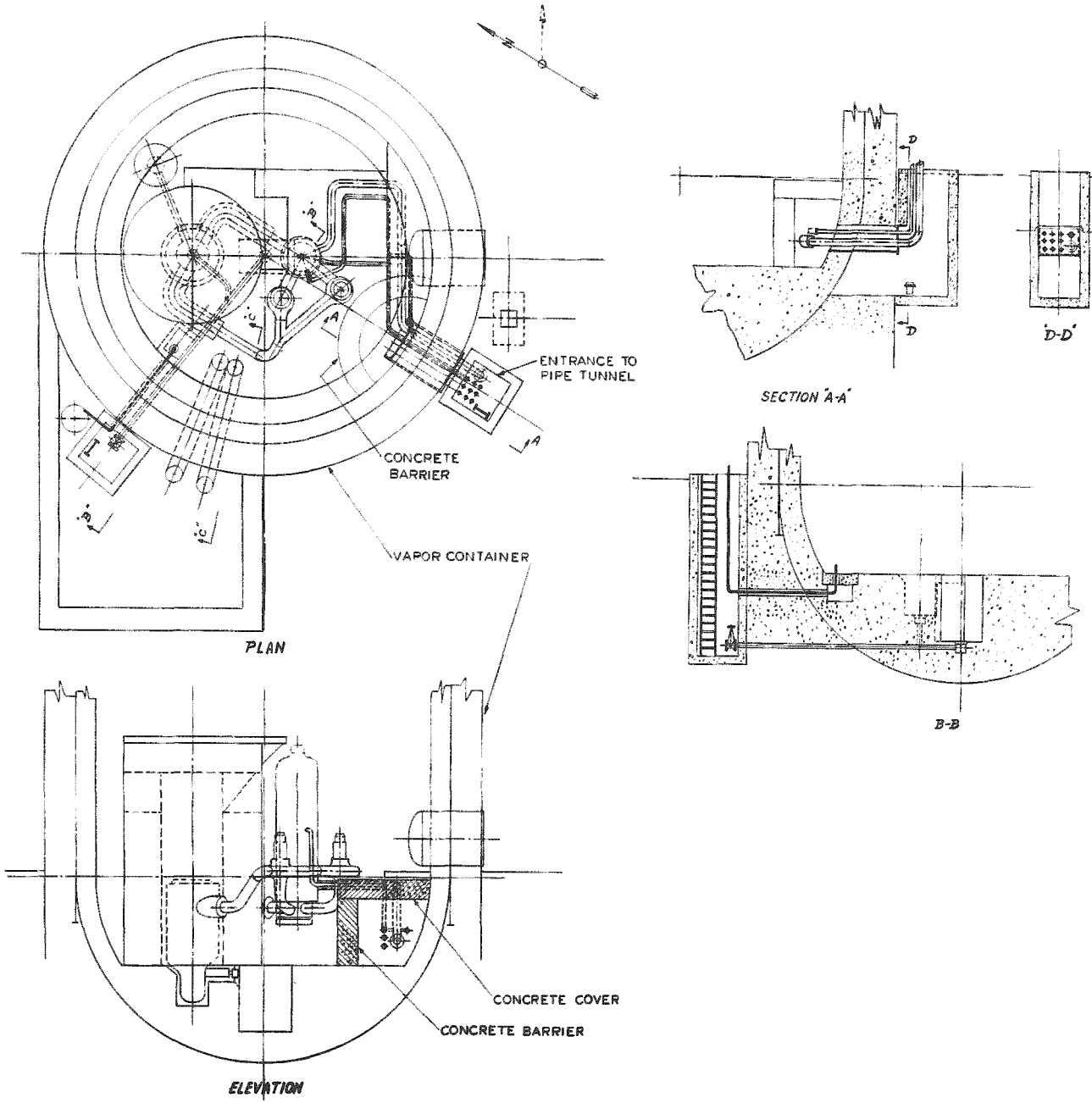

FIG. IV-4 VAPOR CONTAINER STEAM AND WATER LINE PENETRATIONS

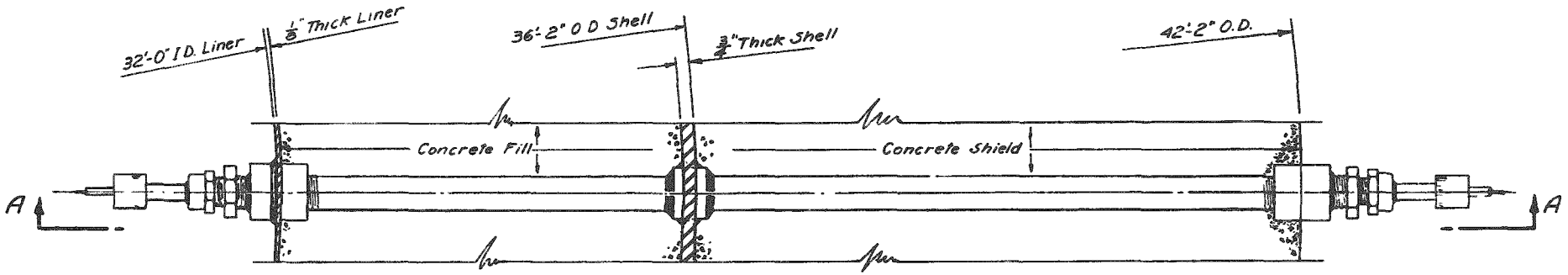

PLAN - TYPICAL ELECTRICAL CONNECTION

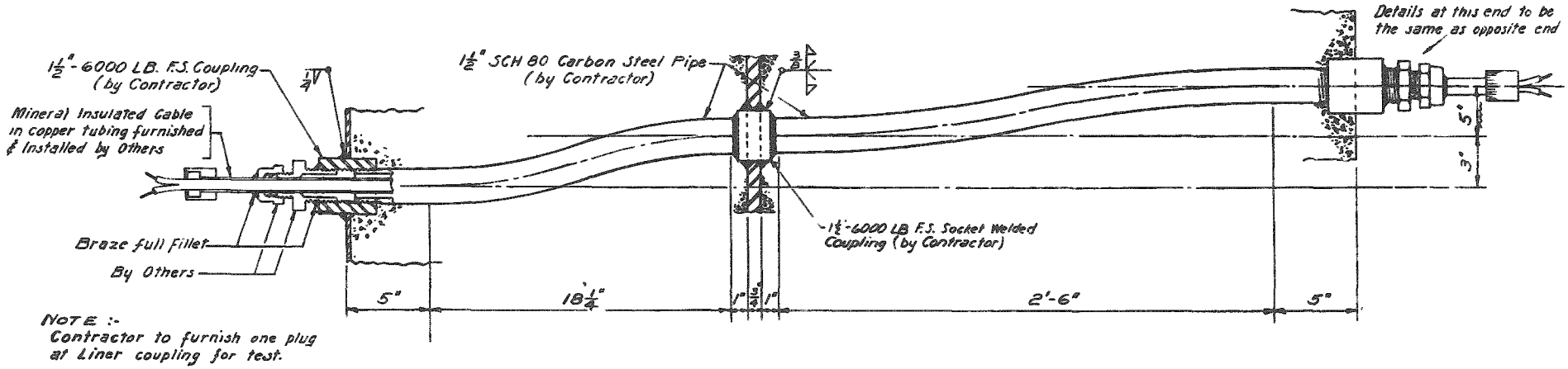

ELEVATION "A-A"

FIG. IV-5 VAPOR CONTAINER CONDUIT PENETRATION

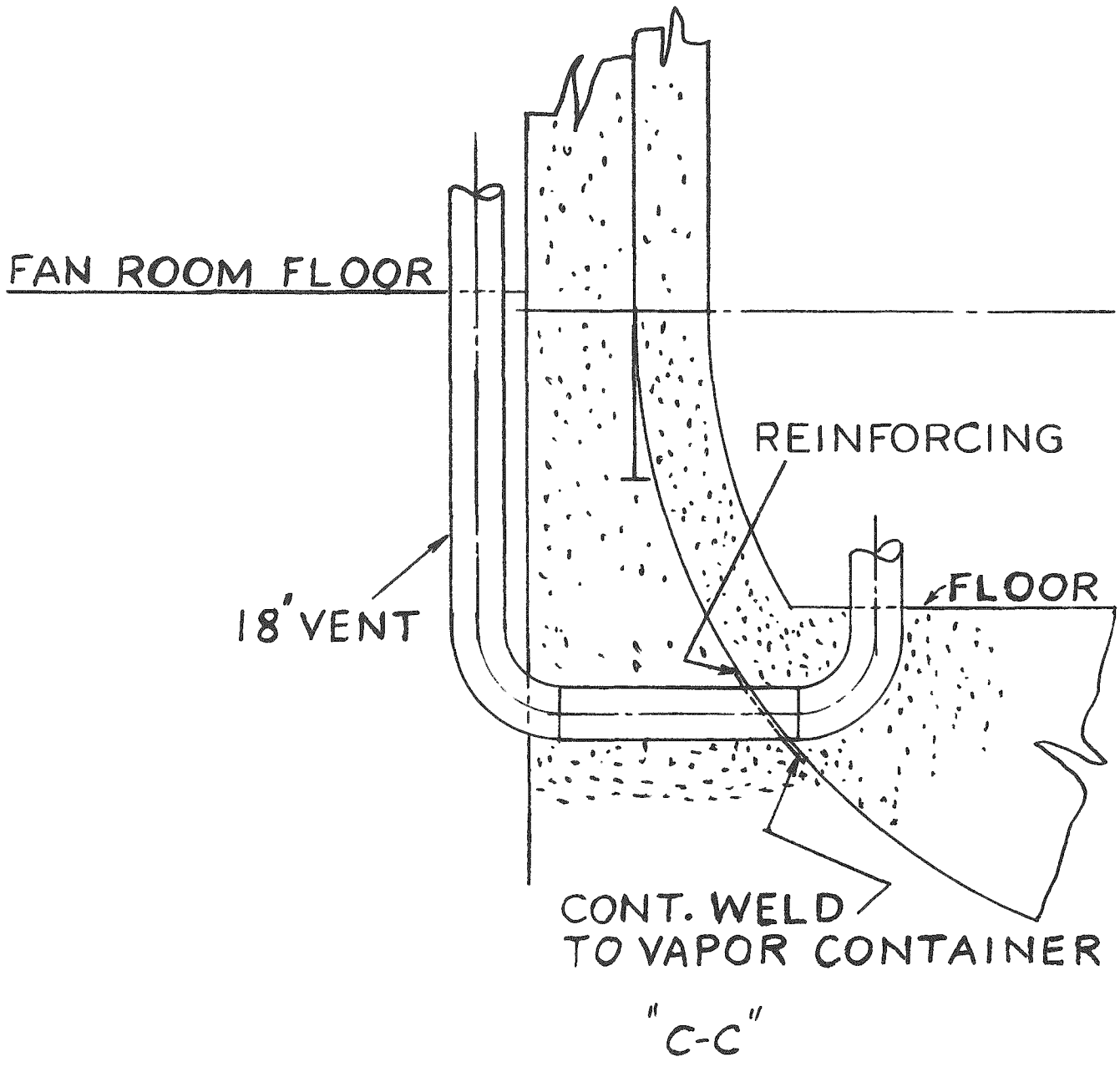

FIG. IV-6 VAPOR CONTAINER AIR DUCT PENETRATION

at full output. Space coolers through which water from Gunston Cove is circulated are provided to maintain temperature within the vapor container at or below 125°F.

A system of spray heads adequately protected from missiles is installed at the top of the container to preclude a secondary pressure rise following a nuclear incident.

The ventilation requirements of the vapor container are such that during any period of occupancy by personnel, the space is ventilated at the rate of six fresh air changes per hour. During reactor operation, the requirement of a leak-tight container governs; consequently, the container is sealed without ventilation. This arrangement obviates the need for normally open ventilation ducts, which must be closed leak-tight in the event of an accident.

The ventilation and decontamination equipment is housed in a concrete building adjacent to the vapor container. The equipment consists of a motor-driven fan of approximately 4000 cfm capacity, suitable air filters, and a set of chemical warfare filters. Air is withdrawn from the top of the vapor container and discharged through the filters back into the container until the air has been decontaminated sufficiently to permit opening the access door. Thereafter the air from the container is discharged to a stack extending approximately 75 feet above the yard level.

The air connections through the vapor container wall consist of steel piping with 150 lb. steel double-disc gate valves. When the reactor is in operation, these valves are kept closed and sealed with water between the discs. The valves are not to be opened until the reactor is completely shut down.

E. Missile Protection

A careful study of missile penetration of the container structure was made

in cooperation with the Department of Docks, U.S. Navy, at Boston, and the Army Ordnance at Aberdeen Proving Grounds. A variety of missiles of various sizes, shapes, and masses were calculated as shown in Appendix B-2.

Missile protection for the body of the vapor container is provided by the two feet of concrete between the inner and outer shells. Protection for the steam and water lines, and the ventilation duct is shown in the detail design of these features referred to previously. The top and lower access openings have inner doors constructed of 2-1/2-inch thick steel to provide the required protection.

All piping carrying incoming fluids are equipped with check valves, both inside and outside the vapor container, to preclude escape of activity to the outside of the container. All piping carrying outgoing fluids are equipped with pressure-actuated valves outside the vapor container which will close in the event the pressure in the vapor container rises to 5 psi above atmospheric pressure.

F. Spent Fuel Pit

A pit for the storage of spent fuel is provided immediately outside of the vapor container as shown in Figure IV-7. It is approximately 28 ft. deep and is lined with white tile. Illumination is provided to facilitate storage of the fuel elements in a lattice of cadmium plated steel at the base of the pit. The cadmium prevents neutron multiplication even with fuel elements at the peak of their reactivity. A steel cover with a lock is provided for the spent fuel pit, with a movable walkway permitting the operator to change his position while storing the fuel elements. Fuel elements are transferred to the storage pit from the reactor vessel through a submerged tube, Figure IV-8. A fuel element may be moved from the reactor vessel to the discharge chute with a minimum of 9.5 feet of water above the element, which

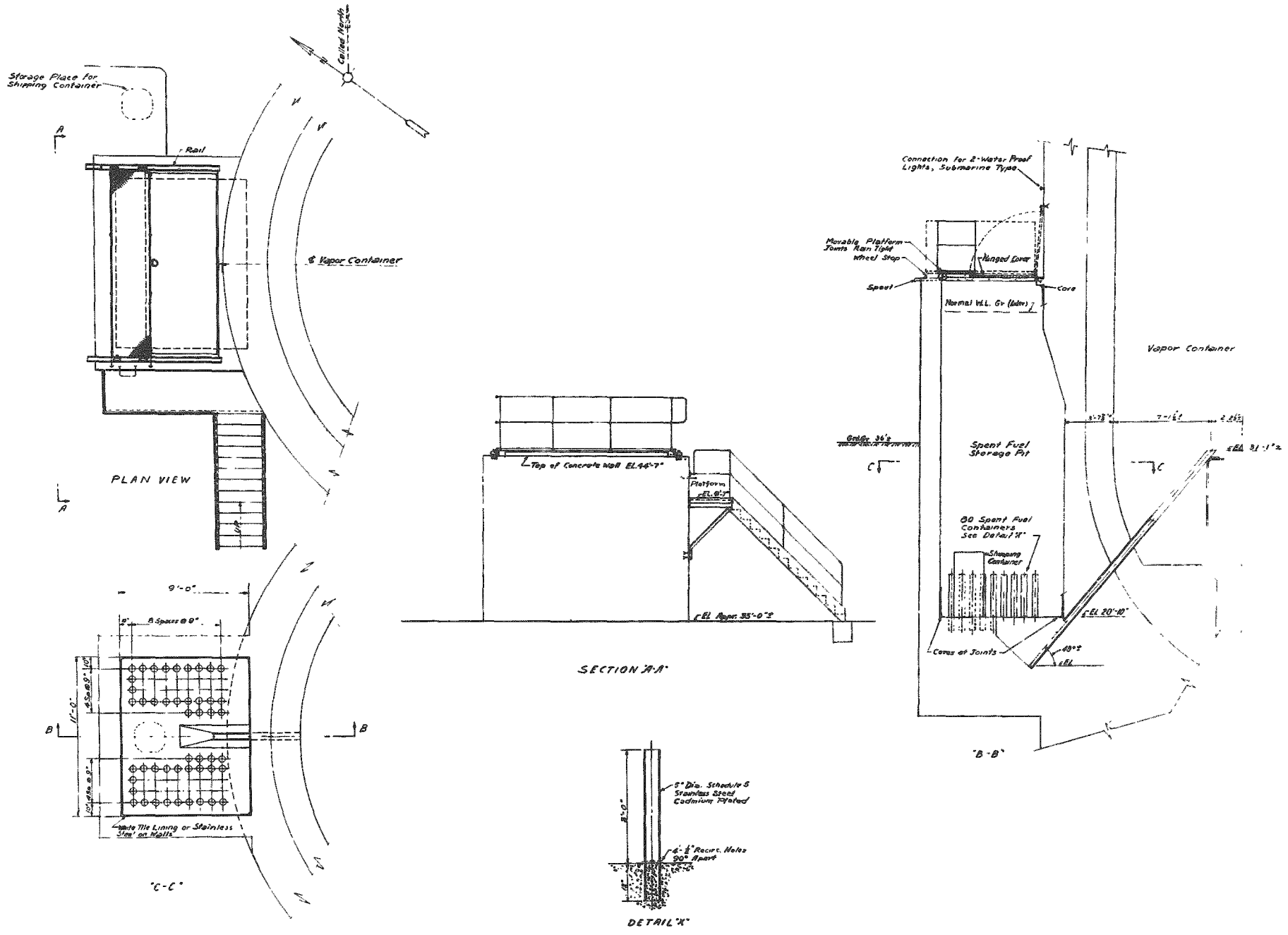

FIG. IV-7 SPENT FUEL STORAGE PIT

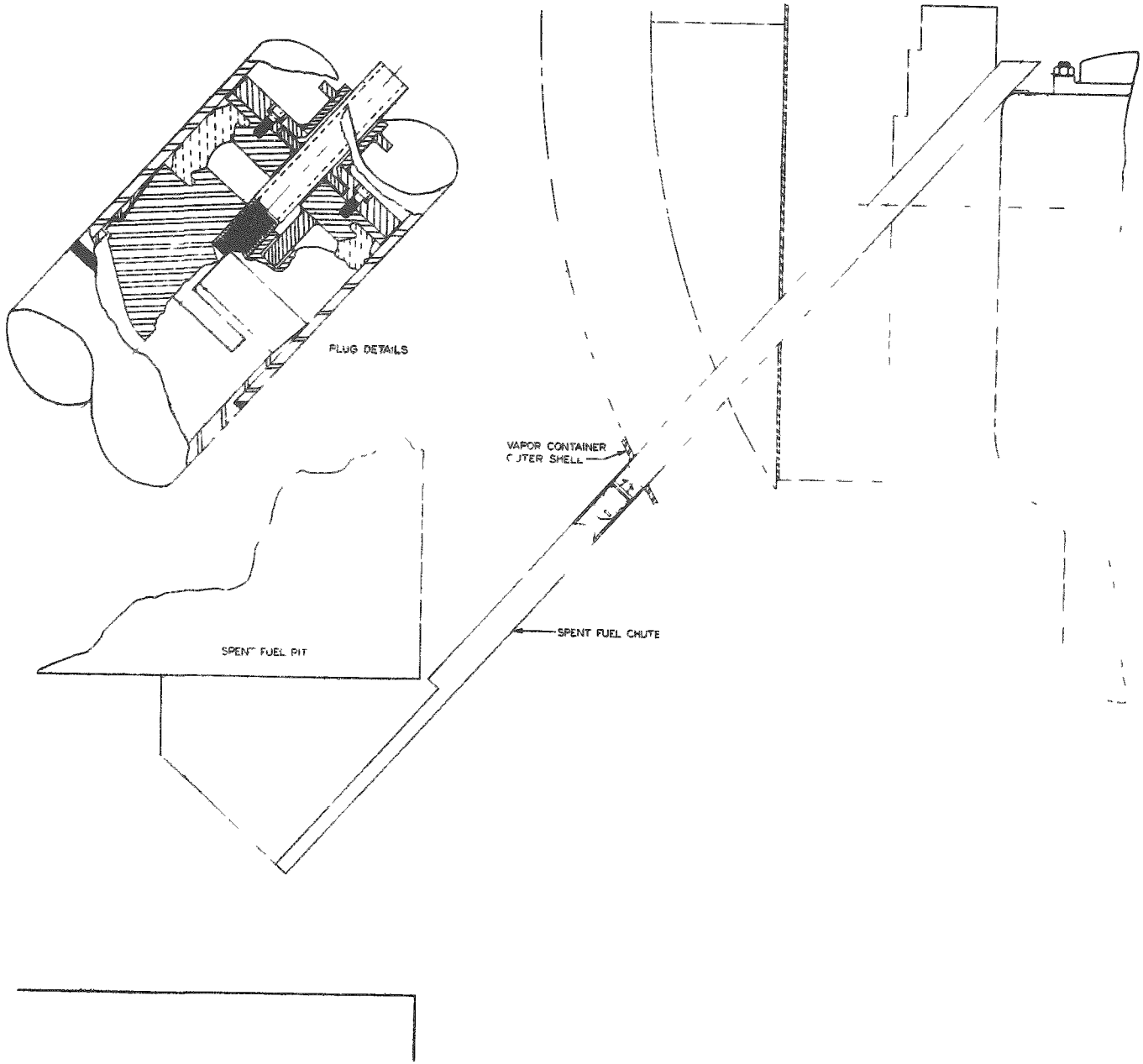

FIG. IV-8 FUEL DISCHARGE TUBE AND PLUG VALVE

provides shielding for the operator during the transfer process.

Since the pit remains full of water at all times, a simple but effective plug valve, shown in Figure IV-8, has been designed for the fuel discharge chute. This valve consists of a two-piece metal plug with a molded rubber compression type sealing element between. The plug is inserted through the top of the spent fuel chute by means of a long-handled tool. Lug members on the plug engage slots in the inner wall of the tube in such a manner that they provide a reaction point to prevent rotation of the plug while the two halves are being drawn toward each other. This is accomplished by means of a threaded member connecting the two halves of the plug and turned by means of the inserting tool. Clamping the two halves together compresses the rubber member between them, thus forming a seal to the tube wall. Removal of the plug is simply the reverse of inserting it. The threaded member is unscrewed, releasing the rubber sealing member and permitting the plug to be turned out of the locating slots and withdrawn.

In the event of build-up of pressure inside the vapor container or if the shield is drained while the spent fuel pit remains filled with water, a pressure difference will exist across the plug valve. The axial force on the valve, resulting from this pressure difference is carried by means of the lugs and slots referred to in the previous paragraph. The structural strength of these members is more than ample to carry the load resulting from the maximum pressure which can possibly exist in the vapor container. The plug valve is physically located outside the pressure containing wall of the vapor container in order to assure pressure integrity in case of mechanical damage to the tube on the inside of the vapor container.

The fuel tube is made of corrosion resistant steel and the plug parts themselves are protected against corrosion.

CHAPTER V - SHIELDING

A. General Considerations

In designing the APPR-1 shielding the objective has been to provide sufficient shielding to meet the accepted practices throughout the Atomic Energy Commission program for radiation levels for operating personnel. Under normal operating conditions, levels for personnel continuously exposed during working hours are restricted to a fraction of the accepted permissible level of 300 mr per week. In certain areas, however, above-tolerance levels are permitted where infrequent access is required for periods of controlled short duration. Taking advantage of this fact permits somewhat greater flexibility of design and operation but at no expense in terms of increased hazards to the operating personnel.

While it is desired to achieve as much of a prototype in the shield design as it is possible to do, one basic compromise was introduced by the desire to locate the facility at Fort Belvoir. In a location such as Fort Belvoir, it is necessary to provide a facility which can be approached at any time and from any angle without being unwittingly exposed to excessive radiation levels. Thus the radiation existing at any point around the building is no higher than the permissible continuous exposure level. This not only makes it possible for modifications to the facility to be considered at a later date with impunity, but it also renders unneeessary a close policing of visitors to prevent them from wandering into areas where radiation exposure may be of some consequence.

A primary shield is provided around the reactor pressure vessel which reduces the gamma rays from the core to a level comparable to the intensity of those gammas arising in the activated water external to the shield. This primary shield

also provides the necessary attenuation for capture gamma rays and reduces the neutron level to a point where no significant activation of the equipment outside the shield occurs.

The dose rate within the vapor container wall is about 20 r/hr which dose is comprised of approximately equal contributions from the core and the primary water outside of the core. Besides the two feet of concrete in the walls of the vapor container, there are three additional feet of concrete as high as the ceiling of the control room. The secondary shield provided by this five feet of concrete brings the dose rate down to two-tenths tolerance in the control room.

The principal source of gamma rays in the primary water is from the O^{16} (n, p) N^{16} reaction. Since the half life of N^{16} is only seven seconds, access may be had to the vapor container within a reasonable period of time after shut down. The shutdown activity in the primary coolant water arises from activated impurities in the system, which result from pick-up of corrosion product ions and impurities in the make-up water.

The calculations of the shield described in the following sections is reported in Reference 3.

B. Secondary Shield

The secondary shield is described in Table V-1. It was designed such that radiation from the primary coolant would give not more than one-tenth of laboratory tolerance for a 40 hour week at any point outside the vapor container up to the full height of the power plant building. The dose rate at a position outside the vapor container due to the important primary coolant components is indicated in Table V-2. Small volumes of primary coolant, such as in the pump, are conservatively

Table V-1
SECONDARY SHIELDING

Description	Material	Outer Radius Inches	Thickness Inches
Vapor Container Lining	Steel	204.1	0.1
Vapor Container Structure	Concrete	224.1	24.0
Vapor Container Wall	Steel	225.0	0.9
Secondary Shield *	Concrete	261.0	36.0

* - To a height of 27 ft. above ground level.

Table V-2
DOSE RATE OUTSIDE VAPOR CONTAINER FROM PRIMARY COOLANT ACTIVITY DURING REACTOR OPERATION

Source	Diameter Inches	Length Inches	Distance from Center to Outside of Shield Near Control Room Feet
Piping	11	144	18
Steam Generator Bundle	44	144	22
Steam Generator Channel	33	18	22

Source	Gamma Flux Outside Shield Photons/Cm^2-Sec.	Gamma Dose Rate Outside Shield Mr/hr
Piping	40	0.31
Steam Generator Bundle	43	0.33
Steam Generator Channel	16	0.12
Total	99	0.76

assumed in the 12-feet of primary piping.

The dose rate just above the spent fuel pit from sources inside the vapor container will be greater than two-tenths tolerance, but it will not exceed tolerance during reactor operation.

Penetrations of the secondary shield by the steam line and several smaller lines are shielded by placing sufficient material around the openings to compensate for the concrete removed. The steam line is oriented so as not to be in a direct line with any major radiation source.

The neutron source from the decay of nitrogen-17 produced by the $O^{17}(n,p)N^{17}$ reaction is lower by several orders of magnitude than the gamma source from nitrogen-16. These neutrons are readily attenuated to a negligible dose by the 5 feet of concrete.

C. Primary Shield

The structural details of the primary shield are described in Chapter II-D. Tables V-3 and V-4 indicate the shielding materials available from the core to the outside of the primary shield in the horizontal and vertical directions, respectively. The primary shield is designed such that the dose rate outside the primary shield due to the reactor is approximately the same as from the primary coolant.

The dose rate with the reactor operating at 10 megawatts, from neutrons and gammas at various points in the radial and top shield are given in Tables V-5 and V-6. The dose from thermal neutrons outside a concrete shield is always much less than the fast neutron dose. The control room, the point for which data is given, is the nearest normally occupied location to the reactor.

The shield was calculated by comparison with Lid Tank and Bulk Shield Reactor experimental data. The BSR spectrum was corrected for the harder gamma

Table V-3
DESCRIPTION OF REACTOR SHIELD - RADIAL

Description	Material	Outer Radius Inches	Thickness Inches
Core	-	11.1	-
Reflector	Primary Water	17.5	6.4
Thermal Shield	Stainless Steel (1)	19.5	2.0
Inlet Passage	Primary Water	24.0	4.5
Pressure Vessel	Steel	26.5	2.5
Insulation	Glass Wool(2)	30.2	4.0
Insulation Cladding	Steel	30.6	0.4
Clearance Space	Void	32.0	1.4
Vessel Support and Shield Tank Wall	Steel	34.0	2.0(3)
1st Cooling Passage	Shield Water	35.0	1.0
1st Shield Ring	Steel	37.0	2.0(3)
2nd Cooling Passage	Shield Water	38.0	1.0
2nd Shield Ring	Steel	40.0	2.0(3)
3rd Cooling Passage	Shield Water	41.0	1.0
3rd Shield Ring	Steel	43.0	2.0(3)
4th Cooling Passage	Shield Water	44.0	1.0
4th Shield Ring	Steel	46.0	2.0(3)
5th Cooling Passage	Shield Water	47.0	1.0
5th Shield Ring	Steel	49.0	2.0(3)
6th Cooling Passage	Shield Water	50.0	1.0
6th Shield Ring	Steel	52.0	2.0(3)

Table V-3 (Cont.)

Description	Material	Outer Radius Inches	Thickness Inches
7th Cooling Passage	Shield Water	53.0	1.0
7th Shield Ring	Steel	55.0	2.0(3)
Neutron Shield	Shield Water	80.0	25.0
Shield Tank Outer Wall	Steel	80.4	0.4

(1) Considered as steel for shielding purposes.

(2) Considered as void for shielding purposes.

(3) Computed at 14.3 in. for the 8 - 2 in. layers.

Table V-4
DESCRIPTION OF REACTOR SHIELD - VERTICAL

Description	Material	Distance from Center of Core To Outer Surface Inches	Thickness Inches
Core	-	11.1	-
Reflector	Primary Water	12.6	1.5
Support Plate	Stainless Steel, Water (1)	14.6	2.0
Header	Primary Water	51.0	36.4
Pressure Vessel Cover	Steel	53.5	2.5
Insulation	Glass Wool(2)	57.2	4.0
Insulation Cladding	Steel	57.6	0.4
Clearance Space	Shield Water	62.0	4.4
Gamma Shield	Steel	64.0	2.0
Neutron and Gamma Shield	Shield Water	164.0	100.0

(1) Since the support plate has holes for coolant water passage, the plate is considered as water for shielding purposes.

(2) Considered as void for shielding purposes.

Table V-5

DOSE RATE FROM REACTOR DURING FULL POWER OPERATION - RADIAL

Location	Gamma Dose Rate Mr/hr	Fast Neutron Dose Rate Mrep/hr
Reactor Surface	2.2×10^{12}	1.8×10^{11}
Outside Shield Tank	6.2×10^{4}	2.6×10^{1}
Inside Vapor Container	9.8×10^{3}	4.1
Outside Vapor Container	0.75	4.6×10^{-6}
One-Tenth Tolerance	0.75	7.5×10^{-2}

Table V-6

DOSE RATE FROM REACTOR DURING FULL POWER OPERATION - VERTICAL

Location	Gamma Dose Rate Mr/hr	Fast Neutron Dose Rate Mrep/hr
Reactor Surface	2.2×10^{12}	1.8×10^{11}
Above Water	4.5×10^{4}	7.1×10^{-2}
Inside Vapor Container	4.4×10^{3}	7.0×10^{-3}
Outside Vapor Container	75	2.8×10^{-5}
10 times Tolerance	75	7.5

radiation anticipated from the APPR-1 core. The attenuation through water was obtained directly from BSR data. The effectiveness of the iron in reducing gammas and fast neutrons was determined from Shield Test Facility data for iron-water shield. The iron in the experimental set-up was closer to the source plate than the thermal shield is to the APPR-1 core, which assures that the secondary gammas are treated on a conservative basis. The attenuation through the secondary shield is calculated by simple exponential attenuation of the flux at the inside of the concrete. A relaxation length characteristic of 7-Mev gammas is used for the gamma flux, as it is indicated that the predominant gammas penetrating to the outside of the shield are hard.

The above calculations have been supported by further calculations described in reference 3.

The inlet and outlet lines are surrounded by 4 inch annuli containing insulation, which offers low resistance to gamma penetration. Although neither pipe is in direct line with the core, a considerable amount of scattered radiation and a significant quantity of direct radiation can escape through the annuli. To prevent this streaming, blocks of steel as shown on Drawing II-1 are added. These rings effectively stop open paths in all directions.

D. Shielding After Shutdown

The gamma dose outside the primary shield has been calculated for various times after shutdown following continuous operation at full power for the various periods specified. The results are shown in Table V-7. The dose which can be expected in case the shield tank water has been lost is also listed.

The core is assumed to have a uniform volume source strength. A linear

Table V-7

DOSE RATE OUTSIDE RADIAL PRIMARY SHIELD FROM FISSION PRODUCT ACTIVITY

	Time After Shutdown Hours	Dose Rate Mr/hr		
		Infinite Operation	1000 Hrs. Operation	100 Hrs Operation
Regular Shield	5	1.4	0.9	0.4
	12	1.2	0.7	0.3
	24	1.0	0.6	0.2
No Water In Shield	5	111	76	33
	12	98	63	24
	24	84	54	15

Table V-8

DOSE RATE EXPECTED ADJACENT TO STEAM GENERATOR OR PIPING AFTER SHUTDOWN FROM CONTINUOUS OPERATION

Time After Shutdown Hours	Gamma Flux Mev/Cm^2-Sec.	Dose Rate Mr/hr
0.1	62	91
1	56	82
12	28	40
24	15	22
48	5.1	7.4

buildup factor has been used as being conservative, but reasonably correct for the low energy of fission product gammas.

The activity level outside various parts of the primary coolant system for selected times after shutdown is shown in Table V-8.

E. Shielding During Spent Fuel Element Transfer and Storage

Spent fuel elements must be shielded during removal from the core, transfer to the spent fuel element storage pit, and storage in the pit.

Table V-9 indicates the dose rate expected from one used fuel element 24 hours after shutdown from 1000 hours of continuous operation, with various thicknesses of water shielding. It is expected that the most active fuel element would have an activity twice the average activity.

Concrete shielding surrounds the fuel element transfer tube. Thirty-six inches of concrete will reduce the dose to 134 mr/hr at the fuel handling position while the fuel element is in the transfer tube.

The water level in the spent fuel storage pit must be the same as in the top shield tank when the transfer tube is open. Thus when the water level in the top shield tank is lowered prior to starting up after changing fuel elements, the water level in the outside pit will be lower also. However, this leaves more than 16 feet of water above the fuel elements in the storage pit. This is completely adequate, as Table V-9 indicates.

Table V-9
DOSE RATE ABOVE WATER FOR A USED FUEL ELEMENT

The fuel element is removed 24 hours after shutdown from infinite operation. The fuel element is assumed to have twice the fission product activity of an average element. The thickness of water is measured to the nearest point of the active core section.

Thickness of Water Feet	Dose Rate Mr/hr
8	270
9	57
10	12
11	2.7
12	0.62

CHAPTER VI - OPERATION & CONTROL

A. Control Features

Because of its strong negative temperature coefficient, the APPR-1 will be a very stable reactor while operating at power. The instrumentation and controls have been designed so as to take full advantage of this inherent stability. With the temperature coefficient being at least -2×10^{-4} per degree Fahrenheit, no additional control mechanism is needed to override rapid transients or power excursions.

A study of such transients has been made on the ORNL Reactor Control Computer and the results are included in Appendix C. The response of reactor power, average fuel temperature, and average coolant temperature following a reduction in power demand from full load to one-fourth load (and also to half load) is shown in Figs. 30 and 31 of Appendix C. In the same figures are shown the response on a sudden demand for full power from these reduced power levels. Only small changes in fuel and coolant temperatures take place.

The APPR-1 incorporates burnout poisoning in the form of boron intimately mixed with the uranium in the fuel plates. Because the boron-10 burns out more rapidly than the uranium, the reactor reaches an excess multiplication of about 7% at operating temperatures and an excess of 16% at room temperature. This phenomenon is explored in more detail in the next chapter. The changes in multiplication over the lifetime of the core will be very slow and will be manifested by a gradual increase in reactor temperature during the first half of the cycle and a similar decrease toward the end. Also, over a period of hours after startup there will be a slow decrease in reactor temperature because of

xenon poisoning. The operator will insert or withdraw the rods to compensate for these changes in operating temperature.

The rods are designed for a total of 25% excess multiplication. The control rod worth as a function of reactor lifetime is being checked by extensive calculations and by critical experiments. During operation of the reactor, the rod positions will be watched closely. If at any time it becomes apparent that more than the anticipated reactivity is appearing, the reactor will be shut down and fuel elements will be removed and replaced by dummy elements.

B. General Description of Instrumentation & Controls

The general arrangement of the instrumentation and controls in the control room is shown in Figure VI-1 and a block diagram of the control and safety circuits is given in Figure VI-2. The three safety chambers will be set to drop the rods at 150% of design power, and the period meter will cause a scram if the reactor period becomes less than three seconds. Details of the operation of the nuclear instrumentations are given in Appendix D. The circuitry is extremely fast and the rods will start to drop in about 60 milliseconds. (See Figure II-5). The rods will drop with an acceleration of about 3/4 g (24 feet per second per second), and 120 milliseconds after the drop starts, 2.0% of negative reactivity will have been introduced.

In addition to the nuclear safety circuits, there will be certain limits in the sensing elements in the primary loop which will initiate a scram.

The design flow rate in the primary loop is 4000 gpm and if this flow drops to 60% while the reactor is at power, a scram is initiated. Below 100

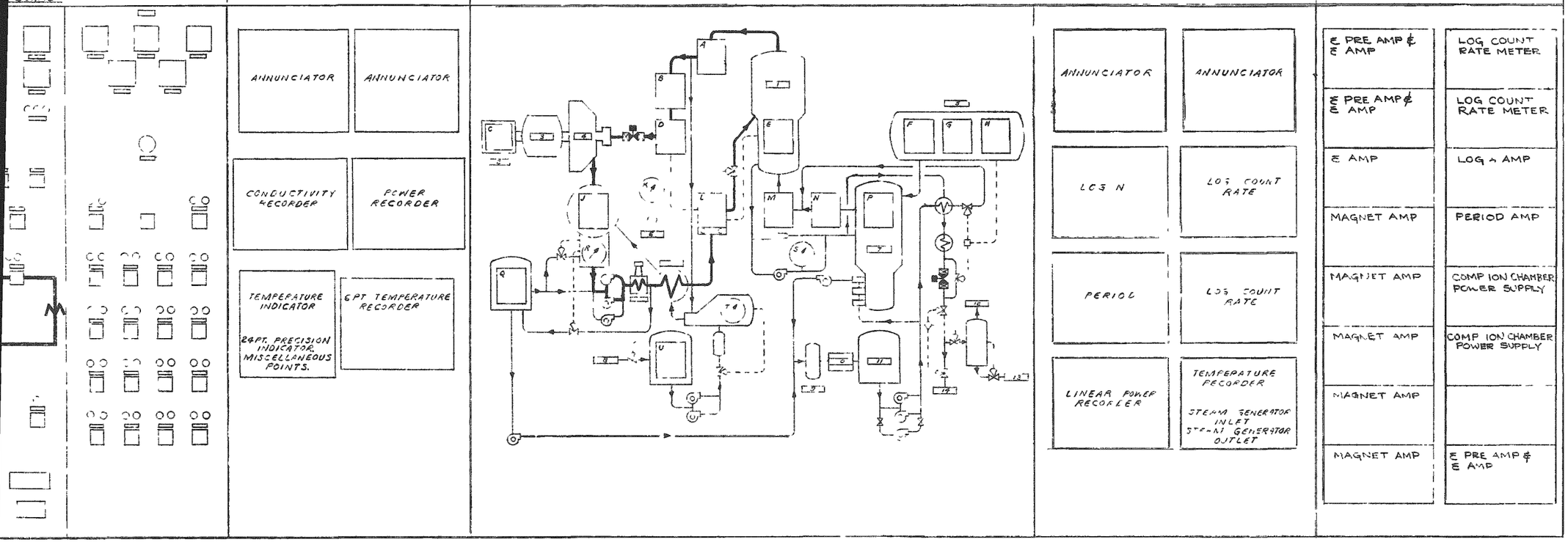

FRONT VIEW OF PANEL
SCALE 3/8" = 1"

EQUIPMENT LEGEND FOR GRAPHIC PANEL

A - STEAM PRESSURE RECORDER
B - STEAM TEMP. RECORDER
C - EXCITER VOLTMETER
D - STEAM FLOW RECORDER
E - STEAM GENERATOR LEVEL CONTROLLER RECORDER
F - PRESSURIZER TEMPERATURE CONTROLLER RECORDER
G - PRESSURIZER PRESSURE CONTROLLER RECORDER
H - PRESSURIZER LEVEL CONTROLLER RECORDER
J - CONDENSER PRESSURE RECORDER
K - RATIO INDICATOR
L - FLOW CONTROLLER RECORDER
M - FLOW RECORDER
N - PRESSURE RECORDER
P - Δ TEMP. RECORDER
Q - DISTILLED WATER LEVEL RECORDER
R - CONDENSER LEVEL INDICATOR
S - DEAD LEG TEMPERATURE INDICATOR
T - EVAPORATOR LEVEL INDICATOR
U - FILTERED WATER LEVEL CONTROLLER RECORDER

NAMEPLATE LEGEND FOR GRAPHIC PANEL :

1 - STEAM GENERATOR
2 - EXCITER
3 - GENERATOR
4 - TURBINE
5 - PRESSURIZER
6 - FEEDWATER RATIO
7 - PRESSURE VESSEL
8 - SERVICE WATER SUPPLY
9 - DEGASSIFIER
10 - FILTER
11 - MAKE UP TANK
12 - VENT TO STACK
13 - TO WASTE
14 - HOT WASTE STORAGE TANK

FIG. VI-1 GENERAL ARRANGEMENT OF CONTROL & INSTRUMENT PANEL

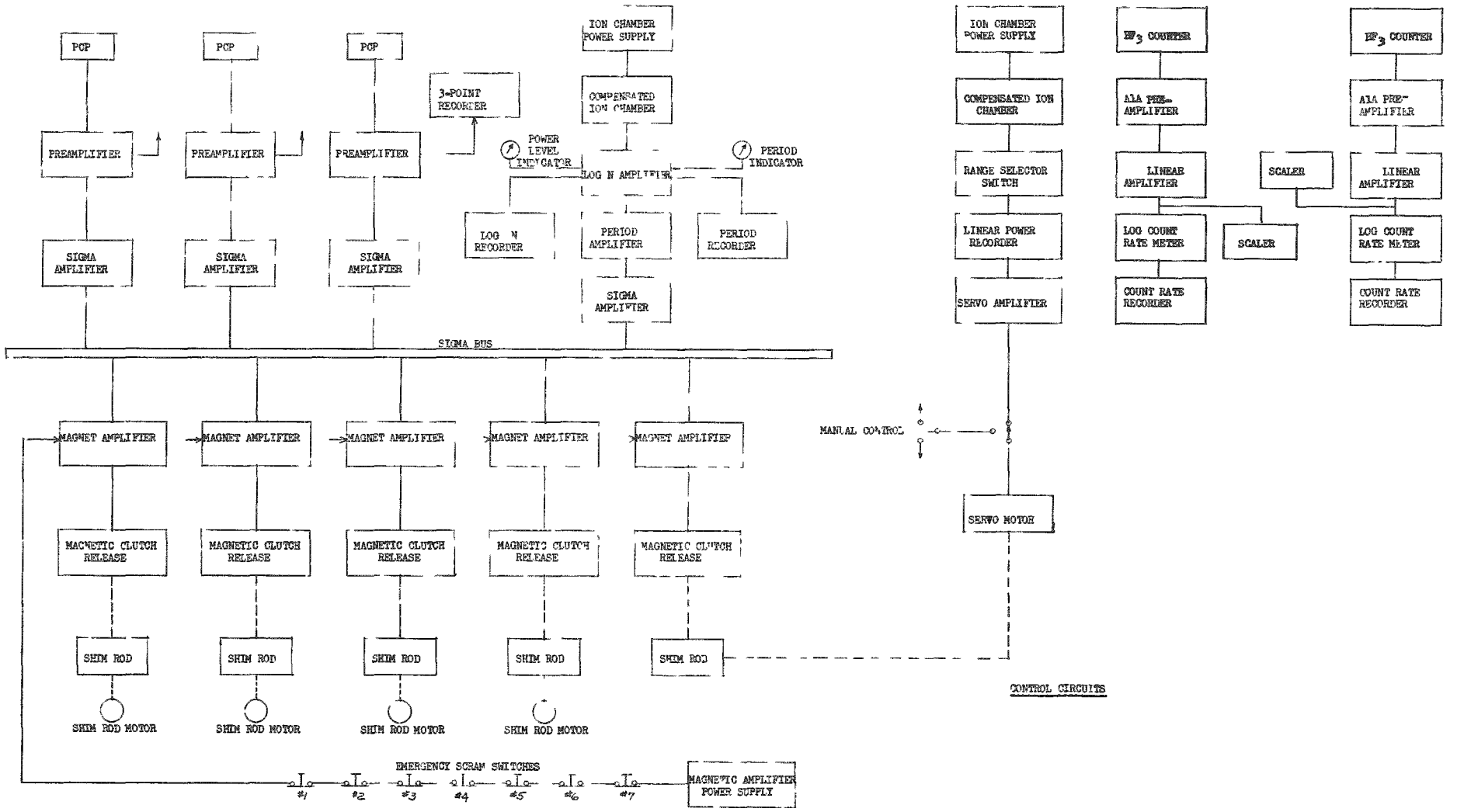

SAFETY CIRCUITS

CONTROL CIRCUITS

FIG. VI - 2 BLOCK DIAGRAM OF CONTROL AND SAFETY CIRCUITS

REACTOR SCRAMS:

1. LOW FLOW - PRIMARY COOLANT
2. REACTOR OUTLET TEMPERATURE - PRIMARY COOLANT
3. SYSTEM PRESSURE - PRIMARY
4. SYSTEM TEMPERATURE - SECONDARY
5. SYSTEM PRESSURE - SECONDARY
6. HIGH PRESSURIZER LEVEL
7. MANUAL SCRAMS

Kw the reactor may be operated without flow. The design pressure in the system is 1200 psi, and a 1450 psi pressure causes a scram. If the reactor outlet temperature goes 20 degrees above the design point of 450° F., there will be a scram. A deliberate back leakage of water is allowed through the standby pump in the primary loop so that the temperature of the water in this dead leg is essentially the same as that in the flowing loop. However, if the temperature in the dead leg drops more than 10° F. below that in the flowing loop, the standby pump can not be started without shutting down the reactor.

C. Preliminary Testing

The utmost importance and necessity for cleanliness of the primary system components during manufacture and shipping is appreciated. It is proposed to use accepted procedures for cleaning components as manufactured and for maintaining this cleanliness during shipment and application.

The primary system pressure vessels and circulating pumps will be tested for leakage by use of helium and the mass spectrometer, as well as by hydrostatic test.

After assembly of the system, it will be checked for leakage by the helium mass spectrometer method. Blank flanges will be used to seal openings for the control rod drives. When the system is clean it will be evacuated and filled with operational quality water with the dummy core in place. By applying pressure with hydrogen at the pressurizer a quick pressure leak check will be made on the system. If there is gas trapped in the system, the pressure addition will cause the level to drop in the pressurizer. If there is any indication of entrapped gas, water will be circulated at maximum velocity until all gas is

removed.

The flanges installed for vacuum and pressure checking will be removed and the rod drives and seals installed. The pressurizer heaters will be energized, the circulating pumps will be started and the special clam shell heaters on the primary circulating piping will be energized. Care will be exercised to be certain that the system pressure is adequate to prevent boiling.

When the system reaches operating temperature and pressure, all operating and emergency controls and instruments will be checked for proper performance. Additional checks will be made at the seals and at any other points where joints may have been disturbed after the hydraulic test.

The system will then be operated for a minimum period of 168 hours to demonstrate its integrity.

After the integrity of the system has been demonstrated it will be allowed to return to room temperature and atmospheric pressure. The shield will be filled with water and the top cap will be removed from the pressure vessel. The fuel bearing control rods will be installed and observed for proper operation, and will be dropped by actuation of the manual scram circuit. The circuits of all nuclear instrumentation will be checked by simulating a chamber signal at a point as close to the chamber as possible. This method will be used to check the nuclear scrams and interlocks, and will also afford a rough check on the flux servo operation.

After the operational checks have been completed, the unloading procedure will be initiated using the dummy fuel elements. The underwater handling tools will be used and the proper operation of the fuel discharge chute will

be demonstrated.

D. Initial Criticality & Zero Power Experiments

After the system has been completely checked out and shown to be operating satisfactorily, the reactor will be loaded with fuel. The fuel elements will be added one by one with a measurement of the subcritical multiplication after each element is added. The BF_3 counters will be mounted temporarily next to the reactor core within the pressure vessel. The reactor will first become critical with the rods almost all the way out. As additional fuel is added, the position of the rods will be noted, giving a calibration of rod worth in terms of fuel addition. The rods will also be calibrated against reactor period. Any additional zero power experiments will now be performed.

E. Power Operation

The cap will then be placed on the pressure vessel and the pressure in the primary system brought up to 1200 psi. With the reactor held critical by the flux servo control, the system will be heated to 450° F. and the temperature coefficient of reactivity measured as the temperature increases. The external heating will then be stopped and the reactor power elevated to about 100 Kw. The vapor container will be sealed at this time. The primary pumps will then be started and by gradually increasing the excitation voltage on the turbo generator, the nuclear power will be increased in steps to 10 megawatts. The xenon buildup will be measured and the system will be observed closely for local boiling in the reactor. After checking the performance of all equipment, the operation of the reactor will then be routine.

F. Shutdown & Hot Fuel Element Handling

When the time comes to change fuel elements, the reactor will be shut down and allowed to cool off for about 24 hours. The air in the vapor container will be changed by blowing out through the stack. While no airborne activity is expected, a monitron will be installed in the stack as a precaution. The vapor container will be entered through the access door and the lid of the pressure vessel removed under water with special tools. The fuel elements will be removed from the core one by one and passed through the discharge chute to the spent fuel pit for storage (See Fig. III-3). All operations are to be performed with the fuel elements under at least 9.5 feet of water.

New fuel elements will then be added, the pressure vessel will be capped, and the reactor will then be ready for further operation.

CHAPTER VII - NUCLEAR EXCURSIONS

A. Positive Reactivity Available

The APPR-1 is designed to operate at 60% of its maximum power of 10 megawatts for two and one-half years without changing fuel elements. To achieve this 15 megawatt-year life time with a minimum of control rods, use is made of a burnout poison. The critical mass at the end of the 15 MW-yr. cycle is 10.2 kg of U-235. The cycle is started with a loading of 17.7 kg of U-235 and is poisoned with 172 grams of boron which is added to the core of the fuel plates during fabrication. Since the poison is effectively exhausted at the end of the first 7 MW-yrs., a peak in reactivity is reached at that time as illustrated in Fig. VII-1. The lower curve in the figure shows the change in multiplication at the operating temperature of 450° F. with a maximum excess multiplication of 7% after 7 MW-years. If the reactor is allowed to cool down to room temperature at any time during the cycle the resultant multiplication can be obtained from the upper curve in the figure. The maximum excess multiplication at room temperature is 16%. It is necessary to provide shim rods in the reactor sufficient to override the 16% excess multiplication. Five rods are used with a total worth of 25%.

B. Control Rod Worth

Since the rods are worth 25% and move in a core 22 inches high, the individual rod worth is 0.23% per inch on the average. The maximum rod withdrawal speed is 3 inches per minute or 0.05 inches per second. On the average, the rate of change of reactivity is 0.011% per second for each rod. However, because of its location the center rod is worth more than the average, and at

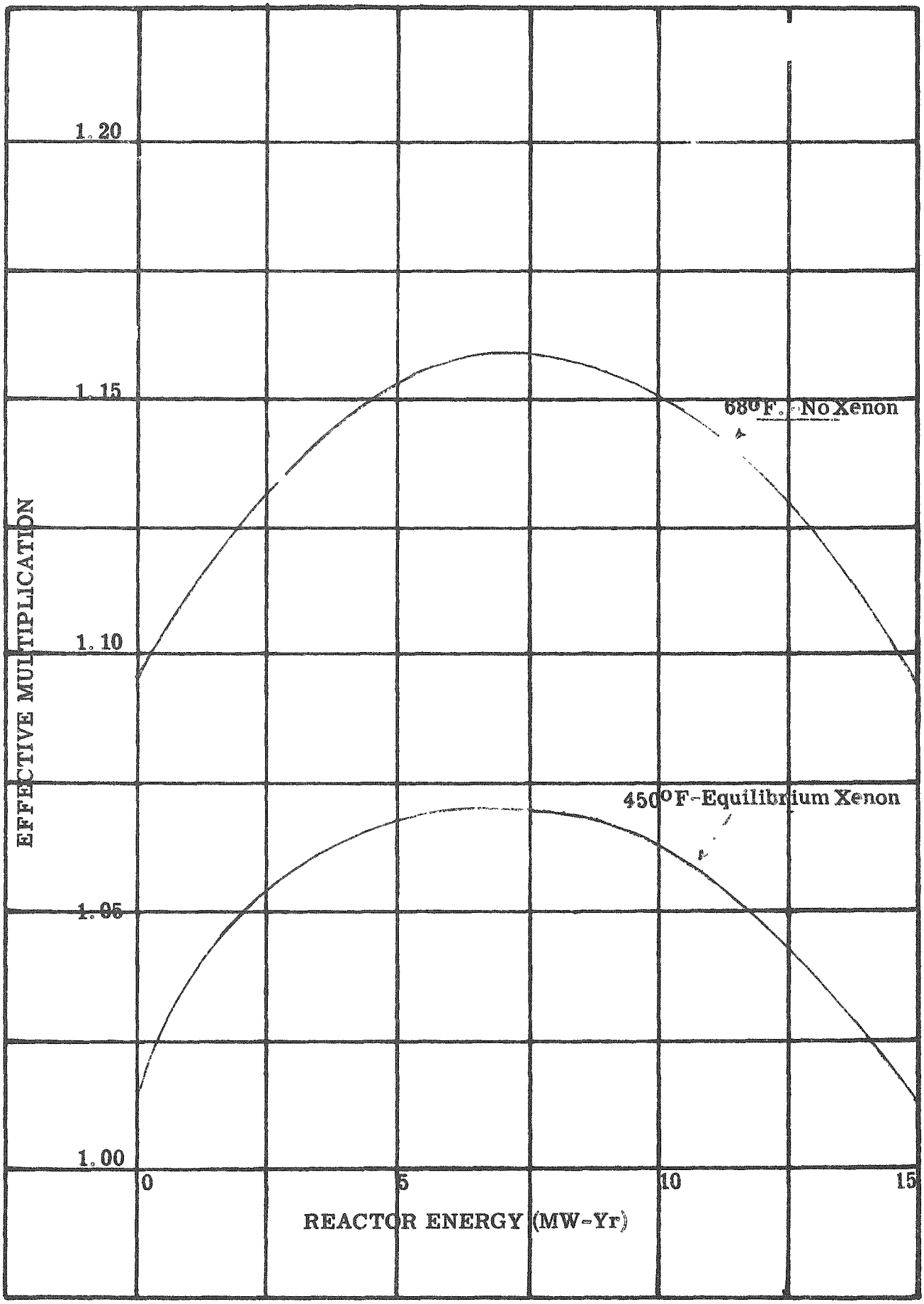

FIG. VII-1 EFFECTIVE MULTIPLICATION AS A FUNCTION OF REACTOR LIFE TIME

its mid position it has a rate of change of reactivity of 0.04% per second. All five rods moving together contribute a maximum of 0.10% per second.

C. Mild Excursions

The kinetic equations of the APPR-1 were simulated on the ORNL Reactor Controls Computer. The results are given in Appendix C and demonstrate that the reactor quickly stabilizes after step changes in reactivity of 0.5% or less. Step changes up to 1.0% have been simulated and indicate a return to stable operation. However, the simulator results are of questionable validity for reactivity steps beyond prompt critical, since the effect of thermal delay in the cladding of the fuel plates was not included. The results at any power level appreciably above design level are questionable as the effect of boiling is not simulated in this model.

The effect of oscillating the power demand was tested on the simulator to ascertain whether a resonance could be obtained. No such behavior appeared likely. The details of these trials are given in Appendix C.

The behavior of the reactor was studied for introduction of water 50 degrees below design inlet temperature for as long as 10 seconds. In the latter case, a peak power of 38 megawatts was reached for a very short time. The reactor quickly stabilized after the transient. Actually this condition cannot be attained since temperature of the water in the standby pump in the primary circuit is maintained within a few degrees of the rest of the water in the circuit, as discussed in a previous chapter.

D. Fuel Plate Melting and Void Fraction

In the APPR-1, an uncontrolled excursion will be limited by one of two

occurrences, void formation from steam bubbles or fuel plate melting. The relationship between the void fraction in the reactor and the multiplication factor is shown in Figure VII-2 for the cold, initial core and for the hot reactor at its mid-life.

The stable reactor period is plotted in Figure VII-3 against the multiplication factor. This is based on a conservatively estimated mean neutron life time of 20 microseconds. It is interesting to calculate the fuel plate temperatures resulting from the introduction of step changes in reactivity. The method of calculation (4), described in detail in Appendix E-1, uses steam formation as the shutoff mechanism. The melting temperature of the fuel plates is 2590^{o} F. From a cold, clean condition this temperature is reached in the center of the fuel plate before shutoff occurs with an excess multiplication of 1.2%. The outer surfaces of the plate will reach the melting point with an excess multiplication of 2.1%. For the reactor at its mid-life and at operating temperature 1.6% excess multiplication is necessary for the center of the fuel plates to reach the melting point before shutoff will occur. The surface will reach the same temperature with a 3.4% addition. The heat release from these excursions is listed in Table VII-1.

The same method of calculation has been used (4) to calculate the results of the Borax experiments. It is interesting to note that the Borax reactor disintegrated when the temperature of the center of the fuel plate reached the melting point (5). From this example it is reasonable to expect that the APPR-1 will disintegrate by the time 1.6% of reactivity is inserted into the reactor. The heat release from such an excursion (less than 70,000 BTU) is negligible compared to the energy released in the maximum credible accident

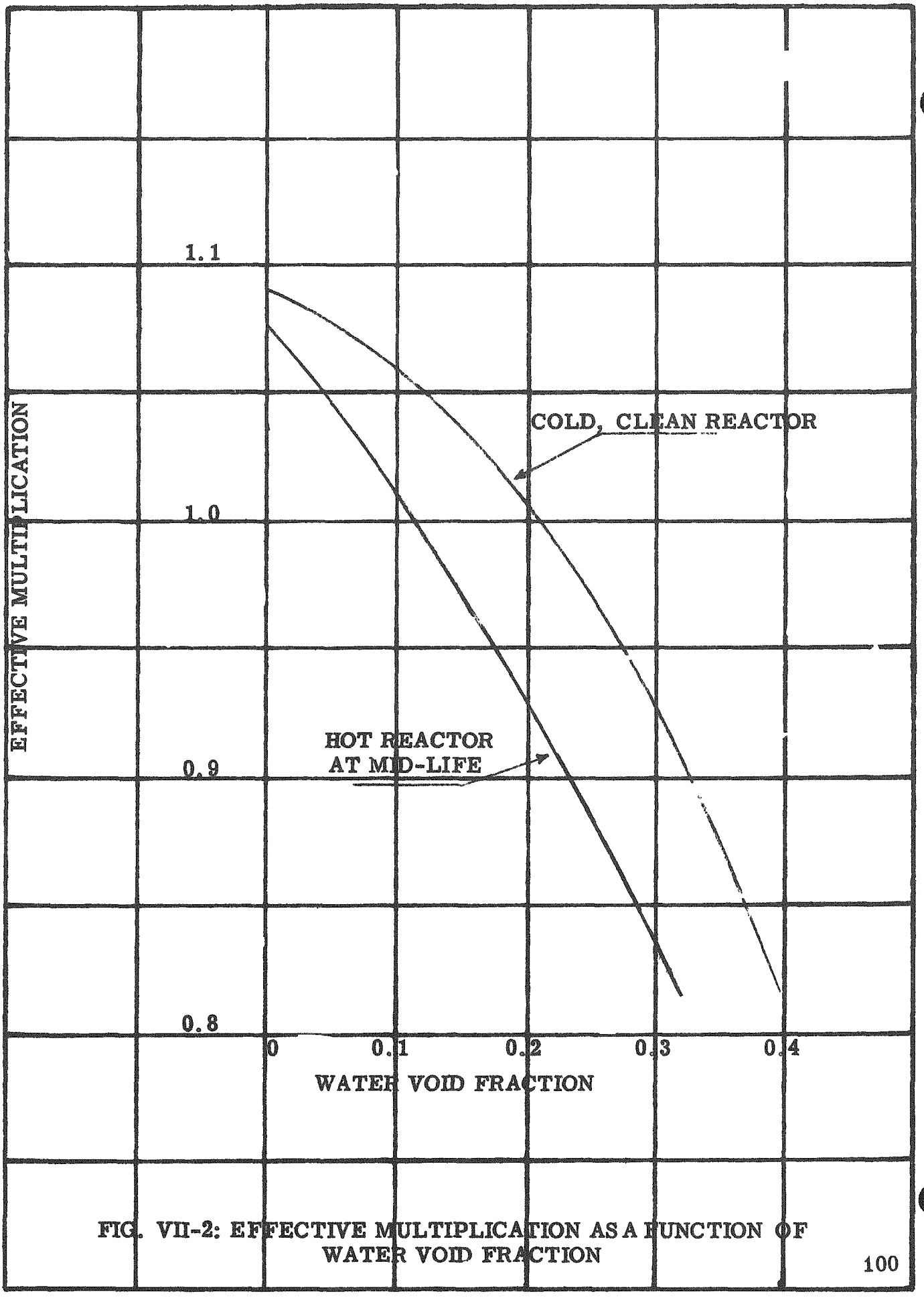

FIG. VII-2: EFFECTIVE MULTIPLICATION AS A FUNCTION OF WATER VOID FRACTION

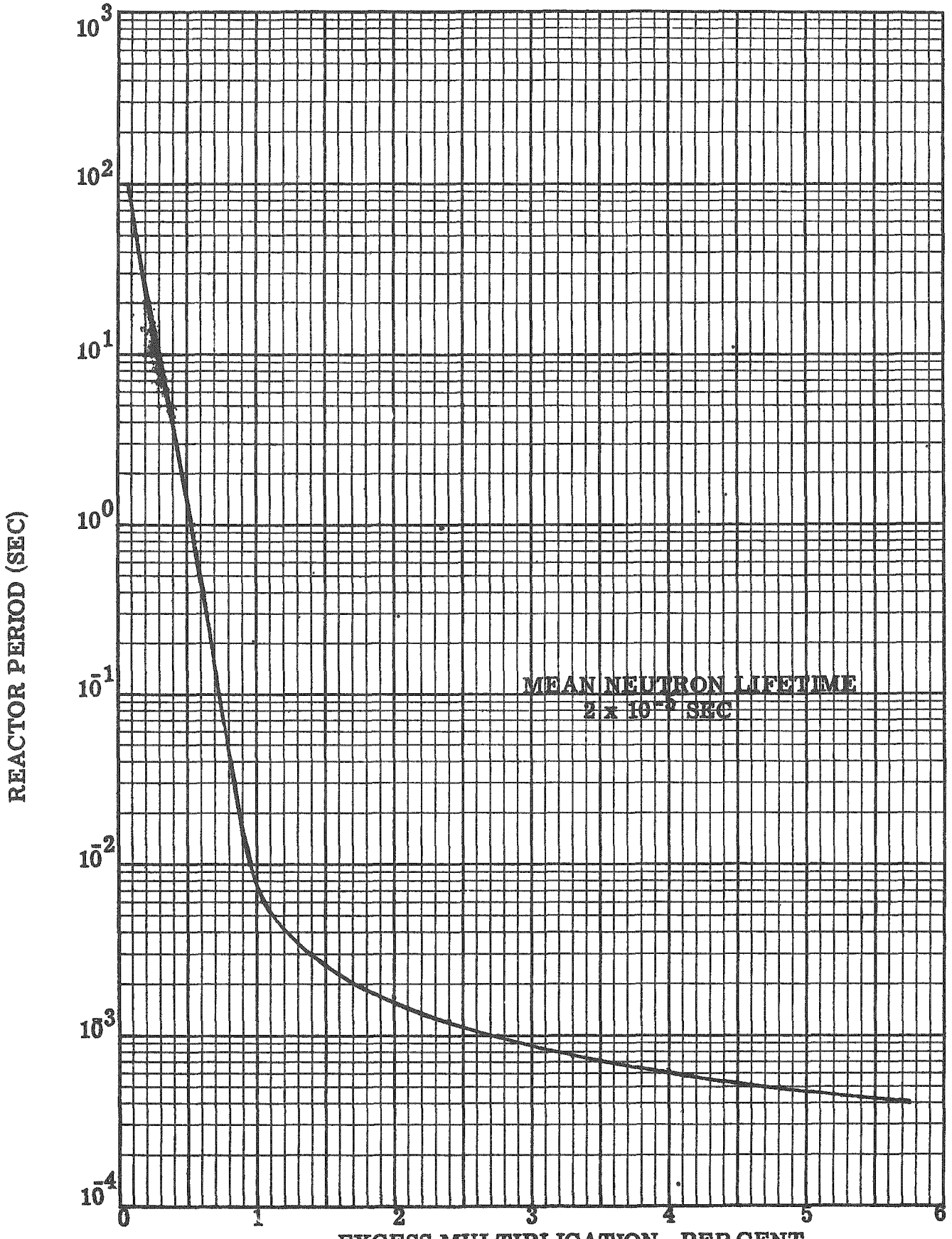

FIG. VII-3 STABLE REACTOR PERIOD AS A FUNCTION OF EXCESS MULTIPLICATION

described in the next chapter.

The energy released as a function of step changes in reactivity is given in Figure VII-4. Based on the model chosen, large step changes will release energy considerably in excess of that for which the vapor container is designed. However, no possible means has been found for large increases in reactivity except by carefully planned sabotage. Even in this case it seems improbable that the reactor would hold together for an excursion greater than 3.4% excess reactivity, in which case the entire fuel elements would be above the melting point.

E. Effect of Withdrawing the Control Rods

It can be postulated that certain coincident equipment failures start withdrawing all five control rods. None of the scram mechanisms operate. For a reactor starting from room temperature, it is assumed that reactivity is added at a rate corresponding to a rod speed of one foot per minute, which is four times the design speed. Calculations in Appendix E-2, based on shut-off of reactivity only by void formation, indicate that the reactor will attain a period of 10 milliseconds and a maximum multiplication of 1.0089. The maximum fuel element temperature is 1200^{o} F. This temperature is well below the melting temperatures of 2590^{o} F., and thus unless some external method is used to counteract the excess multiplication, the reactor will continue to operate. It is expected that the quantitative behavior of the reactor following the initial transient will be similar to the results for a transient arising from rod withdrawal at operating power, as described in the following paragraph.

A different method of analysis has been used to study a withdrawal of five control rods from a reactor at operating temperatures and power. Re-

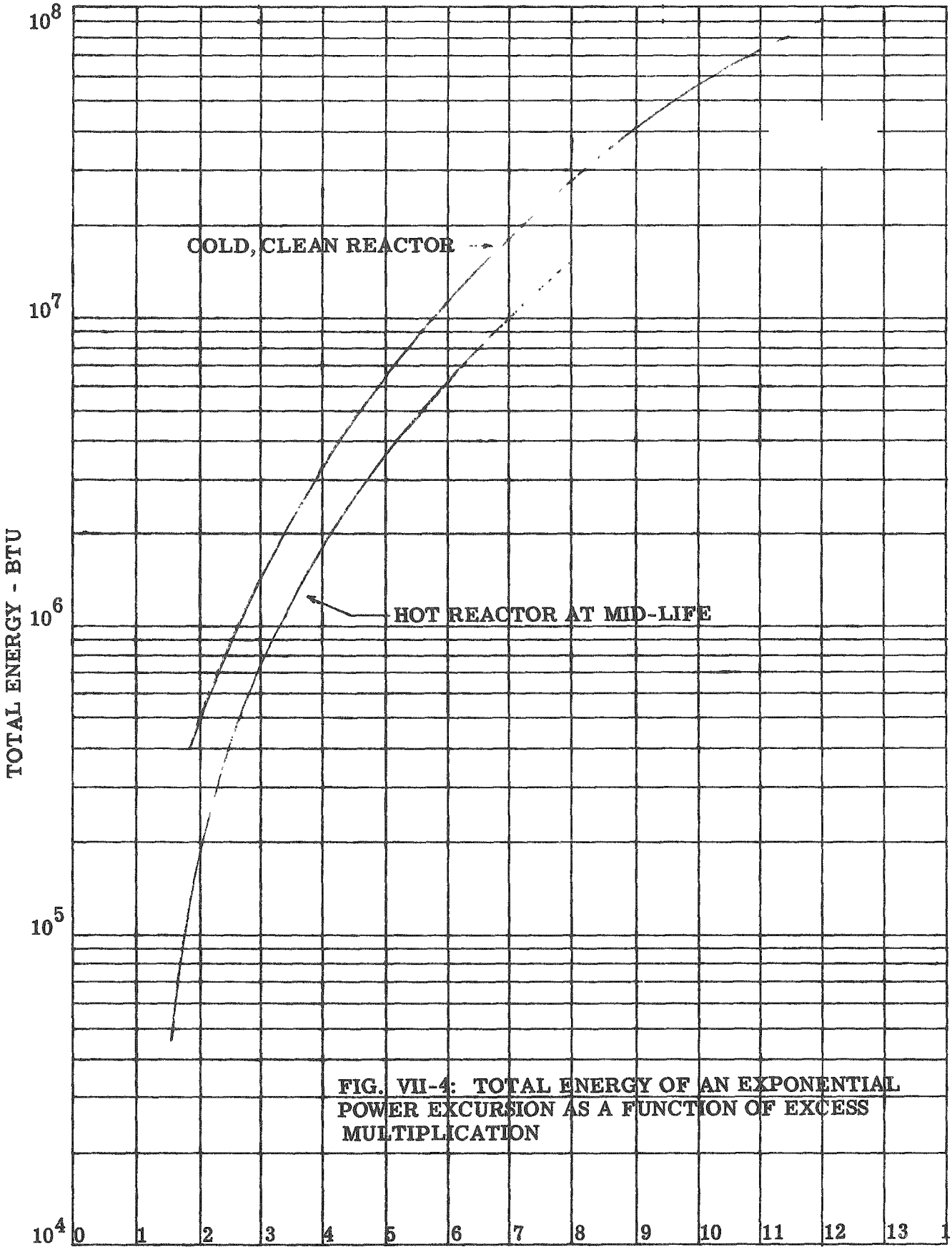

FIG. VII-4: TOTAL ENERGY OF AN EXPONENTIAL POWER EXCURSION AS A FUNCTION OF EXCESS MULTIPLICATION

activity is added at a linear rate of 0.1% per second. Void formation in the water is the only mechanism to reverse the reactivity addition by rod removal. The results of simulation of this problem on an analog computer are presented in Appendix E-3. It is found that no initial peak in power occurs, since very little excess multiplication can be added before boiling begins. The power rises gradually as the rods continue to withdraw, since a higher power is necessary to maintain a larger void volume to compensate for the increasing rod removal. The fuel element temperature follows closely the power rise. After 30 seconds of rod withdrawal, the power has reached 13.7 MW, and the average fuel element temperature, 580° F. A total multiplication of 3% has been added. There is no excursion to add to the maximum credible accident outlined in Chapter VIII.

F. Possibility of Rod Ejection

It can be postulated that with the system at 1200 psia pressure, the outlet pipe ruptures at the exit from the shield tank. (See Fig. II-6). If the incident should occur at room temperature a momentary upward impulse is exerted on the rods lifting them upward 0.031 inches, and introducing a 0.070% reactivity increase which quickly subsides as the rods fall back into place (See Appendix F-1).

If the rupture occurs at the operating temperature of 450° F., the internal energy of the primary water will expel the water into the vapor container and as this primary water rushes out, it will exert an upward force on the control rods.

For higher temperatures than 450° F. this upward force would be even greater. As is described in the next chapter, it is conceivable that the tempera-

ture of the primary circuit can go as high as 596° F. Accordingly the reactor behavior following a primary system rupture at this temperature has been calculated (See Appendix F-2) with the results illustrated in Figure VII-5.

It is assumed that all rods start from their mid position with a rate of addition of reactivity 2.27% per inch of travel. The rods are accelerated upward and the effect of this rod ejection on the multiplication is shown in the upper curve. However, steam bubbles form rapidly. The calculations show that the density of the steam water mixture in the chamber above the core is always less than in the chamber below the core. For conservatism, it is assumed that the steam formation within the core is the same as in the lower chamber. The effect of this water expulsion from the core on the multiplication is shown on the lower curve of Figure VII-5, with the net effect that the reactor is driven subcritical.

It is expected that nearly all of the water will be expelled, as the quasi-equilibrium condition within the vapor container requires an expansion on a volume basis of approximately 180 times. Following the expulsion, it is highly improbable, but still possible that enough water will enter the primary system that the core will again go critical. In this case the ensuing transients will be similar in general characteristics to the behavior described earlier in section VII-E.

G. Summary of Results of Nuclear Excursions

Several possible operating conditions have been studied, to determine if any unusual or extreme conditions result. Small reactivity changes by step and ramp functions, sudden power demand increments or decrements, severe oscillating power demand, and changeover of primary circulating pumps

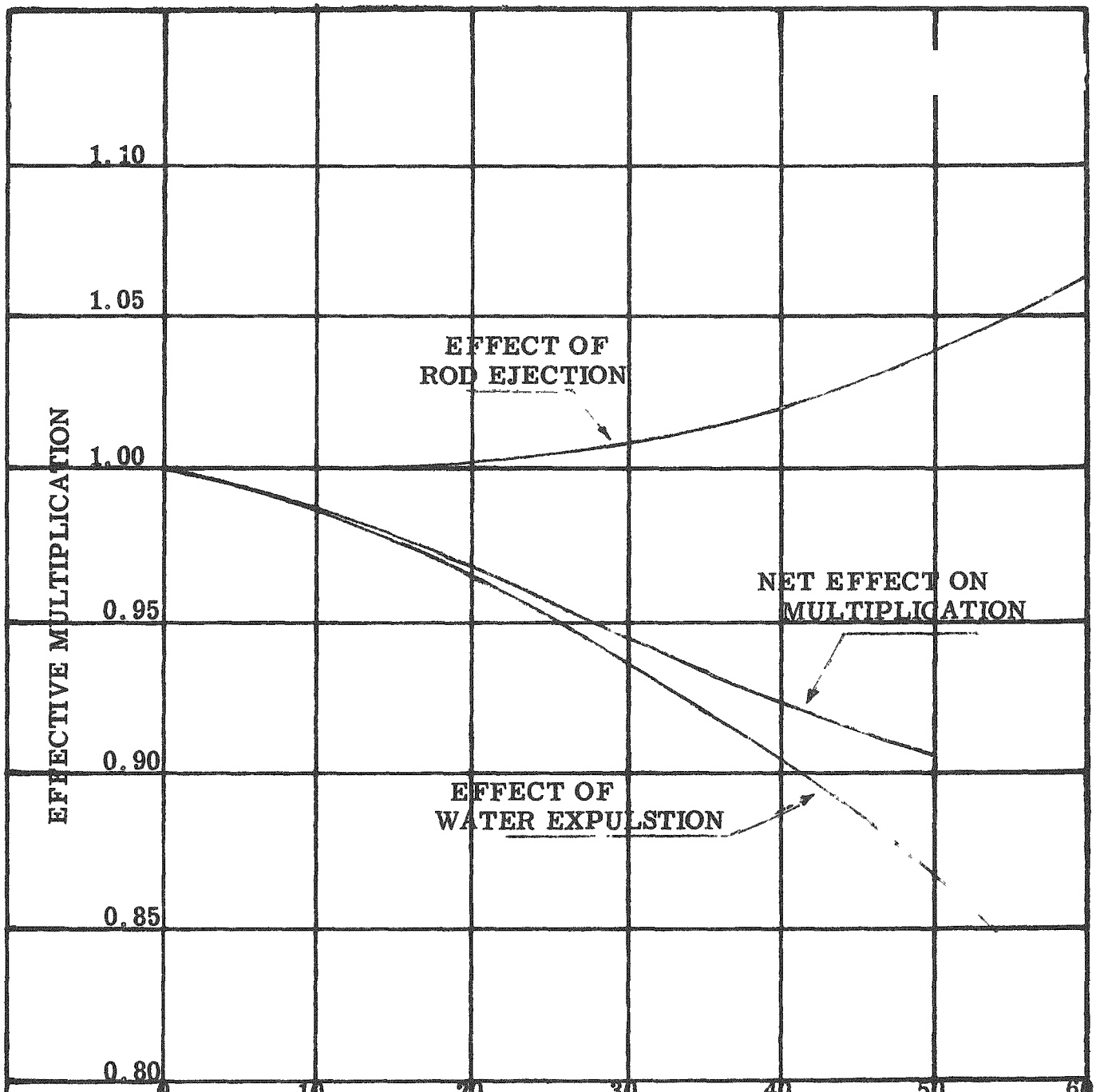

FIG. VII-5 REACTOR BEHAVIOR FOLLOWING A PRIMARY SYSTEM RUPTURE AT 596°F.

have been investigated. Under all operations considered, the reactor was completely self-regulating.

In addition, a number of less credible accidents, such as continuous rod withdrawal with no scram mechanism operating or a rupture of outlet line of primary piping, have been evaluated. It has been shown that the energy release in any incident resulting from sustained control rod operation is small compared to the total energy storage in the water system, as described in the next chapter. The maximum reactivity increment from a system rupture results in a 0.070% reactivity increase which lasts for 30 milliseconds.

Table VII-1

FUEL ELEMENT TEMPERATURES AND ENERGY RELEASES AT TERMINATION OF STEP REACTIVITY ADDITIONS

Reactor Condition	Excess Multiplication Percent	Fuel Plate Temperature at Shutoff, °F		Energy Release to Shutoff BTU
		Center	Surface	
Cold, clean, no power	1.2	2590	990	190,000
	2.1	--	2590	490,000
Hot, mid-life, full power	1.6	2590	900	66,000
	3.4	--	2590	1,070,000

CHAPTER VIII - CONTAINMENT OF THE MAXIMUM CREDIBLE ACCIDENT

A. Definition

In Chapter VII it was shown that a nuclear excursion of sufficient intensity to completely melt the fuel plates in the core releases about one million BTU. However, no mechanism for initiating such an excursion exists, except by deliberate sabotage.

By contrast with this there are 5,000,000 BTU stored as heat energy in the primary and secondary water systems when the reactor is operating at steady state full power. Thus the containment problem centers around the containment of the energy stored in the water system. The maximum credible accident can then be defined as a rupture of the primary and secondary systems at a time when abnormal operating conditions have permitted the energy stored in each of these important components to increase to the maximum attainable level.

B. Conditions Initiating the Maximum Credible Accident

A series of events and failures of equipment can be postulated as in the following paragraphs which will develop the "maximum credible" accident. It is assumed that the first failure is that the operator leaves his post for a period of a few minutes with the reactor and power plant operating. Shortly thereafter a fault in the electrical system develops which causes the turbine and generator to lose their load. This happens at a time when the average system temperature has been adjusted to the high side of the average temperature by the operator.

The resultant sudden loss of load causes the reactor temperature to start to climb while awaiting the effect of the temperature coefficient to bring the reactor power level down to the new equilibrium value. Before this inherent stability can make itself felt, second failure is now postulated. For some unknown reason, the servo comes on,

causing the rod to withdraw at its design rate of three inches per minute.

Under these conditions the reactor will continue to run at a constant power level of ten megawatts. This follows from the fact that the rate of removal of a rod corresponds on an average to approximately 0.6% per minute increase in reactivity, which for the central rod becomes more nearly 0.8% due to the greater effectiveness of the control rod. With a temperature coefficient of $-2 \times 10^{-4}/^{o}F$, a rate of rise of about $40^{o}F$ per minute will compensate for the rate of removal of the rods. The heat capacities of the primary and secondary systems and the heat transfer characteristics are such that at a 10 megawatt power level with no external means of heat removal, a rate of rise of $45^{o}F$ per minute will establish itself. Accordingly, for this incident it is postulated that the reactivity decrease by rise in temperature is just canceled by the reactivity increase by rod withdrawal. In reality this delicate balance would not be achieved, but slow departure from the initial level would occur.

In determining the time relationships discussed in the following paragraphs the system has been reduced to a simple model, consisting of a heat source (reactor), primary heat sink (primary system fluid) and a second heat sink (secondary fluid inside of the steam generator), which is deriving its heat from the primary heat sink (see Appendix G). The time involved is long enough that with seventeen seconds circulation time in the primary system, essential equilibrium will exist throughout the system, yet short enough that the amount of heat transfer to the mass of metal in the system was considered to be negligible.

C. Sequence of Failures

In Fig. VIII-1 there is shown the sequence of events which transpires subsequent to these two initial failures plotted as a function of time starting the instant the turbine

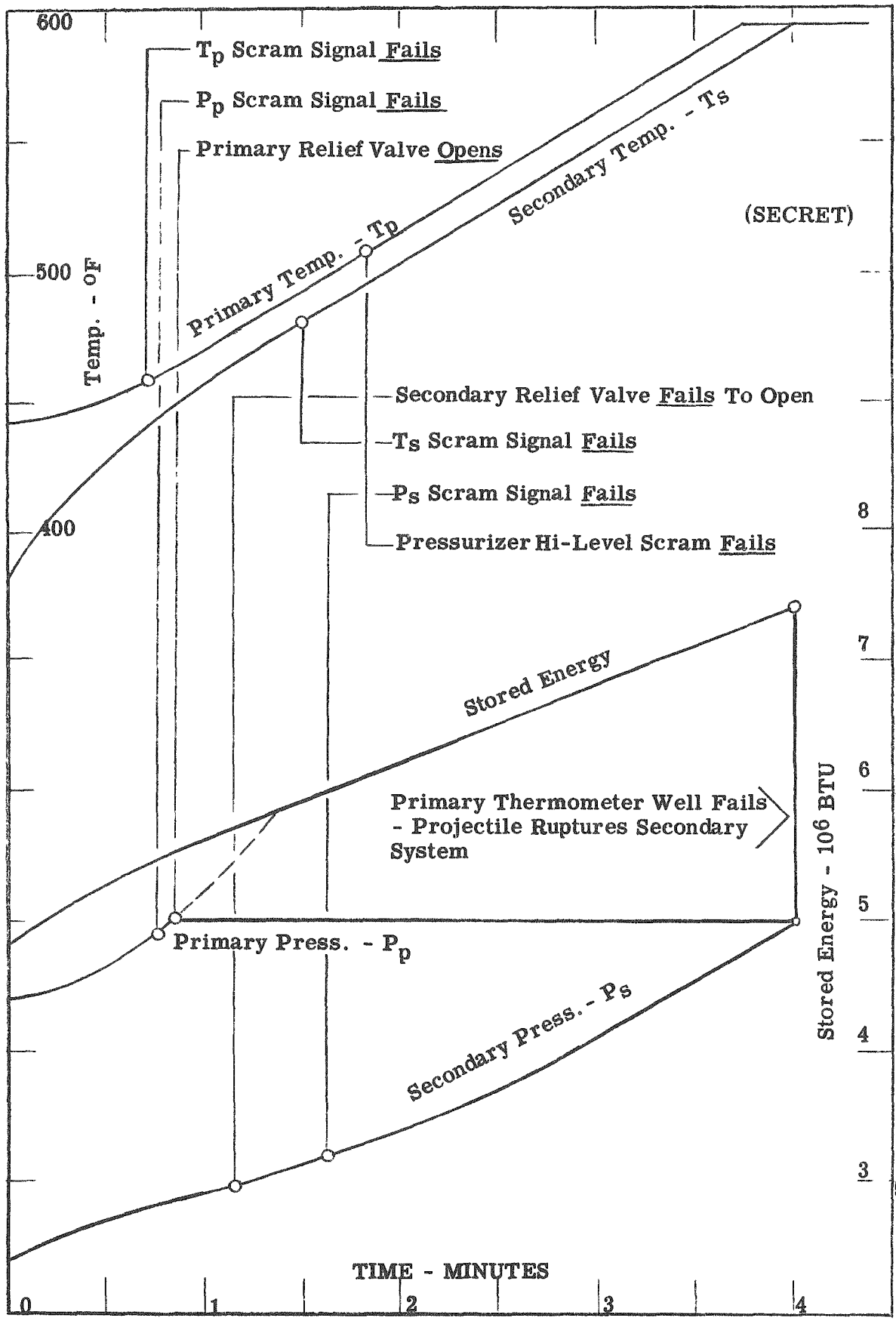

FIG. VIII-1 SEQUENCE OF EVENTS LEADING TO MAXIMUM CREDIBLE ACCIDENT

throttle closes. The significant failures which must occur for the series of events to extend to the maximum credible accident are shown at their proper positions in the time sequence. After approximately 25 seconds have elapsed, the rod is started on withdrawal. At the end of the 39th second the reactor outlet temperature reaches 470°F (10°F above the average temperature plotted in the diagram), which is the level at which the temperature scram should cause shutdown of the reactor. This signal fails so that the temperature and pressures continue to rise.

At the end of 45 seconds the primary system pressure has reached a value of 1450 psi due to the rising temperature of the primary system water. (See pressurizer design, Section III-B). This signal is also presumed to fail in its mission to shut the reactor down.

At the end of 51 seconds the primary system pressure has reached 1500 psi, which is the value at which the primary relief valve is set to open. For the accident to reach its worst proportions, it is necessary for this relief valve to function in its proper manner. The relief valve discharges into the vapor container, thereby conserving within the system the energy which is so released from the primary system. The operation of the valve in its normal manner permits the reactor to continue operation at ten megawatts appreciably longer than would be the case if the relief valve were to stick in the closed position This can be seen in Figure III-5, which shows that if the pressure continued to rise in accordance with the curve for adiabatic compression, the system pressure would reach 2000 pounds per square inch (rupture disc setting) at the end of one minute and twenty seconds. This is approximately two minutes forty seconds earlier than occurs in the sequence that follows opening of the valve in its proper fashion.

At the end of a minute and nine seconds the pressure in the secondary system would reach 500 psi, which is considered an upper limit by which time the relief valve

should be opened and operating. While activation of this is not automatically tied in to the scram signal, it can certainly be considered an alarm, which should recall the operator to the control system for shutdown of the reactor. Since there are nearly three minutes yet remaining before the energy reaches its maximum value, the operator would have adequate time to return to the control room and take action to prevent further departure. This valve is assumed to stick shut, permitting the secondary system pressure to continue to rise.

At the end of a minute and twenty-seven seconds the secondary system will have reached a temperature of $480^{o}F$, which is $40^{o}F$ over the maximum that can be attained with the reactor operating in a normal fashion. Failure of the scram on this limiting value will permit the reactor power to continue unaltered, and temperatures and pressures to climb. At the end of a minute and thirty-eight seconds, the secondary pressure will reach a value of 600 pounds which exceeds the maximum under normal operating conditions by approximately 175 pounds per square inch. A scram signal actuated by this pressure should shut the reactor down, but it is assumed that this also fails.

At the end of a minute and forty-six seconds the primary system average temperature has reached a value of $510^{o}F$. The change in density of the primary coolant causes displacement of ten cubic feet of water from the primary system into the vapor container. The rate of this displacement so far exceeds the possible rate of removal for normal purge purposes that the level within the pressurizer has risen well above the normal design limits. This is the last possible point for scramming the reactor. Failure on the part of this scram signal will permit continuation of reactor operation at the ten megawatt level without any control by the operator.

D. Final Rupture of the System

The pressures and temperatures of both the primary and secondary systems continue

to rise in accordance with the curves shown in Fig. VIII-1 At the end of the fourth minute after the turbine throttle was closed, the primary system has reached saturation temperature at 1500 pounds per square inch, the relief valve setting With no means of relief for the secondary system, the pressure and temperature in that part of the system have also risen to saturation value at 1500 pounds per square inch. The curve of stored energy shows that at this point a total of 7.4×10^6 BTU are stored in the system. No further energy can be accumulated because the reactor power level will inherently cut back as the system reaches saturation temperature, and steam formation takes place within the reactor core. Since the reactor has approached this point at a slow rate, it is anticipated that generation of steam will occur in an orderly fashion and reduce the power level of the reactor to a level consistent with the rate at which heat is leaking from the system thru the thermal insulation When this condition exists the reactor has succeeded in storing the maximum amount of energy that can be stored.

With the conditions just described, the maximum accident is triggered by the abrupt failure of a thermometer well in the primary system. The energy imparted to the thermometer well and its location are such that the well becomes a missile which ruptures the shell on the secondary side of the steam generator. The stored energies of both the primary and secondary systems are released within the vapor container While several seconds or perhaps a few minutes could elapse before all of the superheated water could escape from both systems, the rate is still sufficiently rapid that it may be considered as instantaneous release of this stored energy The pressure in the container rises essentially instantaneously to a pressure peak, which is determined by the relation between total stored energy and volumes of water and vapor container Once this peak has been reached, the time relationship of pressure and temperature is the resultant of heat leakage through the vapor container walls and into the primary

shield water, plus the additional heat released from the metal parts (approximately one-half million BTU) and from the decay of equilibrium fission products reaching a total of approximately fourteen million BTU at the end of forty-eight hours).

E. Pressure-Time Relationship Within Vapor Container

In the long time aspect of the containment problem (36 to 48 hours after rupture), the heat capacity of the primary shield and of the vapor container structure is of major consequence. In Figure VIII-2 the pressure-time relationship existing within the container is shown for 48 hours following the rupture. Supporting data is presented in Appendix I. The initial peak upon rapid release of the stored energy is dissipated within approximately the first hour after the rupture has occurred During this hour the heat stored in the nearly 50,000 pounds of primary system metal is released to the water, while at the same time heat leakage to the walls of the container and to the primary shield mass is taking place. At the end of the hour the metal parts are essentially in equilibrium with the surrounding water. During this hour and for nearly 48 hours after the rupture the rate of heat released from the decaying fission products can be taken into account. An additional fourteen million BTU will be released in 48 hours from this source alone. Fortunately the time interval is great enough that the effect of the large bulk of water in the primary shield and the heat capacity of the vapor container make themselves felt. The result of these competing factors is a secondary pressure peak of minor proportions as shown in Figure VIII-2. Water sprayed into the vapor container by a manually controlled emergency system to provide a large additional heat sink results in further reduction of the secondary peak as shown.

F. Requirements for Containment

The actual design of the vapor container to confine the results of the accident

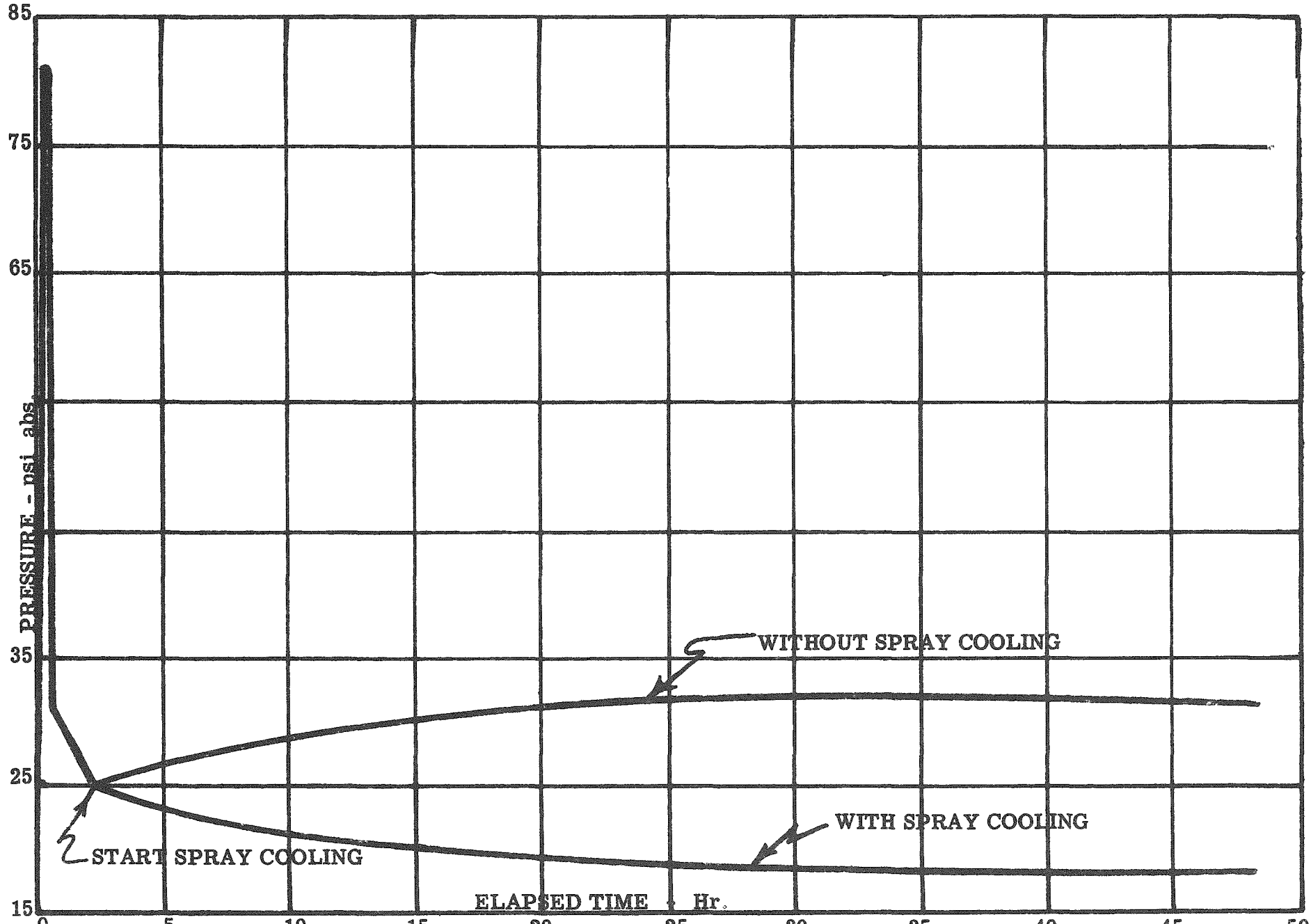

FIG. VIII - 2 PRESSURE VS. TIME IN VAPOR CONTAINER AFTER A MAXIMUM CREDIBLE ACCIDENT

can follow no prescribed guide lines While a vessel of the characteristics described in Chapter IV could be considered as an unfired pressure vessel, designing to this standard is felt to be unnecessarily conservative. The objective of the pressure vessel code is to provide a container which can be used continuously under operating conditions, whereas this vessel is to be used but once under the conditions of maximum credible accident In the light of this major condition in utilization it is believed logical to base the design upon permitting the stress in the containment to approach 80% of the yield point of the structural material (32,000 psi minimum for the steel used in the design)

The design of vapor container proposed for this installation has been analyzed to develop the relationship between the amount of heat released in an accident and the resultant stress in the containment vessel Figure VIII-3 is the curve of stress vs heat release from which it can be seen that a total of 9.5×10^6 BTU can be released essentially instantaneously within the vapor container without exceeding 80% of the yield point of the containment material Under these conditions the internal pressure will amount to approximately 90 to 95 pounds per square inch Since the maximum credible accident only releases 7.4×10^6 BTU, the pressure rises only to about 65 psi which produces a stress of 18,000 psi - only 56% of the minimum yield strength

In calculating this stress and equilibrium pressure no allowance was taken for heat leakage into the walls of the vapor container or into the mass of water which constitutes the primary reactor shield While this is conservative it was not believed to be unduly so since the release of pressure from the primary and secondary systems can occur in a matter of twenty to thirty seconds, during which time the amount of heat transferred to the primary shield and the container would obviously be insignificant

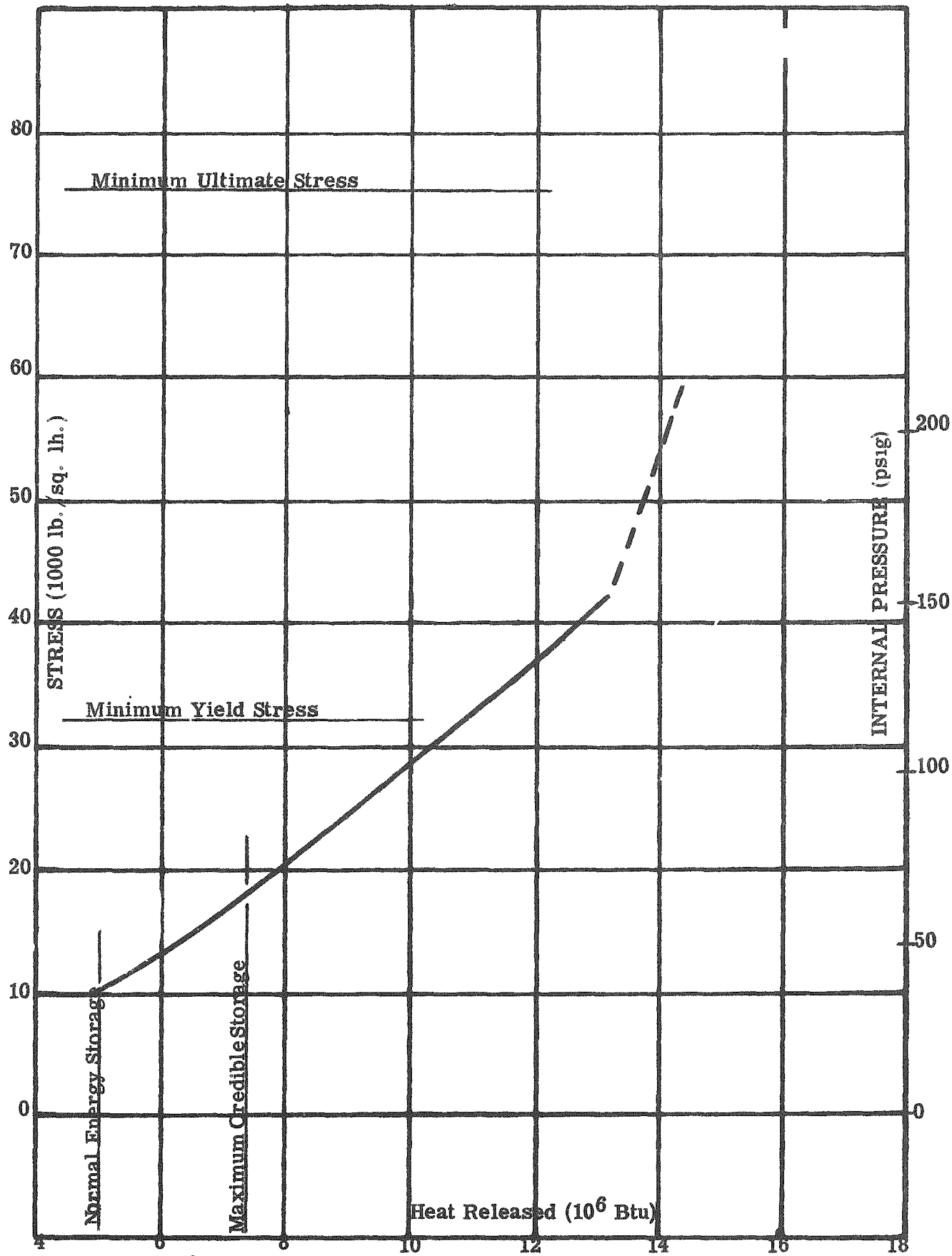

FIG. VIII-3 STRESS VS. HEAT RELEASE IN VAPOR CONTAINER

While it is true that rupture of the primary shield tank would release 150,000 to 160,000 pounds of water to mix with the superheated water, it cannot be guaranteed that such rupture would occur. Lacking this assurance conservatism indicates that it cannot be relied upon as a major source of energy absorption for the immediate storage problem following rupture of the system.

G. Variations from the Maximum Credible Accident

The accident described in the previous paragraphs is the worst that can be postulated with credulity Eight failures in proper sequence must occur to attain the maximum energy release of 7.4×10^6 BTU. Variations from the runaway described can be considered. If the runaway occurs at a faster rate so that the reactor gets on a fast period, both the period and level scrams will be actuated. In addition, on a fast excursion, there is a much higher probability that boiling will occur in the core which will reduce the reactivity. In any event no more than the maximum energy of 7.4×10^6 BTU can be stored in the system.

If the runaway occurs at a slower rate than that described, again no more than 7.4×10^6 BTU can be stored in the system. In this case the probability is increased that the operator can shut down the plant before the final system rupture occurs

Attention is called to a nuclear excursion which might result from expulsion of the control rods as described in the previous chapter. While the calculations indicate that for a cold reactor the energy released would be considerably larger than the vapor container could confine, this is not considered as a credible accident because no mechanism has been found which would permit expulsion of the rods under this condition. The only source of energy is that stored in the system pressurizer, but at the most this would manifest itself as a shock wave traversing the fuel element

in a period of 400 microseconds. The impact given to the rods is sufficient only to give a minor and temporary increase in reactivity.

The possibility of expulsion of the rods with the reactor hot is increased because of the energy stored within the reactor coolant. An abrupt rupture, causing release of pressure in the exit plenum chamber would permit establishment of a pressure drop across the control elements in such a direction as to propel them from the reactor. As discussed in the previous chapter and in Appendix F-2, the pressure drop which furnishes the driving force for expelling the rods also causes steam formation at a rate so fast that the net changes in reactivity is negative.

CHAPTER IX - HAZARD TO SURROUNDING AREA IN THE EVENT OF A CATASTROPHE

A. Events Leading to a Catastrophe

It has been shown in the preceding chapters that the vapor container of the APPR-1 will contain an accident resulting from any credible sequence of failures Yet to be considered are the consequences of the simultaneous occurrences of an accident releasing a large quantity of fission products and a rupture of the vapor container by sabotage, aerial bombing, or an act of God. In the latter category are fire, windstorm, flood and earthquake The only inflammable material of significance is the hydrogen used to inhibit corrosion in the primary system If the entire contents of a hydrogen cylinder were drained into the vapor container and ignited the energy released would be only 71,500 BTU. Wind velocities up to 100 miles per hour have been encountered in the Washington area but the vapor container will withstand wind velocities much higher than this. The vapor container itself would withstand a flood and its lowest elevation is 14 feet above the normal level of Gunston Cove. No seismic disturbances of sufficient intensity to cause a structural damage are on record in the Washington area.

Accordingly, the only reasonable events which can lead to a rupture of the vapor container are sabotage or aerial bombing.

B. Types of Accident Postulated

This reactor is located at Fort Belvoir, Virginia, approximately 17 miles south-southwest of Washington, D C A review of the climatology of the site is presented in Appendix A-1. The following facts should be kept in mind. The wind direction at the proposed site is from the south and south-southwest approximately

20% of the time; precipitation can be expected in the Washington area about 120 days per year; and stable atmospheric conditions may be expected 40 to 60% of the time, mostly during the nighttime hours

The hazard calculations are based on the long time (912 days) operation of the reactor at a power level of 10 megawatts

Two types of accident are postulated In the first it is assumed that rapid vaporization of the reactor occurs liberating 1.6×10^6 BTU of heat into the container volume of 1048 m^3 and that all of the heat goes into the temperature rise of the air in the container. It is further assumed in this incident that 50% of the fission products in the reactor are released into the container volume. The heated air and fission products are assumed to escape instantaneously from the reactor shell and to rise due to buoyancy. This type of event will be referred to as the "hot" cloud

The second type of calculated incident is a release of 100% of the fission product activity into the vapor container and to just crack the shell so that all of the activity leaks out at a constant rate over a 12-hour period. The leak is assumed to take place at the ground and no rise of the plume is considered. This event will be referred to as the "cold" cloud

A special incident is postulated concerning the radioactive concentration expected in the Potomac River in event of a "total washout" of the "hot" cloud at the APPR-1 site.

C. Method of Calculation

Three methods of irradiation are considered for each of the first two above incidents, namely, external gamma radiation from the traveling cloud using the method and nomographs developed by Holland (6), inhalation of fission products using Sutton's

(7) (8) diffusion formulae with geometrical adaptations developed by Holland (9), and estimating source strengths and dosages based on Burnett's treatment of a "30 isotope" mixture (10), and external gamma radiation resulting from ground deposition of fission products by removal from the traveling cloud by rain; Chamberlain's (11) modifications of Sutton's equations and some work by Holland (9) provide methods for treating this latter problem. In computing dosages a decay correction based on a decay rate of $t^{-0.2}$ was made for the external gamma and deposition cases. In the inhalation case the half life of the "30 isotope" mixture is long enough to permit the neglect of decay in these computations.

Each irradiation method is examined for two representative meteorological situations First, the "day" case with good diffusion and moderate wind speeds; and second, the "night" situation with a stable atmosphere and light winds

For the "hot" cloud computation, the height of rise in a stable atmosphere is 1300 meters However, there is considerable doubt and no available experimental data to confirm whether or not the relatively small heat release will actually result in cloud rises of this magnitude For the sake of conservatism it was assumed that the "hot" cloud would rise to 1000 meters in the daytime and to 500 meters at night. This approach has essentially no effect on the external gamma dosages which are already very small with clouds rising to 500 meters, nor does it affect "washout" dosages since rainfall would usually originate from elevations above 1300 meters in any case.

In the special case, a most pessimistic situation is clearly indicated when it is assumed the activity in the "hot" cloud is instantaneously and completely "washed out" at the origin. Also, no corrections are made in the calculations for sediment

fixation, decay, surface winds, tide and water density differential All but the last two items would generally tend to reduce the concentration.

The calculations are summarized in Appendix H.

D. Results

Figures IX-1 to IX-8 summarize the results for each type of incident postulated.

In examining the results of the dosage computations for the various methods of irradiation it can be seen that the limiting hazard is that of dosage resulting from inhalation of the fission products Values greater than the maximum permissible exposure occur at approximately 6 miles for the "day" "hot" cloud and from approximately 9 to beyond 60 miles for the "night" case. The computations for the stable "night" case were not extended beyond 100,000 meters since, with a 2 mps wind, times in excess of 14 hours would be required for the cloud to travel greater distances. Except in unusual circumstances, 14 hours represents a reasonable duration of stable conditions.

For a continuous release the "cold" cloud dosages exceed the maximum permissible exposure out to 25 miles for the "day" case, and for all distances out to beyond 60 miles for the "night" meteorological conditions.

The possible dosages from continuous precipitation "washout" may exceed 100 roentgens out to 3 and 4 miles for "day" conditions and 4 and 10 miles for the "night" situations for the "hot" and "cold" clouds respectively.

The Potomac river activity concentration caused by an instantaneous "total washout" of the "hot" cloud at the APPR-1 site is highly significant as values far in excess of the accepted provisional maximum permissible concentration of 10^{-7}

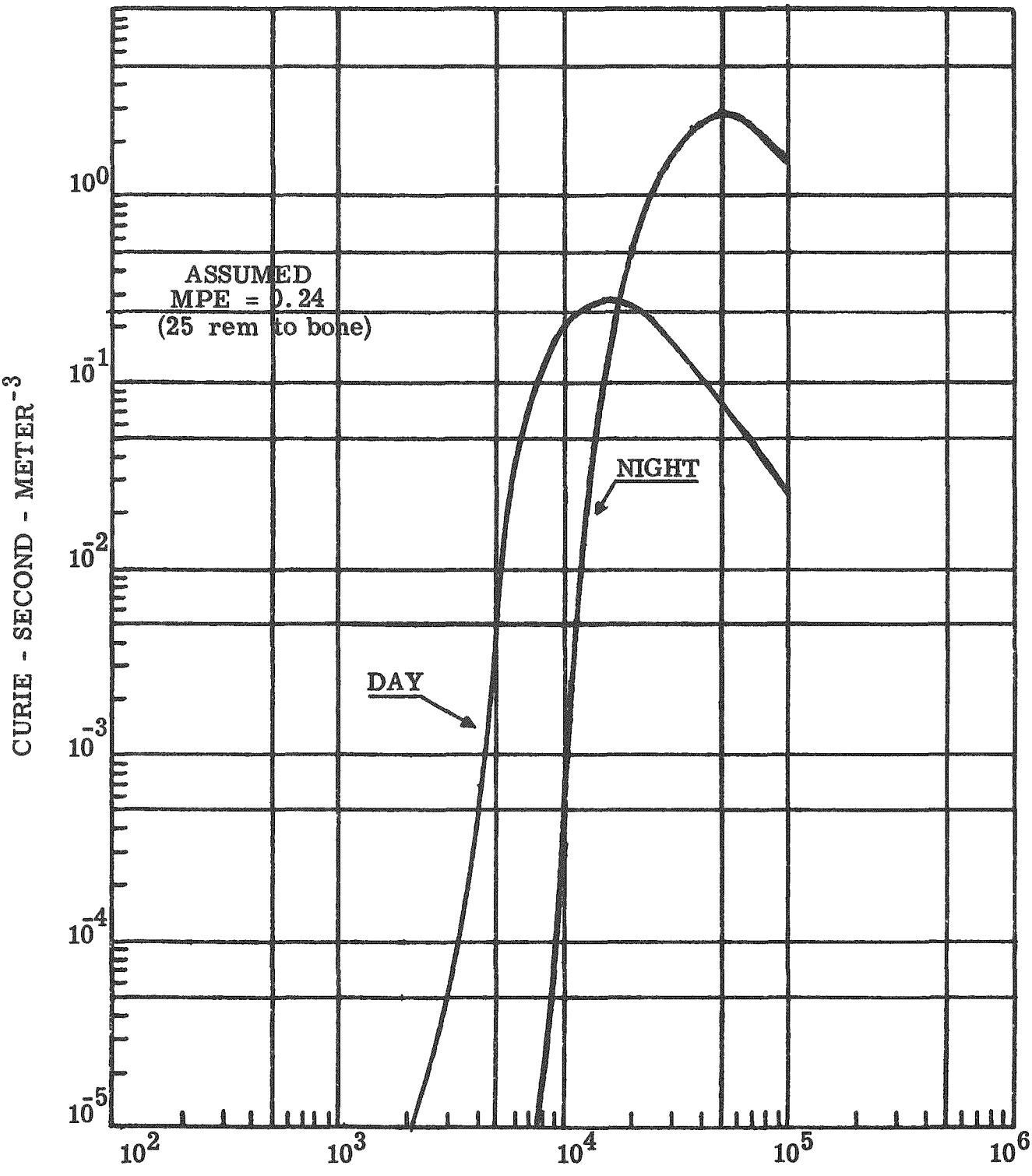

Inhalation Dosage - "Hot" Cloud

FIG. IX-1 (See TABLE H-3)

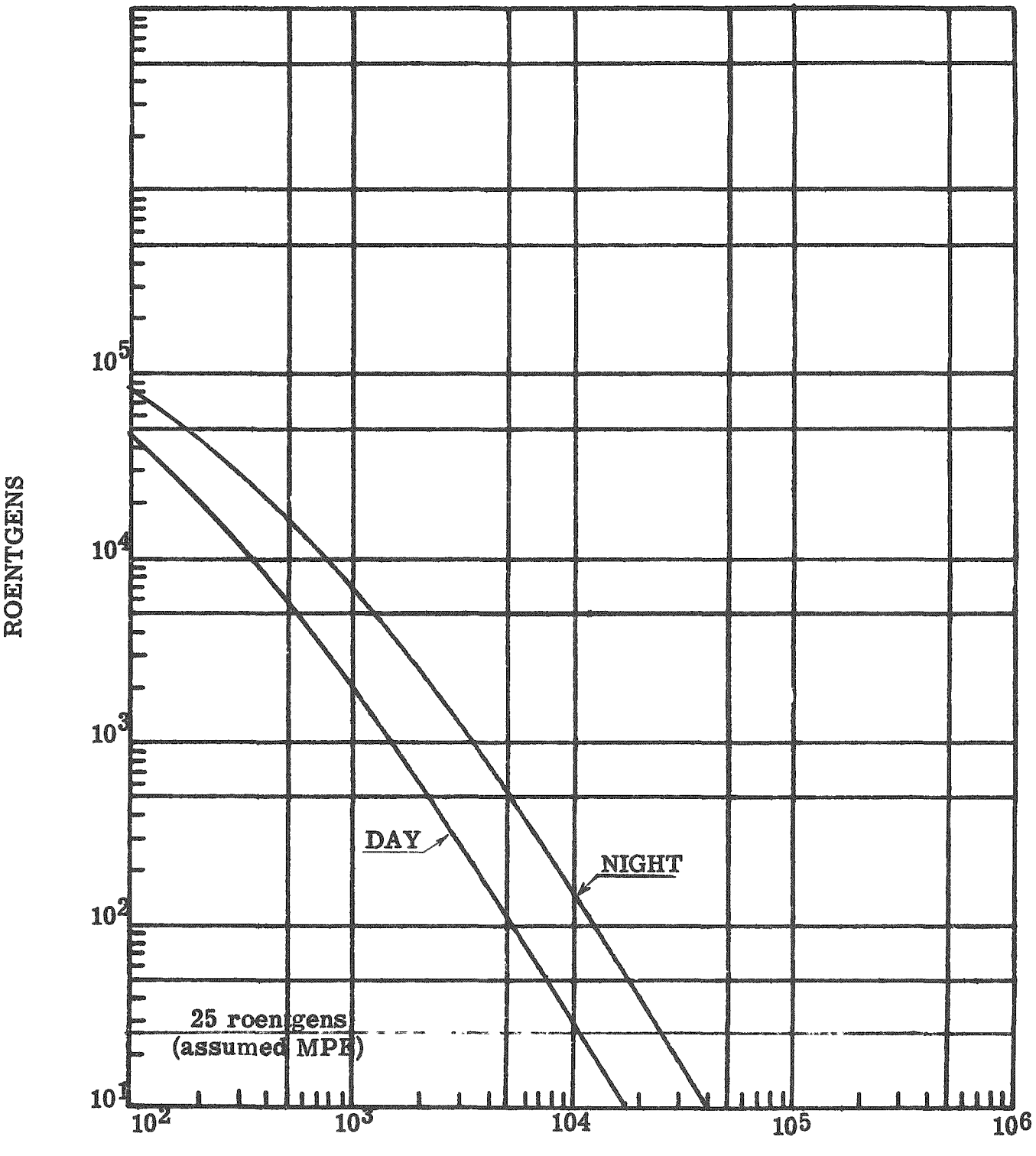

Integrated Gamma Dosage From Deposition By Continuous Precipitation - "Hot" Cloud

FIG. IX-2 (See TABLE H-5)

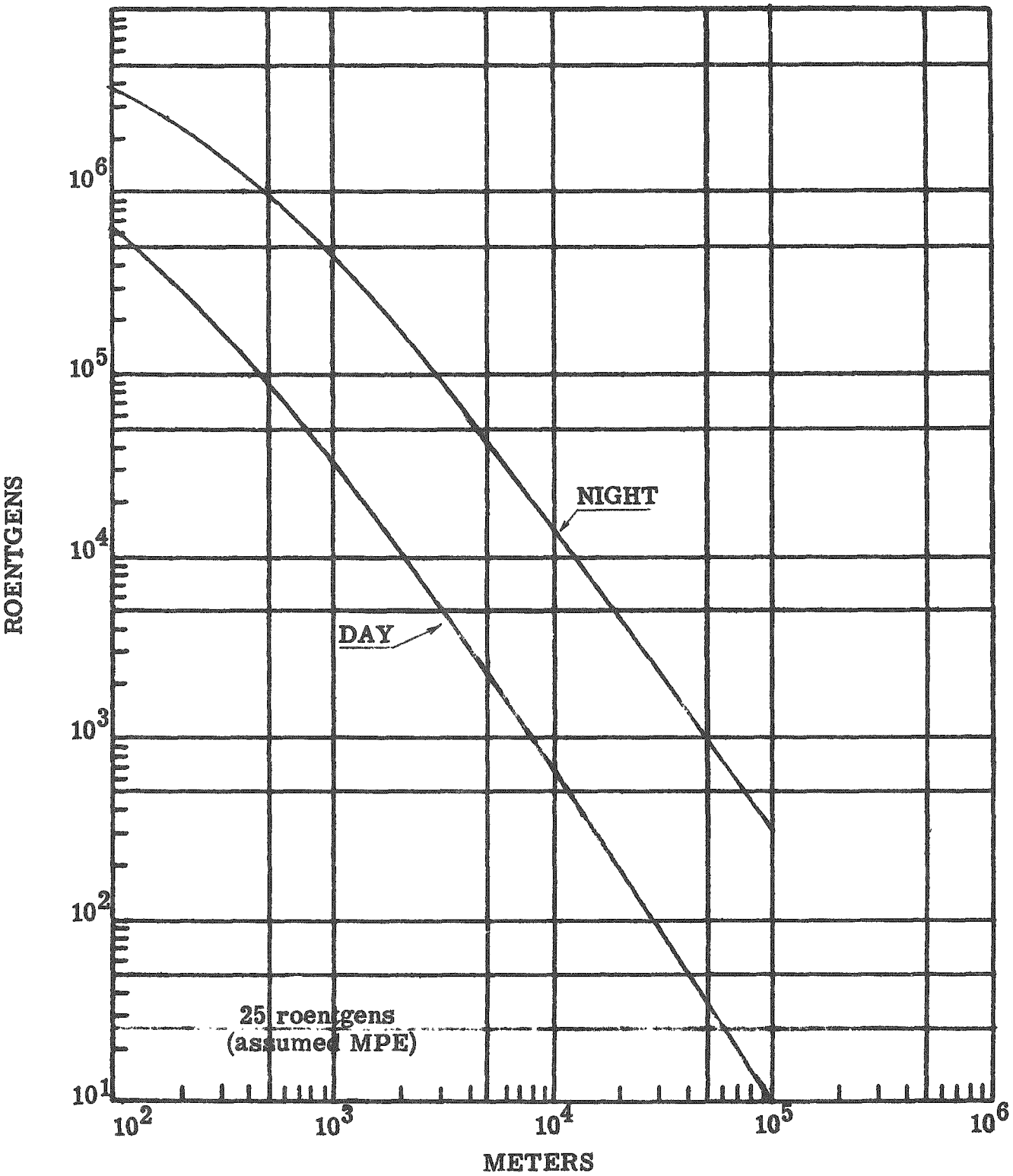

Integrated Gamma Dosage From Deposition By
Instantaneous "Total Washout" -"Hot" Cloud

FIG. IX-3 (See TABLE H-7)

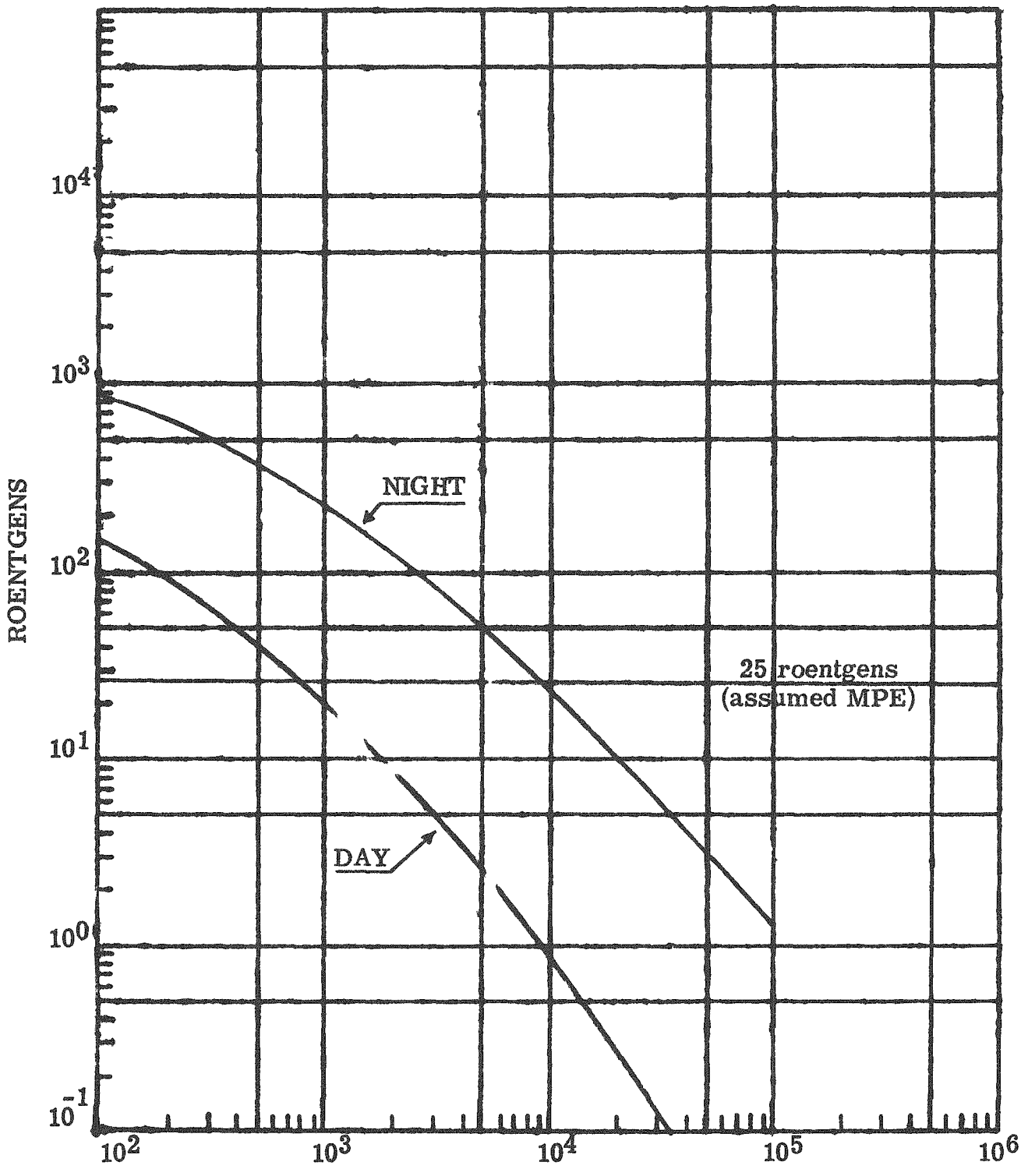

External Gamma Dosage From Continuous Release
"Cold" Cloud

FIG. IX-4 (See TABLE H-8)

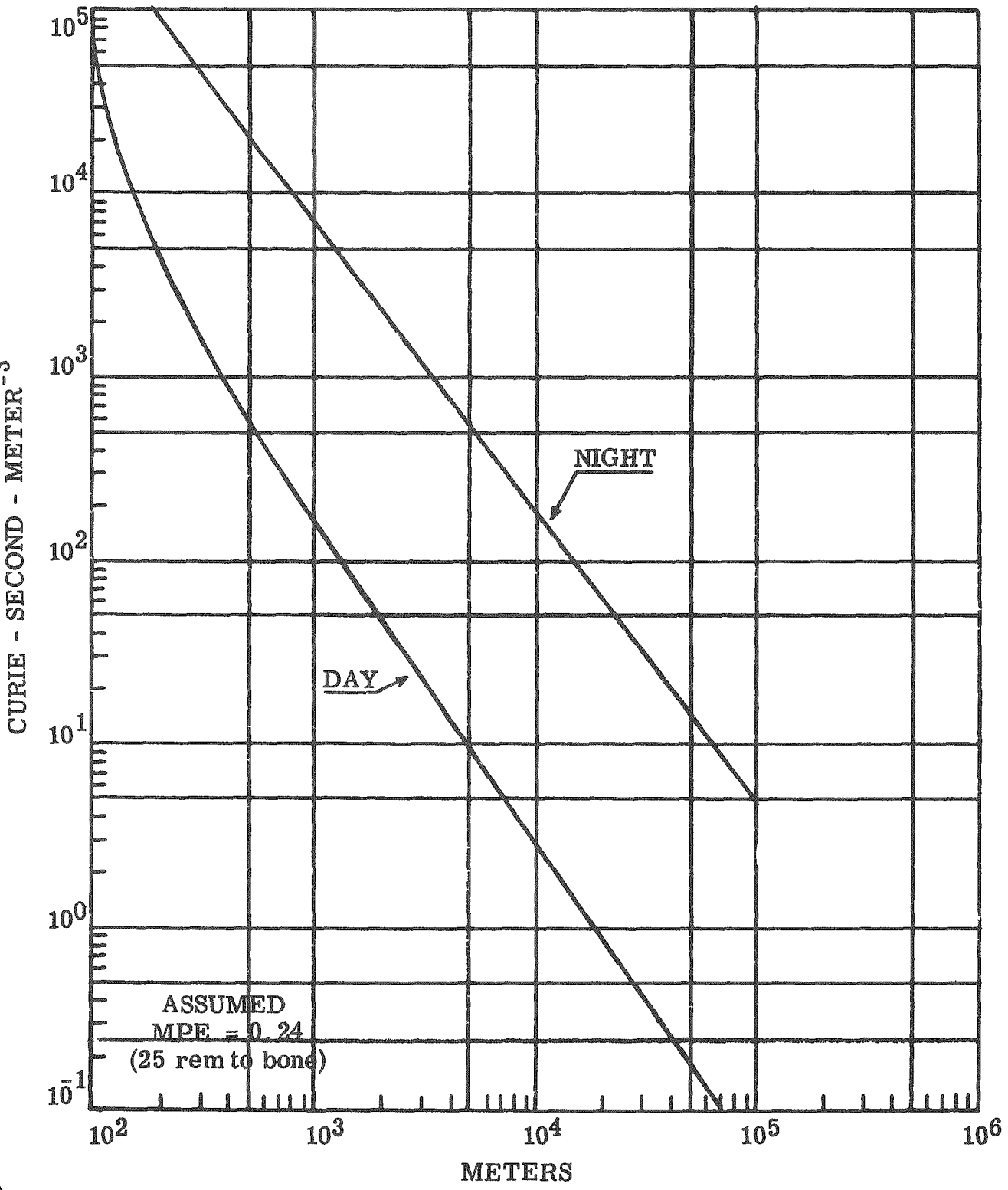

Integrated Inhalation Dosage - "Cold" Cloud

FIG. IX-5 (See TABLE H-9)

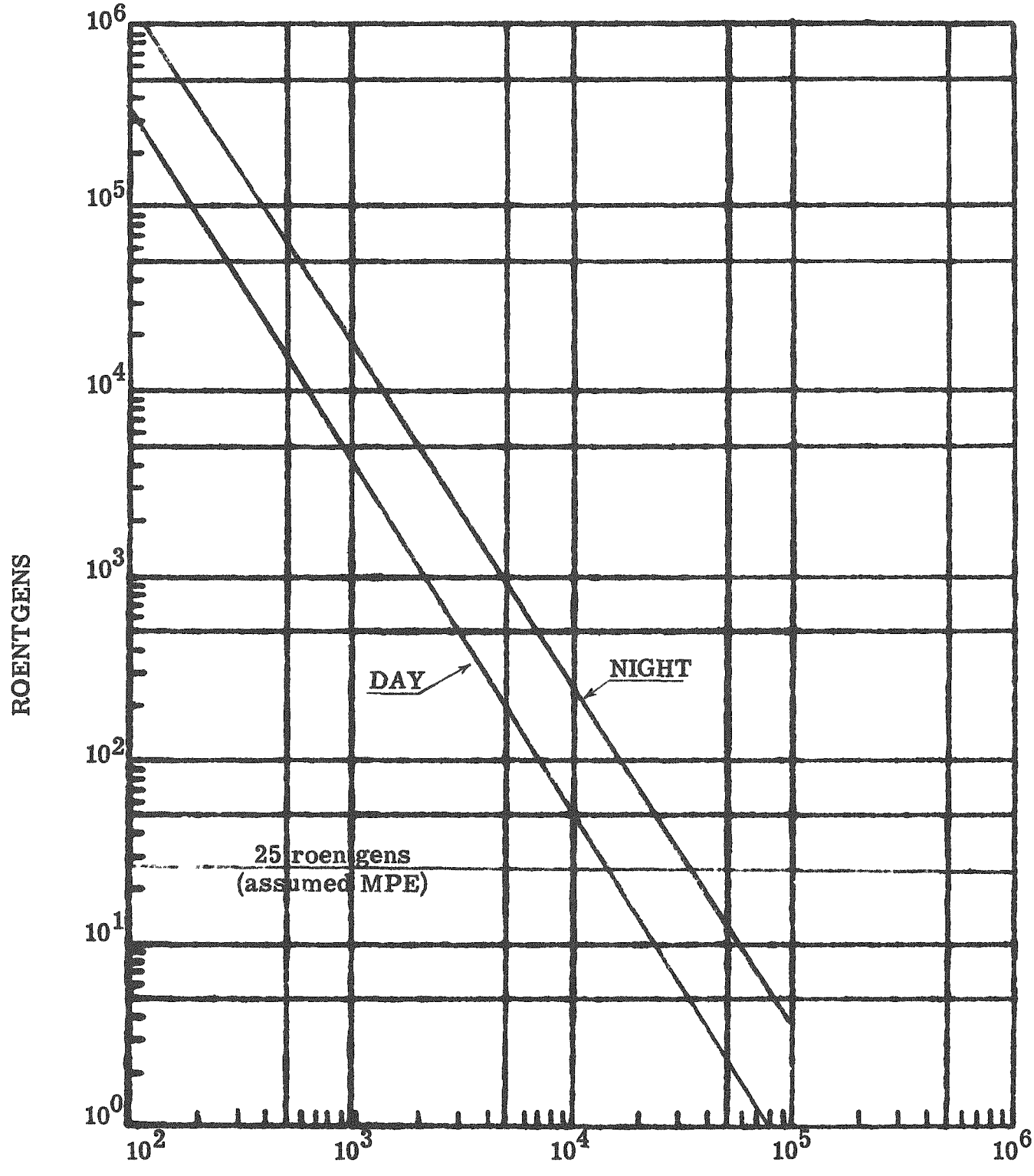

Integrated Gamma Dosage From Deposition By
Continuous Precipitation - "Cold" Cloud

FIG. IX-6 (See TABLE H-11)

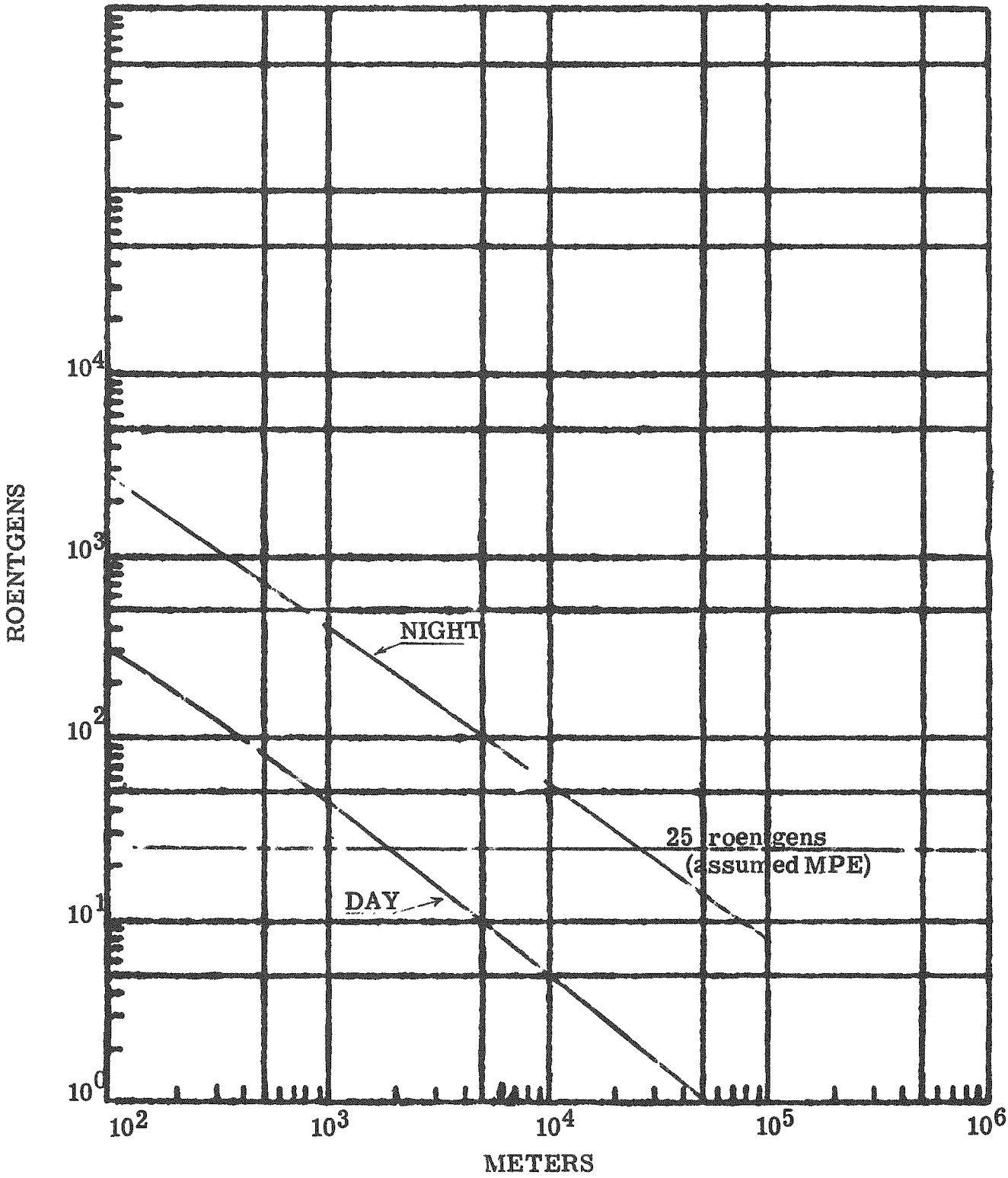

Integrated Gamma Dosage From Deposition by Instantaneous "Total Washout" – "Cold" Cloud

FIG. IX-7 (See TABLE H-13)

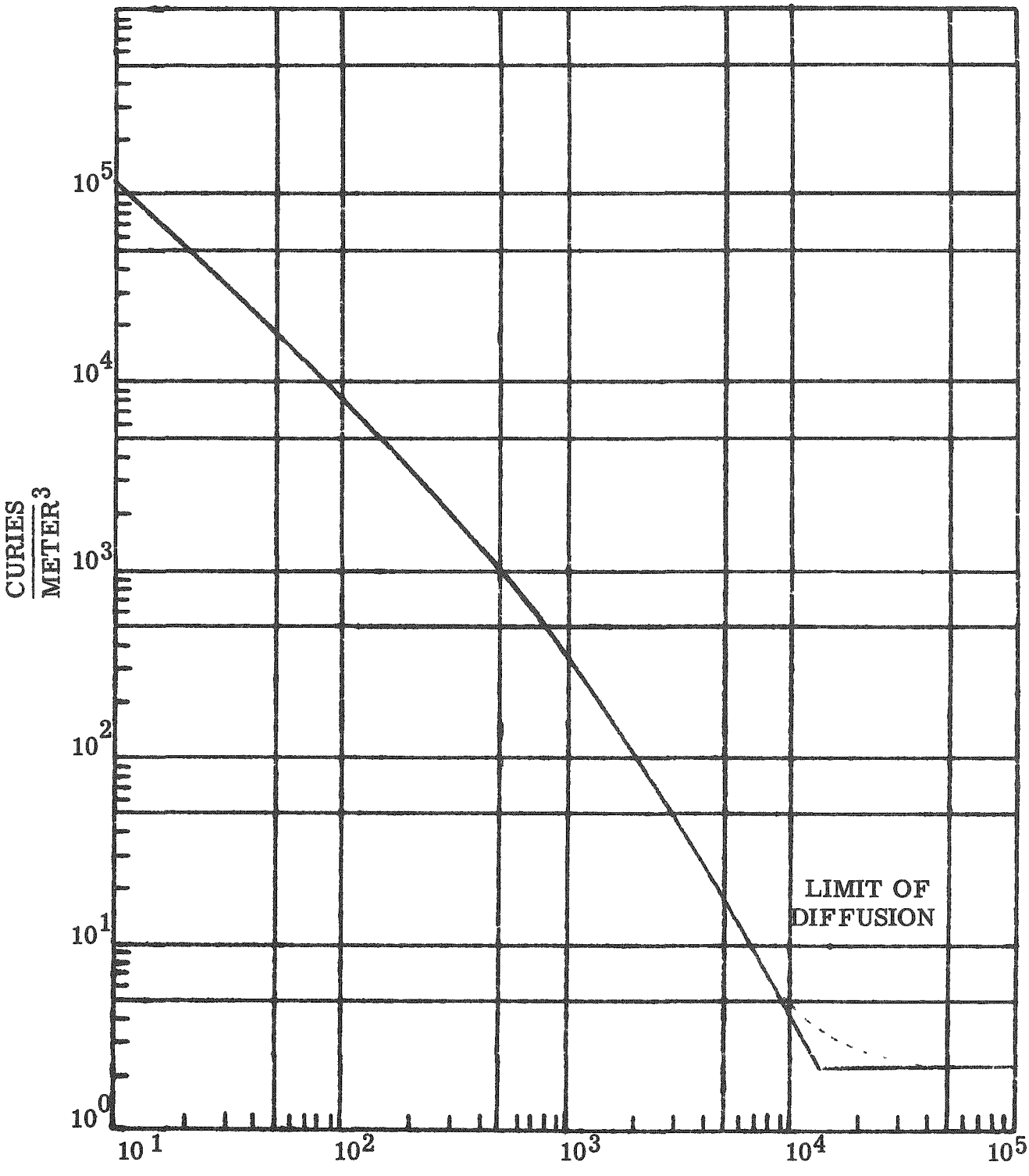

Activity Concentration in Potomac River by Instantaneous "Total Washout"-"Hot" Cloud

FIG. IX-8 (See TABLE H-14)

curies/meter^3 for unknown fission products can be expected to enter the Chesapeake Bay. The possible external dosage to any person in or on the river would be less than that indicated for ground deposition by "total washout" of the "hot" cloud. Although the river is subject to reverse flow under unfavorable wind and tide conditions, the District of Columbia sewage disposal plant at Washington has recorded effluent a maximum of 2-1/4 miles upstream (12), thus it could be expected that no hazard to Alexandria or Washington would result from this unfavorable condition.

APPENDIX A-1 - METEOROLOGY AND CLIMATOLOGY

Introduction

Ft. Belvoir, Va., is located approximately 17 miles SSW of Washington, D.C. just to the west of the Potomac River and between Dogue and Pohick Creeks. The latter creek flows into Gunston Cove which forms the southern boundary of the military reservation. The proposed location of the Army Package Reactor (APPR-1) installation is to be on the south shore of this relatively small Ft. Belvoir penninsula facing Gunston Cove. The terrain in the immediate vicinity of the proposed reactor location slopes upward steeply from the river's edge, from approximately two feet msl to 130 ft. msl in 1/3 of a mile. The entire peninsula is also heavily timbered.

Source of Data

Although no meteorological data exist for the proposed APPR-1 site itself or for Ft. Belvoir, very complete meteorological records have been taken for many years at both the Central Office of the Weather Bureau in Washington and at the Weather Bureau Airport Station at the Washington National Airport (WNA). The latter office is also located along the Potomac River 13 miles NNE of the proposed APPR-1 site. Climatological data from the Quantico Marine Corps Air Station (20 miles SW of the site, also along the Potomac) have also been examined.

Climatological Review

For the most part, there does not appear to be any significant change in the general meteorology of the area between Ft. Belvoir and Washington, D.C., so that for most engineering purposes, the published data for Washington, D.C., may be used.

Washington, D. C. lies at the western edge of the middle Atlantic coastal plain,

about 50 miles east of the Blue Ridge Mountains and 35 miles west of Chesapeake Bay. Elevations range from a few feet above sea level to about 400 feet in parts of the NW section of the city.

Summers are warm and humid and winters mild; generally pleasant weather prevails in the spring and autumn. The coldest weather normally occurs in late January and early February, when average low temperatures are in the upper twenties and average high temperatures in the middle forties. The warmest weather normally occurs during the middle of July with average daily high temperatures in the upper eighties. The record high temperature of 105.6° occurred on July 20, 1930. The record low temperature of -14.9° occurred on February 11, 1899, just preceding the worst blizzard in Washington's climatic record.

The average annual snowfall is near 20 inches, and the greatest recorded single fall was 28 inches, which occurred in the two days of the so-called Knickerbocker Storm of January 1922. This storm, in which the snowfall accumulation caused the collapse of the Knickerbocker Theater roof, resulted in the loss of many lives. Snowfalls approaching the magnitude of this storm, however, are rare, and the snow accumulation of the normally bad winter storms in Washington is nearer ten inches than thirty. Also, thanks to temperature and sunshine, these 10-inch falls usually melt off rapidly enough not to be too seriously inconvenient for more than two to four days - though while the fall is fresh (and usually very wet) driving is hazardous, traffic snarls frequent, foot-locomotion uncomfortable-to-impossible, schools have to be closed, and community disorganization is more or less general.

The normal annual precipitation is near 41 inches. No well pronounced wet and dry seasons are evident, rainfall being well distributed throughout the year. The

greatest amount for a 24 hour period was 7.31 inches, which occurred on August 11-12, 1928. The longest period without appreciable rainfall extended from October 15 to November 11, 1901 - a total of 28 days.

The average date of last killing frost in spring is April 10 and the latest recorded date May 12, 1913. The average date of the first killing frost in the fall is October 28 and the earliest recorded date October 2, 1899. The average length of the growing season is 200 days.

Washington averages 33 days a year with thunderstorms. During summer months they often bring sudden and heavy rain showers and may be attended by damaging winds, hail, or lightning. On June 9, 1929 a violent local thunderstorm with wind gusts up to 100 miles an hour was recorded. Two severe hailstorms with resultant damage estimated at $100,000 or more are recorded - one in April 1938 and one in May 1953.

Tornadoes rarely occur, but two are recorded with resultant damage of $100,000 or more - one in April 1923 and one in November 1927.

Tropical disturbances occasionally, during their northward passage, influence Washington's weather - mainly with high winds and heavy rainfall; but extensive damage from this cause is rare.

Floods occur in the Potomac River about once every two years.

Surface wind direction and speed

The hourly wind observations for an 8-year period 1945-1952 for both Washington National Airport and Quantico Marine Station were studied in detail. Tables A-1 and A-2 present the percentage frequency of the wind direction and wind speeds. As is indicated in Table A-1 the wind direction frequency in this area appears to have two maxima, one from the south and one from the northwest. This results from the fact

that the prevailing winds are from the south during the summer months and from the northwest during the winter These average wind directions should be applicable to the proposed APPR-1 site.

It is necessary to examine the wind structure during periods of precipitation to consider the effect of washout of possible waste contaminants. Table A-2 presents the percentage frequency of wind direction for WNA during those hours when precipitation is falling (this is approximately 11% of the time). As may be noted, the prevailing direction in these cases is from the NNE and NE while there is a secondary maximum from the S and SSW.

Wind direction is also important when the lower atmosphere is very stable and atmospheric diffusion is at a minimum. The frequency of this type of condition is discussed later in this report, but the wind direction frequencies are included in Table A-2. The prevailing direction associated with inversion conditions is southerly. It is also noteworthy that night-time inversions (0300 G.C.T.) are accompanied by a larger than average frequency of calms.

In Table A-3, it will be noted that a larger frequency of weaker winds (3-7 knot interval) have been observed at Quantico than at WNA and vice-versa for the stronger wind class intervals. This difference in wind speed frequencies must be due, in part, to the fact that the anemometer at WNA is somewhat higher above ground level. More than likely, because of the proposed location of the APPR-1 site, it is our estimate that a significantly larger frequency of weaker winds should be expected. This estimated frequency is included in Table A-2. These weak winds will be very predominant during the night and early morning hours (2200 to 0800). From records at Washington, D.C., the average velocity is 7 mph and may range from an average

of 10.7 mph for a windy month to 5.0 mph for a calm month. The maximum speed ever observed which existed for at least 5 minutes was 53 mph from the NE. An instantaneous gust of 77 mph has been observed once in 74 years of record.

Precipitation

As is indicated in the Climatological Review, the APPR-1 area should receive approximately 40 inches of precipitation annually which will be spread over approximately 120 days. The heaviest precipitation will be observed during the summer and spring months. The maximum amount of precipitation ever recorded in Washington, D.C., (74 years) over a 24-hour period was 7.3 inches; over 12 hours, 6.2 inches; over 3 hours, 4.1 inches; over 30 minutes, 2.4 inches; and over 10 minutes, 1.2 inches.

The average snowfall is 13.1 inches which falls on approximately four days during the winter months. The greatest amount ever recorded for a 24-hour period was 25.0 inches, and for one storm 28.0 inches. The maximum depth on the ground was 34.2 inches.

Temperature

The APPR-1 site should experience temperatures ranging from 0 to 100 degrees over a year. The average temperature will be approximately 56^{o} and the average number of degree days will be approximately 4300.

Atmospheric Stability

To study the diffusion potentiality of the Washington area, the twice daily radiosonde observations (1000 and 2200 EST) during the period October 1945 through September 1950 from WNA were examined for a five-year period to determine the frequency of atmospheric inversions. (An inversion is present if the temperature in-

creases with height, hence diffusion is retarded.) During the period investigated, there were a total of 3600 radiosonde observations. An inversion condition was found to be present 8% of the time at 1000 and 41% at 2200. It should be kept in mind that the inversion data presented here are for the time of the radiosonde observations. For the 2200 EST observations, which are shortly after the onset of the nightly inversion, fewer stable periods are experienced than would be expected during the early morning hours. Undoubtedly, if data were available for 0400 to 0600 EST, this frequency of inversion conditions would be much greater.

Hourly visibility observations for both Washington National Airport and Quantico were also examined for the 8-year period mentioned earlier. On the average, 9% of the hourly observations at WNA and 12% at Quantico were reduced to 6 miles or less by fog which is another indication of stable atmospheric conditions and poor diffusion probabilities. Fog at the APPR-1 site may be expected slightly more than that experienced at Quantico, say 15% of the time. As with the atmospheric inversion conditions mentioned above, fog should be more frequent during the night and early morning hours.

Table A-1

PERCENTAGE FREQUENCY OF WIND DIRECTION

(Based on hourly observations January 1945 - December 1952)

	Washington National Airport	Quantico
N	3.6%	5.7%
NNE	5.5	2.4
NE	5.3	5.8
ENE	3.4	4.0
E	2.3	2.8
ESE	2.2	2.3
SE	3.4	5.8
SSE	6.6	5.8
S	10.1	8.5
SSW	10.9	5.0
SW	4.9	6.0
WSW	3.3	2.9
W	3.9	9.8
WNW	8.1	7.4
NW	10.1	9.7
NNW	7.0	8.1
CALM	9.2	8.0

Table A-2

PERCENTAGE FREQUENCY OF WIND DIRECTION

(Based on hourly observations October 1945 through September 1950)

	When Precipitation Is Falling	When Inversion Base Is Below 500 ft. MSL	
		0300GCT	1500 GCT
N	5.4%	2.0%	1.5%
NNE	12.8	2.1	3.6
NE	12.8	3.1	3.9
ENE	6.7	1.5	0.6
E	3.6	1.1	2.2
ESE	3.3	0.5	4.7
SE	4.0	2.2	3.6
SSE	5.9	6.2	23.7
S	8.1	13.8	15.8
SSW	9.0	21.8	10.4
SW	4.4	10.8	6.8
WSW	2.5	3.8	0.8
W	2.4	3.2	4.3
WNW	3.8	4.2	5.3
NW	6.8	5.9	3.1
NNW	6.8	4.1	6.2
CALM	3.5	14.0	3.6

Table A-3

PERCENTAGE FREQUENCY OF WIND SPEED GROUPS (KNOTS)

(Based on hourly observations January 1945 - December 1952)

	Calm	3-7	8-12	13-20	21-30	31-40	40
Washington National Airport	9.2	27.6	33.8	24.7	4.5	0.2	*
Quantico	8.0	52.1	30.8	8.6	5	*	0
Estimate for APPR-1 Site	12	60	20	5	3	-	-

* Less than 0.1%.

APPENDIX A-2 - GEOLOGY AND HYDROLOGY

Area of Investigation

The Fort Belvoir Military Reservation lies in both the Coastal Plain and the Piedmont Plateau Physiographic provinces. The proposed reactor site, however, lies only in the Coastal Plain province. References to the Piedmont Plateau Physiographic province will be limited to subsurface geologic and hydrologic information that might have a bearing on the site.

The proposed reactor site which is about 500 feet square, extends from the water's edge, Gunston Cove, back and up the slope in a northeast direction to an elevation of about 60 feet above mean sea level. This area lies between two small streams that rise a short distance back from Gunston Cove which joints the main channel of the Potomac River about 500 yards southeast of the site.

Geology

Immediately underlying the proposed site are unconsolidated deposits of Cretaceous age. These deposits are about 450 to 500 feet thick, and dip to the southeast at a rate of about 30 feet to the mile. Below the unconsolidated strata are granitic rocks of the same type as those which crop out a short distance northwest of the area under consideration. These granitic rocks comprise the so-called "bedrock", and are of the pre-Cambrian age.

The unconsolidated rocks, which are Cretaceous in age, consist of sands, gravels, and clays. These strata have been correlated with the Potomac group, which includes three formations - The Patuxent, Arundel, and Patapsco in Maryland. In this area, however, these sediments are represented by near shore, or even terrestrial deposits, and no differentiation of all formations has been possible.

The logs in table A-4 show the Cretaceous rock penetrated in the drilling of wells at the Fort Belvoir Military Reservation. The logs show the nature of sediments penetrated and the depth to bedrock at these points. The elevation of land surface at these wells is estimated.

Earthquake History

This is not an area of frequent earthquakes. Only one earthquake is reported in N. H. Heck's Earthquake History of the United States. This earthquake occurred at 5:22 a. m., August 31, 1861. The quake's epicenter was at 38.8° north latitude and 77.0° west longitude. The intensity of this shock was 5 on the Rossi-Forel scale of intensity. A quake with an intensity of 5 on this scale is described as a shock of moderate intensity, generally felt by everyone; disturbance of furniture and ringing of some bells.

Surface-Water Hydrology

The proposed reactor site, as mentioned above, is adjacent to Gunston Cove. Gunston Cove, an inlet of the Potomac River, is formed by the submersion of the lower parts of valleys of the Accotink and Pohick Creeks.

There are no published data on temperatures and chemical quality of the Potomac River water near this site. Oral reports from Interstate Commission on the Potomac River Basin, however, indicate that the temperature of samples of water from the Potomac River between Marshall Hall and Hallowing Point ranged from 32°F. to 90°F. The river is tidal, but the chloride content of the water at these same points has not exceeded 20 parts per million. It should be noted, however, that these temperatures and chloride determinations are not the result of a continuous sampling over an extended period of time. They are, rather, isolated determinations made over a period

of years, and the conditions under which the samples were taken are not known The chloride content of course might be different at different depths and in different parts of the channel. Discharge of the river and the tides also may cause differences in chloride content.

As the Fort Belvoir Military Reservation is between the sampling points for the analysis mentioned above, it is reasonable to expect that the chloride content of the river opposite the proposed reactor site might be comparable to that noted above

However, another factor to consider in evaluating the temperature and chemical quality of surface water near the proposed reactor site is that Gunston Cove is an inlet of the Potomac River, which receives fresh water from two small streams (Accotink and Pohick Creeks). This fresh-water discharge into the cove tends to freshen and/or hold out salt water from the Potomac.

Ground Water Hydrology

Occurrence and Movement of Ground Water

Precipitation falling to the earth's surface either percolates down through the soil, evaporates, or moves along the land surface until it enters surface streams, lakes, or the ocean.

The water that percolates downward into the soil either is intercepted by roots of vegetation or percolates down to the zone of saturation, the upper surface of which is the water table. When water is added to the zone of saturation it tends to make a high point on the water table. These points of high water table are characteristic of points of recharge, whereas points of discharge such as springs, seeps, or wells are low points on the water table. Ground water moves from point of recharge to points of discharge through the interstices of unconsolidated rocks, and through fractures in consolidated rocks.

In the Fort Belvoir area ground water occurs in both consolidated and unconsolidated rocks. In the area northwest of the proposed reactor site consolidated rocks consisting of granites and gneisses crop out at the surface. The consolidated rocks are relatively impervious, but they have been fractured and ground water occurs and moves through these fractures. The productivity of wells drilled into these rocks is dependent upon the size and number of fractures intercepted. As the size and number of fractures generally decrease, the chances of getting water are very poor at depths of more than about 350 feet in rocks of this type. Yield of such wells is small, and some of them yield little or no water.

At the proposed reactor site the area is underlain by unconsolidated gravels, sands, and clays for a depth of about 500 feet. In these unconsolidated deposits ground water occurs in the sands and gravels in which the water moves through the interstices between sand grains. In these deposits a properly constructed well drilled into a saturated sand would produce water. The amount of water that can be produced from such a sand is dependent upon the hydrological characteristics of the aquifer. Wells in aquifers of this type usually are more uniform in production than wells in fractured consolidated rocks.

Ground Water Use at Fort Belvoir

Little factual information is available regarding ground water in the Fort Belvoir Military Reservation. The water supply for the reservation itself is obtained from Accotink Creek. Three drilled wells, however, are interconnected with this surface-water supply, but they are used only for emergencies and supplemental supplies. In addition to the three wells mentioned above, the Engineer Research and Development Laboratories have one drilled well, used to supply cooling water to the climatological laboratories.

Table A-5 shows the available information on the records for these four wells. Chemical analysis of water from each well is given in table A-6.

Evaluation of the Proposed Site

It is believed that the proposed site, considering the geologic and hydrologic factors, is a reasonably satisfactory one for the construction and operation of a portable power nuclear reactor.

It is understood that the loading of the reactor will be less than 4,000 pounds per square foot. From the only logs available showing subsurface materials, table A-4, it is surmised that in the excavation for this proposed reactor building the material believed to underly the site should support 4,000 pounds per square foot of loading.

The earthquake history of this area indicates no potential problem from possible earthquakes. Insofar as is known, there is no reason to believe that the occurrence and intensity of earthquake shocks would be any different from what they have been in the past.

The proposed site offers reasonably good facilities for using an abundant source of river water for cooling during most of the time in any year. In that small part of the year when the temperature of the river water would be too high for efficient cooling, ground water offers a potential source of cooling water. (The availability of ground water is discussed in one of the following paragraphs.) The limited available records of temperature and chemical quality of river water indicate a fair quality of water.

The 450 to 500 feet of unconsolidated sands, gravels and clays that lie beneath the reactor site form potentially good aquifers. The four wells now on the military reservation give some indication of the quantities and quality of water available. It is reasonable to expect that a well drilled at the proposed reactor site would produce water of

of reasonably good chemical quality at a rate of 200 gallons per minute, or more. It is possible that two or more aquifers are present in this 500 foot section of alternating sands, gravels, and clays.

Ground water, if available at the reactor site, could be mixed with water from the river to lower the effective temperature of the cooling water. Ground-water temperatures will remain constant at about 60°F summer and winter, whereas the river water will range from 32 to about 90°F.

Another consideration in choosing a site for a reactor is the potential dangers of contamination of water by radioactive material and subsequent dangers to public water supplies downstream and/or down dip from the reactor site. Under normal operations the Health-Physics regulations would control any such potential contamination, but such regulations and operation standards do not take into account danger from accidental spillage. This proposed reactor site is believed to be very well situated in relation to this problem. In case of an accidental spilling of radioactive material on the ground, its possible course of travel is as follows:

If the radioactive fluid were to run overland, due to the inability of the soil to absorb it - a probability in periods of high precipitation or frozen ground - the contaminants would be intercepted by either the small streams northwest or southeast of the site or by Gunston Cove. If intercepted by the small streams the contaminant would still be discharged into Gunston Cove. From Gunston Cove the contamination would move into the Potomac River, and then into Chesapeake Bay. In no case is a public water supply taken from the Potomac River below Gunston Cove. However, there is considerable recreational use made of the lower Potomac and Chesapeake Bay area. Also damage to a highly developed fishing industry would have to be considered. Whether

an accidental spillage of radioactive fluid would contaminate the lower Potomac and Chesapeake Bay area is dependent upon the type and concentration of the fluid. However, there would be a very large dilution factor in this reach of the stream and bay.

If the radioactive fluid percolates into the soil, rather than running overland to surface streams, the probability of damage to a public supply would be very remote. The rate of travel through the soil and sub-surface material would be much slower than surface travel. Ground-water flow is measured in feet per year, rather than miles per day, as for surface flow. Whether the delay in travel time encountered in the slower flow of ground water would be enough to neutralize the contaminating fluid would, of course, depend upon the nature of the fluid.

The dangerous elements in a radioactive fluid possibly would be absorbed on the clay particles of the underlying formations, or removed from the fluid by base-exchange. If, however, the radioactive elements did reach the water table they would then move down gradient. Due to the fact that the site itself is on a peninsula-like projection of land on Gunston Cove, the elements probably would be discharged into the cove itself. In this case, it would then follow the travel course outlined in a preceding paragraph; however, there would be a considerable delay in time from the occurrence of the accident until the contamination appeared in the cove.

If the contaminated ground water did not discharge into Gunston Cove, it would slowly continue down dip in the aquifer. Eventually, the contamination might reach a public supply down dip, however, enough information is not now available to evaluate the probability of such an event.

From all considerations of the geology and hydrology, the proposed reactor site in the Engineer Research and Development Laboratories section of Fort Belvoir appears to be as satisfactory a site as could be selected in the Metropolitan Washington, D.C. area.

Table A-4
DRILLERS' LOGS OF WELLS DRILLED AT FORT BELVOIR

Fort Belvoir Well #1

Layne Well #1

Depth in feet	Thickness in feet	Material Penetrated
0	5	Gravel
6	1	Boulders
25	19	Heavy Gravel
31	6	Gravel and sand
44	13	Blue sandy clay
54	10	Fine gray sand
57	3	Brown sandy clay
67	10	Fine brown sand
79	12	Medium sand and gravel
90	11	Gray sand, some clay
100	10	Blue sand, and boulders
108	8	Dark sandy clay
216	108	Brown sandy clay
237	21	Blue sand
253	16	Hard sand and boulders
		Rock to 278', core to 290'

Fort Belvoir Well #2
Sydnor Well #2

Depth in feet	Thickness in feet	Material Penetrated
5	5	Soft sandy mud and gravel
25	20	Red clay
30	5	Red clay
40	10	Gray clay
43	3	Sticky blue clay
55	12	Sticky gray clay
58	3	Sticky gray clay
75	17	Gray clay and sand, no water
80	5	Gray sandy clay
90	10	Sticky sandy clay
100	10	Sand and clay, no water
102	2	Sand and clay, no water
112	10	Pasty sand and clay
120	8	Blue clay
138	18	Blue clay

Table A-4 (Cont.)

Depth in feet	Thickness in feet	Material Penetrated
143	5	Sandy clay
144	1	Hard streak
158	14	Sticky clay, streaked
175	17	Sticky streaked clay
180	5	Streaked clay, sticky
190	10	Red clay, sticky
200	10	Streaked clay, sticky
214	14	Sticky streaked clay
225	11	Clay with some sand
238	13	Sand and clay
240	2	Sticky blue clay
245	5	Sticky blue clay
265	20	Silty solid clay
280	15	Sandy clay
300	20	Coarse sand and clay
311	11	Coarse sand and clay
317	6	Hard sand and clay
326	9	Hard sand and clay
330	4	Shale rock
333	3	Shale rock

Table A-5

DATA ON WELLS AT FORT BELVOIR

Well Location	#1 Filter Plant	#2 About .7 Miles NNE of Filter Plant	#3 About 1.1 Miles NE of White Stone Pt.	#4 ERDL Area Climatological Laboratory
Elevation (in feet)	24	105	95	87
Depth (in feet)	245	322	375	372
Diameter (in inches)	18-10-8	10-8	8	10
Depth to Bedrock (in feet)	253	320*(2)	500*(2)	525*(2)
Water Bearing Formations (Elevations)	97-102 231-253	------	------	110-135 252-382
Water Level (in feet) (Below Land Surf., Est'd.)	8	96	84	86
Gallons (GPM)	185*(1)	136*(1)	236*(1)	175
Drawdown (in feet)	86	64	74	34
Remarks	Post Well #1 (Layne #1) Behind Filter Plant	Post Well #2 (Sydnor #2) West of Outdoor Amphitheater	Post Well #3 (Sydnor #4) About .15 miles NW of Sewage Disposal Plant #2	Post Well #4 (Sydnor #3)

*(1) 72 Hour Test - March 1945

*(2) Estimated from report test drilling near by

Table A-6
CHEMICAL ANALYSIS OF WATER SAMPLES
FROM WELLS AT FORT BELVOIR, VA.

Analyses by Geological Survey, United States Department of the Interior
(parts per million)

Laboratory	49109	49110	49111	49112
Date of collection 1954	May 18	May 18	May 18	May 18
Silica (SiO_2)	44	25	30	33
Iron (Fe), dissolved 1/	.33	.59	.56	.02
Iron (Fe), total	.59	1.2	1.6	.03
Manganese (Mn), dissolved 1/	—	—	—	—
Manganese (Mn), total	—	—	—	—
Calcium (Ca)	2.8	7.1	1.0	.7
Magnesium (Mg)	2.0	6.7	.1	.1
Sodium (Na)	—	—	—	—
Potassium (K)(Calc.)	4.1	26	7.5	9.2
Bicarbonate (HCO_3)	0	0	0	0
Carbonate (CO_3)	10	107	14	12
Sulfate (SO_4)	8.4	11	3.6	4.6
Chloride (Cl)	5.5	2.1	2.8	4.9
Fluoride (F)	.1	.1	.1	.1
Nitrate (NO_3)	.2	.3	1.6	.5
Dissolved solids Sum Residue on evaporation at 180°C	79	126	58	61
Hardness at $CaCO_3$	16	47	4	2
Non-carbonate 2/	8	0	0	0
Specific conductance (micromhos at 25°C)	75.3	177	34.4	39.6
pH	6.3	7.4	6.1	5.8
Color	3	4	35	3
Carbon Dioxide (CO_2)(Calc.)	8.0	6.7	15	30

For notes 1/ and 2/ see next page.

Table A-6 (Cont.)

1/ In solution at time of analysis.

SAMPLE NUMBER	FORT BELVOIR WELL NUMBER	LOCATION see table A-5
Laboratory No. 49109	#1	Accotink filter plant
Laboratory No. 49110	#2	.7 mile NNE Filter Plant
Laboratory No. 49111	#3	1.1 miles Northeast Whitestone Pt.
Laboratory No. 49112	#4	ERDL area.

2/ Includes hardness of all polyvalent cations reported.

APPENDIX B-1 - LEAK TESTING

Prior to the hydrostatic proof test, a bubble test is to be made using an internal air pressure of 15 psig on the container. All welded seams are to be checked for leakage by coating with detergent type soap and water. Any leaks found are to be repaired and a retest made prior to the hydrostatic proof test.

The sketch shown on page 153 indicates the equipment and connections required to make hydrostatic and leakage tests.

The test chamber is to be mounted just above the top of the vapor container shell. The test chamber is not to be connected in the circuit for the first hydrostatic test which shall be made at 75 psig. This pressure is to be held for one hour. Upon successful completion of this test a twenty-four hour leakage test is to be made. An air pressure of 75 psig $\pm$ 2 psig shall be maintained above the water in the test chamber (with vapor container completely filled with water) for a period of 24 hours. During this period, leakage shall not exceed 4 cu. ft., as indicated by fall of level in the test chamber gauge glass.

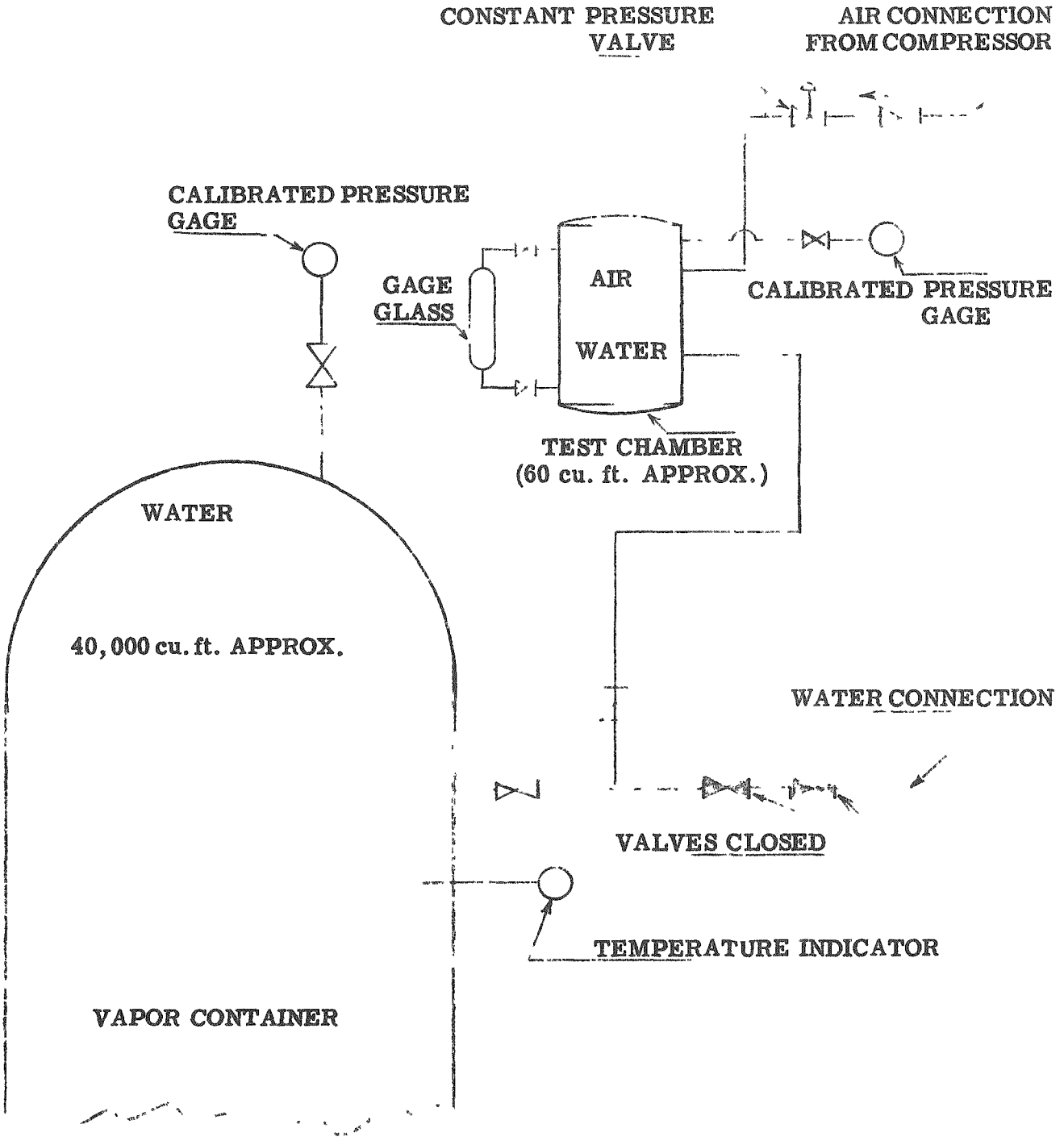

EQUIPMENT ARRANGEMENT DIAGRAM
LEAKAGE TEST PROCEDURE

APPENDIX B-2 - VAPOR CONTAINER-MISSILE PENETRATION

The selection of the maximum credible missile during a nuclear incident in the vapor container is not subject to precise calculation. The selection of the missile is a matter of judgment. Credible missiles include objects which might become free during a nuclear incident and be propelled by an expanding jet of vapor against the wall of the vapor container.

Several credible missiles were considered as outlined in the following description.

A 2 inch, 1500 lb. (test) steel globe valve. This valve weighs 50 pounds. The complete projected area of such a valve is 30 sq. in. in the bottom-on position. The projected area in the end-on position is approximately 7 sq. in. but after the initial impact the bonnet and stem would also resist penetration so that the estimated average penetrating area of this valve is 18 sq. in.

A heavy wall thermometer test well, normally welded into the primary coolant circuit, weight 5 lbs. and an area of 1.25 sq. in.

A 2 ft. length of 2 in. steel bar with a weight of 21 lbs. and an area of 3 sq. in.

A 4 ft. length of 2 in. schedule160 steel pipe with a weight of 30 lbs. and an area of 4.4 sq. ft.

The worst missiles are those which combine maximum weight in minimum area of impact.

The above credible missiles are summarized on the following page.

Type	Weight, Lb.	Projected Area of Impact, Sq. In.
2in., 1,500 lb. steel globe valve	50	18
Thermometer test well	5	1.3
2in., steel bar, 2 ft. long	21	3
2in., schedule 160 steel pipe 4 ft. long	30	4.4

VELOCITY OF MISSILE

Missiles can acquire velocity either by being struck by a jet of vapor issuing from the point of fracture and being propelled by that jet, or if the missile is hollow and contains fluid at the time of rupture, the missile can be self-propelled by the expanding fluid.

The problem becomes one of determining the velocity of the missile and its kinetic energy and establishing whether or not such a missile will penetrate the vapor container wall.

SELF-PROPELLED MISSILES

Of the above tabulated credible missiles, the only one which could contain fluid and be self-propelled is the 2 inch schedule 160 pipe.

If the pipe were initially filled with 1,200 psi, 450^{o}F water, the available energy in the fluid when expanded to final pressure in the vapor container (assumed atmospheric as the worst case) is 38 BTU per lb. of fluid. The weight of water per foot of pipe is 0.8 lb. and this has a kinetic energy, if all the thermal energy were converted, of 23,000 ft-lb per ft of pipe. Assuming that the pipe, which weighs 7-1/2 lb per ft. and half the weight of the water is accelerated through the entire travel, the corresponding final velocity is 435 fps. The available maximum travel within the vapor container is

approximately 40 ft. and such an object would reach a velocity of approximately 435 fps in that distance.

Similarly, if such pipe were filled with 425 psi saturated steam at the instant of detachment, the available heat energy for expansion to atmospheric pressure is 255 BTU per lb. The weight of such fluid in one foot of pipe is 0.17 lb. and the kinetic energy of the steam is 30,000 ft.lb. per ft. of pipe. This results in a velocity of 510 fps, if all the thermal energy of the fluid went into developing kinetic energy. Again, such an object would reach a velocity of approximately 510 fps in 40 ft. of travel.

Consequently, the velocity of a self-propelled missile has been taken at 500 fps, which is conservative, since it has been assumed that all the energy of a fluid is transferred into kinetic energy of the missile at 100% efficiency.

JET PROPELLED MISSILE

A credible missile upon being detached may be propelled by the jet of escaping fluid and continue in that jet of fluid until it strikes the wall of the vapor container. The jet, which has mass and velocity, imparts impulse to the missile from which the increase in velocity of the missile from an initial state of rest can be determined. With the impulse force known, first the acceleration and then the final velocity of the missile in 40 ft. of travel can be calculated.

The fluid pressure,initially at 1,200 psi and 450°F, drops very rapidly to saturation pressure of 423 psia by the expulsion of a few pounds of water at the rupture opening. The 423 psia fluid expands into the vapor container and when expanded to 15 psia reaches a peak velocity a few feet from the orifice of rupture. The missile is propelled by and accelerated in this jet of vapor. After the jet has fully expanded, that is, when the jet has reached vapor container pressure, the assumption is made that the jet continues to

propel and accelerate the missile until the missile impinges on the vapor container wall. Since no data have been found which would determine the shape of the jet between its point of maximum expansion and the vapor container wall, it has been assumed that the jet moves at constant velocity with all elements of the jet remaining parallel to each other rather than continuing to expand at some angle. This is conservative. The impulse of the vapor jet acting on the missile provides force to accelerate it. There is neither distance nor time for the missile to reach the velocity of the jet, but it does reach the theoretical velocity calculated below.

RATE OF FLOW OF PROPELLING JET

The rate of release of fluid in the jet depends on the area of the rupture and the velocity of the issuing fluid. It has been assumed that a missile of the above type would be associated with an opening approximately 3 in. in diameter as might result from a 2 in. valve or other object tearing out a 2 in. nipple by which it was attached to the primary coolant circuit. Since the size and shape of such a rupture opening is unknown, no coefficient of contraction has been used. Use of a conventional coefficient of 0.7 would indicate a 3.6 in. diameter opening.

In the following:

Subscript m refers to the missile
Subscript f refers to the fluid

With an isentropic expansion between 423 psia initial pressure and atmospheric pressure and a coefficient of velocity of 0.9 due to friction in the orifice, the velocity of the jet will be given by:

$$V = C_v \sqrt{2g \frac{\Delta P}{\rho}}$$

$$\rho = 52 \text{ lb/ft}^3$$

$$V = 243 \text{ ft/sec.}$$

that is, the velocity of the issuing jet near the orifice of rupture is 243 fps.

The area of a 3 in. hole is .049 sq. ft. and the weight rate of flow of the fluid is given by:

$W_I = V_I \rho$ $\quad$ A = 629 lb/sec

that is, fluid issues from the orifice at 629 lb. per sec. Neglect of the velocity of the first few pounds of fluid accelerated as the pressure drops from 1200 to 423 psia is more than compensated for by the conservative assumptions of the missile remaining in the jet at 100% efficiency for its full travel.

ANGLE OF JET

The weight of fluid actually impacting on the missile decreases after the jet expands, starting at 629 lb. per sec. at the point of rupture and decreasing as the missile moves further and further from the point of rupture, since the total weight of fluid in the jet remains constant, but as the area of the jet increases, the weight of fluid actually striking the missile on its projected area continually decreases. Thus the final velocity of the missile depends upon the assumption as to the angle of the jet.

Data obtained from the U.S. Department of Defense, Ballistics Research Laboratory in paper No. 843, AFSWP No. 768 indicate that the advancing front of jet of air suddenly released from an orifice expands at an angle of 60-70 deg. from the orifice pressure down to atmospheric pressure. On the other hand, in steam turbine practice, nozzles are designed with an angle of 10 to 15 deg. since with a greater angle the jet does not expand fast enough to maintain contact with the walls. With an unconfined and uncontrolled expansion within the vapor container and with the jet issuing from a ragged opening, it is considered that the angle is more likely to approach the greater value above, but calculations have been made both for a 12^o and a 60^o angle.

The force of the jet acting on the missile, assuming the latter to be a flat plate surface and that it turns the jet through a 90^{o} angle, is given by

$$F = \frac{W_f}{g} (V_f - V_m)$$

This force is a maximum when V_m is 0 at the start and the force becomes 0 when the V_m is equal to V_f (V_m never reaches V_f in the available distance of travel). In the above expression, the drag coefficient of the jet acting on the missile has been assumed equal to unity. For sharp edged objects the drag coefficient is reported as 0.8 to 1.0 and independent of Reynold's Number.

Computations of the impulse of the jet on the missile have been undertaken for the 2 in., 1,500 lb. valve weighing 50 lb. The computation is one by trial and error. An assumption is made of the final velocity of the missile which permits computing the impulse force from the above expression. Knowing the force, the acceleration of the missile is computed from the expression -

$$a_m = \frac{g}{W_m} \times F$$

From the acceleration, the final velocity is computed from the expression

$$V_m = \sqrt{2as + V_o^2}$$

where s is the distance traveled.

The result of the computations for the 2 in., 1,500 lb. (test) valve weighing 50 lb. with a projected area of 30 sq. in., assuming both a 12^{o} and a 60^{o} angle of expansion for the jet are:

Item	12° Angle	60° Angle
Weight of missile, lb.	50	50
Projected area of missile, sq. in.	30	30
Final velocity of fluid on expansion from 1,200 psia to 15 psia, fps	1,277	1,277
Weight rate flow of fluid from orifice, lb per sec	629	629
Distance from orifice at which the jet reaches 15 psia, ft.	7.8	1.43
Velocity of missile when jet has reached atmospheric pressure, fps	480	210
Distance jet travels at constant velocity, ft	32.2	38.7
Final velocity of missile on traveling total distance of 40 ft., fps	700	500

Since both the self-propelled missile and the jet propelled missile with an expansion angle of 60° reach a theoretical velocity of 500 fps, it is considered that this represents a credible velocity. Nevertheless, further calculations have also been made with the 700 fps missile velocity corresponding to 12° jet angle, although this is considered to be greater than a credible velocity.

The calculation of missile velocity has been made only for the 2 in., 1,500 lb. valves weighing 50 lb. The velocity reached with the other missiles would be less. As stated above, force is proportional to the weight of the fluid and since acceleration is proportional to force divided by the weight of the missile, acceleration is proportional to the weight of fluid divided by the weight of the missile. Since the weight of the fluid striking the missile is proportional to the projected area, acceleration is, in turn, proportional to the area of the missile divided by the weight of the missile. That missile which has

the greatest ratio of area to weight will obtain the greatest acceleration and hence the greatest final velocity. In the following tabulation this ratio is greatest for the 2 inch valve. Hence, other missiles would have a smaller final velocity.

Missile	Ratio of Area to Weight of Missile
2 inch steel valve	.60
Thermometer well	.25
2 inch steel bar	.14
2 inch steel pipe	.15

MISSILE PENETRATION THROUGH VAPOR CONTAINER

The degree of penetration of the wall of the vapor container has been investigated by several formulations of a semi-empirical nature which predict the penetration of steel and concrete by an object possessing kinetic energy. These have been made available by the U.S. Department of Defense. The first is that used by the Ballistics Research Laboratory. The second is that used by the Navy in their publication Nav Docks Bulletin No. P-51.

The vapor container consists of a 1/8 inch steel plate inner liner, 2 ft. of reinforced concrete and a 3/4 inch outer steel shell. The inner liner has been neglected. Manhole covers are 2-1/2 inch steel plate.

The BRL formulation for concrete is

$$P = \frac{6Wd^{1/5}}{d^2} \times \left(\frac{V}{1,000}\right)^{4/3}$$

where

P = penetration of missile, in.
W = weight of missile, lb.
d = diameter, in.
V = velocity, fps

BRL recommend that the calculated penetration in concrete be multiplied by a factor of 1.3 to insure no complete penetration due to the cracking of concrete ahead of the point where the missile stops. Since in the vapor container the 2 ft. layer of concrete is followed by 3/4 in. steel, this 1.3 factor is not considered absolutely essential.

The penetrations of the several missiles with a missile velocity of 500 fps are as follows:

Missile	2in. Steel Valve	Thermometer Well	2in. Steel Bar	2in. Steel Pipe
Weight, lb.	50	5	21	30
Area, sq. in.	18	1.3	3	4.4
Diameter, (Equiv.),in.	4.8	1.3	2	2.4
If velocity= 500 fps				
penetration, in.	7	7.5	14.5	15
penetration x 1.3, in.	9	10	19	19.5
If velocity= 700 fps				
penetration, in.	10	11	21	22
Penetration x 1.3, in.	13	14	27	29

It will be noted with the above, that none of the missiles with 500 fps penetrate the concrete nor do the missiles at 700 fps penetrate except when using the 1.3 factor. Navy Docks states that in a compound wall of steel and concrete, 1 in. of steel is equivalent to 12 in. of concrete so that if the complete vapor container wall is considered equivalent to 33 in. of concrete, there is no penetration even with 700 fps missile velocity.

The BRL formulation for penetration of steel is expressed by -

$$t^{3/2} = \frac{1/2\ m\ V^2}{K^2 \times 17,400 \times d^{3/2}}$$

where

t = wall thickness, in.

m = mass of the missile, slugs

V = velocity of missile, fps

K = a constant depending on the grade of steel and =1

d = the diameter of the missile, in.

Using the above formulation, the missile penetrations are as follows:

Missile	2 in. Steel Valve	Thermometer Well	2 in. Steel Bar	2 in. Steel Pipe
If Velocity = 500 fps				
Penetration, in.	1	.8	1.5	1.5
If Velocity = 700 fps				
Penetration, in.	1.5	1.3	2.3	2.3

Thus the 2-1/2 in. steel plate, where there is no concrete, is sufficient to prevent penetration even with 700 fps missile velocity.

The above penetrations may be rechecked with Nav Docks formulation. This is

$$D = K\ A_p\ V'$$

where

D = Depth of penetration, ft.

K = A coefficient depending on the nature of the concrete and is .00799 for mass concrete, .00426 for normal reinforced concrete, such as would be used in building construction and is .00284 for specially reinforced concrete.

$$V' = \log_{10}\left(1 + \frac{V^2}{215,000}\right)$$

V = The velocity of the missile, fps

A_p = weight of missile per sq. ft. of projected area, lb. per sq. ft.

Using the above formulation, the following calculated penetrations result:

Missile	2 in. Steel Valve	Thermometer Well	2 in. Steel Bar	2 in. Steel Pipe
Weight, lb.	50	5	21	30
Area, sq. in.	18	1.3	3	4.4
A_p, lb. per sq. ft.	400	550	1,000	1,000
If velocity = 500 fps				
Penetration, in.	8	10	19	19
If velocity = 700 fps				
Penetration, in.	12	16	30	30

With a velocity of 500 fps concrete is not penetrated. With a velocity of 700 fps, which is more than a credible velocity, two of the missiles penetrate the concrete but considering the total equivalent thickness of steel in concrete of 33 in., there is still no theoretical penetration.

APPENDIX C
ANALOG SIMULATION OF THE THERMAL KINETIC EQUATIONS

The kinetic equations describing the thermal behavior of the package reactor have been solved for a number of different perturbing factors by the ORNL Reactor Controls Computer (13). The results are presented in the form of curves of power and temperature vs. time.

The equations were derived in Reference 14. The time delay equations have been modified to describe different types of flow. In order to cover all types of flow three mathematical models were used to simulate the kinetics of the piping and plenum chamber. They are:

1. The flow of the coolant was assumed to be slug flow in the piping with some but not complete mixing in the plenum chambers.
2. Complete mixing throughout plenum chambers and piping
3. Slug flow throughout plenum chambers and piping.

It is believed that (1) is the most logical representation of the actual physical situation and therefore most of the tests were made with this type of flow.

All of the curves from Figure 1 through Figure 38 have the coolant flow represented by slug flow in the piping and some but not complete mixing in the plenum chambers of the reactor vessel. The curves from Fig. 39 through Fig. 45 are for complete mixing and the curves from Fig. 48 through Fig 50 are for slug flow.

The temperature coefficient of reactivity for the reactor has been calculated to be approximately $-2 \times 10^{-4}/^{o}$ F. However, it was desirable to

determine the effect on reactor power and the various temperatures by making the coefficient more positive. For this reason three values of the coefficient were used. For Figs 1 through 8 and Figs. 27 through 50, the temperature coefficient of reactivity is $-2 \times 10^{-4}/^{o}F$ and for Figs 18 through 26 it is $-5 \times 10^{-5}/^{o}F$ Figs 9, 10 and 11 have the coefficient as a parameter.

Fig. 1 shows the reactor power following step changes in $\Delta k/k$ of $\pm$ 0 30%, $\pm$ 0 20% and $\pm$ 0 10%. The power, after rising sharply returns to 10 Mw since the power demand was held at 10 Mw. Figs. 2 and 3 show the mean fuel, mean coolant and steam temperature, θ_F, θ_C and θ_S, for these changes in reactivity There is very little over-shoot on the fuel temperatures and none on the coolant and steam temperatures. Fig. 4 shows the coolant temperature, θ_{B_1}, at the inlet of the steam generator, the mean coolant temperature in the steam generator θ_B, and the coolant temperature at the core inlet, θ_{C_1}, for $\Delta k/k$ steps of $\pm$ 0 30%

Fig. 5 shows the effect of larger step changes in $\Delta k/k$, namely $\pm$ 0.50%, $\pm$ 0 40% and $\pm$ 0.30% on the reactor power. For this test the initial power was reduced to five megawatts.

Figs. 6 and 7 show the fuel, coolant and steam temperatures for these conditions. Fig. 8 shows the coolant temperature as it enters the steam generator, the mean coolant temperature in the steam generator and the coolant temperature at the core inlet for $\Delta k/k$ steps of $\pm$ 0.50%.

Fig 9 shows the effect of still larger changes in $\Delta k/k$, namely $\pm$ 1.0% and $\pm$ 0.75% in the reactor power. The initial reactor power was reduced to two megawatts for this test. Reducing the temperature coefficient of reactivity from $-2 \times 10^{-4}/^{o}F$ to $-1 \times 10^{-4}/^{o}F$ increases the power excursion as

would be expected. Figs. 10 and 11 show the effects of these Δ k/k steps and changes in temperature coefficient on fuel temperature, mean coolant temperature and steam temperature.

The curves shown in Figs. 12, 13 and 14 are the same tests as the curves of Figs. 1, 2 and 3 except that the temperature coefficient of reactivity has been reduced from $-2 \times 10^{-4}/^{o}F$ to $-1 \times 10^{-4}/^{o}F$. The power now shows some oscillations since there is less damping for the smaller coefficient. The fuel and the coolant temperatures show some over-shoot in this case. In Fig. 14, the negative Δ k/k steps of 0.30%, 0.20% and 0.10% were applied at the end of the fourth minute while the curves indicate that the steps were applied at the end of three minutes. The curves will be correct if the center horizontal portion of each curve is extended one minute.

Figs. 15, 16 and 17 are for the same tests as Figs. 5, 6 and 7 in which the initial power was five megawatts and the reactivity steps were $\pm$ 0.50%, $\pm$ 0.40% and $\pm$ 0.30%, but the temperature coefficient is now $-1 \times 10^{-4}/^{o}F$. The power does not oscillate as it did when the initial power was 10 Mw. The other conditions are unchanged.

Figs. 18, 19 and 20 should be compared with Figs. 1, 2 and 3 and Figs. 12, 13 and 14. The temperature coefficients of reactivity are different for each of the three groups of figures but the other conditions are the same. Brush recorder traces were taken of reactor power for all + Δ k/k steps. The shortest period indicated, for steps less than prompt critical, was 4.5 seconds and occurred for the + 0.3% step shown in Fig. 18. Figs. 21, 22 and 23 are comparable with Figs. 5, 6 and 7 and Figs. 15, 16 and 17. Figs. 23, 25 and 26

are comparable with Figs. 9, 10 and 11.

Figs. 27, 28 and 29 show the effect of oscillating the power demand. The purpose of the test was to determine whether or not a strong resonance could be obtained and consequently dangerous temperatures and pressures built up. No such dangers are apparent.

Figs. 30, 31 and 32 show the effect of power demand on reactor power, fuel, coolant and steam temperatures. In the first test the power demand was reduced from 10 Mw to 5 Mw in a step and at 4.5 minutes the power demand was raised in a step to 10 Mw. The test was repeated with the power demand reduced to 2.5 Mw. After full power was demanded, a minimum positive period of 25 seconds was produced. These tests were repeated for different flow conditions and the results shown in Figs. 43, 44, 45, 49 and 50.

The curves at the left in Fig. 23 indicate how the reactor power follows a slowly changing power demand. The curve on the right in Fig. 33 shows the reactor power as the power demand was raised to 300% rated power, held there for a few seconds and then a Δ k/k ramp of -1.0% per second was applied to scram the reactor.

Figs. 34 and 35 show the effect on power and temperature of cold water injection into the core. A step change in coolant temperature of -50° F. was applied to the core for periods of one, five and ten seconds after which a step change of $+50^{\circ}$ F. was applied to raise the coolant temperature to 431.6° F, the design point temperature.

Figs. 36, 37 and 38 are for Δ k/k ramps. The first curve of Fig. 36 shows the effect on the power of a 0.30% Δ k/k step followed by an optimum

manual compensation using a ` k/k ramp of -0 10%/sec after the initial disturbance. The ramp was three seconds long The second third and fourth curves show the effect of control rod movements on reactor power beginning at two megawatts. Twenty seconds after the 0 025%/sec ramp was initiated a sustained period of seven seconds was reached. Seven seconds after 0 15%/sec ramp was initiated, a sustained period of 2 2 seconds was reached Three and a half seconds after the 0.40%/sec. ramp was initiated, a sustained period of 0.8 second was reached. The fuel temperatures are shown in Fig 37 for the first and fourth curves of Fig 36. The steam temperature is shown in Fig 38 for about the first 10 seconds of the 0.4%/sec. ramp

If it is assumed that the coolant mixes completely in the plenum chambers and in the piping, the curves of Figs. 39, 40 and 41 are obtained for k/k steps of $\pm$ 0.30%, $\pm$ 0 20% and $\pm$ 0.10%. Here the power is seen to oscillate and fuel, coolant and steam temperatures over-shoot.

Fig. 42 shows the steam generator inlet temperature and the core inlet temperature for _ k/k steps of $\pm$ 0 30% The reactor was at 10 Mw when the step was applied.

Fig. 43 shows the reactor power for step changes in power demand The curve for a power demand of three megawatts is broken at 4 5 minutes and a portion of the curve during which the power was three megawatts was removed That part of the curve to the right of the 4.5 minute ordinate shows the power rise after the power demand was increased to 10 Mw. Figs 44 and 45 show how the fuel, coolant and steam temperature are changed by changing power demand.

Figs. 46, 47 and 48 show the effect of _ k/k steps of 0 30% ` 0 20%

and 0.10% on reactor power, fuel, coolant and steam temperature. The coolant flow for these tests is assumed to be slug flow. Note that power and temperature change suddenly.

Figs. 49 and 50 show the response of the reactor power, fuel and coolant temperature to step changes in power demand for the case of slug flow.

A comparison of the responses of the three flow models to reactivity changes indicate in general that the largest transient excursions occur with the first and third models, transport (slug) flow and combination (mixing plus slug) flow, being practically equivalent. The first order approximation model (complete mixing) gives a conservative picture of power excursions by a small percentage, and at the same time gives the least conservative picture concerning system stability.

LIST OF SYMBOLS USED IN APPENDIX C

k	Multiplication factor
P_d	Secondary power demand, Mw
P_o	Design power, 10 Mw
α	Temperature coefficient of reactivity, $^{o}F^{-1}$
θ_B	Mean primary coolant temperature in steam generator, ^{o}F
θ_{B_1}	Primary coolant temperature entering steam generator, ^{o}F
θ_C	Mean coolant temperature in core, ^{o}F
θ_{C_1}	Coolant temperature entering core, ^{o}F
θ_F	Mean fuel element temperature, ^{o}F
θ_S	Steam temperature, ^{o}F

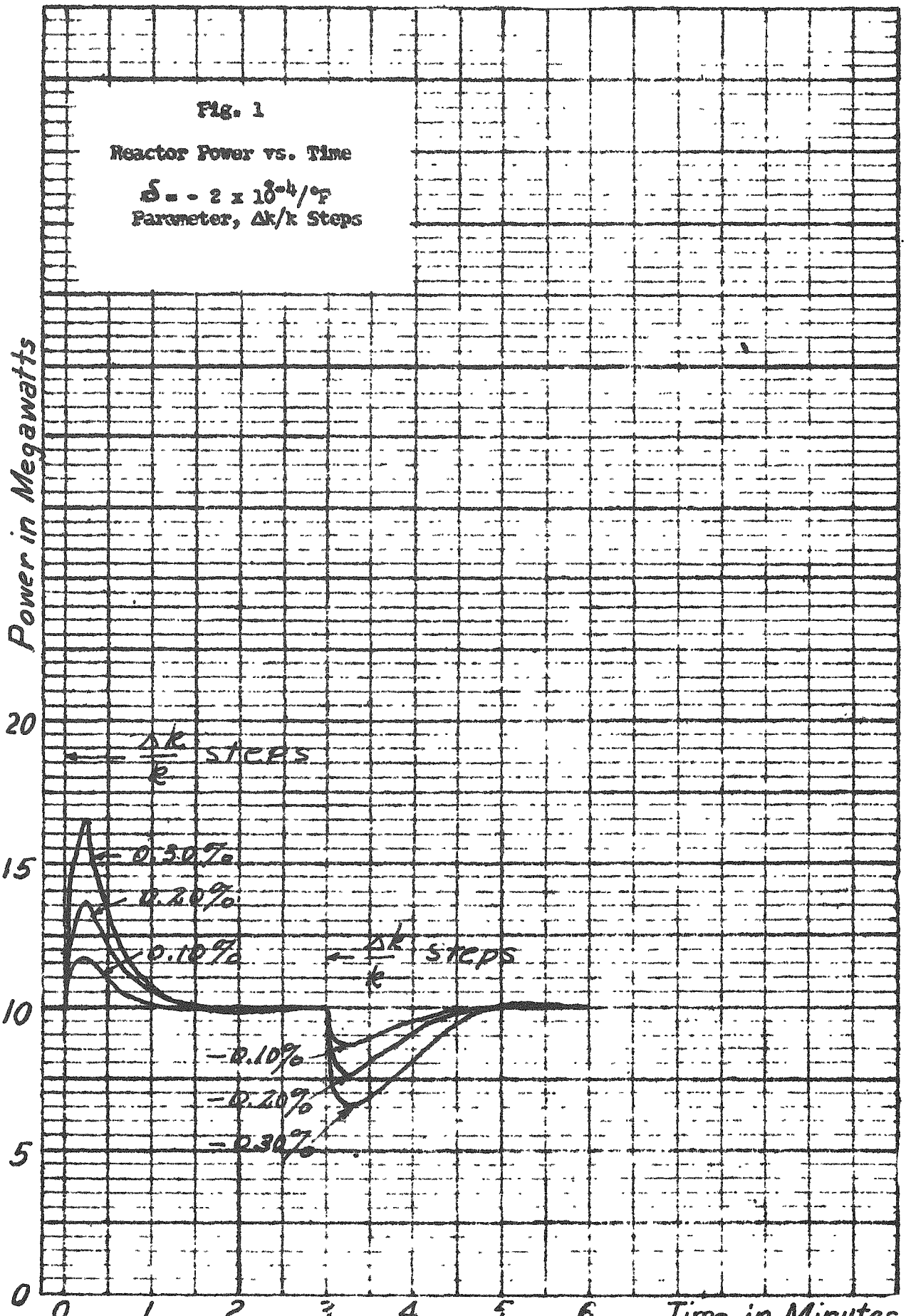
Fig. 1
Reactor Power vs. Time
δ = - 2 x 10^{-4}/°F
Parameter, Δk/k Steps
Power in Megawatts
20
15
10
5
0
0
1
2
3
4
5
6
Time in Minutes
$-\frac{\Delta k}{k}$ steps
-0.30%
-0.20%
-0.10%
$-\frac{\Delta k}{k}$ steps
-0.10%
-0.20%
-0.30%

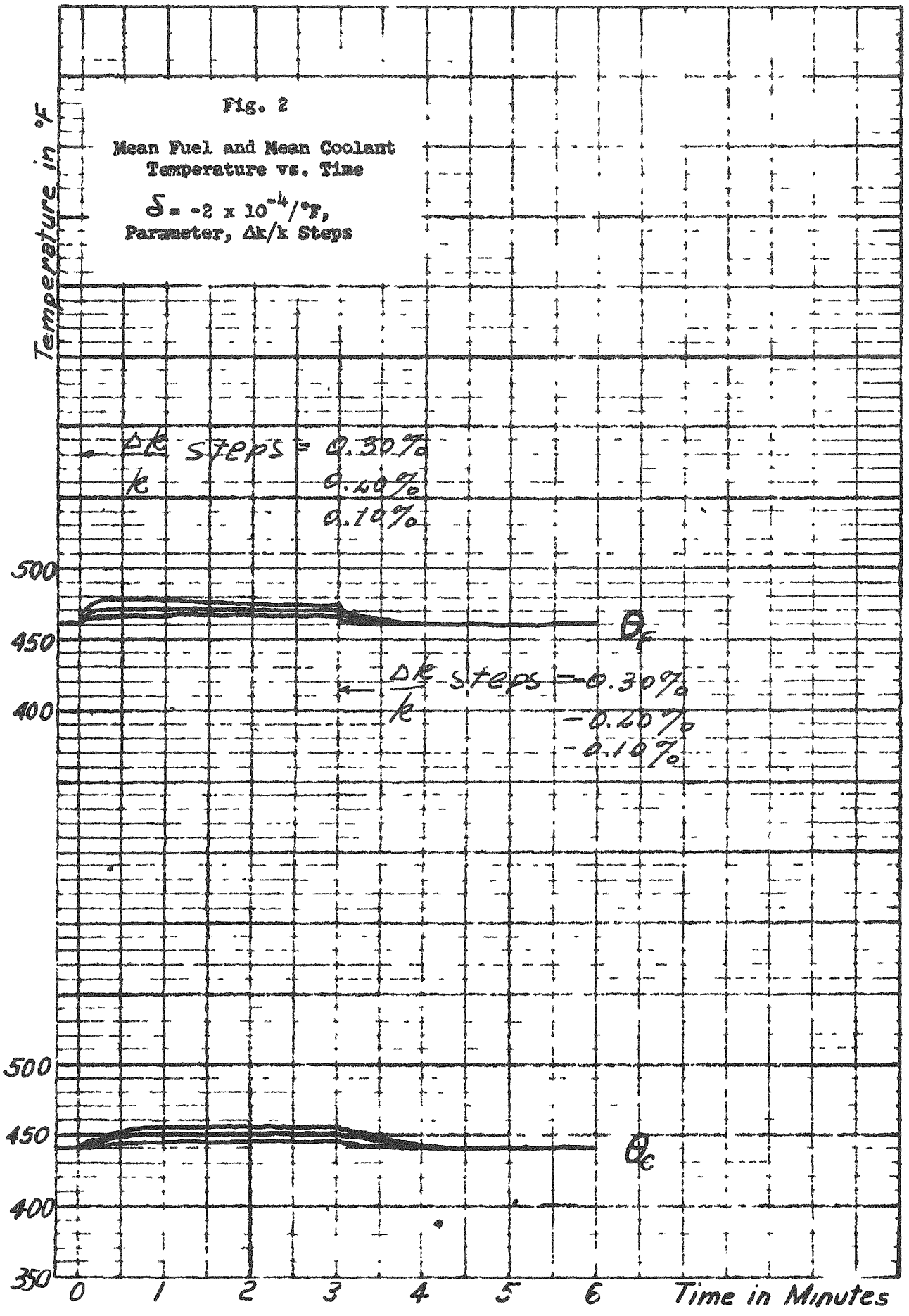
Fig. 2
Mean Fuel and Mean Coolant Temperature vs. Time
δ = -2 x 10⁻⁴/°F,
Parameter, Δk/k Steps
Temperature in °F
Δk/k steps = 0.30%
0.20%
0.10%
500
450
400
θf
Δk/k steps = -0.30%
-0.20%
-0.10%
500
450
400
350
θc
0
1
2
3
4
5
6
Time in Minutes

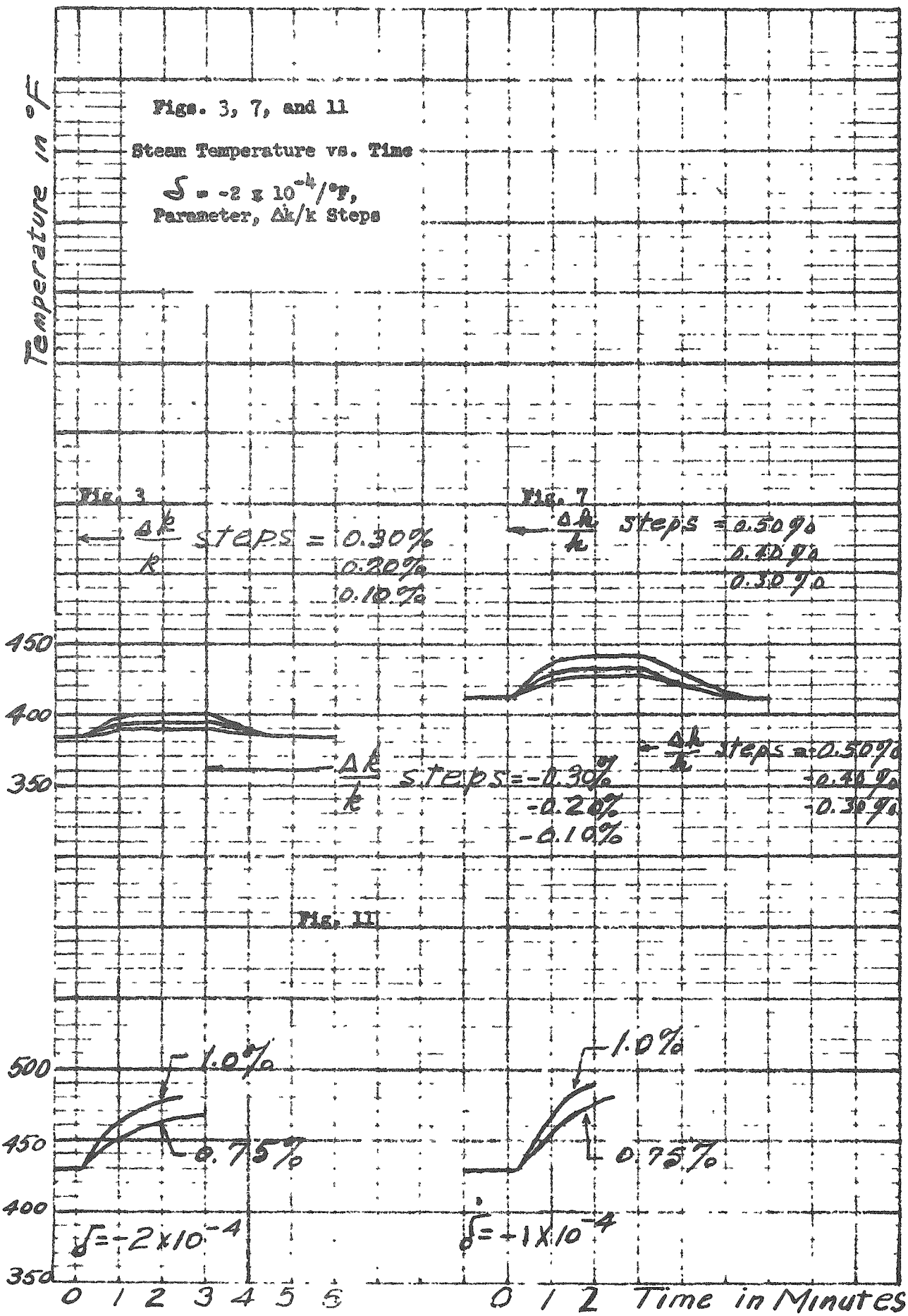
Figs. 3, 7, and 11
Steam Temperature vs. Time
$\delta = -2 \times 10^{-4}/°F$,
Parameter, Δk/k Steps
Temperature in °F
Fig. 3
$\frac{\Delta k}{k}$ steps = 0.30%
0.20%
0.10%
Fig. 7
$\frac{\Delta k}{k}$ steps = 0.50%
0.40%
0.30%
$-\frac{\Delta k}{k}$ steps = -0.30%
-0.20%
-0.10%
$-\frac{\Delta k}{k}$ steps = -0.50%
-0.40%
-0.30%
Fig. 11
1.0%
0.75%
$\delta = -2 \times 10^{-4}$
$\delta = +1 \times 10^{-4}$
350
400
450
500
0 1 2 3 4 5 6
0 1 2
Time in Minutes

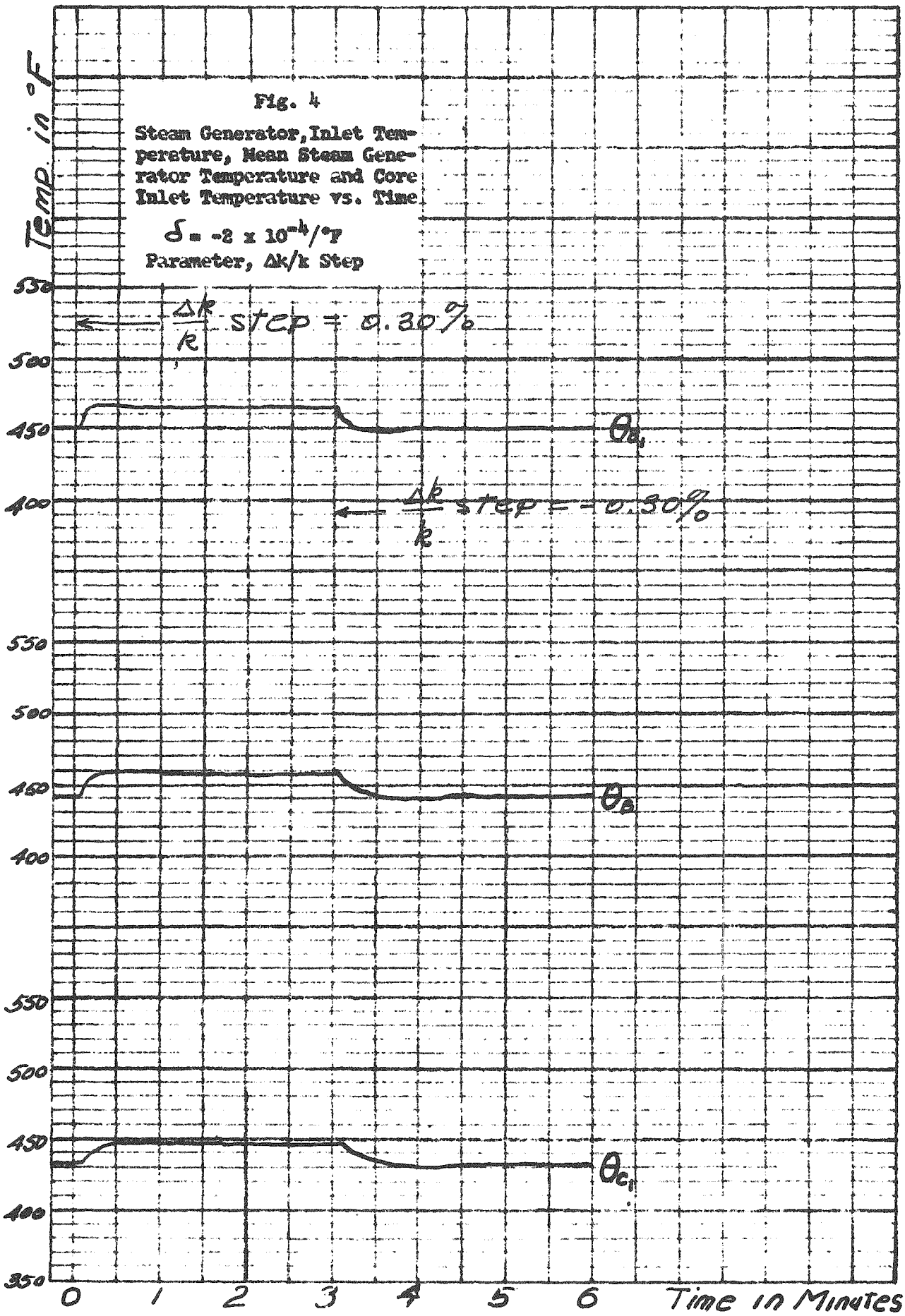
Fig. 4
Steam Generator, Inlet Temperature, Mean Steam Generator Temperature and Core Inlet Temperature vs. Time
$\delta = -2 \times 10^{-4}/°F$
Parameter, Δk/k Step
Temp. in °F
550
500
450
400
$\frac{\Delta k}{k}$ step = 0.30%
θ_{a_1}
$\frac{\Delta k}{k}$ step = -0.30%
550
500
450
400
θ_a
550
500
450
400
350
θ_{c_1}
0
1
2
3
4
5
6
Time in Minutes

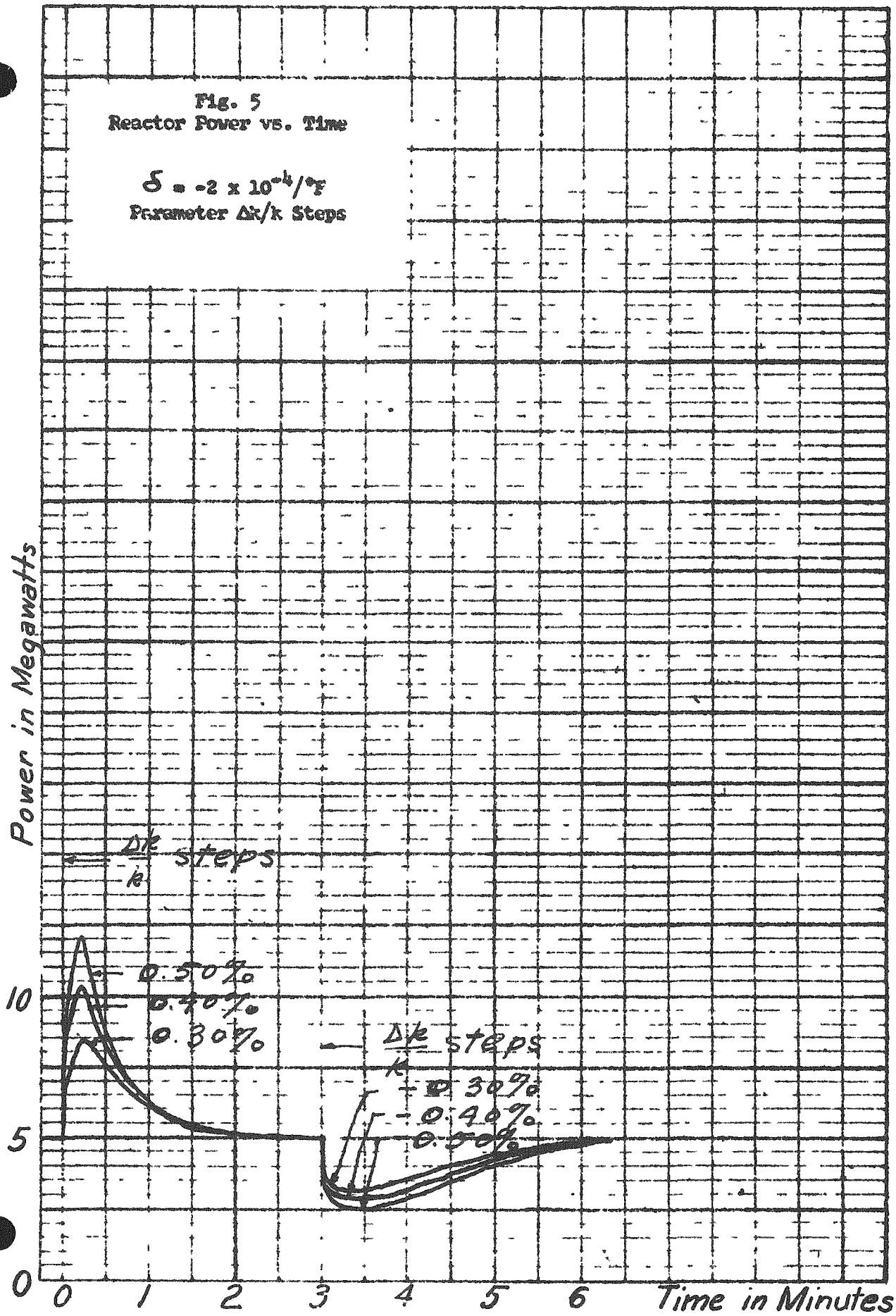
Fig. 5
Reactor Power vs. Time
δ = -2 x 10⁻⁴/°F
Parameter Δk/k Steps
Power in Megawatts
Δk/k steps
0.50%
0.40%
0.30%
Δk/k steps
+0.30%
-0.40%
-0.50%
10
5
0
0
1
2
3
4
5
6
Time in Minutes

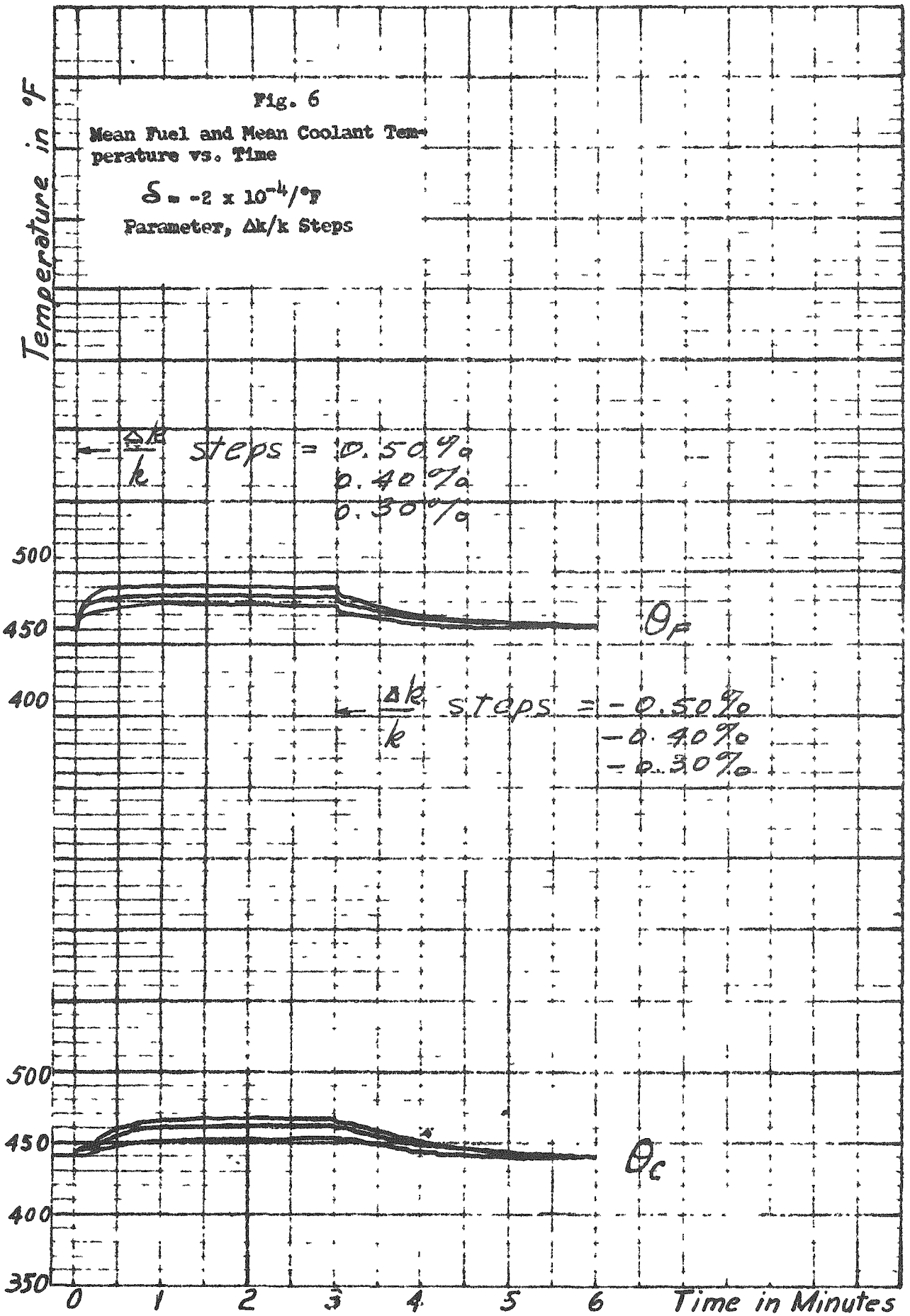
Fig. 6
Mean Fuel and Mean Coolant Temperature vs. Time
δ = -2 x 10⁻⁴/°F
Parameter, Δk/k Steps
Temperature in °F
Δk/k steps = 0.50%
0.40%
0.30%
Δk/k steps = -0.50%
-0.40%
-0.30%
θF
θC
500
450
400
500
450
400
350
0
1
2
3
4
5
6
Time in Minutes

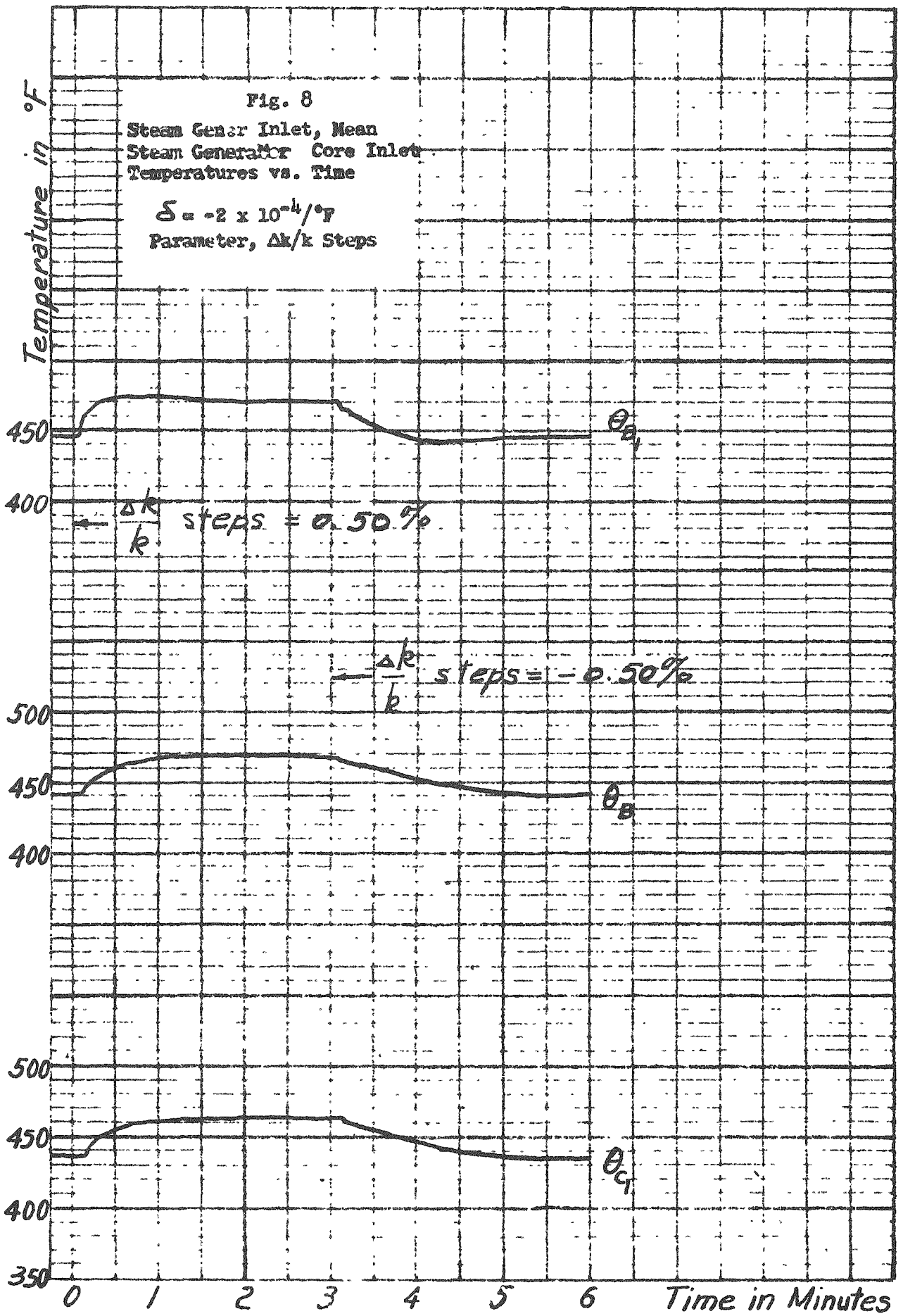
Fig. 8
Steam Gener Inlet, Mean
Steam Generator Core Inlet
Temperatures vs. Time
δ = -2 x 10⁻⁴/°F
Parameter, Δk/k Steps
Temperature in °F
450
400
Δk/k steps = 0.50%
Δk/k steps = -0.50%
500
450
400
500
450
400
350
θA
θB
θC
0
1
2
3
4
5
6
Time in Minutes

Fig. 9

Reactor Power vs. Time

Parameters $\Delta k/k$ Step and δ

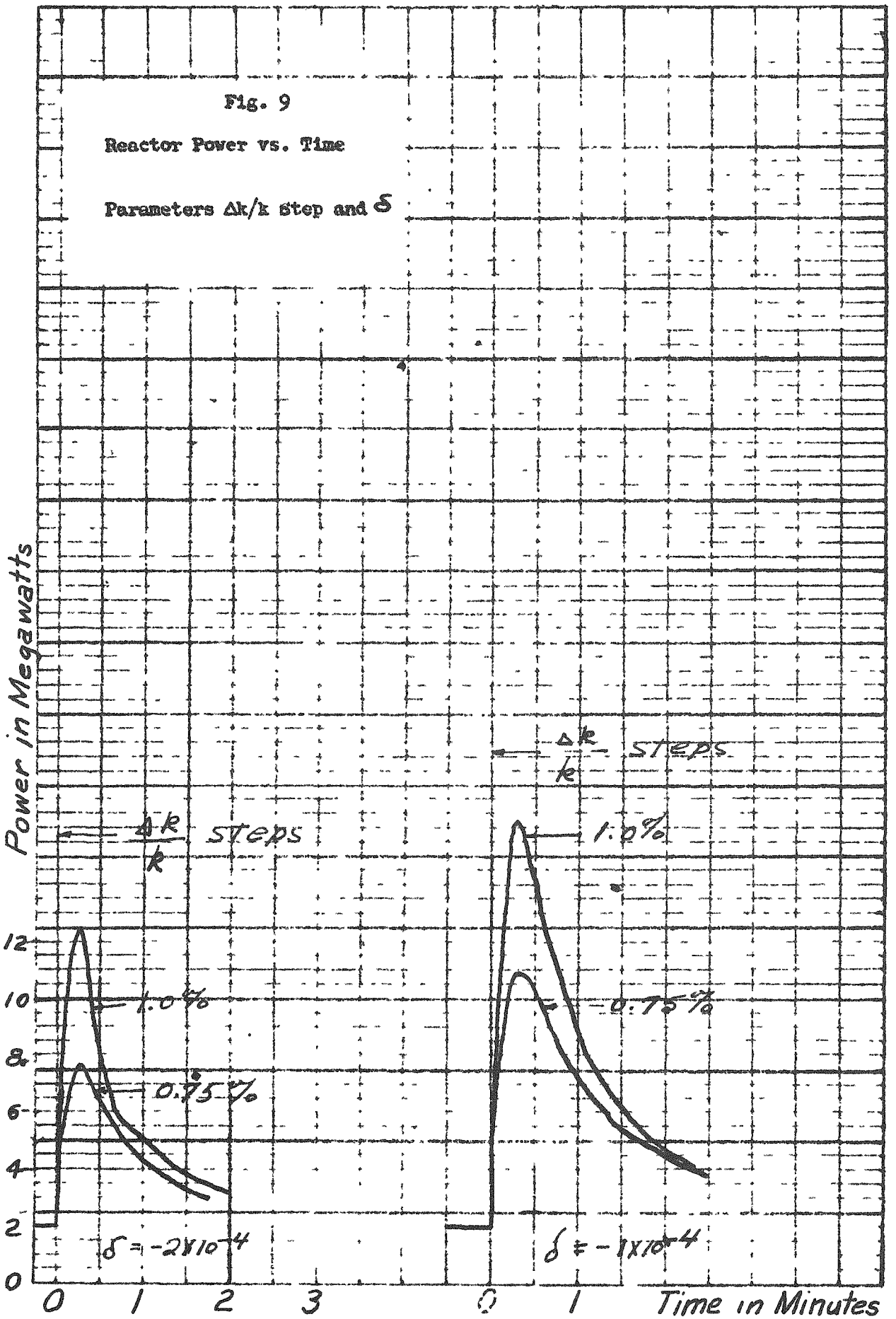

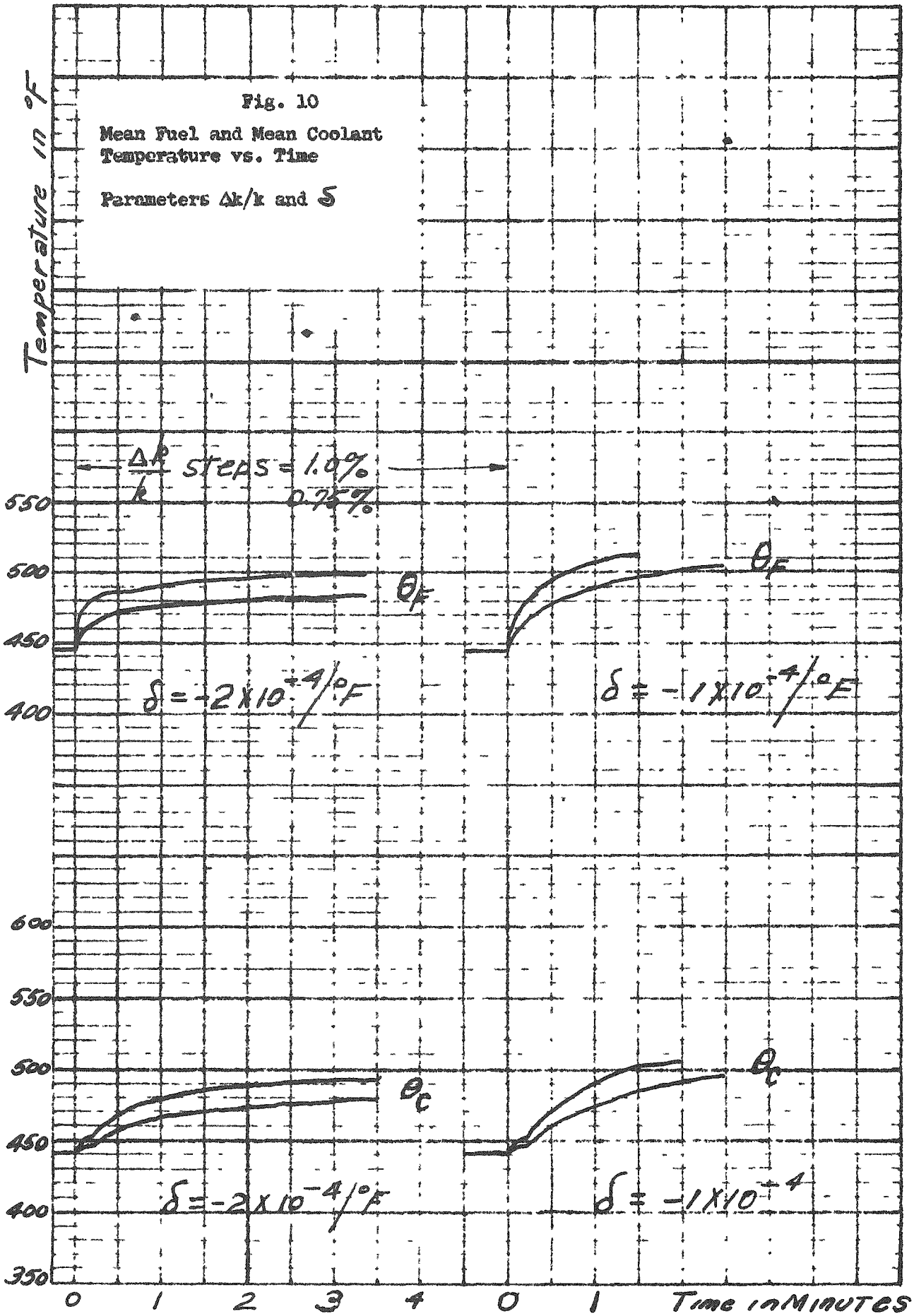
Fig. 10
Mean Fuel and Mean Coolant Temperature vs. Time
Parameters Δk/k and δ
Temperature in °F
Δk/k steps = 1.0%
0.75%
550
500
450
400
600
550
500
450
400
350
θF
θF
θc
θc
δ = -2X10⁻⁴/°F
δ = -1X10⁻⁴/°F
δ = -2X10⁻⁴/°F
δ = -1X10⁻⁴
0
1
2
3
4
0
1
Time in MINUTES

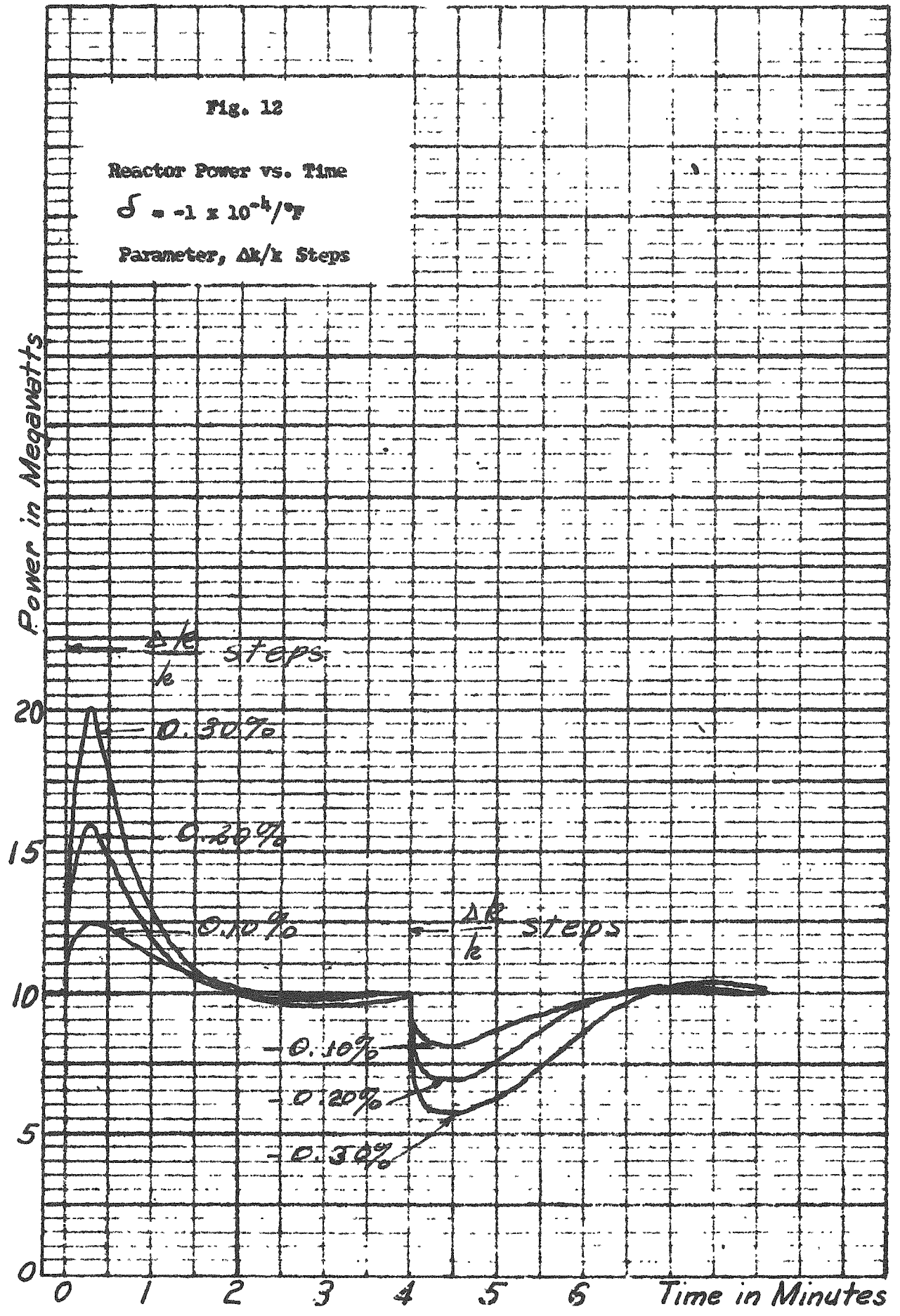
Fig. 12
Reactor Power vs. Time
$\delta = -1 \times 10^{-4}/\tau$
Parameter, Δk/k Steps
Power in Megawatts
Time in Minutes
0
5
10
15
20
0
1
2
3
4
5
6
$\frac{\Delta k}{k}$ steps
+0.30%
+0.20%
+0.10%
$\frac{\Delta k}{k}$ steps
-0.10%
-0.20%
-0.30%

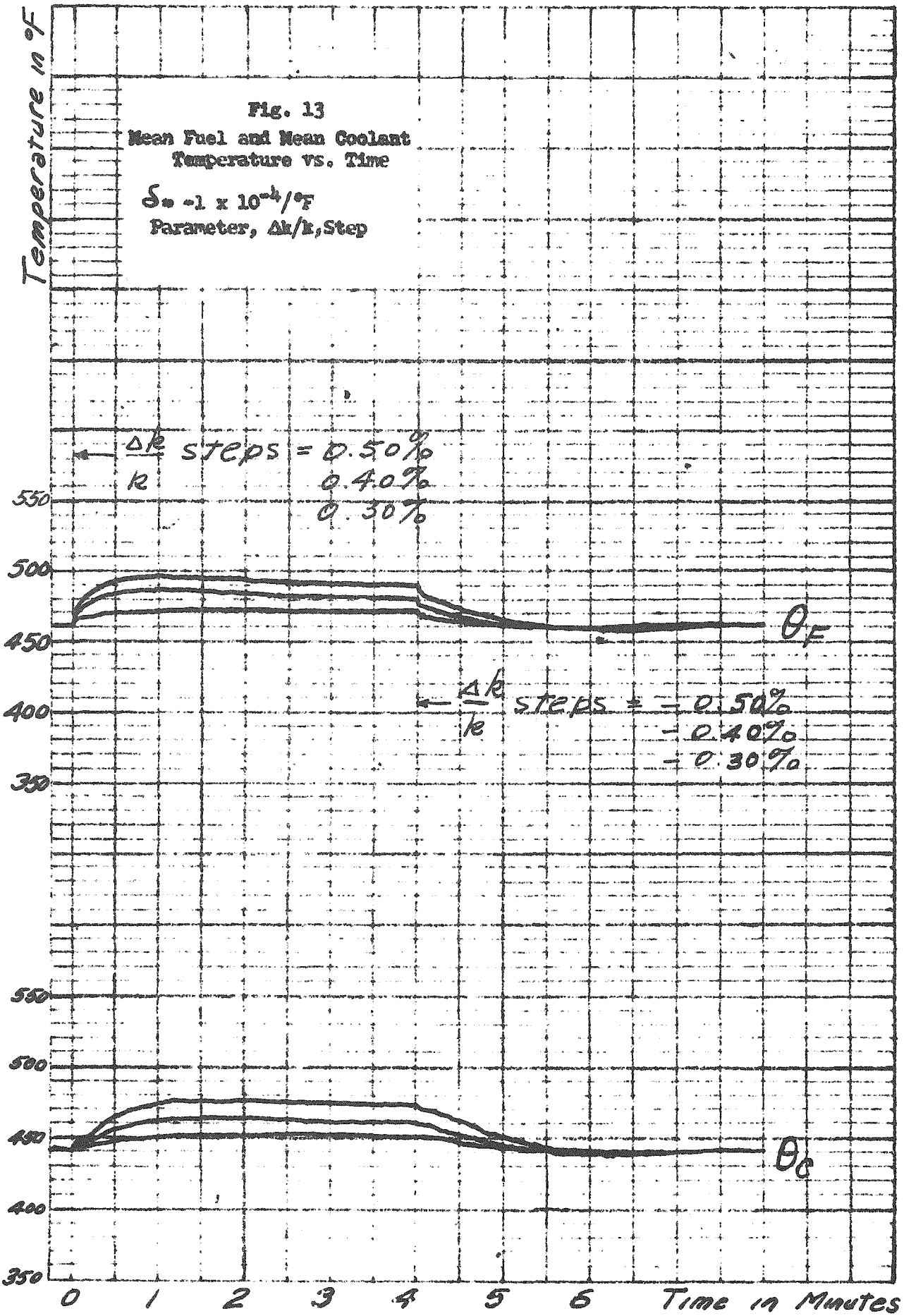
Temperature in °F
Fig. 13
Mean Fuel and Mean Coolant Temperature vs. Time
$\delta_* = -1 \times 10^{-4}/°F$
Parameter, Δk/k, Step
Δk/k steps = 0.50%
0.40%
0.30%
Δk/k steps = −0.50%
−0.40%
−0.30%
θ_F
θ_C
550
500
450
400
350
0
1
2
3
4
5
6
Time in Minutes

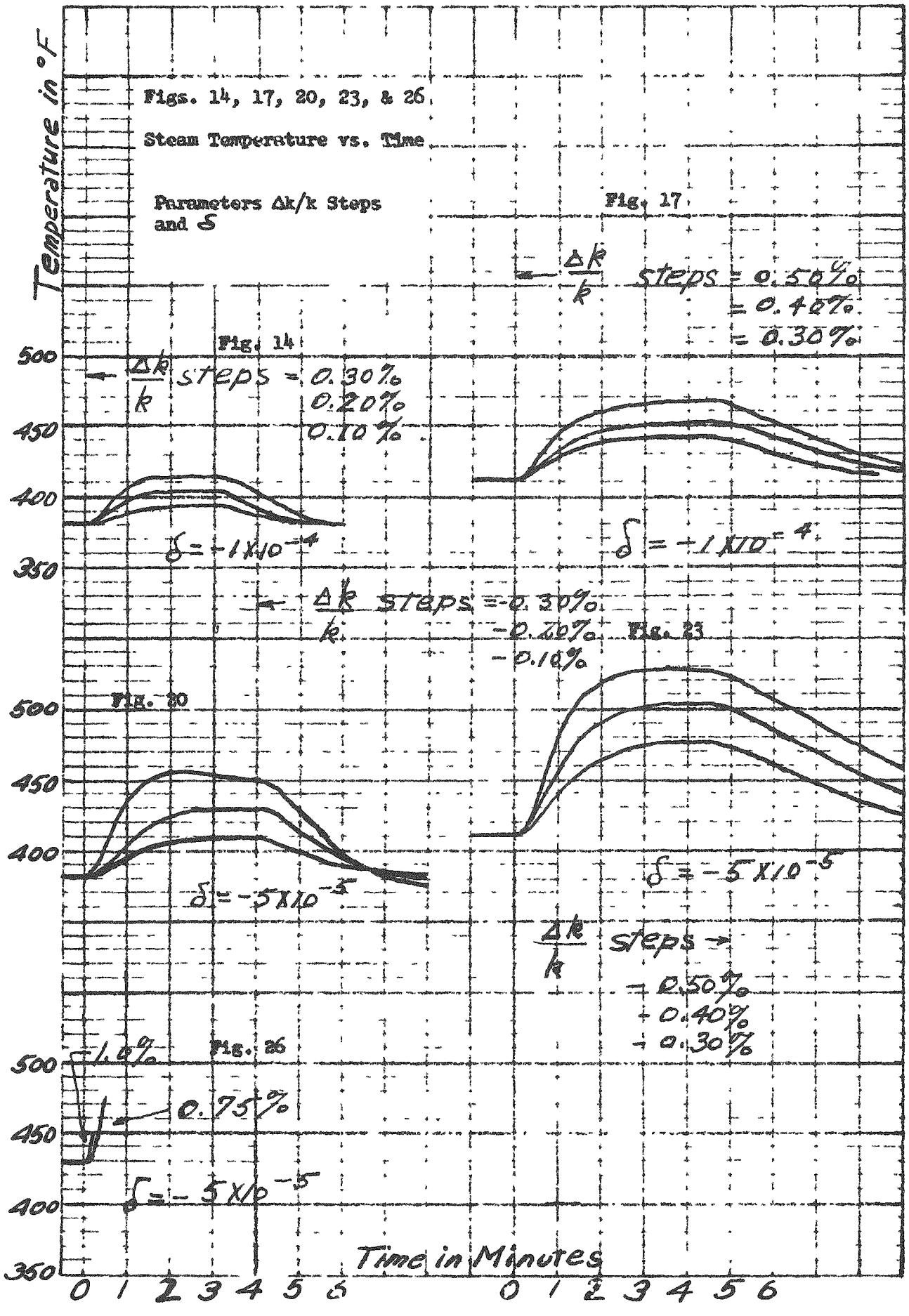
Figs. 14, 17, 20, 23, & 26
Steam Temperature vs. Time
Parameters Δk/k Steps and δ
Temperature in °F
Time in Minutes
Fig. 14
Δk/k steps = 0.30%
0.20%
0.10%
δ = -1X10⁻⁴
Fig. 17
Δk/k steps = 0.50%
= 0.40%
= 0.30%
δ = +1X10⁻⁴
Fig. 20
δ = -5X10⁻⁵
Fig. 23
Δk/k steps → -0.30%
-0.20%
-0.10%
δ = -5X10⁻⁵
Δk/k steps →
+0.50%
+0.40%
+0.30%
Fig. 26
-1.0%
-0.75%
δ = -5X10⁻⁵
500
450
400
350
0 1 2 3 4 5 6

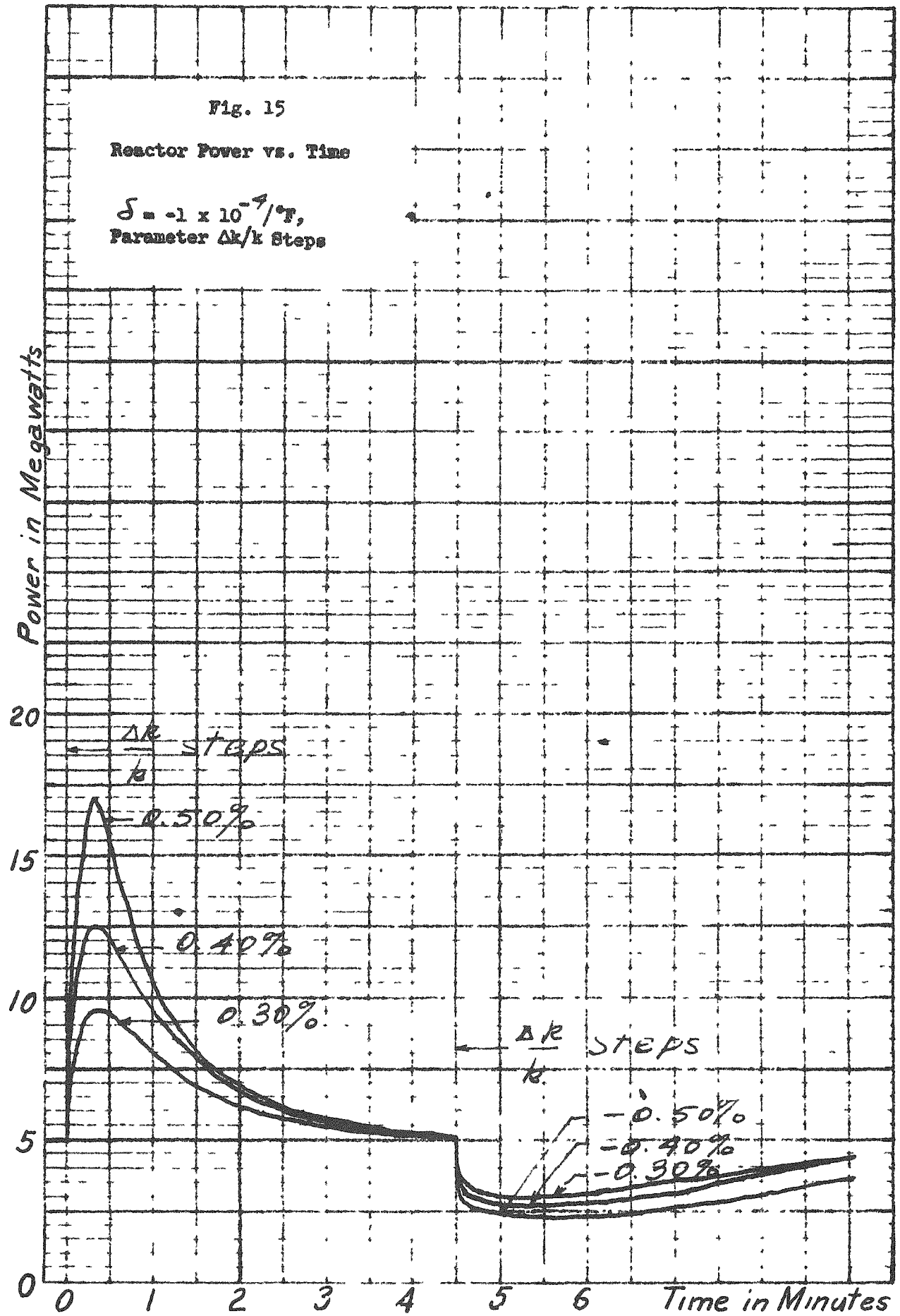
Fig. 15
Reactor Power vs. Time
$\delta = -1 \times 10^{-4}/°F$,
Parameter Δk/k Steps
Power in Megawatts
20
15
10
5
0
Δk/k steps
-0.50%
-0.40%
-0.30%
Δk/k steps
-0.50%
-0.40%
-0.30%
0 1 2 3 4 5 6
Time in Minutes

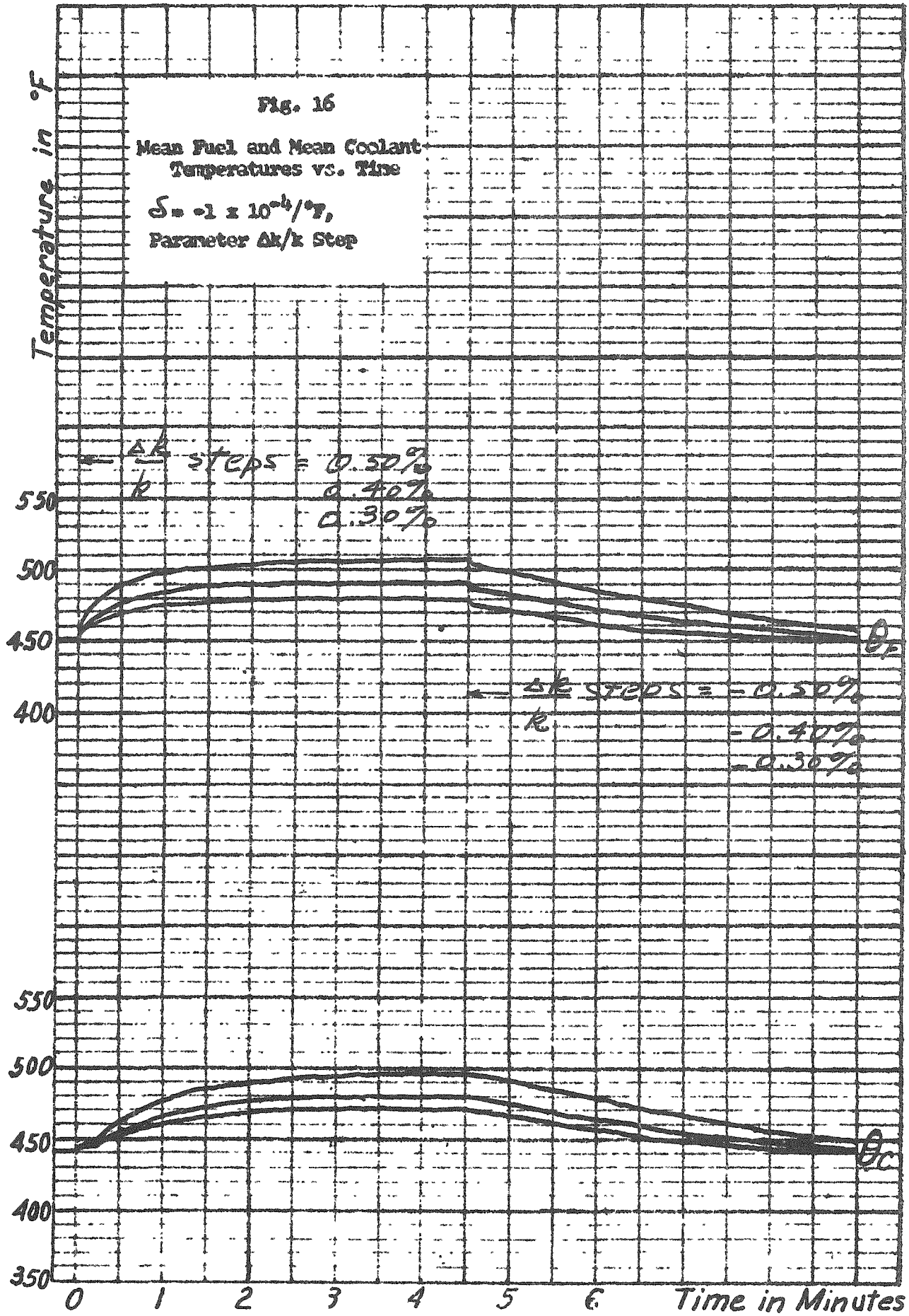
Fig. 16
Mean Fuel and Mean Coolant Temperatures vs. Time
$\delta = -1 \times 10^{-4}/°F$,
Parameter Δk/k Step
Temperature in °F
$-\frac{\Delta k}{k}$ steps = 0.50%
0.40%
0.30%
$\frac{\Delta k}{k}$ steps = -0.50%
-0.40%
-0.30%
θ_F
θ_C
550
500
450
400
350
0
1
2
3
4
5
6
Time in Minutes

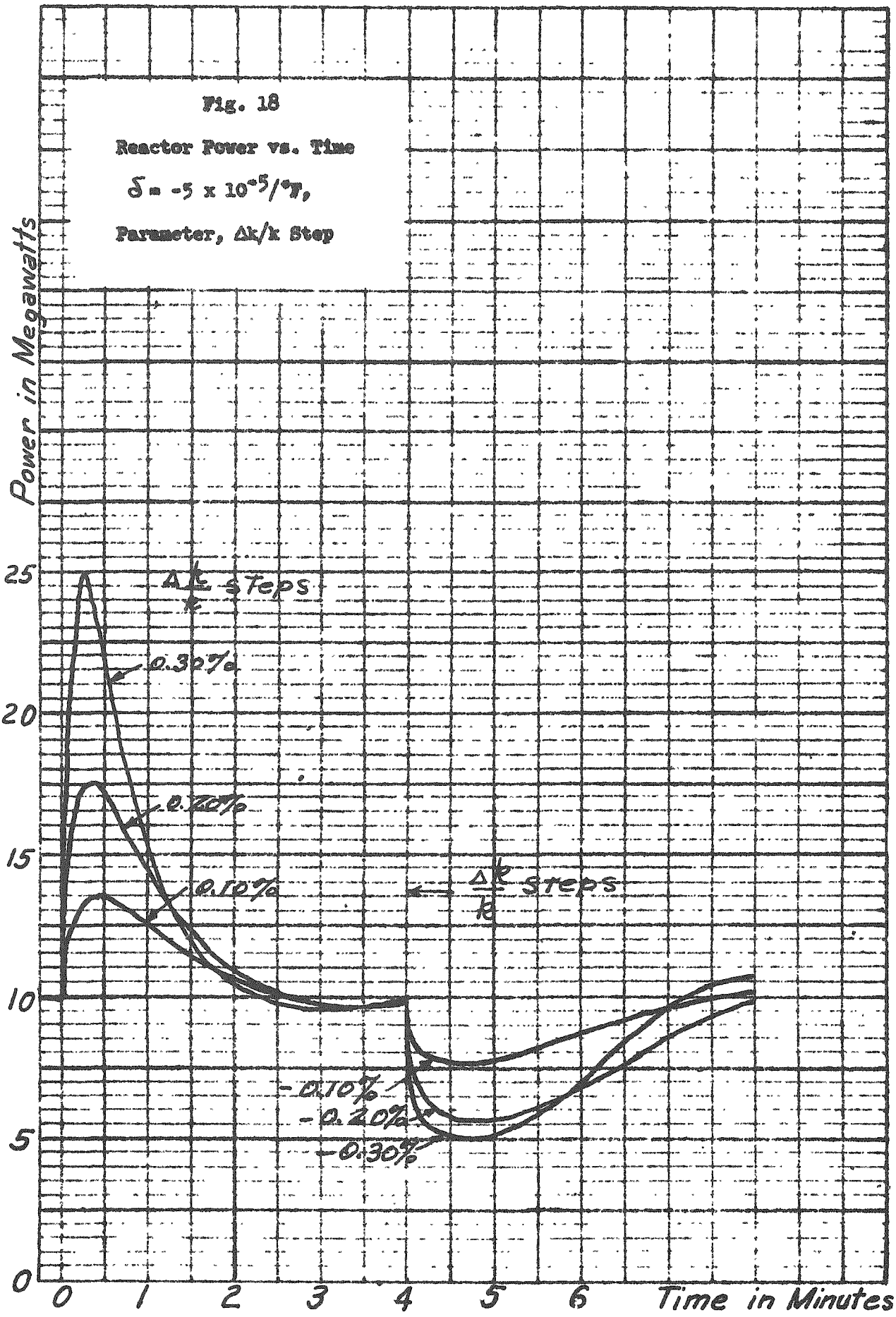
Fig. 18
Reactor Power vs. Time
δ = -5 x 10^-5/°F,
Parameter, Δk/k Step
Power in Megawatts
25
20
15
10
5
0
Δk/k steps
0.30%
0.20%
0.10%
Δk/k steps
-0.10%
-0.20%
-0.30%
0
1
2
3
4
5
6
Time in Minutes

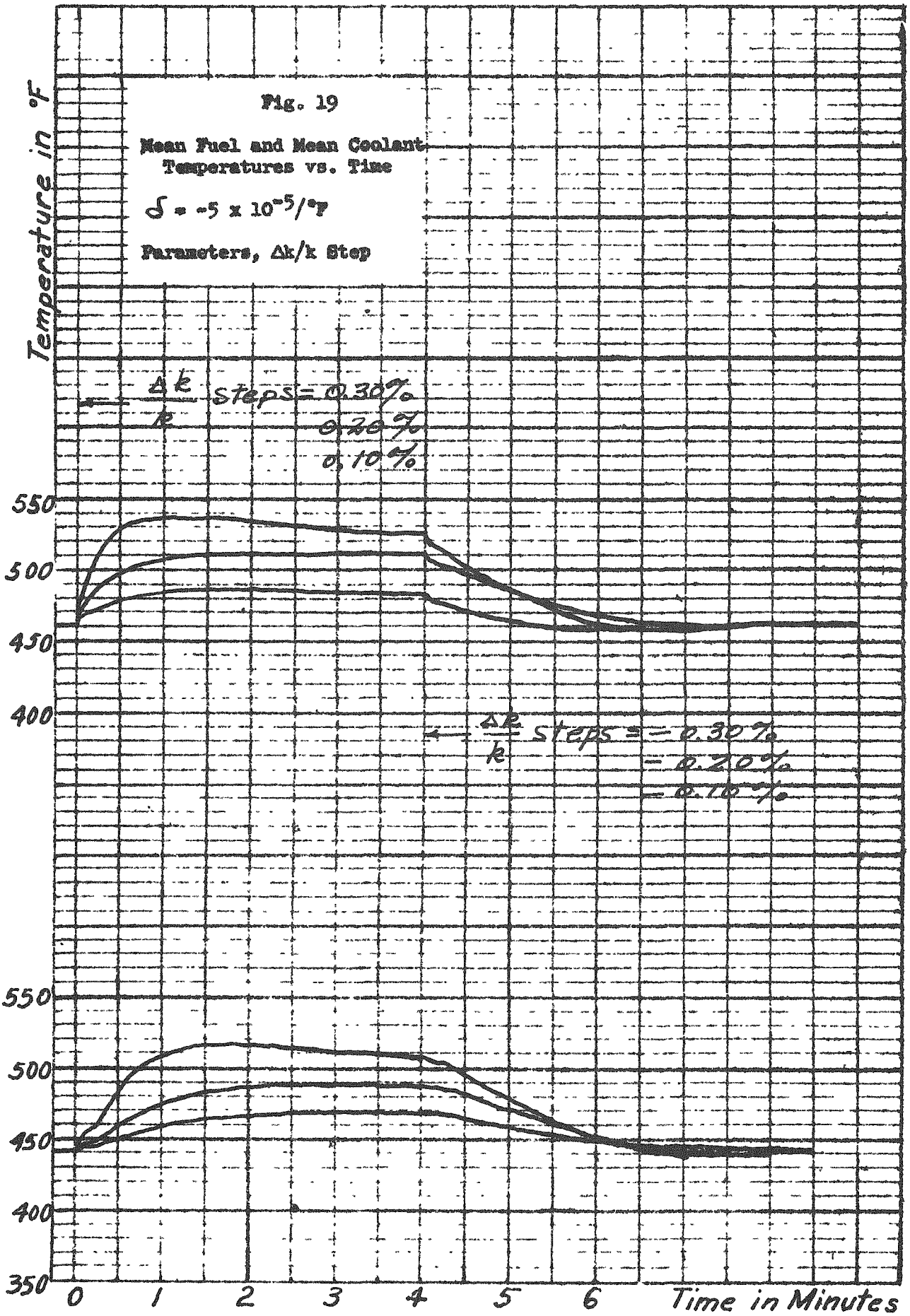
Fig. 19
Mean Fuel and Mean Coolant Temperatures vs. Time
$\delta = -5 \times 10^{-5}/°F$
Parameters, Δk/k Step
Temperature in °F
$\frac{\Delta k}{k}$ steps = 0.30%
0.20%
0.10%
$\frac{\Delta k}{k}$ steps = −0.30%
−0.20%
−0.10%
550
500
450
400
350
0
1
2
3
4
5
6
Time in Minutes

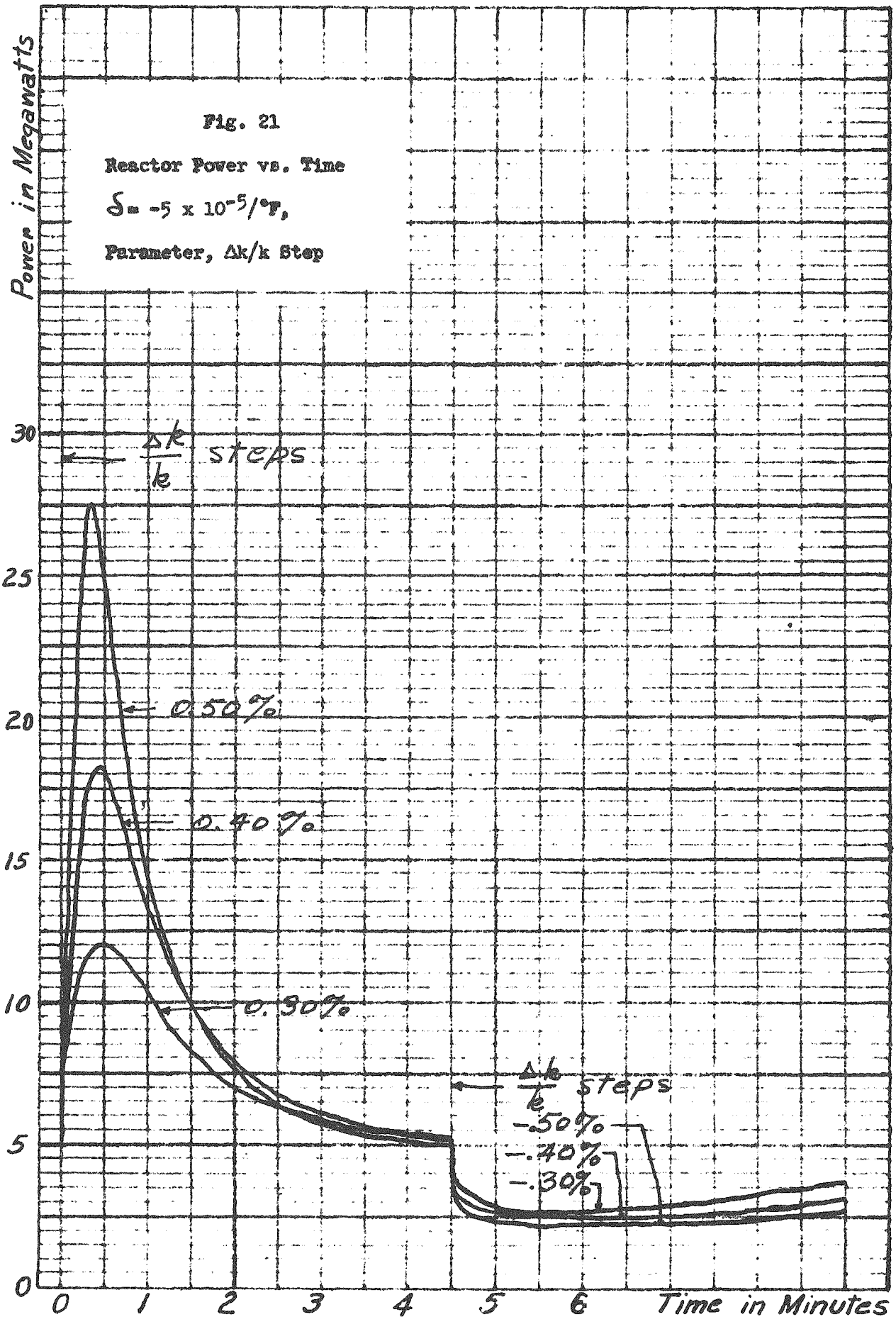
Power in Megawatts
Fig. 21
Reactor Power vs. Time
δ = -5 x 10⁻⁵/°F,
Parameter, Δk/k Step
Δk/k steps
0.50%
0.40%
0.30%
Δk/k steps
-.50%
-.40%
-.30%
0
5
10
15
20
25
30
0
1
2
3
4
5
6
Time in Minutes

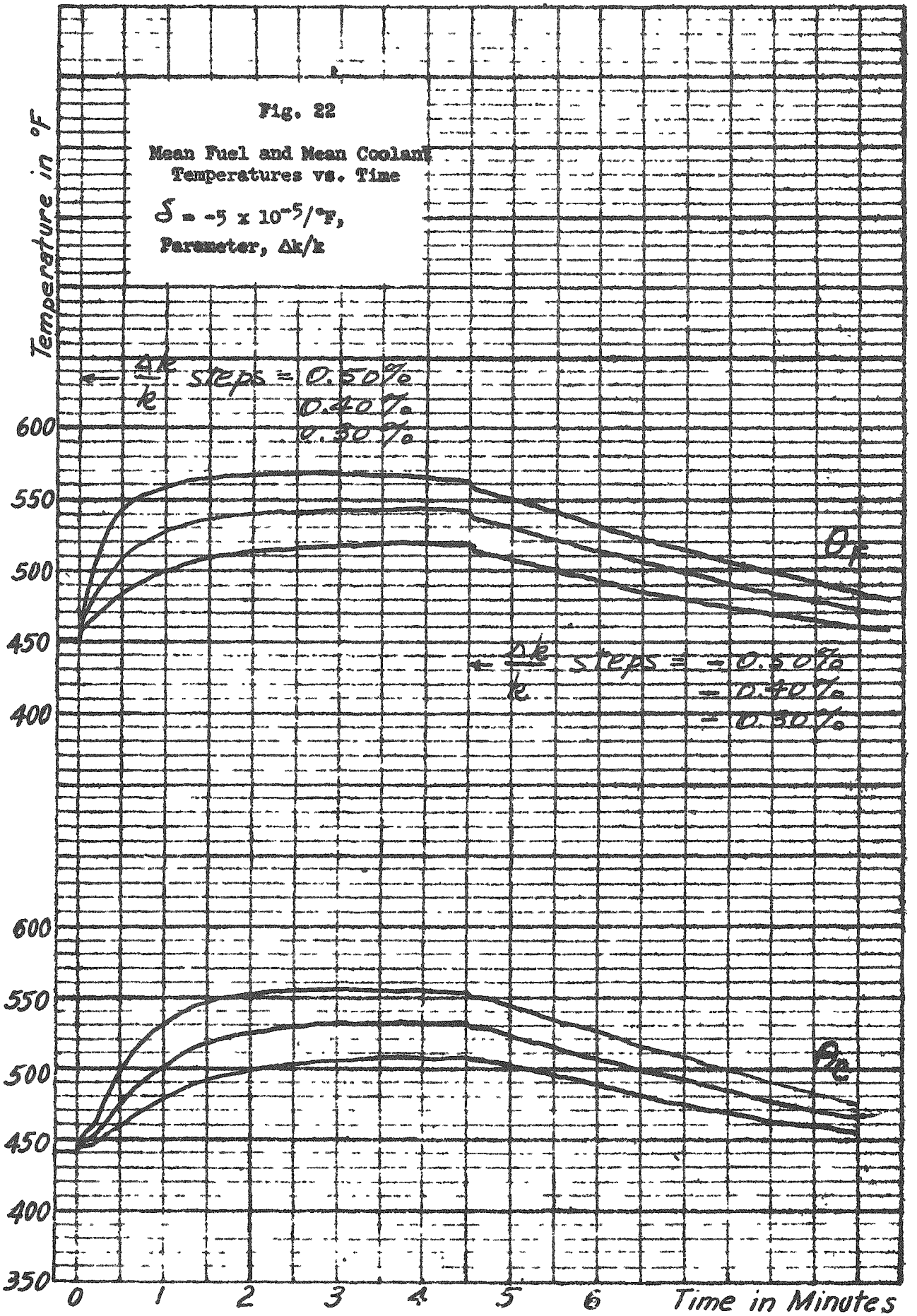
Fig. 22
Mean Fuel and Mean Coolant Temperatures vs. Time
$\delta = -5 \times 10^{-5}/°F$,
Parameter, $\Delta k/k$
Temperature in °F
$\leftarrow \frac{\Delta k}{k}$ steps = 0.50%
0.40%
0.30%
600
550
500
450
400
θ_F
$\leftarrow \frac{\Delta k}{k}$ steps = −0.50%
−0.40%
−0.30%
600
550
500
450
400
350
θ_C
0
1
2
3
4
5
6
Time in Minutes

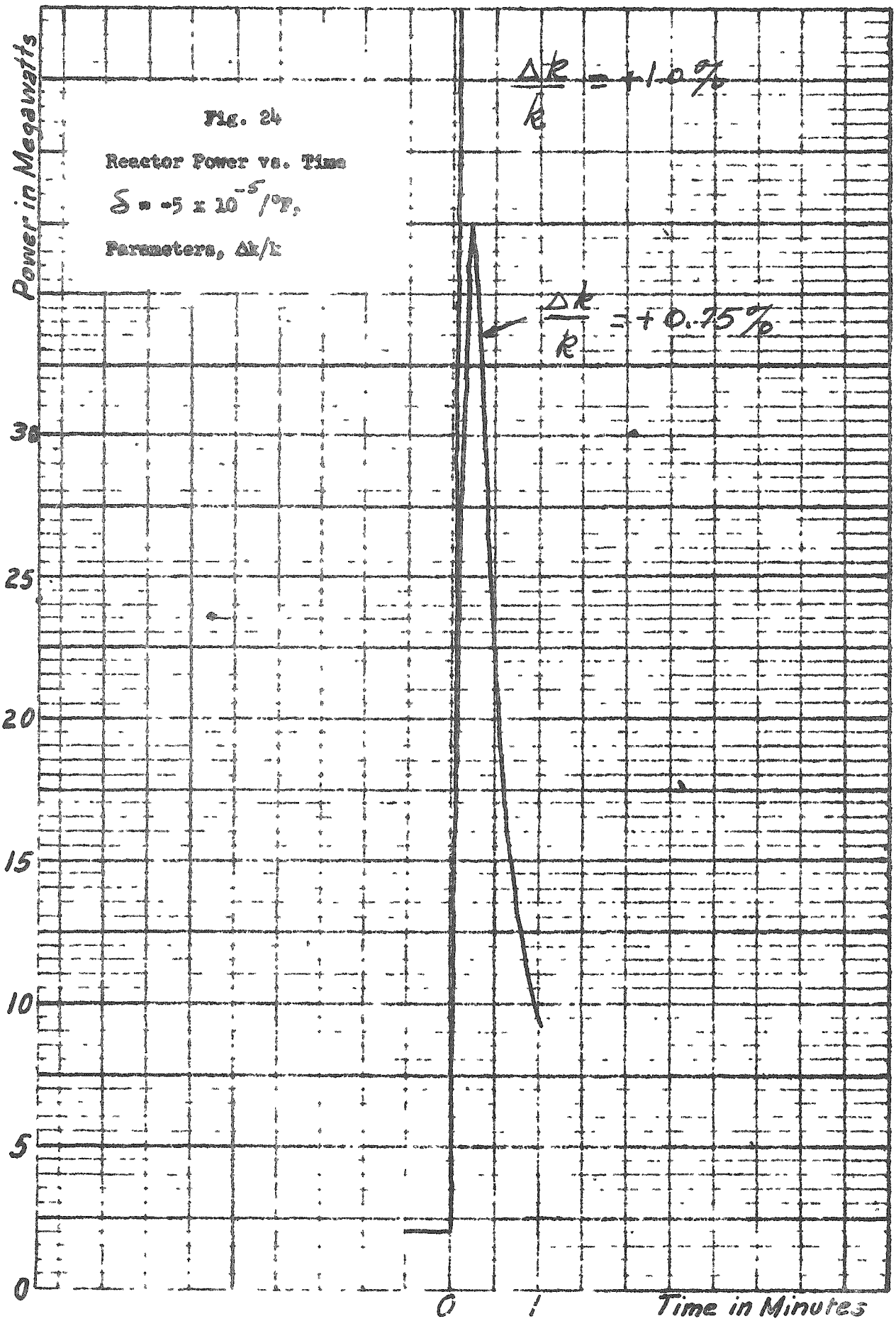

Fig. 24

Reactor Power vs. Time

$\delta = -5 \times 10^{-5}/°F.$

Parameters, $\Delta k/k$

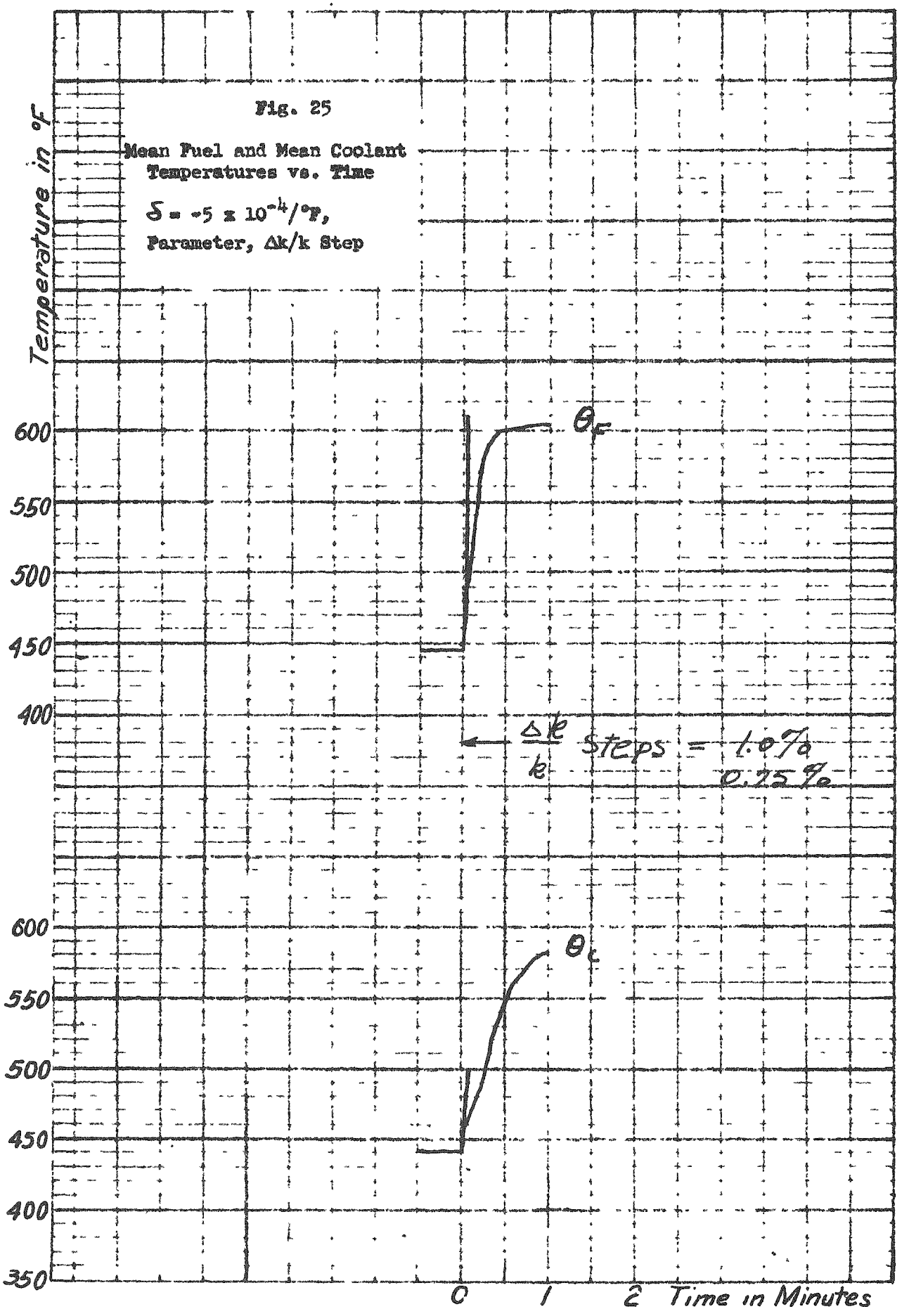
Fig. 25
Mean Fuel and Mean Coolant Temperatures vs. Time
δ = -5 x 10⁻⁴/°F,
Parameter, Δk/k Step
Temperature in °F
600
550
500
450
400
600
550
500
450
400
350
θF
θC
Δk/k steps = 1.0%
0.75%
0
1
2
Time in Minutes

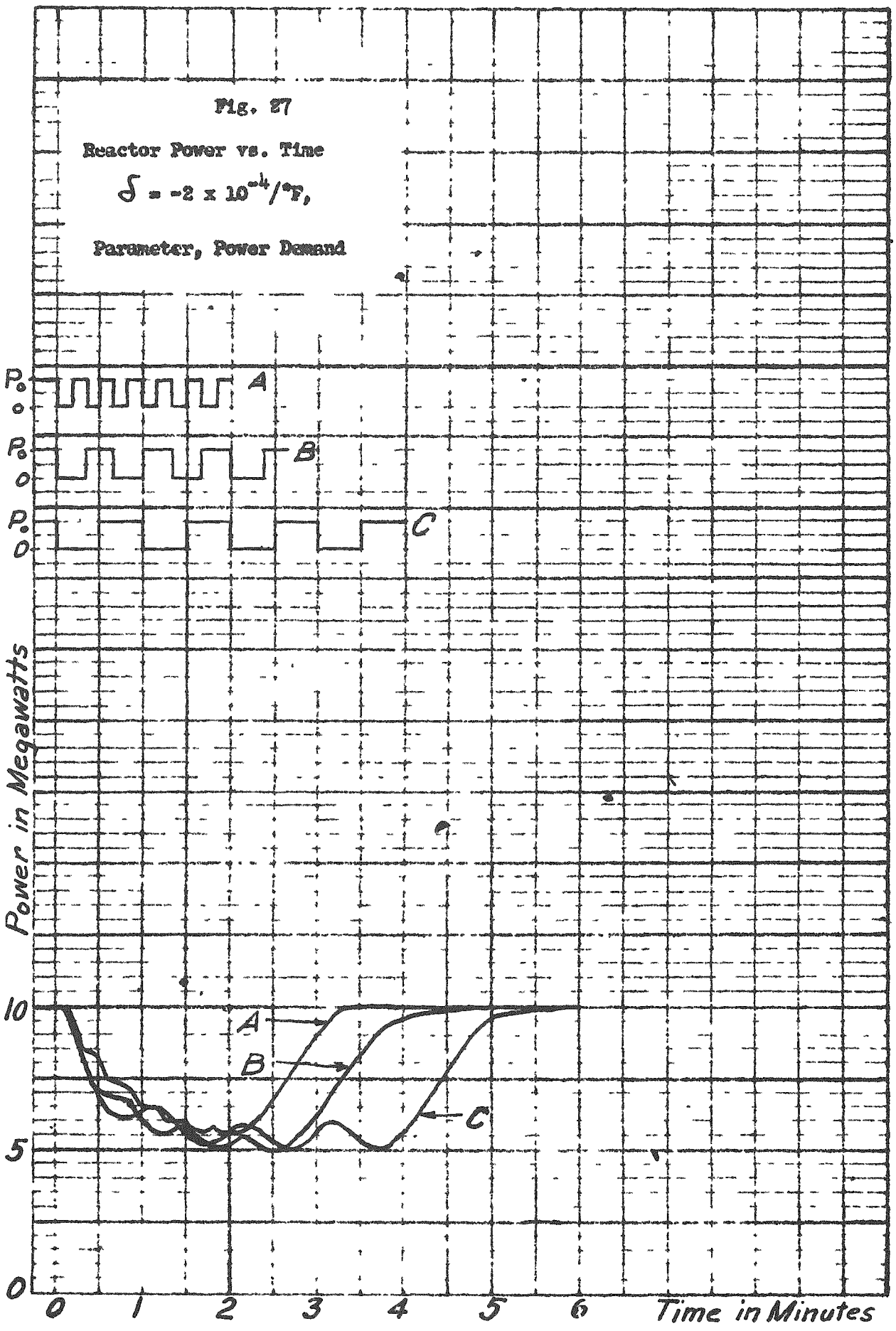
Fig. 27
Reactor Power vs. Time
$\delta = -2 \times 10^{-4}/°F$,
Parameter, Power Demand
P
A
B
C
0
Power in Megawatts
10
5
0
A
B
C
0
1
2
3
4
5
6
Time in Minutes

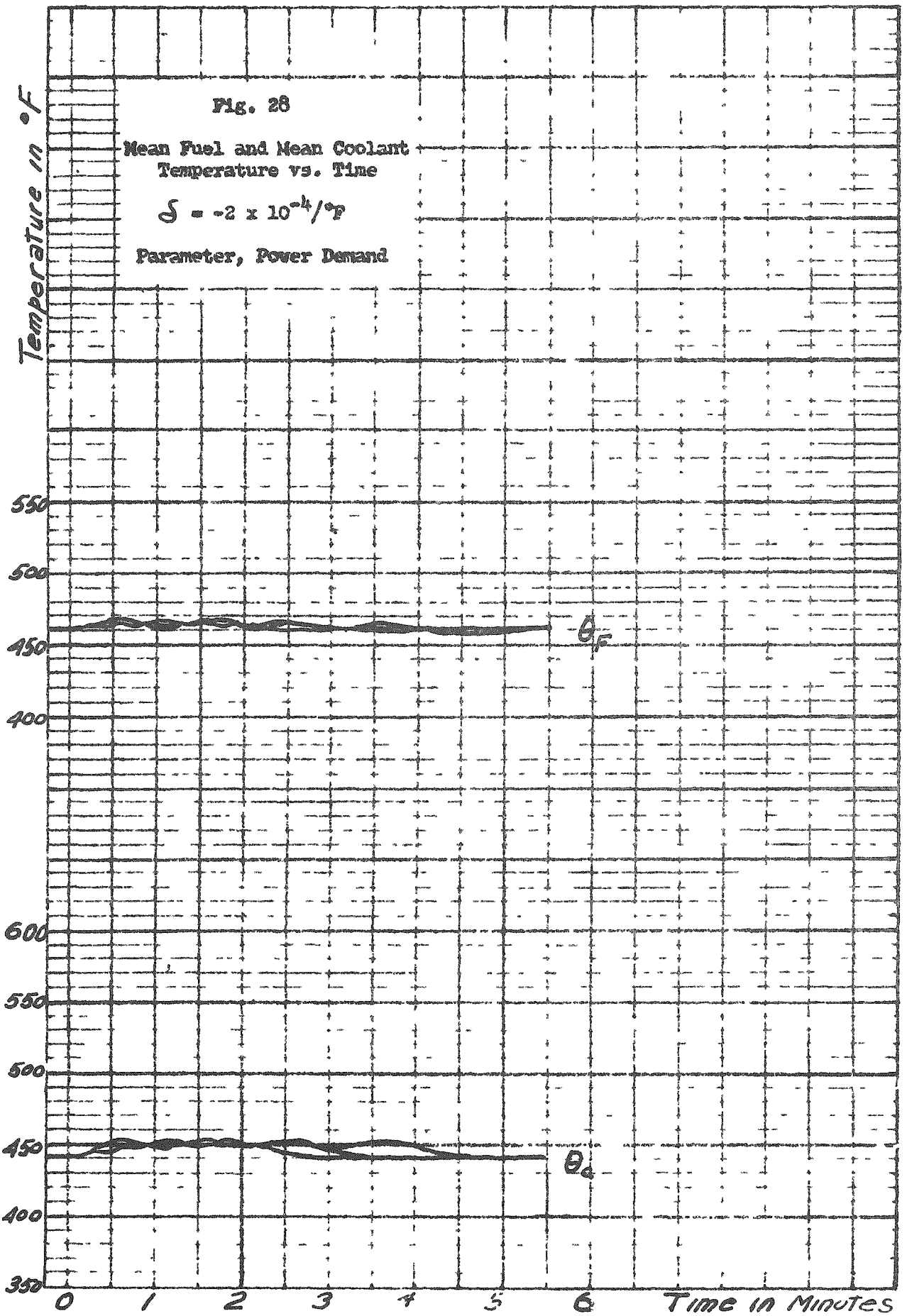
Fig. 28
Mean Fuel and Mean Coolant Temperature vs. Time
$\delta = -2 \times 10^{-4}/°F$
Parameter, Power Demand
Temperature in °F
550
500
450
400
600
550
500
450
400
350
θ_F
θ_c
0
1
2
3
4
5
6
Time in Minutes

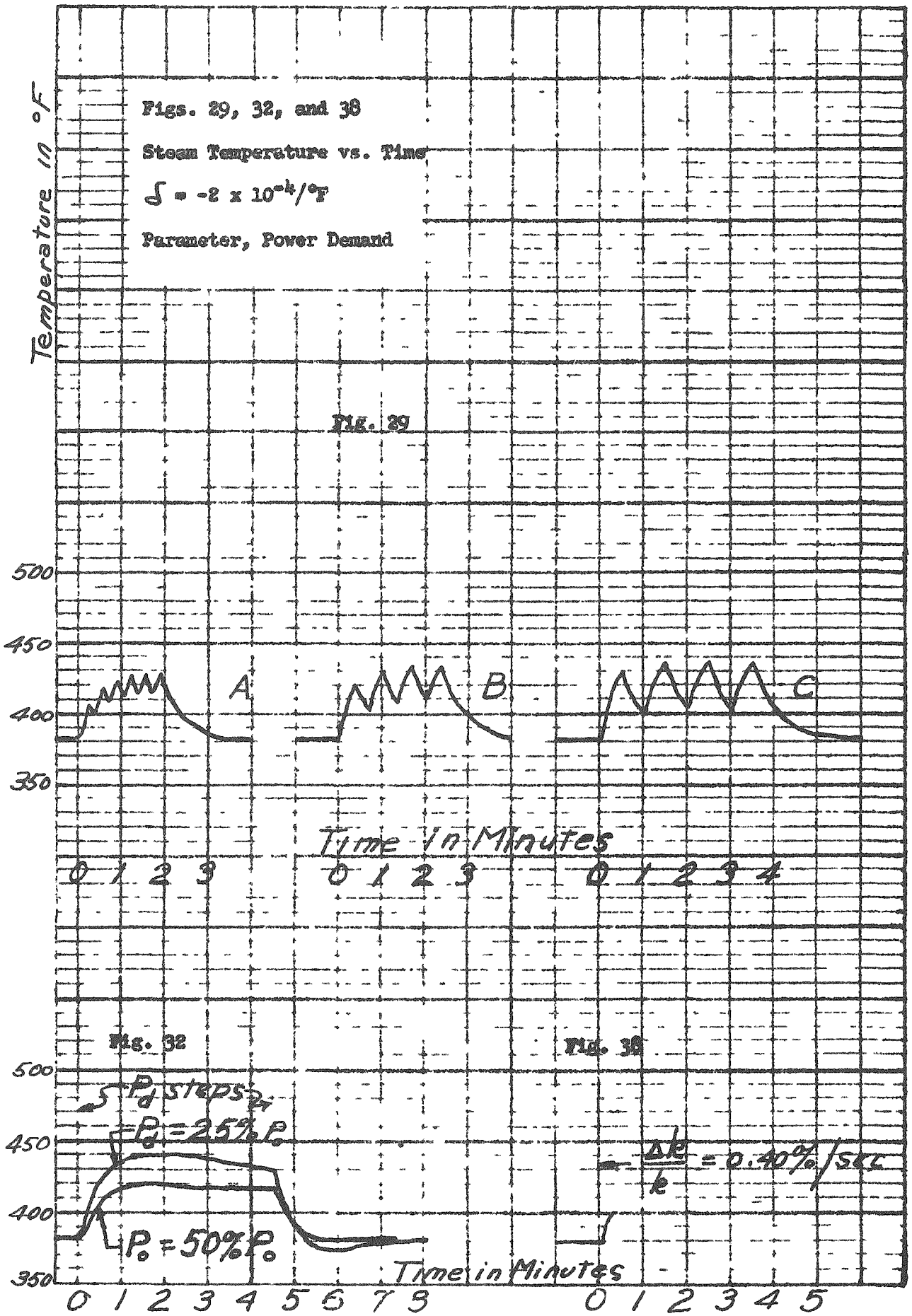
Figs. 29, 32, and 38
Steam Temperature vs. Time
$\alpha = -2 \times 10^{-4}/°F$
Parameter, Power Demand
Temperature in °F
Fig. 29
500
450
400
350
A
B
C
Time in Minutes
0 1 2 3
0 1 2 3
0 1 2 3 4
Fig. 32
Fig. 38
5 P_d steps
$P_o = 25\% P_o$
$P_o = 50\% P_o$
$\frac{\Delta k}{k} = 0.40\%/sec$
Time in Minutes
0 1 2 3 4 5 6 7 8
0 1 2 3 4 5

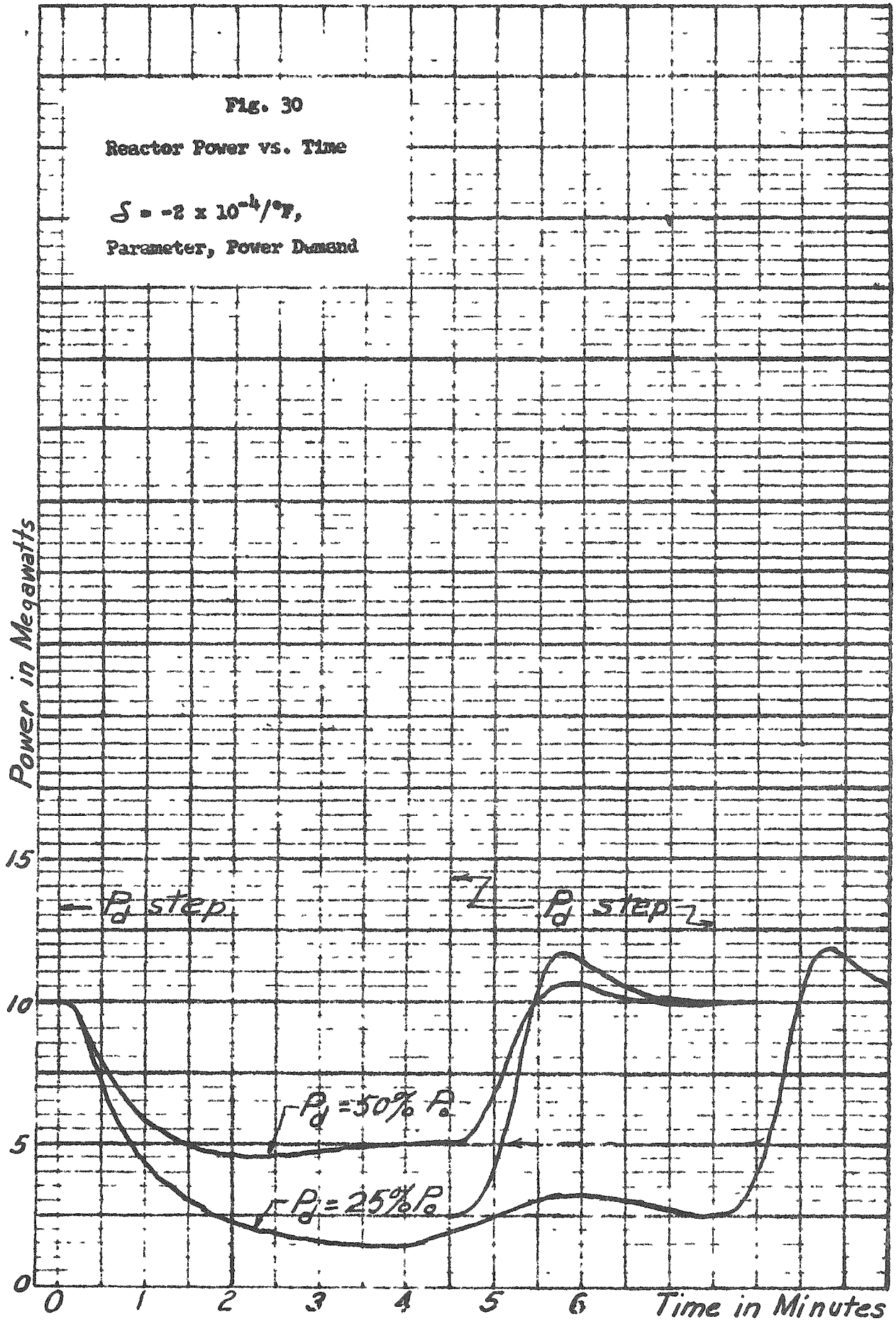

Fig. 30

Reactor Power vs. Time

$\delta = -2 \times 10^{-4}/°F$,

Parameter, Power Demand

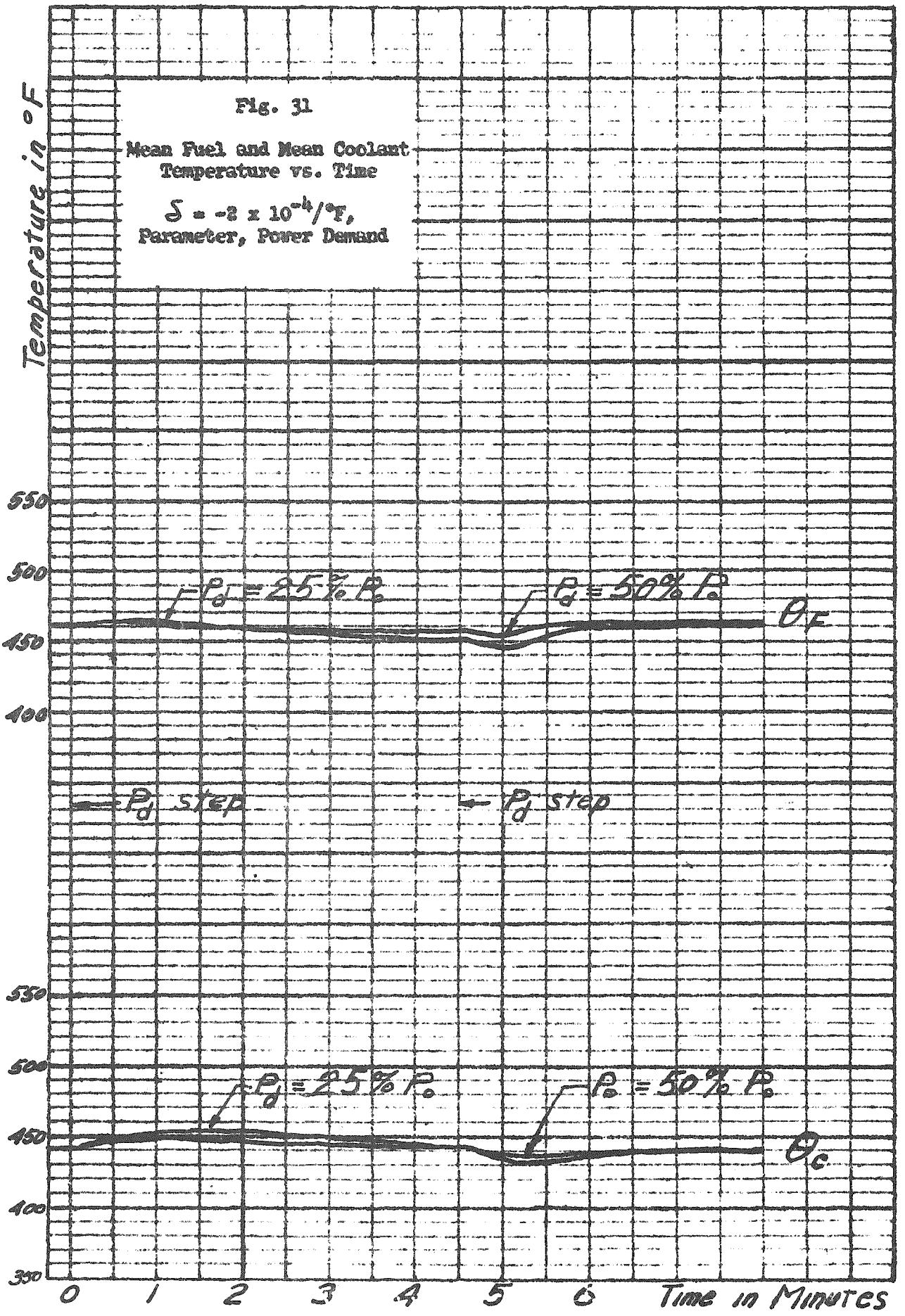

Fig. 31

Mean Fuel and Mean Coolant Temperature vs. Time

$\delta = -2 \times 10^{-4}/°F$, Parameter, Power Demand

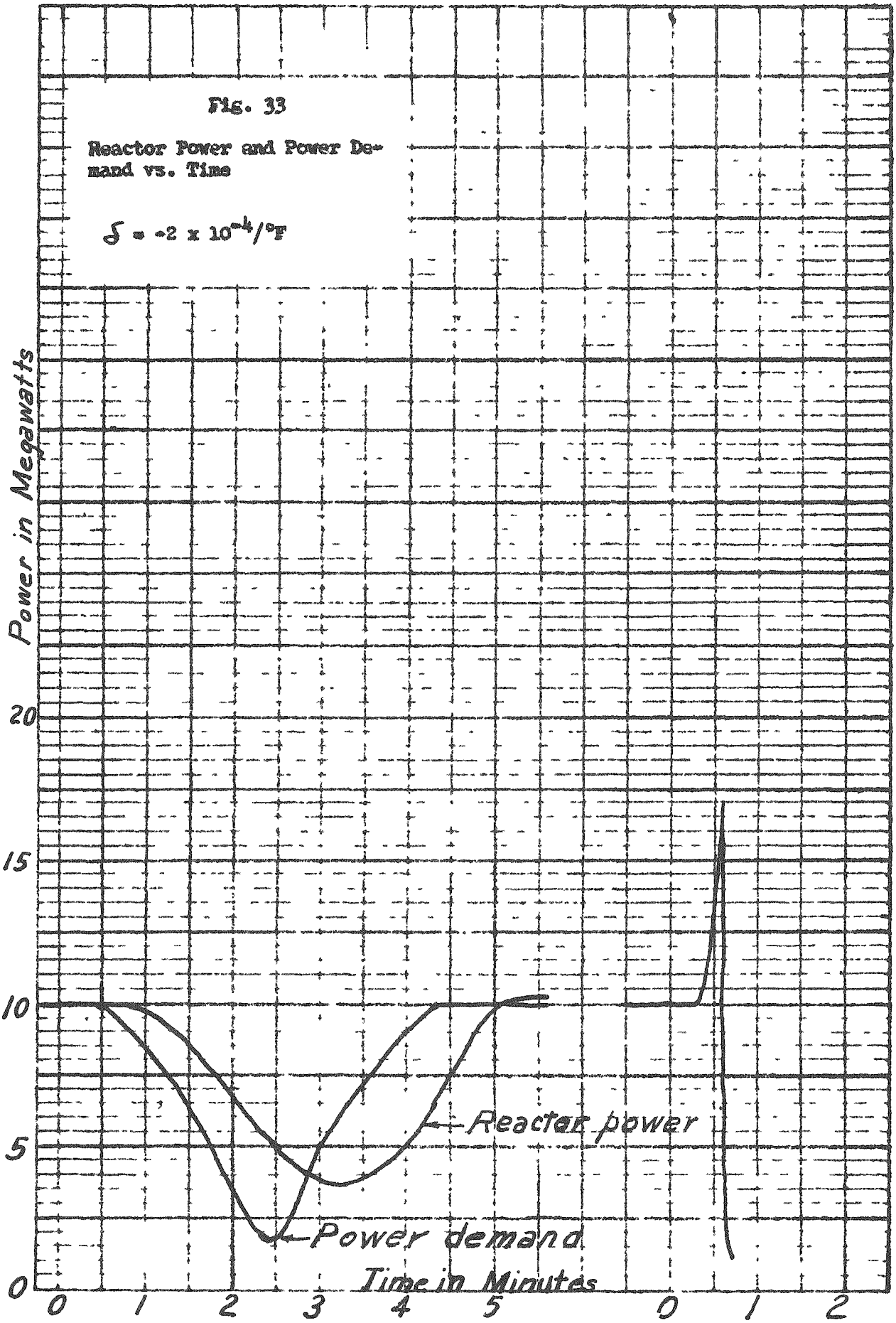

Fig. 33

Reactor Power and Power Demand vs. Time

$\delta = -2 \times 10^{-4}/°F$

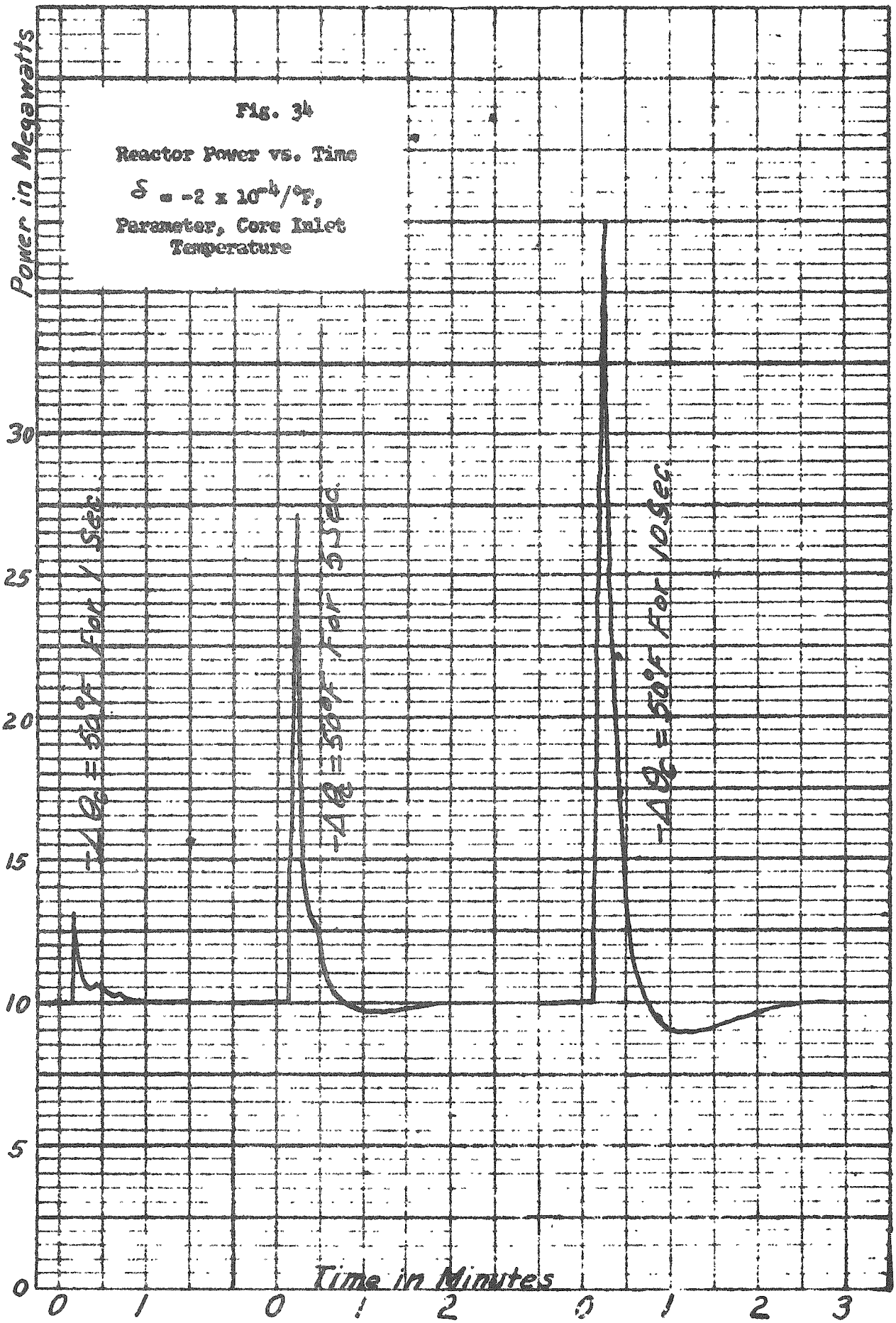

Fig. 34

Reactor Power vs. Time

$\delta = -2 \times 10^{-4}/°F$,

Parameter, Core Inlet Temperature

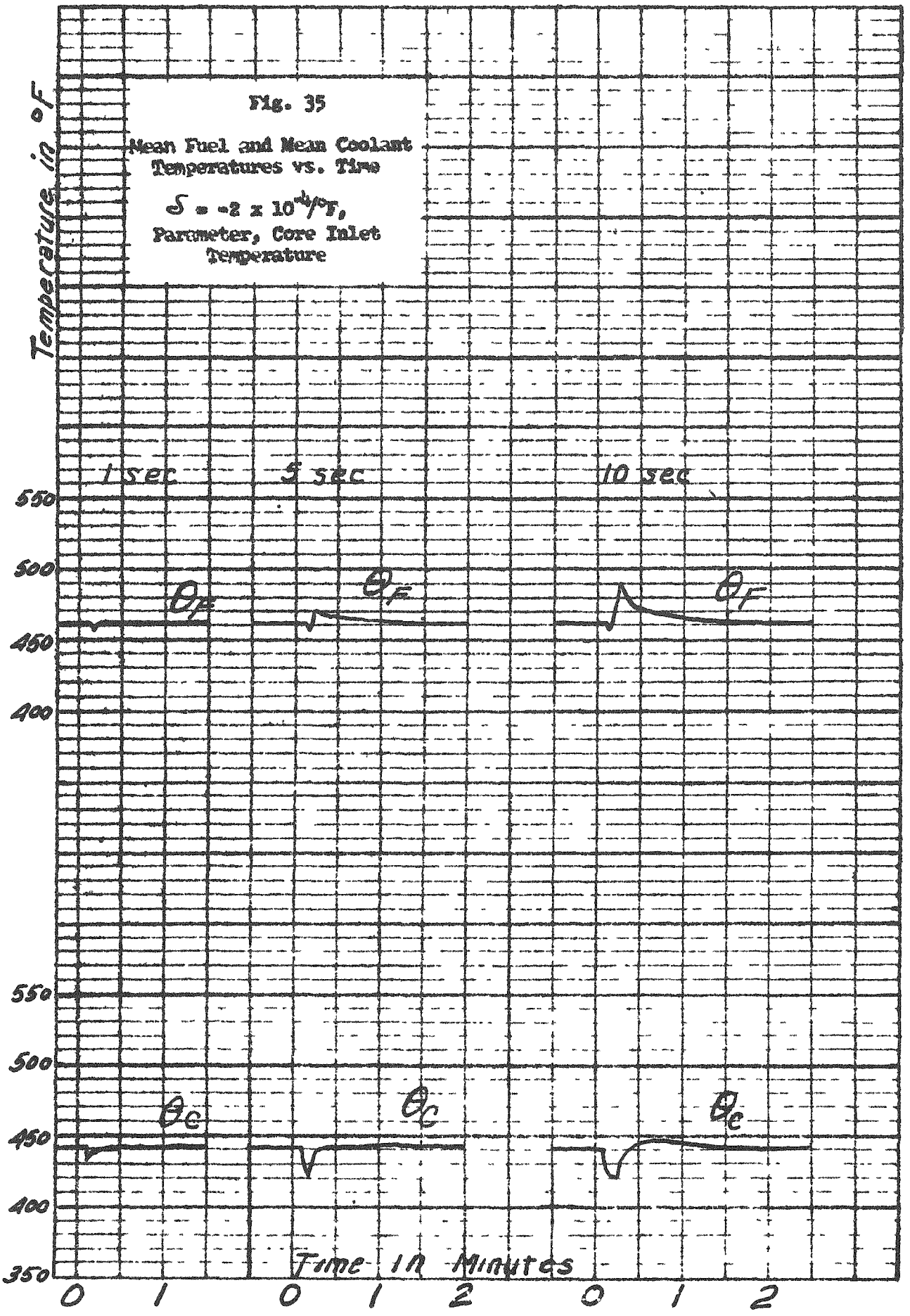
Fig. 35
Mean Fuel and Mean Coolant Temperatures vs. Time
$\delta = -2 \times 10^{-4}/°F$,
Parameter, Core Inlet Temperature
Temperature in °F
1 sec
5 sec
10 sec
θ_F
θ_F
θ_F
θ_c
θ_c
θ_c
550
500
450
400
550
500
450
400
350
Time in Minutes
0 1 0 1 2 0 1 2

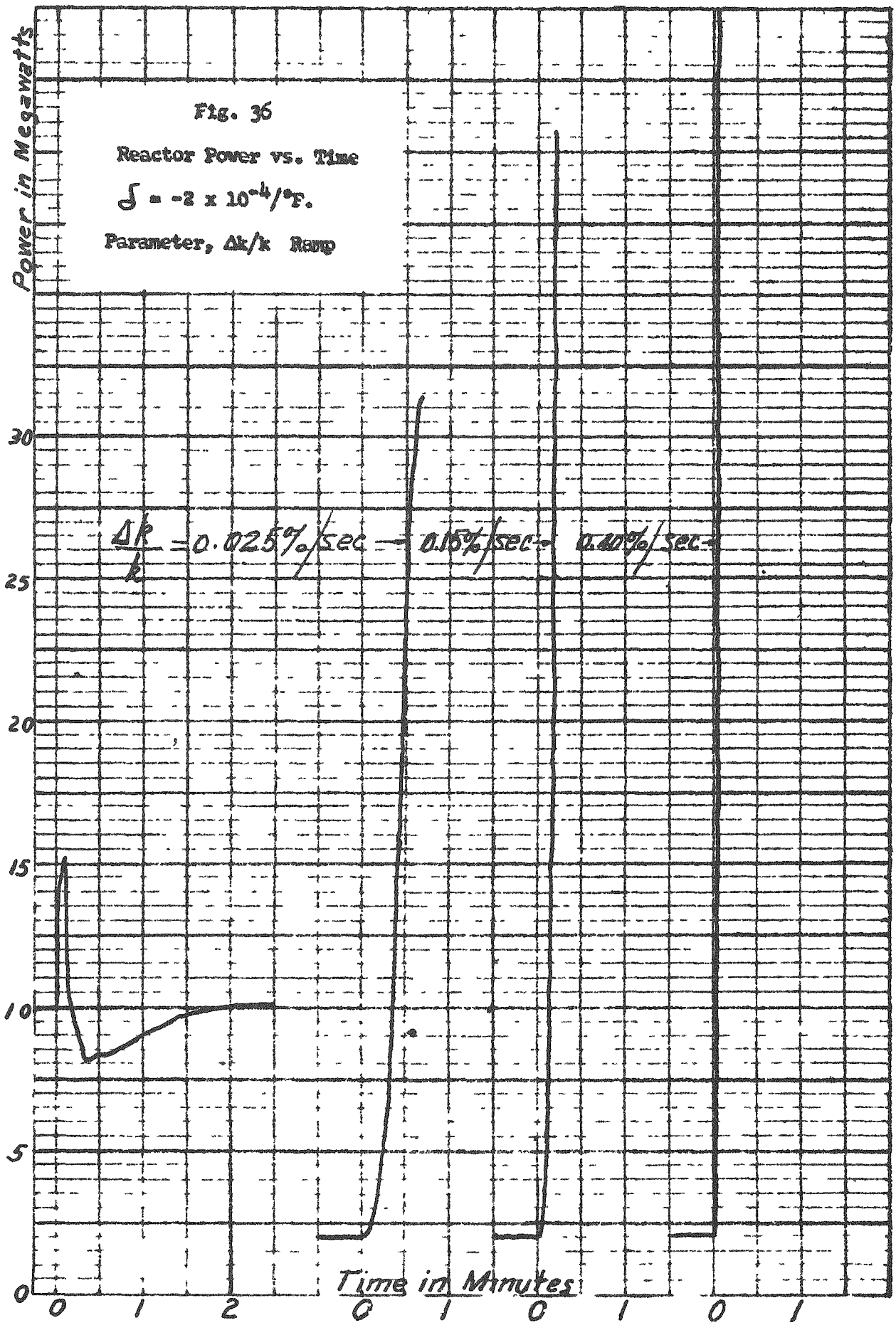
Power in Megawatts
Fig. 36
Reactor Power vs. Time
$\alpha = -2 \times 10^{-4}/°F.$
Parameter, Δk/k Ramp
$\frac{\Delta k}{k}$ = 0.025%/sec — 0.15%/sec - 0.40%/sec
30
25
20
15
10
5
0
0 1 2 0 1 0 1 0 1
Time in Minutes

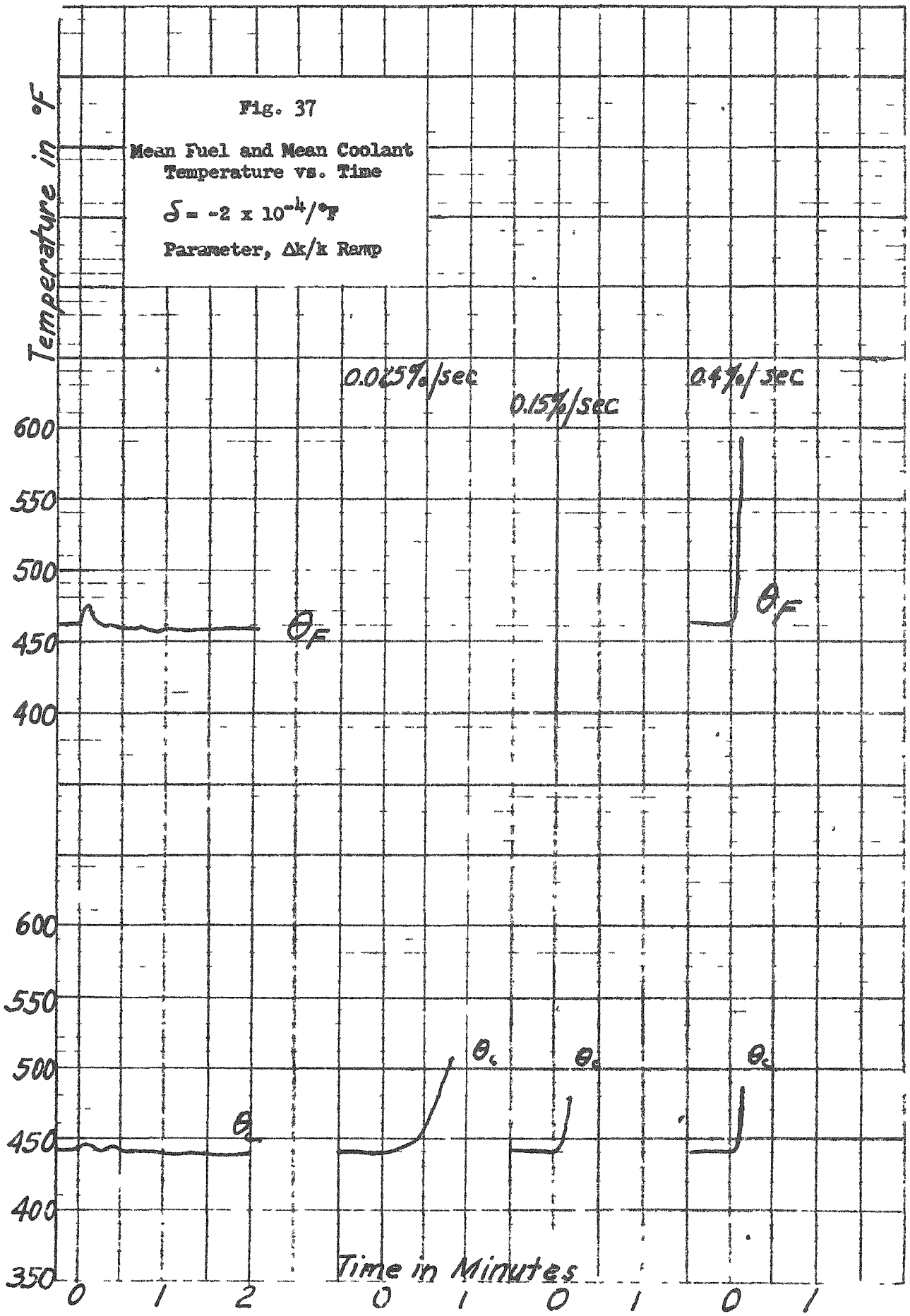
Fig. 37
Mean Fuel and Mean Coolant Temperature vs. Time
δ = -2 x 10⁻⁴/°F
Parameter, Δk/k Ramp
Temperature in °F
0.05%/sec
0.15%/sec
0.4%/sec
600
550
500
450
400
350
θF
θc
Time in Minutes
0
1
2

Fig. 39

Reactor Power vs. Time

$\delta = -2 \times 10^{-4}/°F$

Parameter, $\Delta k/k$ Steps

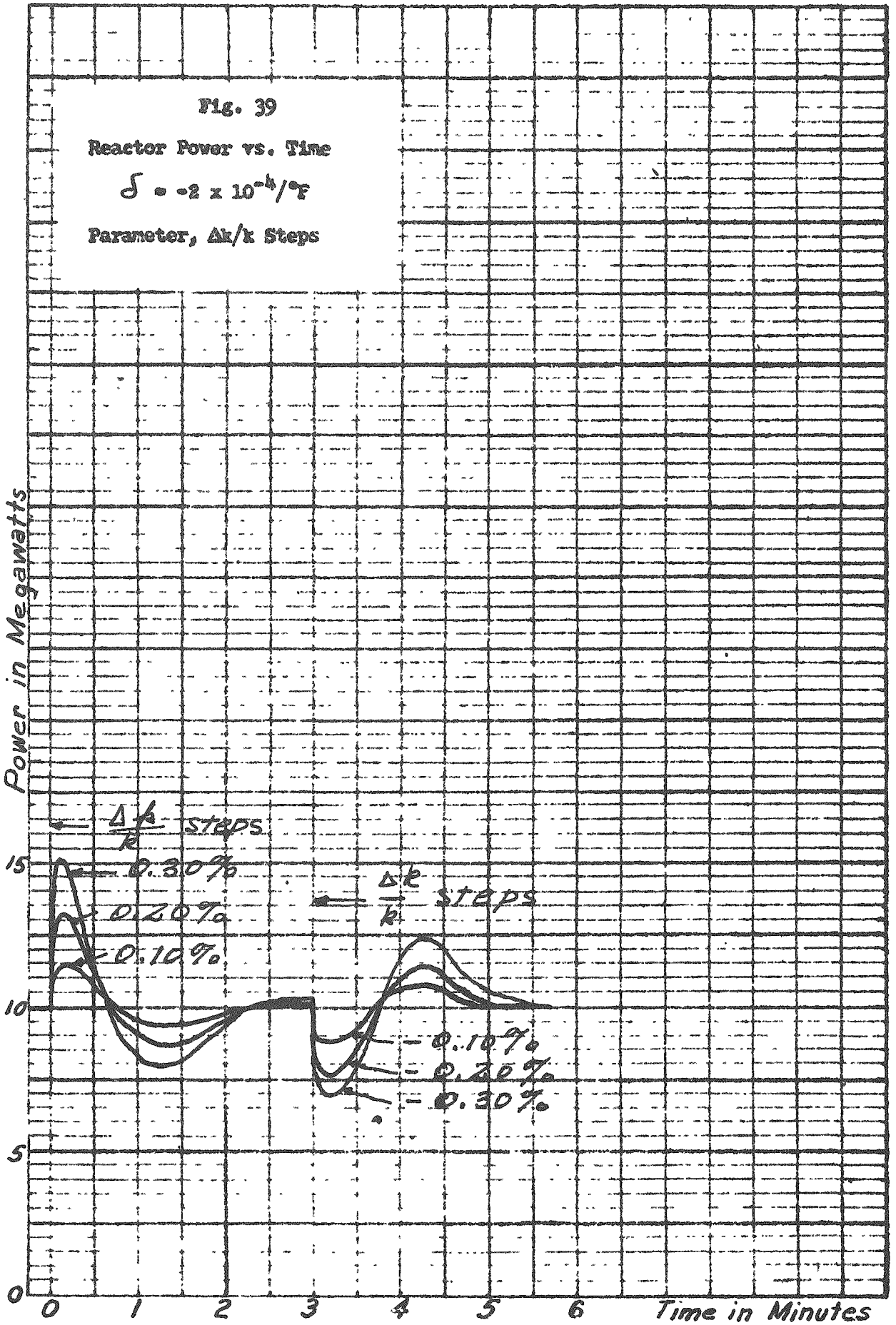

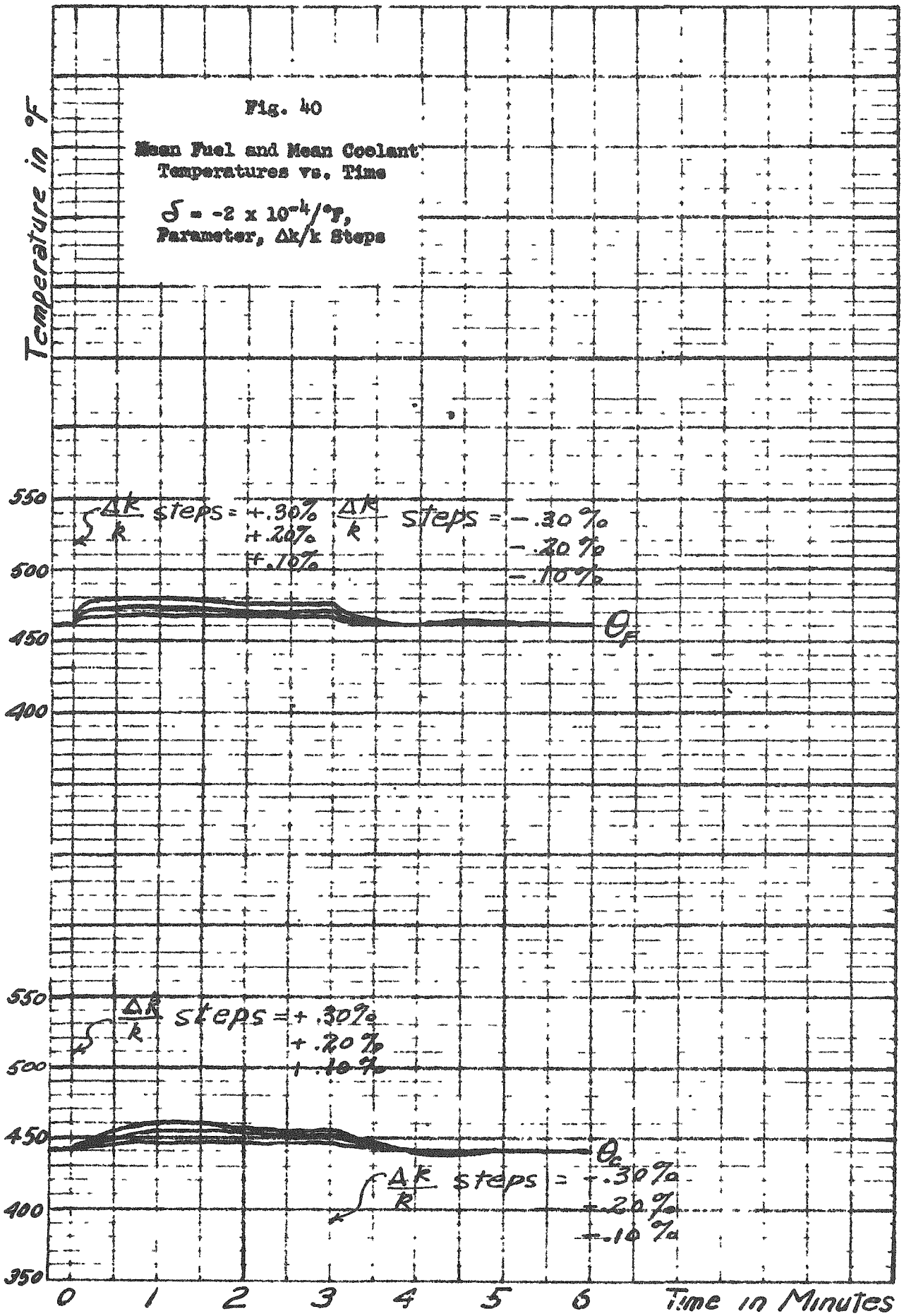
Fig. 40
Mean Fuel and Mean Coolant Temperatures vs. Time
δ = -2 x 10^{-4}/°F,
Parameter, Δk/k Steps
Temperature in °F
550
500
450
400
Δk/k steps = +.30%
+.20%
+.10%
Δk/k steps = -.30%
-.20%
-.10%
θ_F
550
500
450
400
350
Δk/k steps = +.30%
+.20%
+.10%
θ_c
Δk/k steps = +.30%
+.20%
+.10%
0
1
2
3
4
5
6
Time in Minutes

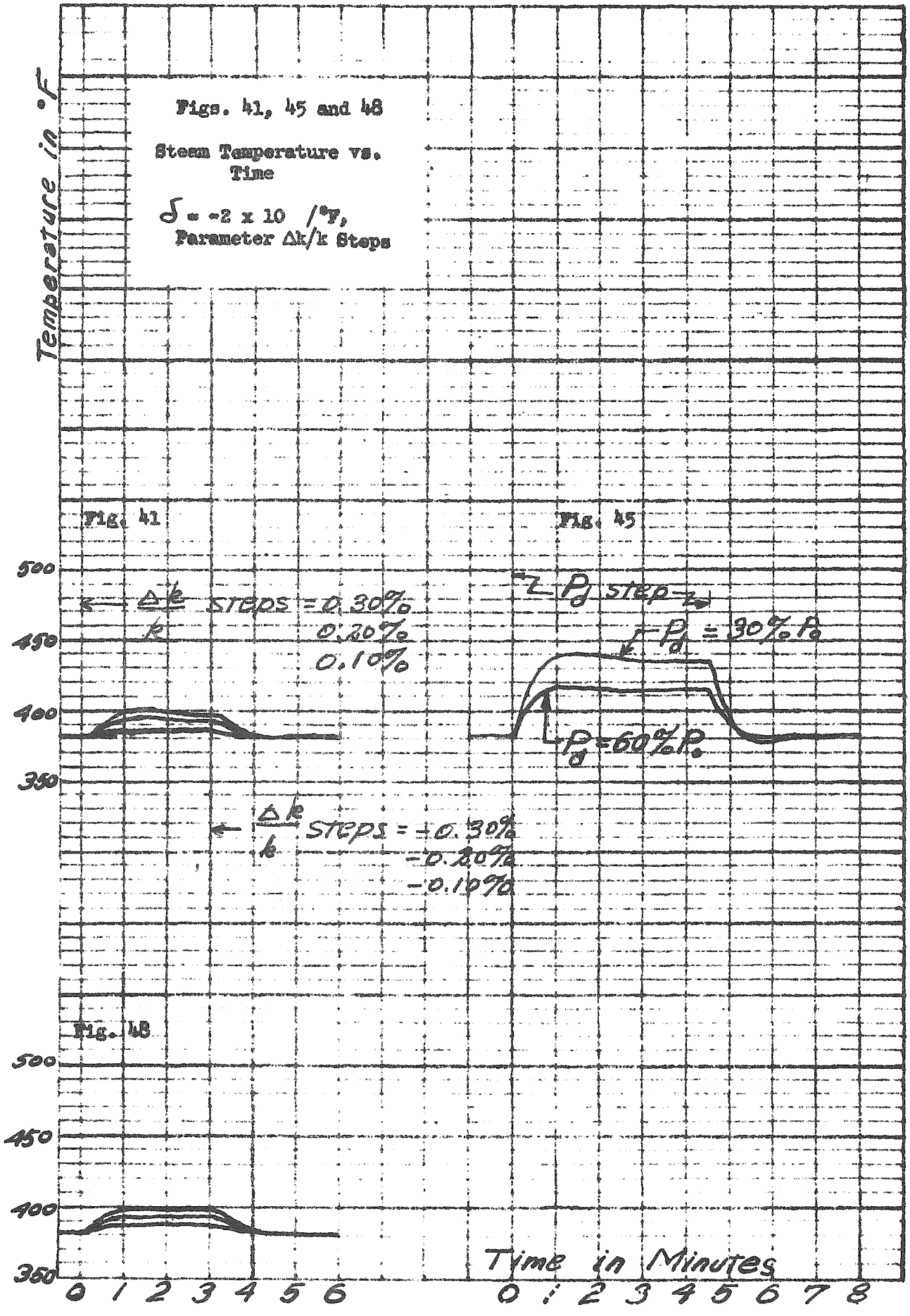
Figs. 41, 45 and 48
Steam Temperature vs. Time
δ = -2 x 10 /°F,
Parameter Δk/k Steps
Temperature in °F
Fig. 41
Fig. 45
500
450
400
350
Δk/k STEPS = 0.30%
0.20%
0.10%
Pd STEP
Pd = 30% Po
Pd = 60% Po
Δk/k STEPS = -0.30%
-0.20%
-0.10%
Fig. 48
500
450
400
350
Time in Minutes
0 1 2 3 4 5 6
0 1 2 3 4 5 6 7 8

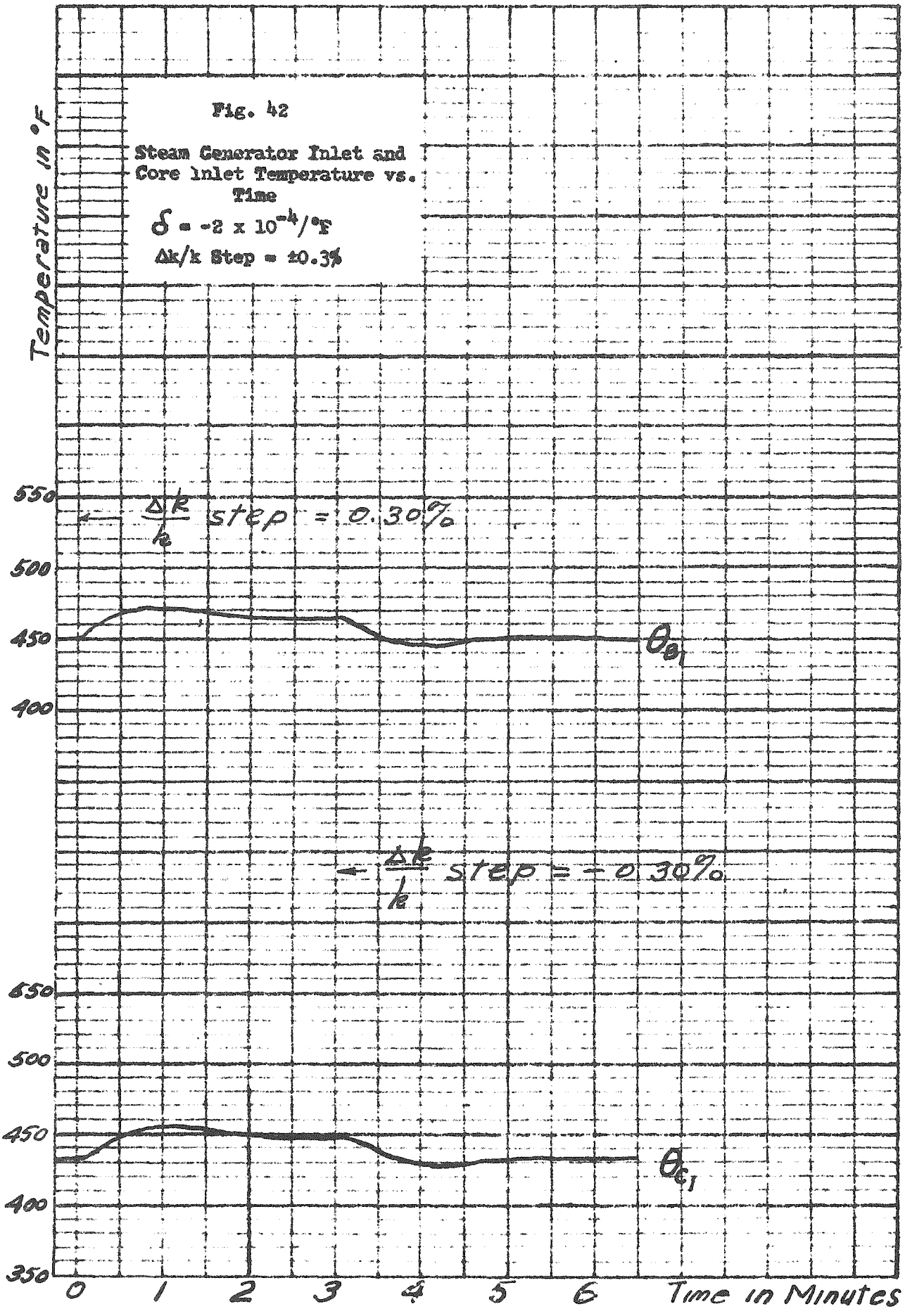
Fig. 42
Steam Generator Inlet and Core Inlet Temperature vs. Time
δ = -2 x 10⁻⁴/°F
Δk/k Step = ±0.3%
Temperature in °F
550
500
450
400
650
500
450
400
350
Δk/k step = 0.30%
Δk/k step = -0.30%
θ_a
θ_c
0
1
2
3
4
5
6
Time in Minutes

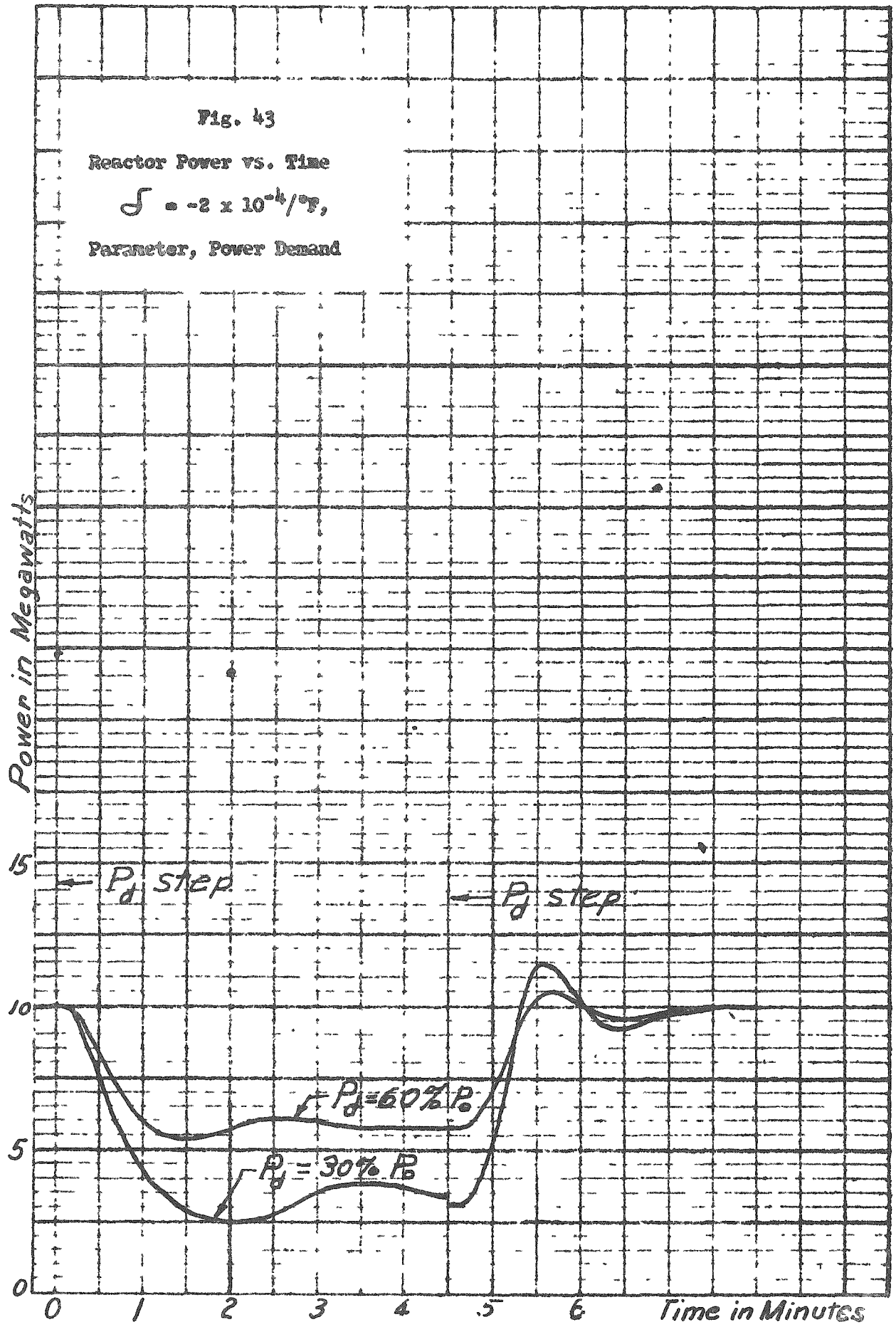

Fig. 43

Reactor Power vs. Time

$\alpha = -2 \times 10^{-4}/°F$,

Parameter, Power Demand

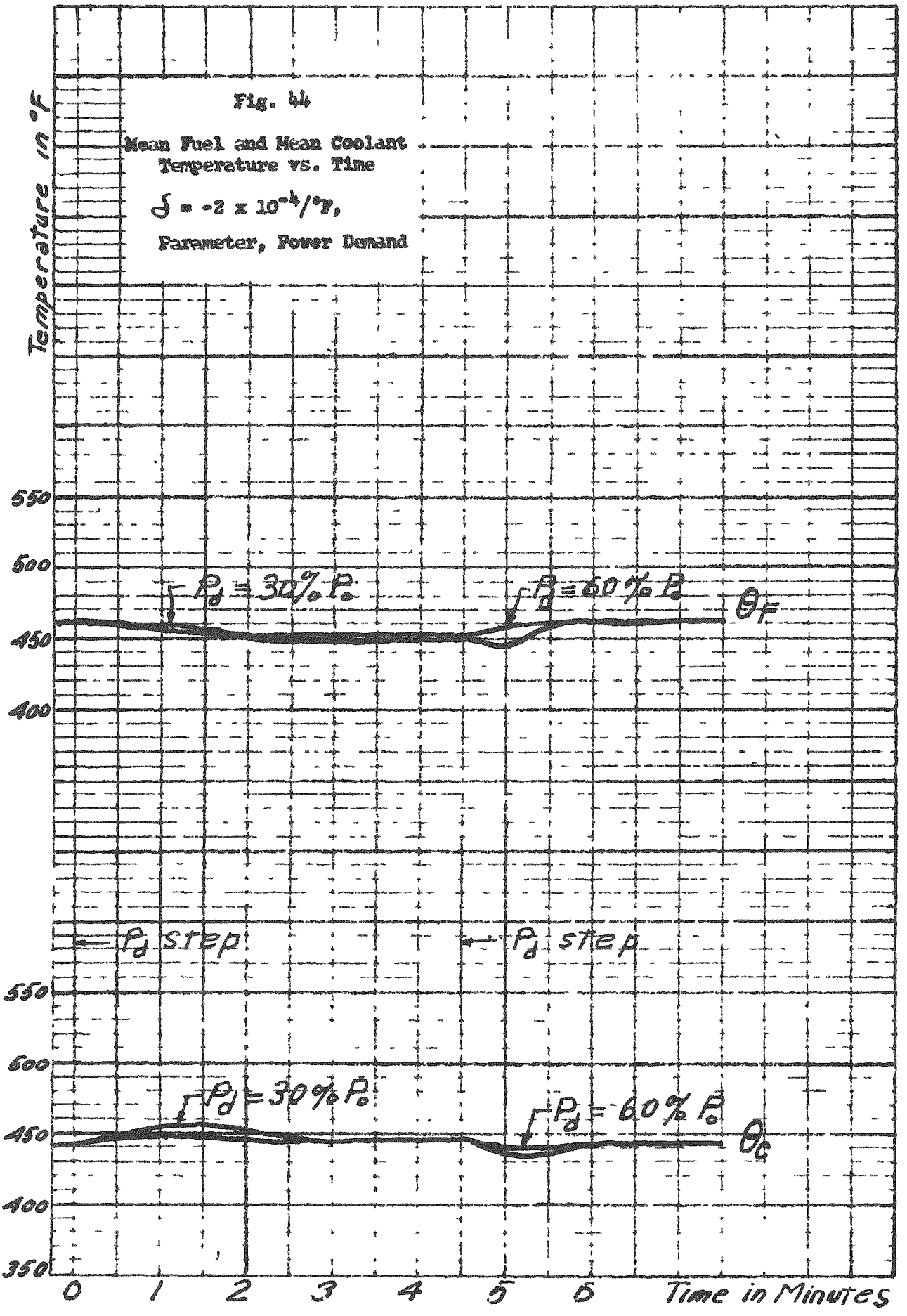
Fig. 44
Mean Fuel and Mean Coolant Temperature vs. Time
$\delta = -2 \times 10^{-4}/°F$,
Parameter, Power Demand
Temperature in °F
550
500
450
400
$P_d = 30\% P_o$
$P_d = 60\% P_o$
θ_F
P_d step
P_d step
550
500
450
400
350
$P_d = 30\% P_o$
$P_d = 60\% P_o$
θ_C
0
1
2
3
4
5
6
Time in Minutes

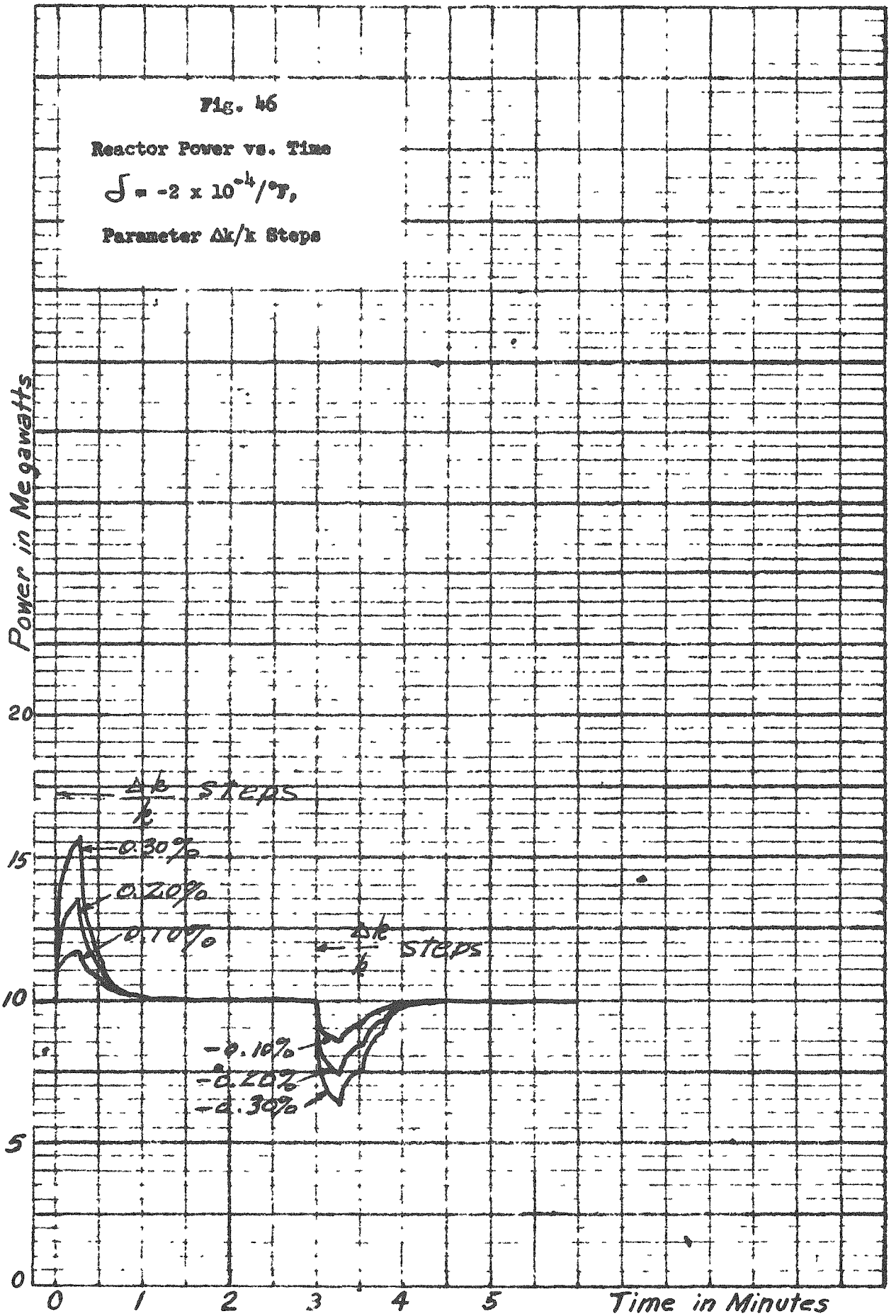
Fig. 46
Reactor Power vs. Time
$\alpha = -2 \times 10^{-4}/°T$,
Parameter Δk/k Steps
Power in Megawatts
0
5
10
15
20
0
1
2
3
4
5
Time in Minutes
Δk/k steps
-0.30%
-0.20%
-0.10%
Δk/k steps
-0.10%
-0.20%
-0.30%

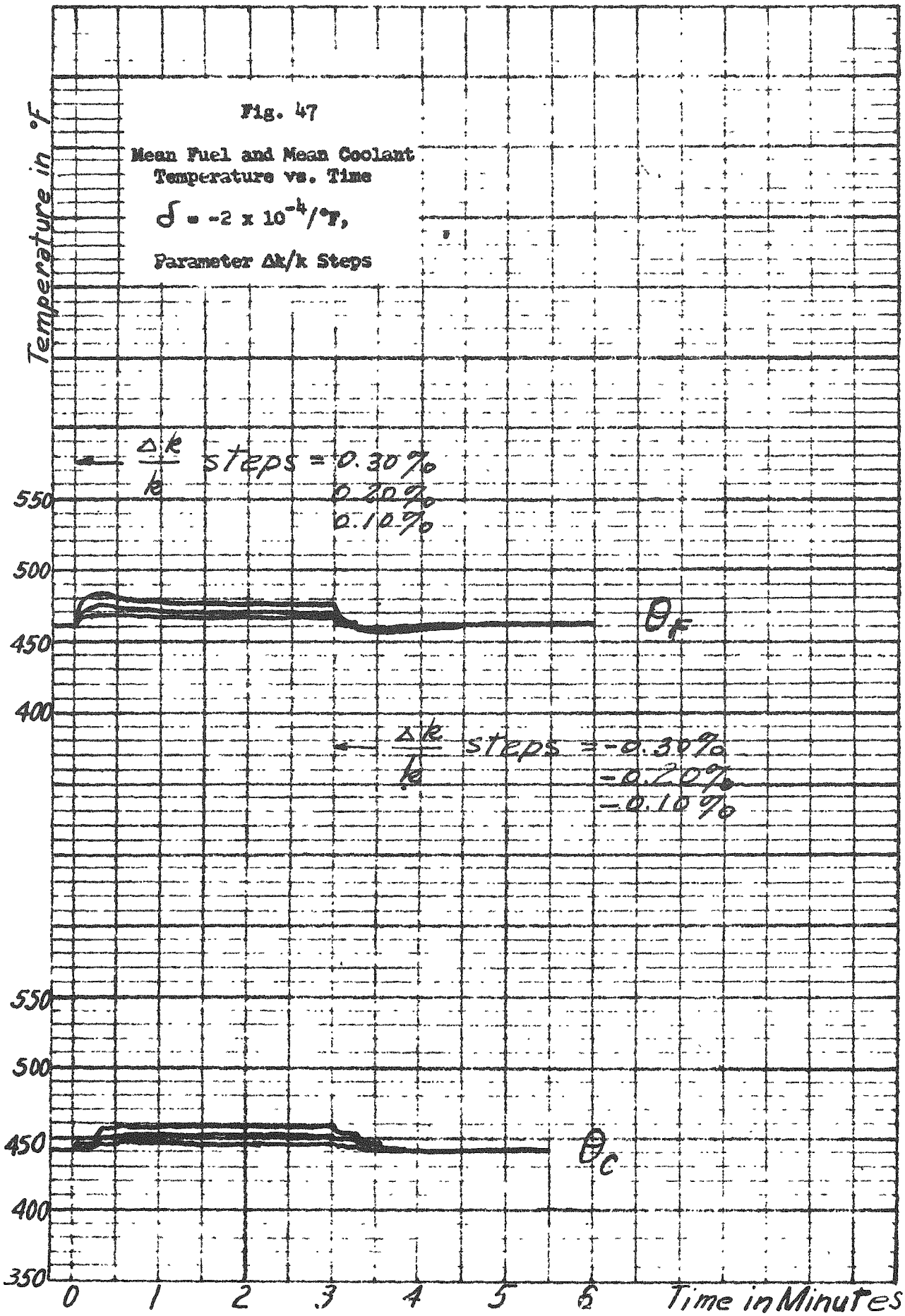
Fig. 47
Mean Fuel and Mean Coolant Temperature vs. Time
$\delta = -2 \times 10^{-4}/°F$,
Parameter Δk/k Steps
Temperature in °F
Δk/k steps = 0.30%
0.20%
0.10%
θ_F
Δk/k steps = -0.30%
-0.20%
-0.10%
θ_C
550
500
450
400
350
0
1
2
3
4
5
6
Time in Minutes

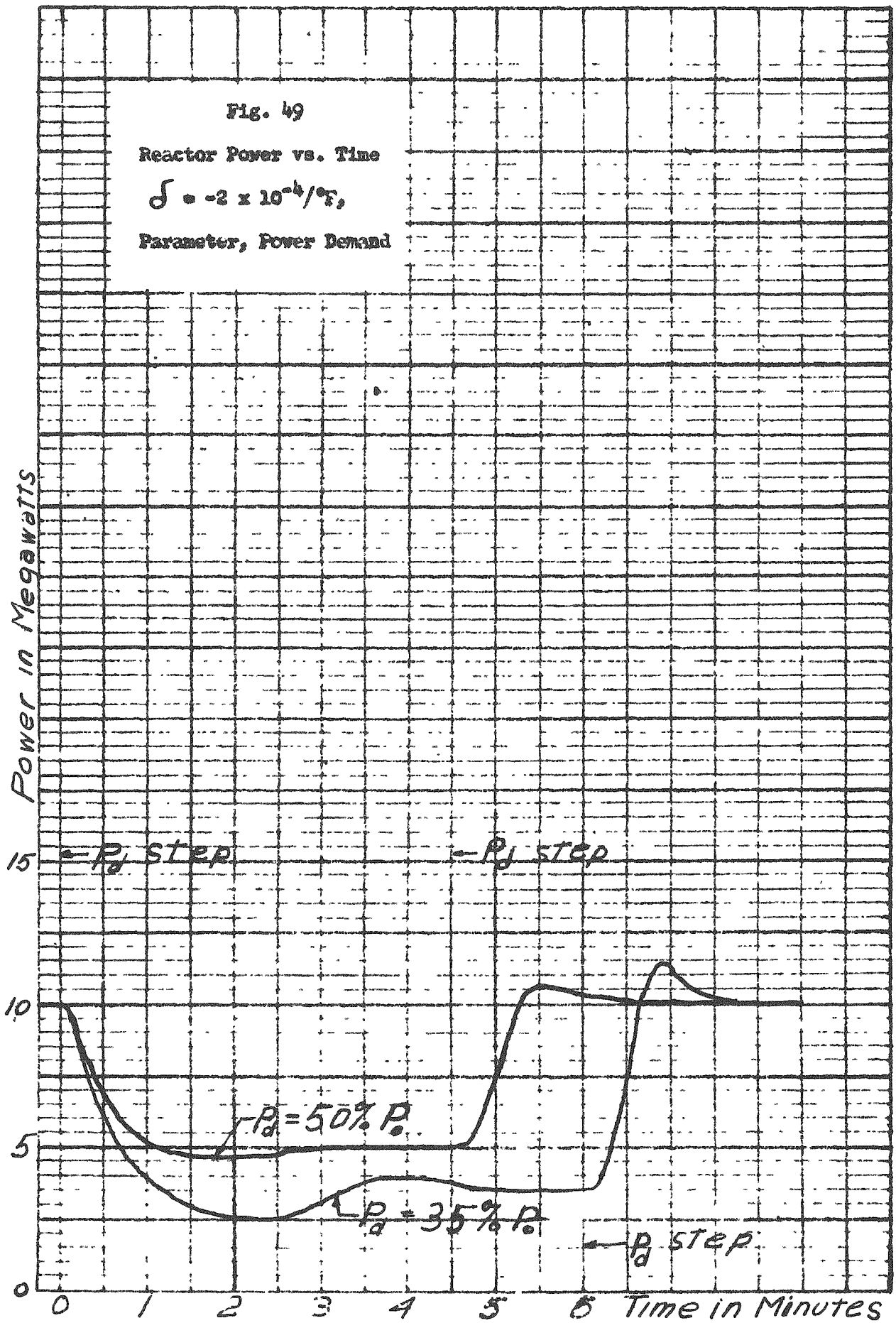
Fig. 49
Reactor Power vs. Time
$\delta = -2 \times 10^{-4}/\tau$,
Parameter, Power Demand
Power in Megawatts
15
10
5
0
P_d step
P_d step
$P_d = 50\% P_o$
$P_d = 35\% P_o$
P_d step
0 1 2 3 4 5 6 Time in Minutes

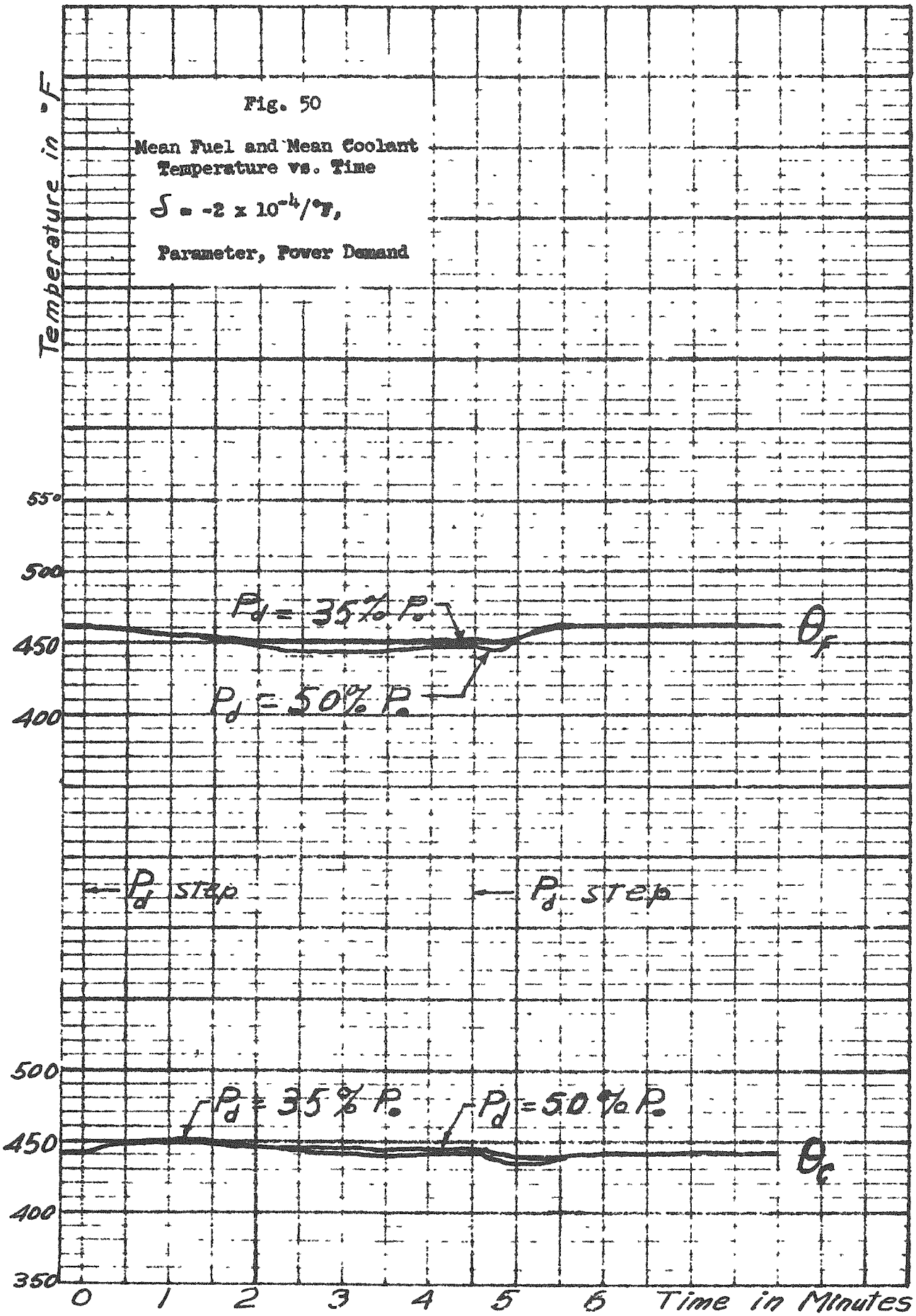
Fig. 50
Mean Fuel and Mean Coolant Temperature vs. Time
$\alpha = -2 \times 10^{-4}/°F$,
Parameter, Power Demand
Temperature in °F
550
500
450
400
$P_d = 35\% P_o$
$P_d = 50\% P_o$
θ_f
P_d step
P_d step
500
450
400
350
$P_d = 35\% P_o$
$P_d = 50\% P_o$
θ_c
0
1
2
3
4
5
6
Time in Minutes

APPENDIX D - DESCRIPTION OF REACTOR SAFETY CIRCUITS

As mentioned in Chapter VI-B, there are three PCP chambers which will cause a scram if the neutron flux exceeds 150% of the flux at 10 megawatts reactor power. In addition, the signal from a compensated ionization chamber is fed to the period circuit which will cause a scram if the reactor period becomes shorter than three seconds. A block diagram of the control and safety circuits is given in Figure VI-2.

The parallel-circular plate ionization chamber (PCP) is designed for high-speed response to changes in neutron flux level. The active section of the counter consists of a set of graphite disks. Each disk is completely coated with boron-10. Under neutron irradiation the reaction B^{10} (n, α) Li^{7} takes place. An ionization current of approximately 50 microamperes is reached at the operating flux of 10^{10} n/cm^2-sec. The materials used in the construction of the chambers are such that they do not become highly radioactive under neutron bombardment and can be handled without elaborate shielding. This instrument is used for safety and servo circuits and has a power-level range greater than 10^3.

The compensated ionization chamber is designed to give a reliable measurement of neutron flux over a large range, particularly in the presence of intense gamma radiation. The chamber is constructed with two separate volumes. An inner volume is contained between a movable cup electrode and a fixed inner electrode shell; the outer volume is between this inner shell liner and outer electrode shell. The two volumes are approximately equal.

The outer volume is made sensitive to neutron radiation by boron-10 coatings applied to the electrode surfaces. The cup electrode is held at a negative potential and the outer shell electrode at a positive potential with respect to the inner shell; the net current carried by the inner shell will, therefore, be a measure of neutrons only. Close balance of the two volumes for zero gamma signal is obtained by moving the cup electrode, thus varying the inner volume. The chamber has a range of 10^6 and gives 100 microamperes current at full operating level of 10^{10} n/cm^2-sec and 10^{-4} microamperes at the bottom of the range. The instrument is used to supply the signal to the log-N and period circuits.

The reactor period and power level instruments operate as follows: The log-N amplifier operates from the output of the compensated ionization chamber. It consists of a thermionic diode. The voltage across the diode is proportional to the logarithm of the current passing through the diode over a range of greater than 10^6; thus the output of the amplifier is the logarithm of the reactor power level. The log-N signal is amplified and recorded on the log-N recorder to give a record of the power level. The log-N amplifier also furnishes a signal which is passed through an RC differentiator This signal is inversely proportional to the reactor period and is recorded on the period recorder. The period amplifier also differentiates the signal from the log-N amplifier to produce a signal suitable for operation of the safety circuits.

The sigma amplifiers are essentially direct current amplifiers which operate in the following manner: The imput signal to the sigma amplifier is furnished by a PCP chamber and a pre-amplifier or from a period amplifier.

An increase in signal to the sigma amplifier causes the grid of a triode to go more positive. This in turn causes the sigma bus to be driven more positive since the cathode of the triode is connected to the bus. If this action occurs in only one of the four sigma amplifiers, then the cathodes of the other three amplifiers are also carried positive and the tubes tend to cut off. In this manner the amplifier receiving the highest signal can take control and all other amplifiers follow along, assuming the same cathode potential.

The magnet amplifiers receive their input signal from the sigma bus. In operation the clutch current can be set to release the clutch when a certain flux is reached. As the power of the reactor is increased the clutch current remains essentially constant until full load is approached. The amplifier output then decreases as the flux increases until the point is reached where the current is insufficient to support the clutch torque. The value of neutron flux to initiate a fast scram is set at 150% of full-load reactor power. The current which the output tubes of the amplifier supply the clutch is furnished from a separate transformer. The emergency scram switches are connected in series with this circuit providing a convenient means for manually scramming the reactor

Two types of scram are therefore possible; fast scram by amplifier action and slow scram by interruption of clutch power. An accidental ground on the sigma bus would result in the clutches being de-energized and the rods dropping.

APPENDIX E-1 - ENERGY RELEASE FOR VARIOUS AMOUNTS OF EXCESS MULTIPLICATION ADDED INSTANTANEOUSLY

In considering instantaneous additions of excess multiplication, a method originated by Golian[4] was followed. The procedure involves a mathematical analysis of the thermal conditions resulting from an exponential power excursion in a parallel plate fuel element. This analysis is divided into two parts (1) the transient until the metal-coolant interface reaches boiling temperature, (2) and the transient from this time until suitable moderator void is formed to cause shut-down.

In the first part of this problem, the coolant is considered to be stagnant for periods less than 25 millisec. The problem is then treated as a one-dimensional, three-region problem in which heat is transferred by conduction only. The time-dependent source term is assumed zero except in the fueled core where it is considered uniform.

After boiling begins, it is postulated that shut-off will occur when sufficient moderator void has been formed to overcome the excess multiplication added but that the void will have no effect prior to this time. The formation of the void volume depends only on introducing enough heat to raise the temperature of the water and supplying the latent heat of vaporization. Further, it is postulated that steam is formed in a laminar layer adjacent to the fuel plate. Additional steam is formed by conducting heat through this layer to the water which increases thickness of the layer.

Using the equations resulting from this analysis, the integrated energy release for various excess multiplications were calculated. In the first calculations the reactor was considered to be at zero power with the coolant flowing at the design rate and pressure but at room temperature ($68^{\circ}F$). The core at this point is loaded with 17.7 kg of U-235 and 32 g of B-10. The effective multiplication is 1.096 and the curve of effective

multiplication as a function of void fraction, Figure VII-2, uses this value as an initial point.

In this condition, the maximum excess multiplication (15 per cent) is available. If this total 15 per cent is added to the core instantaneously, the reactor will proceed on a power excursion whose asymptotic period is 1.41×10^{-4} sec. The void fraction necessary to terminate this excursion obtained from Figure VII-2 is 27 per cent. The heat required to produce this much void is 1.79×10^{3} BTU. When the clad-core interface reaches boiling the power is 1.67×10^{7} Mw. The total energy of the excursion to this point is 2.2×10^{6} BTU.

In addition, it is found that 6.82×10^{-4} seconds after boiling begins, a sufficient steam void has been formed to terminate the power excursion. When the shut-off occurs, the power of the excursion is 2.12×10^{9} Mw and the total energy of the complete excursion is 2.8×10^{8} BTU. The central core temperature when boiling begins is about 7×10^{4} ^{o}F and, of course, shows that this impossible excursion would terminate by fuel meltdown before the water began to boil.

This excursion along with some credible ones is plotted in Figure VII-4 as integrated energy versus per cent excess multiplication.

In the second excursion, the reactor is considered to be at zero power, with the coolant flowing at the design flow rate and pressure and at operating temperature (450^{o}F). The core is considered to be loaded with 14.0 kg U^{235} and 8 grams B^{10}. This corresponds to the conditions at reactor mid-life. For these conditions, the effective multiplication of the reactor is 1.076. If 7 per cent total excess multiplication is added to the reactor instantaneously, the reactor will proceed on a power excursion whose asymptotic power period is 3.20×10^{-4} sec. The void fraction necessary to

terminate such an excursion obtained from Figure VII-2 is 9.3 per cent. The heat required to vaporize enough water in the core to produce such a void fraction is 617 BTU.

Using the same method as before, it is found that when the metal-coolant interface is at the boiling temperature, the central core temperature is 3600°F. The power of the excursion at the time when this occurs is 3.21×10^5 Mw and the total energy of the excursion up to this point is 97×10^3 BTU.

Also, it is found that 1.54×10^{-3} seconds after boiling begins, a sufficient steam void has been formed to terminate the excursion. When the shut-off occurs, the central core temperature is 5.1×10^5 °F and the metal-coolant interface temperature is 15,000°F. The power of the excursion at this time is 3.98×10^7 Mw and the total energy of the complete excursion is 12.1×10^6 BTU. Results for a number of excess multiplication additions are shown in Figure VII-4.

The amount of excess multiplication necessary to produce melting at the center of the fuel plates was calculated for a neutron lifetime of 20×10^{-6} sec. For the cold, clean reactor, it was found that the center of the plates would reach the melting temperature (2590°F) before shut-off occurs if the excess multiplication is greater than 1.16 per cent. For these conditions, the surfaces of the fuel plates would have a temperature in excess of 990°F.

For the same reactor conditions (clean and cold), it was found that the outer surfaces of the fuel plates reach the melting temperature before shut-off occurs if the excess multiplication is greater than 2.06 per cent.

When the reactor core has reached the half-way mark in its usable life and is at operating temperature, the center of the fuel plates would reach the melting temperature before shut-off occurs if the total excess multiplication is greater than 1.65 per

cent. For these conditions, the surface of the fuel plates would have a temperature in excess of 900°F.

For these same reactor conditions, it was found that the outer surfaces of the fuel plates would reach the melting temperature before shut-off occurs if the excess multiplication is greater than 3.39 per cent.

APPENDIX E-2 - CONTROL ROD WITHDRAWAL AT ROOM TEMPERATURE

A startup accident is defined here as the sequence of events following the continuous withdrawal of all control rods from a reactor initially at source level. All scram mechanisms are assumed to be inoperative. Thus, in order to reduce the reactivity, self-induced reactivity effects must be brought into play. In the following analysis, it is assumed that void formation in the coolant moderator is the only means effective in reducing reactivity for the type of accident considered.

Since void formation in the moderator will not occur until the fuel element surface is at saturation temperature, it is possible to treat the pile kinetic equations and the heat conduction equations independently until the fuel element surface reaches saturation temperature. The first part of the analysis will be devoted to the behavior of the reactor power level and the fuel element temperature up until the time at which boiling begins.

Consider first the pile kinetic equations:

$$\frac{dn}{dt} = \frac{k(1-\beta)-1}{\ell} n + \sum_{i=1}^{6} \lambda_i C_i + S \qquad \text{(E-1)}$$

$$\frac{dC_i}{dt} = \frac{k\beta_i}{\ell} n - \lambda_i C_i \quad ; \quad i = 1, 2, \cdots 6 \qquad \text{(E-2)-(E-7)}$$

where N = neutron content in reactor at time, t

C_i = delayed neutron emitter content of i^{th} kind in reactor at time, t

λ_i = decay constant for C_i, sec^{-1}

β_i = fractional yield of delayed neutrons of i^{th} kind

ℓ = prompt neutron generation time, sec

S = source contribution to neutron content of reactor, neutrons/sec

k = multiplication of neutron content at time, t

$\beta = \sum_{i=1}^{6} \beta_i$

At time t=o, it is assumed that the reactor is in subcritical equilibrium. The source level is such that the reactor is 10^{-10} of operating power level. The multiplication at t = o is assumed to be k(o) = 0.95. The time dependence of k is assumed to be

$$k(t) = k(o) + \Delta k\left(\frac{t}{110} - \frac{\sin\frac{\pi t}{58}}{2\pi}\right); \qquad o < t < 110$$

where k (o) = 0.95

Δ k = 0.211

and the rod withdrawal speed = 1 ft/min (four times design speed).

With these conditions, the reactor will be delayed critical at about t = 40 sec. and prompt critical at about t = 42 sec.

Equations (E-1) - (E-7) were solved numerically for $\ell = 6.5 \times 10^{-5}$ sec. This solution was utilized to obtain the solution for $\ell = 2 \times 10^{-5}$ sec. in the following manner. In equation (E-1) $\frac{dn}{dt} \ll \frac{1-(1-\beta)k}{\ell} n$ when $k \ll 1 + \beta$. To illustrate this, the solution for $\ell = 6.5 \times 10^{-5}$ sec. was used to make the following table -

t, sec	k	$\frac{1-(1-\beta)k}{\ell}\left(\frac{n}{\frac{dn}{dt}}\right)$
41.00	1.00456	28.3
41.20	1.00521	17.0
41.40	1.00582	8.92
41.60	1.00654	3.65

The usefulness of the approximate solution here (neglecting $\frac{dn}{dt}$) derives from the fact that Equations (E-1) - (E-7) can be written in terms of the variable $\frac{n}{\ell}$. It may be shown that the initial value of $\frac{n(t)}{\ell}$ and S are independent of ℓ, and hence the solution of n(t) for any ℓ may be obtained from the solution available for $\ell = 6.5 \times 10^{-5}$ sec. in the time interval $o < t < 41.60$ sec.

In order to extend the solution for arbitrary ℓ beyond t = 41.60 sec., a different approximation is used. Hurwitz (15) has derived an approximation solution which is valid if the reactivity does not change appreciably over a time interval comparable to the asymptotic period characteristic of the excess multiplication. The Hurwitz approximation was used to check the exact solution for $\ell = 6.5 \times 10^{-5}$ sec. for $t > 41.60$ sec. Several check points are shown in Figure E-1. Also shown in Figure E-1, are the exact solution for $\ell = 6.5 \times 10^{-5}$ sec. and the extended solution for $\ell = 2.0 \times 10^{-5}$ sec. The scale is such that log y equals 10 for the reactor at full power.

The solution of the thermal problem was obtained using the time dependent power generation obtained from the solution of the pile kinetic equations. A one-dimensional model was used to characterize the temperature distribution of the reactor fuel elements. The following illustrates the geometry of the fuel plate model.

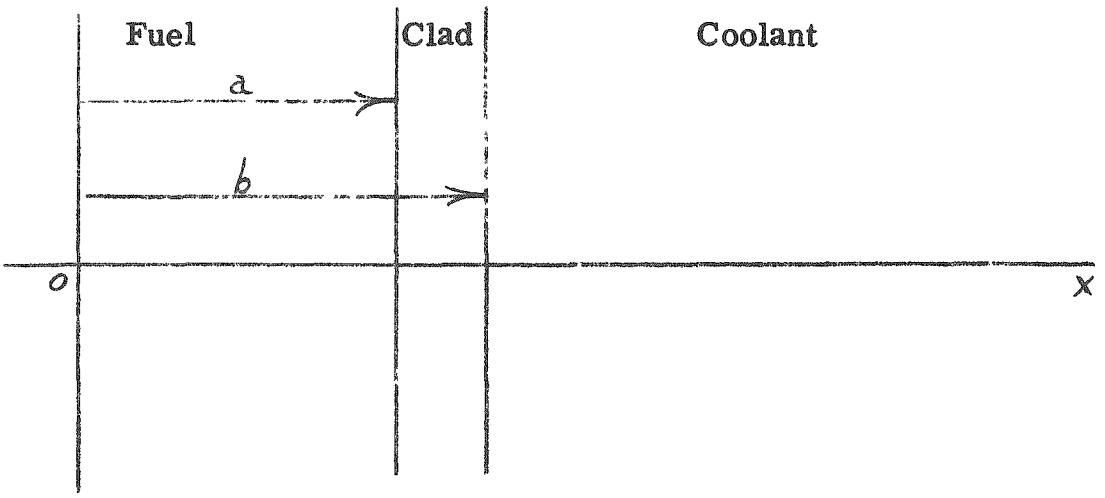

The equations which govern the temperature distribution in the fuel element are as follows:

$$\frac{\partial^2 T}{\partial x^2} = \frac{c_p \rho}{k} \frac{\partial T}{\partial t} - \frac{Q(x,t)}{k}$$

$$Q(x,t) = Q(t) \qquad (o \leq x < a \;,\; t > o)$$

$$= o \qquad (a < x < b \;,\; t > o)$$

$$\left(\frac{\partial T}{\partial x}\right)_{x=o} = o \qquad (t > o) \qquad \text{E-8}$$

$$\left(\frac{\partial T}{\partial x}\right)_{x=b} = -\frac{h}{k} T(b,t) \qquad (t > o)$$

$$T(x,o) = o \qquad (o \leq x \leq b)$$

The boundary value problem described by the above equations includes the following assumptions:

1. The mean coolant temperature is used as a reference temperature and does not vary with time.
2. The steady state coolant boundary condition is valid under transient conditions.

3. The heat source term is independent of temperature, and hence no temperature induced reactivity effects are considered.

The solution of boundary value problem (E-8) was obtained for arbitrary Q(t) by utilizing Laplace transform techniques. In particular the solutions for T (o,t) and T(b,t) were obtained in the following forms:

$$T(o,t) = \int_o^T h_1(u)\, Q(t-u)\, du$$

$$T(b,t) = \int_o^T h_2(u)\, Q(t-u)\, du \qquad \text{E-9}$$

where the functions $h_1(u)$ and $h_2(u)$ have the forms

$$h_1(u) = \sum_{u=1}^{\infty} A_n e^{-x_n^2 u}$$

$$h_2(u) = \sum_{u=1}^{\infty} B_n e^{-x_n^2 u}$$

From the forms (E-9), the time at which boiling occurs at x = b was found and the maximum fuel temperature at x = o was computed. For the two generation times the following table gives the pertinent information about the transient at the time boiling begins:

CHARACTERISTICS OF INITIAL TRANSIENT IN THE START-UP ACCIDENT

Generation Time, Sec.	Max. Fuel Temp., °F		Period of Transient, Sec.	Multiplication
	Boiling	Shutoff		
6.5×10^{-5}	770	1060	0.023	1.0104
2.0×10^{-5}	950	1200	0.010	1.0089

The second phase of the analysis seeks to furnish some quantitative estimates for the system behavior during the period of time that the shutoff mechanism (void formation) functions. These estimates are based upon the type of analysis considered in NRL-4495. In this analysis it is assumed that the transient will terminate if sufficient voids are created to compensate for the excess prompt multiplication. A complete description of the analysis and the assumptions employed is given in NRL-4495. The results of these calculations for the maximum temperature at shutoff are given in the preceding table. These temperatures are well below the melting temperature of 2590^{o} F and, therefore, unless some external means of counteracting the excess multiplication is used, the reactor may continue to operate. The qualitative behavior of the reactor power during the time after the initial transient will be discussed in the next section.

APPENDIX E-3 - CONTROL ROD WITHDRAWAL AT OPERATING TEMPERATURE AND POWER

This accident occurs after the reactor has been operating at design power and temperature. Again all rods are assumed to be withdrawn continuously at the maximum rate and all safety mechanisms fail to function. As before, the void formation is assumed to be the only method of reducing the reactivity. However, in this case, the boiling occurs very shortly after the accident is initiated, and consequently the heat transfer and pile kinetics must be considered simultaneously.

The pile kinetic equations are, of course, the same as before

$$\frac{dn}{dt} + \frac{1-(1-\beta)k}{\ell} n = \sum_{i=1}^{6} \lambda_i C_i$$

$$\frac{dC_i}{dt} = \frac{k\beta_i}{\ell} n - \lambda_i C_i$$

In addition, the equation

$$\frac{\ell}{\ell\tau}\frac{dV_f}{dt} + \frac{V_f}{T_1} = m\left(\frac{T_M}{T_B} - 1\right), \text{ if } \frac{T_M}{T_B} > 1$$

$$= 0, \text{ if } \frac{T_M}{T_B} < 1$$

is used to relate the rate of change of void fraction to the metal temperature and the residence time in the core.

Here,

V_f = void fraction

T_1 = residence time

T_M = the metal temperature - mean coolant temperature

T_B = boiling temperature - mean coolant temperature

and m = a constant

The metal temperature is dependent on the heat generation rate which, in turn, is determined by the neutron flux. This relationship is expressed as

$$c_p \rho \frac{\partial T_M}{\partial t} + \frac{h T_M}{\Delta x} = g n$$

where

h = heat transfer coefficient

and g = a constant

Finally, the effective multiplication can be written as

$$k = 1 + at - bV_f$$

where b is a constant determined from the slope of the void fraction curve near zero void fraction.

By proper substitution, these five equations can be reduced to the following four equations,

$$\frac{dy}{dt} + \frac{1-(1-\beta)h y}{\ell} = \sum_{i=1}^{6} \lambda_i X_i$$

$$\frac{dX_i}{dt} = \frac{k \beta_i}{\ell} y - \lambda_i X_i \quad , \quad i = 1, 2, \cdots 6$$

$$\frac{dk}{dt} + \frac{k}{t} = \frac{1 + a T_1 + at}{T_1} - bm(z-1) \qquad z > 1$$

$$= \frac{1 + a T_1 + at}{T_1} \qquad z \leq 1$$

$$\frac{dz}{dt} + \frac{z}{T_2} = \frac{y}{T_2}$$

where $\overline{l_2} = \frac{\nu_i \rho}{h}$

$y = \frac{n}{n_o}$

and $X_i = \frac{c_i}{n_o}$

$z = \frac{T_M}{T_B}$

These equations were set up on the differential analyzer using the following constants.

$a = 10^{-3}$ $\Delta k/sec$,

$b = 0.466$,

$m = 1.62\ sec^{-1}$,

$\beta = 0.00755$,

$T_1 = 0.44$ sec ,

and $T_2 = 0.100$ sec

The initial conditions assumed for solving this problem were

$y(o) = 0.884$,

$X_i(o) = \frac{k(o)\beta_i}{\ell \lambda_i}, (o)$,

$k(o) = 1.00$,

and $z(o) = 0.884$

The power as a function of time for a typical excursion is shown in Figure E-2. No initial peak occurs since very little excess k has been added before boiling begins. The effect of changing the time constant T_1, can also be seen in Figure E-2. It may also be noted that the fuel temperature follows closely the power rise in Figure E-3.

The qualitative behavior of the system as disclosed by this simple analysis can be taken as an indication of the behavior of the system following the initial power pulse of the previous start-up accident from room temperature.

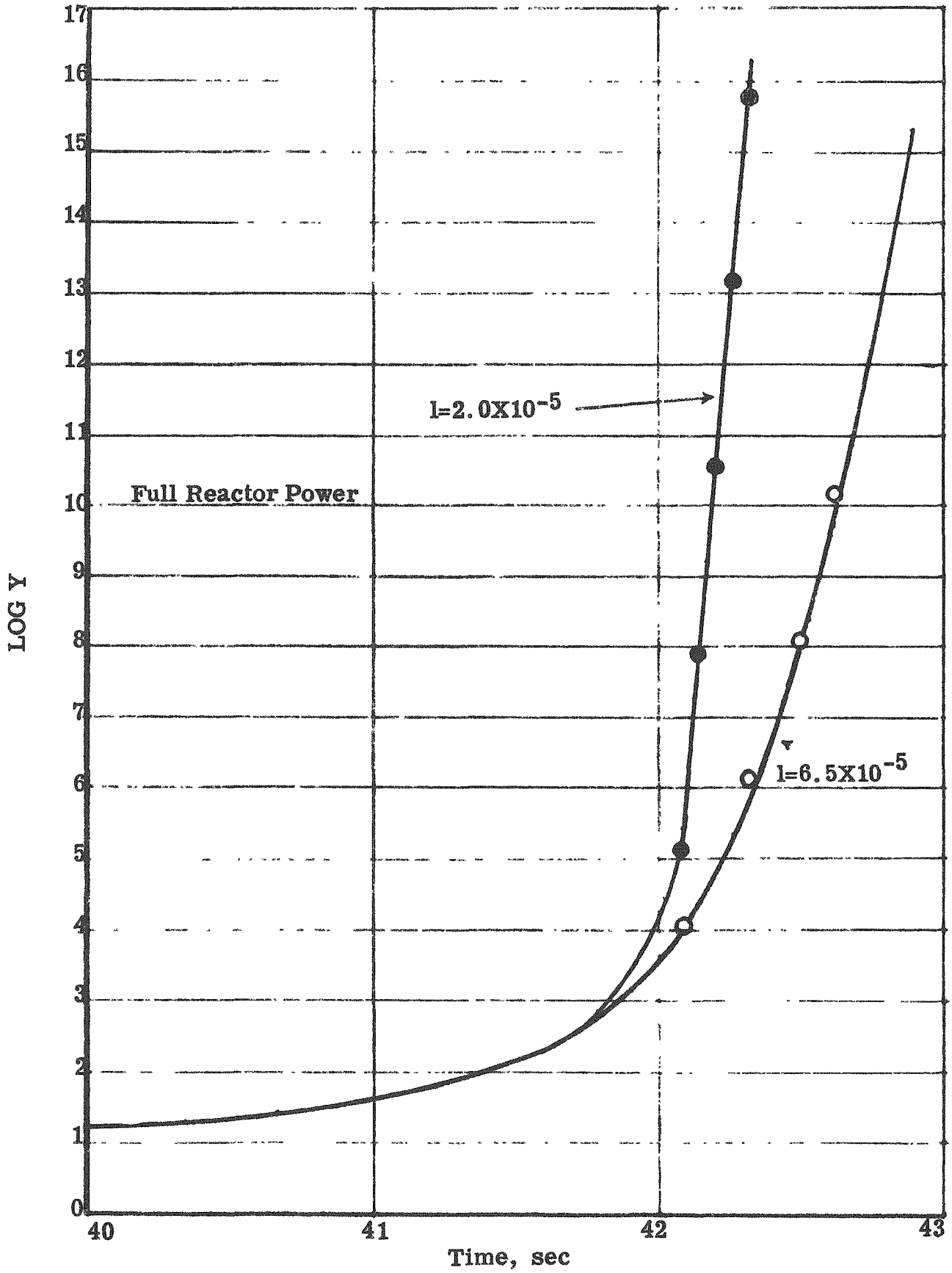

FIGURE E-1 TRANSIENT BEHAVIOR DURING START-UP

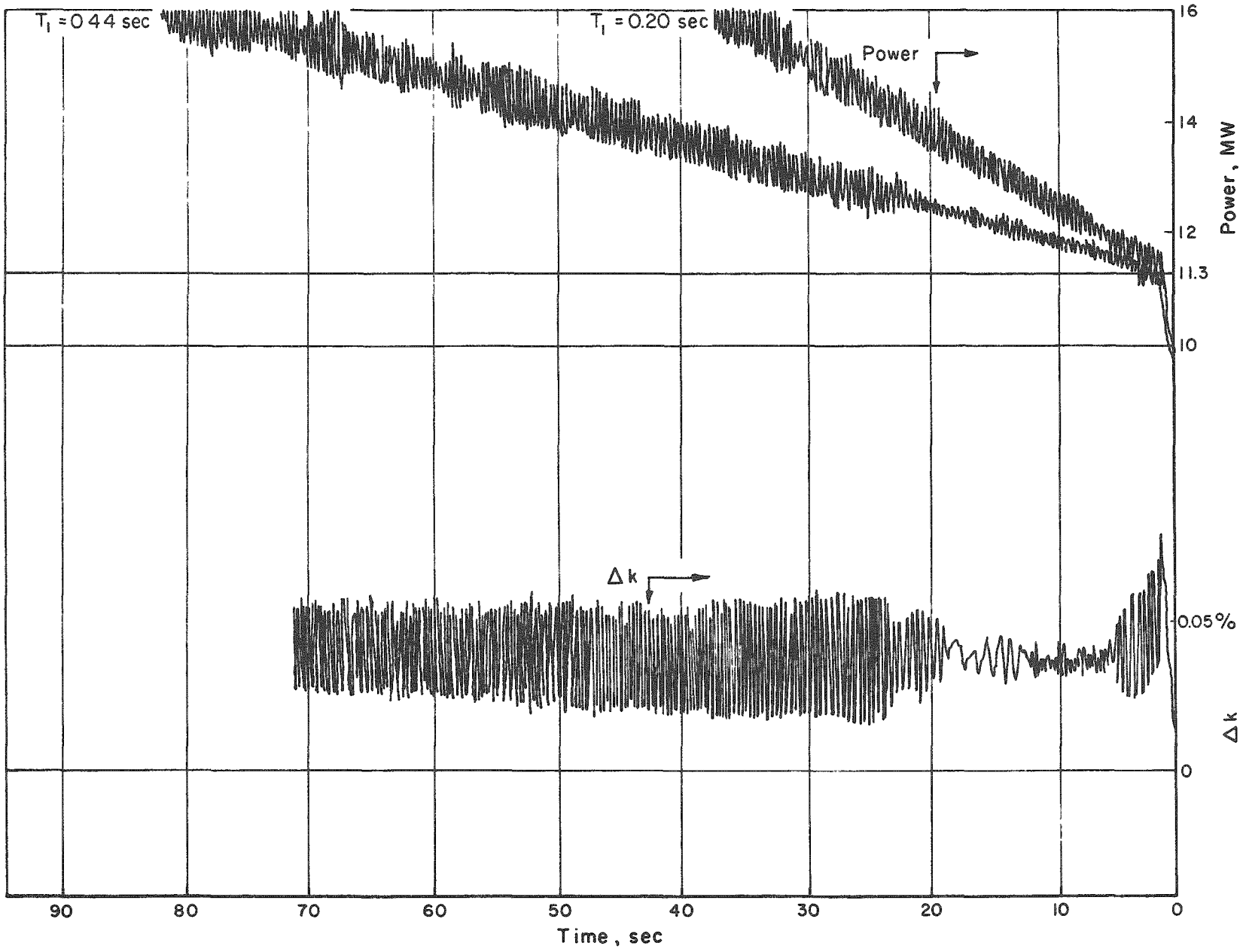

FIGURE E-2 POWER AND Δk VERSUS TIME

A-15064

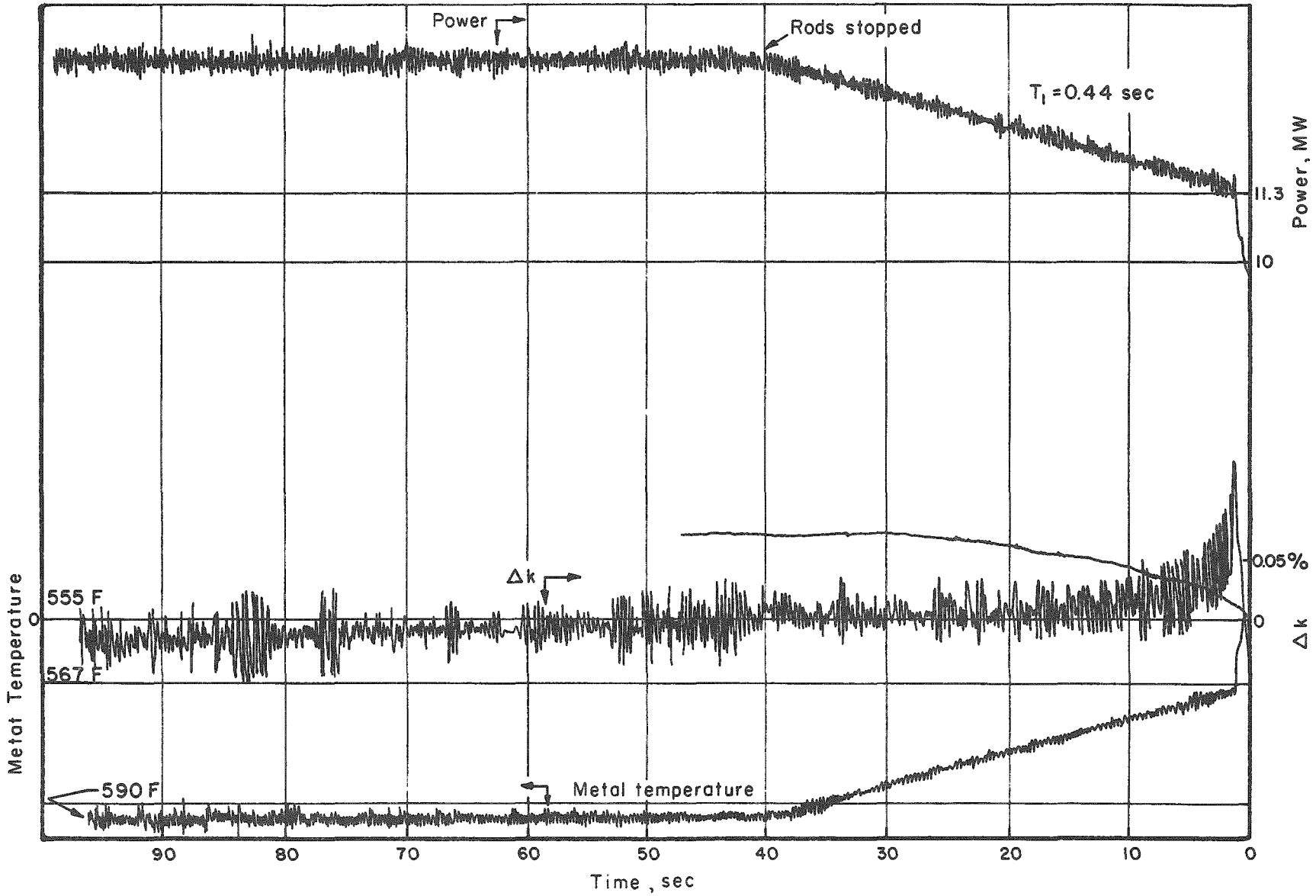

FIGURE E-3 POWER METAL TEMPERATURE AND Δk VERSUS TIME

A-15062

APPENDIX F-1 - EJECTION OF CONTROL RODS RESULTING FROM A RUPTURE OF COLD, PRESSURIZED PRIMARY SYSTEM

A rupture of the primary system in the cold, pressurized condition will result in a pressure wave that travels at the speed of sound or faster throughout the primary loop. The pressurizer, containing hot liquid and steam, will gradually expel fluid from the pressurizer, but this will occur over a considerably longer period than is required to relieve the pressure of compressed liquid in the primary loop. Thus, the actual pressure relief will be more gradual than would result from releasing only compressed liquid.

During the time the pressure wave travels the length of the core, there is a net force exerted upward on the control rods. It is conservatively assumed that a pressure wave of 1200 psi travels through the core with the velocity of sound in water, 4800 fps. Actually the pressure wave will not be so great because of the pressurizer influence, and the speed of sound increases significantly with increased pressure differential.

During the 400 microseconds the pressure wave travels through the control element fuel plates, an impulse of 0.82 pound-seconds is imparted to the 75-pound control rods, which results in a rise of the control rod, if unrestrained, of 0.0008 inches and a final velocity of 0.35 fps. This velocity will cause a total control rod lift of 0.031 inches, as the effect of gravity restores the rod to its initial position. Based on a total control rod worth of 25% and a maximum-to-average effectiveness axially of 2, this lift corresponds to a 0.070% maximum increase in reactivity from all five rods, lasting for 30 milliseconds.

APPENDIX F-2 - EJECTION OF CONTROL RODS RESULTING FROM A RUPTURE OF THE HOT PRESSURIZED PRIMARY SYSTEM

An investigation has been carried out to determine the upward force which might be applied hydraulically to the control rods following a major rupture of the primary system, and its effect on their position or motion. The concurrent growth of voids in the reactor has been calculated and the net change of reactivity from these opposing influences has been computed. A summary of the results of these computations is shown graphically in Figure F-1.

Assuming the accident to be a complete, instantaneous rupture of the 12-inch primary line on the discharge side from the reactor, a pressure drop and flow from bottom to top of the reactor would develop tending to lift the control rods. On the other hand, as this flow builds up in excess of the normal flow through the reactor, steam bubbles will form which will lower and finally completely stop the reactivity. This flashing to steam results from stored energy and is independent of reactor response to the accident. It is assumed that the control rods are de-clutched from the control mechanism at the same initial instant to permit them to fall freely and scram the reactor. However, this freedom would also permit their being lifted instead, as soon as the combined effect of pressure gradient, entrainment force and flotation exceed the weight of the rods.

The worst possible condition preceding the accident was taken to be the point in the maximum credible accident sequence when the primary pressure has risen to 1500 psia (the setting of the pressure relief valve) due to overheating of the entire primary water content and compression within the steam dome due to expansion of the water, followed by a further temperature rise to the saturation value of 1500 psia at 596°F. This con-

stitutes a far greater quantity of stored energy than could be reached before rupture if the pressure relief valve failed to open.

Since the time required to reach this 1500 psia and 596°F. point is 3.7 minutes, compared to 17 seconds required for primary fluid to complete its circuit, this initial condition has been taken as applicable for both the upper and lower portions of the reactor vessel. The following values were used:

Liquid volume above core ("B" Chamber), ft^3	27.4
Liquid volume below core ("A" Chamber), ft^3	50.0
Area of opening discharging B (severed 12 in. pipe), ft^2	0.71
Area of opening discharging A (core passages), ft^2 actual	2.08
effective	0.90

The effective core passage area is derived from the calculated pressure drop through the reactor at rated primary circulation, consisting predominantly of frictional loss, by considering the core as an orifice with the characteristic $v^{1.8} \cdot 2gH$, where the difference between the exponent 1.8 and the standard value of 2.0 is the variation of friction coefficient with velocity.

Two major premises of this analysis are that:

a) Conditions and properties of liquid and gas in each chamber will, of their own accord, rigorously follow saturation equilibrium values during the blow-down.

b) The whole incident will be completed so rapidly that neglibible gravitational separation of water and steam can take place. Instead the two will reamin together in a fairly homogeneous mixture of liquid and vapor bubbles.

The following nomenclature will be used in explaining the method of analysis:

Symbols -

P = Pressure, psia

T = Temperature, ^{o}F

v_s = Specific volume, ft^3/lb

u = Internal energy of fluid, $\frac{Btu}{lb.}$

V = Velocity, ft/sec

W = Weight, lbs.

Θ = Time, milliseconds

Subscripts, etc. -

ℓ = liquid

g = vapor

ev= increment of the function grained or lost during evaporation

m = mixture

B = "B" chamber (above the core)

A = "A" chamber (below the core)

' = mean value for the time or weight increment under calculation

The calculating procedure is as follows:

A. Blowdown Sequence for Each Chamber Treated Independently

1. Prepare from standard steam tables a graph of saturation P, T, v_s, g, $v_{s,\ell}$ and u_{ev}, all versus u_ℓ as the abscissa.
2. For either chamber assume successive weight increments of water (or water-steam mixture) expelled, without reference to the time required for this to take place.

3. Determine the volume thus made available for steam, recognizing that after the first step some of the expelled material will be steam, and that the remaining steam will expand as the pressure decreases.

4 Calculate the weight of liquid which can evaporate into the space made available, the internal energy required to do this, and the resulting reduced value of u_ℓ for the unevaporated liquid remaining in the vessel.

5. By maintaining a running plot of the resulting values of u_ℓ and of %-evaporated -by-weight versus quantity expelled, and extrapolating to the mid and end points of each new interval, the effective values of $v_{s,\ell}$, $v_{s,g}$ and u_{ev} needed for each step can be obtained from the steam table chart. The new values of P and T can also be read off this chart and $v'_{s,m}$ derived, while percent reduction in density is figured directly from the weight expelled. A trial and error method is used to compute the performance in the first interval.

6. The corresponding graph for the other chamber is prepared by plotting the same derived conditions against values of weight expelled corrected in the ratio of the total volumes of the two chambers.

B. Combined Blowdown of A & B Chambers versus Time

1. Assume intervals of time (10 to 50 millisecond range)

2. Estimate P' and $v'_{s,m}$ for each chamber for the period.

   Note: By trial and error for first one or two points,

   by extrapolation of running graph thereafter.

3. Calculate velocity for discharge from B:

$$V = \sqrt{2g \cdot 144\ (P_B' - 14.7)\ v_s',\ mB}$$

4. Calculate velocity for discharge from A to B:

$$V = \frac{1.8}{}\sqrt{2g \cdot 144\ (P_A' - P_B')\ v_s',mA}$$

where the radical 1.8 is used instead of 2 to allow for the high L/D ratio and resulting frictional characteristics of the core passages. (See Discussion of equivalent area on the preceding page).

The working chart prepared to expedite this and the next step checked closely with independently derived points of pressure drop vs flow in the pertinent range, using standard methods and Pigott's friction factors, based on water.

5. Calculate volume and weight flow out of B, from A to B, and resultant net for B, for the period.
6. Determine from the previously prepared working charts the new values of P, T, and $v_{s,m}$ for A and for B.
7. By plotting cumulative net weight expelled from B and from A versus time and extrapolating the lines, obtain these values for midpoint of the next time interval.
8. Tabulate and plot, in addition to the cumulative values of W expelled, P_A, P_B, $(P_A - P_B)$ and percent reduction in density.

C. Resulting Rod Ejection Sequence

1. The effect on the control rod assemblies of the developing pressure gradient and primary coolant flow has been analyzed, taking account of the actual geometry of a complete control rod assembly and of the flow through it. The overall pressure drop between A and B has been broken down into its component fractions, taking account of kinetic and frictional effects. These were multiplied by their appropriate projected areas, to determine the force applied to the rod for each value of overall pressure gradient.
2. Rod displacements have been calculated based on the total equivalent mass of the rods, racks and engaged rotating assembly, acted on by the total force calculated

as described on the preceding page, plus the flotation effect. Friction of the rotating assembly has been neglected, since this is the more pessimistic treatment yielding more rapid rod ejection.

The results of this investigation are presented in Chapter VII, and illustrated by Figure VII-5.

The actual reduction in reactivity will be more rapid than shown for two reasons:

a) The controlling reduction in density will be an integrated mean within the core, roughly 30% of the way from chamber A conditions to those of chamber B. This would amount to a 22.5% reduction, for example, concurrent with 18% in A.

b) The calculations have ignored the continuing heat generation of the core, which would actually accelerate the local boiling and density reduction in the core. Thus 20 BTU/lb working in the range where u_{ev} = 600 BTU/lb. could produce additional evaporation of 3 1/3% of each pound passing through, or an additional reduction in density of about 3%.

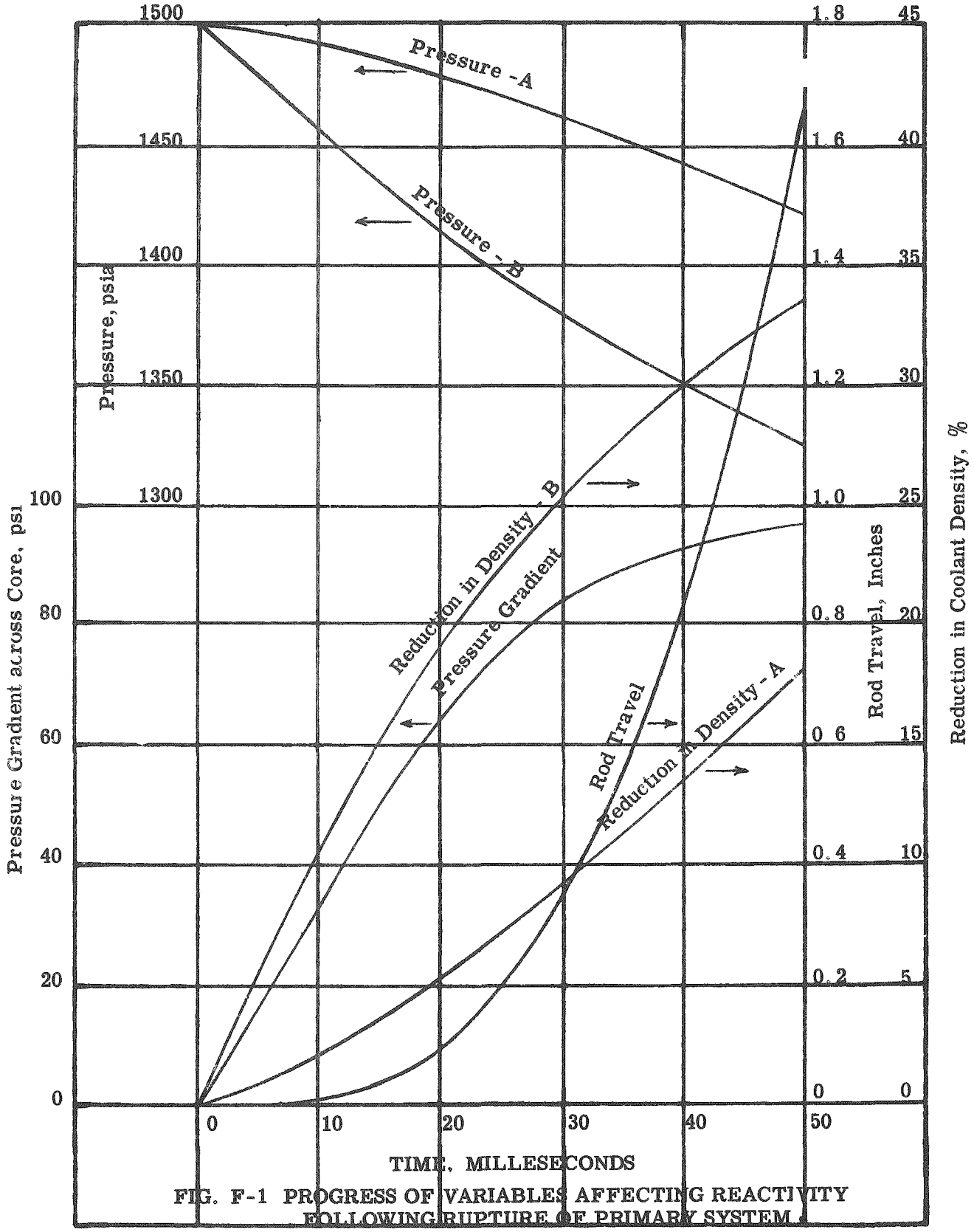

FIG. F-1 PROGRESS OF VARIABLES AFFECTING REACTIVITY FOLLOWING RUPTURE OF PRIMARY SYSTEM

APPENDIX G - 10 Mw CONSTANT POWER RUNAWAY

In determining the time dependence of the important variables of the reactor power plant system during the events leading up to the maximum credible accident, a simple analytical model can be employed because of the relatively long period of time involved. The more important of the simplifying assumptions may be summarized as follows:

1. With a primary loop circulation time of less than twenty seconds and an overall excursion measured in terms of minutes, the primary system can be considered to be at a uniform average temperature.

2. The reactor, primary loop and the secondary loop may be simplified to a three element system, such that the heat developed in the reactor is transmitted to the primary heat sink. Part of this heat energy is accumulated in the primary heat sink and part of it is transmitted to the secondary heat sink, which is the water existing in the steam generator.

3. The heat absorbing capacity of the metallic structure can be neglected since the time for the excursion is short enough that the amount of heat transferred into the metal will be insignificant. Further, the heat so stored is not available for the pressure peak developed after the rupture but will be released over a considerable time interval after the rupture.

4. The heat transfer coefficient of the steam generator is constant throughout the incident.

With these simplifying assumptions the heat balance of the system at any instant may be written as:

$$q = W_p C_p \dot{T}_p + W_s C_s \dot{T}_s \qquad \text{(G-1)}$$

where

C	= Specific heat of water	BTU/lb-^oF
q	= Reactor power	BTU/sec.
W	= Weight of Water	lb
T	= Water temperature	^oF

and subscripts p and s refer to the primary and secondary systems respectively. Dotted quantities indicate derivatives with respect to time.

The primary and secondary temperatures may be related through the heat transfer characteristics of the steam generator. Since it has been assumed that the characteristics of the steam generator are constant during the incident,

$$W_s C_s \dot{T}_s = hA\,(T_p - T_s) \qquad \text{(G-2)}$$

where

A	= Heat transfer area of steam generator	ft^2
h	= Heat transfer coefficient of steam generator	BTU/ft^2-^oF-sec

From this relationship it is possible to determine T_p in terms of the first and second time derivatives of T_s. Substituting these values in equation (G-1), the differential equation for the system may be written as:

$$\ddot{T}_s + \frac{ha\,(W_p C_p + W_s C_s)\,\dot{T}_s}{(W_p C_p)\,(W_s C_s)} = \frac{hA}{(W_p C_p)\,(W_s C_s)}\,q \qquad \text{(G-3)}$$

For the case of a constant power excursion q = constant, and the solution to equation (G-3) is:

$$T_S = T_{is} + \frac{(W_p C_p)(W_s C_s)}{hA\,(W_p C_p + W_s C_s)}\left[\frac{hA\,(T_{ip} - T_{is})}{W_s C_s} - \frac{q}{W_p C_p + W_s C_s}\right]\left[1 - e^{-\frac{hA(W_p C_p + W_s C_s)\,t}{(W_p C_p)\,(W_s C_s)}}\right]$$

$$+ \frac{qt}{W_p C_p + W_s C_s} \qquad \text{(G-4)}$$

where the subscript i refers to the initial value.

The primary temperature can then be found from equation (G-2) to be:

$$T_p = \frac{W_s C_s \dot{T}_s}{hA} + T_s$$

$$+ \frac{W_s C_s}{hA}\left[\frac{hA\,(T_{ip} - T_{is})}{W_s C_s} - \frac{q}{W_p C_p + W_s C_s}\right] e^{-\frac{hA\,(W_p C_p + W_s C_s)\,t}{(W_p C_p)\,(W_s C_s)}}$$

$$+ \frac{q\,W_s C_s}{hA\,(W_p C_p + W_s C_s)} + T_s$$

For the particular conditions of the APPR-1, when the power level of the reactor remains constant during the incident, these equations reduce to:

$$T_S = 415.5 - 33.5e^{-0.069t} + 0.75t$$

and $$T_p = 430.5 + 11.5e^{-0.069t} + 0.75t$$

The performance of the system has also been investigated for the case in which reactor power varies with time, the manner of this variation having an important effect upon the time response of the system. In view of the strong negative temperature coefficient of the system, a fair approximation to reality can be obtained by assuming a linear variation of power with time. Thus the reactor power may be written as:

$$q = q_o + Qt$$

where Q = Rate of increase of reactor power.

The differential equation of the system becomes:

$$\ddot{T} + B\dot{T} = q_o + Qt$$

The solution to which may be written as:

$$T = Ce^{-Bt} + \frac{Q}{2B}t^2 + \left(\frac{q_o}{B} - \frac{Q}{B^2}\right)t + \left(\frac{Q}{B^3} - \frac{q_o}{B^2} + D\right)$$

where C and D are constants of integration. B, q_o and Q refer to the system parameters and operation characteristics.

Numberical results were obtained for the APPR-1 system for linear power increases with rates of rise as high as 2000 kw/sec. Simulator results (Appendix E-3) have shown even without the inclusion of a negative temperature coefficient, local boiling will limit the rate of power rise to very low values so that the constant power case is considered to be a satisfactory approximation.

APPENDIX H - CALCULATIONS OF HAZARD TO SURROUNDING AREA IN THE EVENT OF A CATASTROPHE

The calculations are based on the following data and formulae:

1. External exposure: Nomographs by Holland.

2. Inhalation:

$$X = \left[\frac{2Q}{\pi C^2 \bar{u} (\bar{u}t)^{2-n}} \right] e^{-\frac{h^2}{C^2 (ut)^{2-n}}}$$

$$X_{max} = \frac{2Q}{e \pi \bar{u} h^2}$$

$$\ell_{max} = \left(\frac{h^2}{C^2} \right)^{\frac{1}{2-n}}$$

3. Deposition:

Continuous washout

$$\omega = \frac{Q}{e \pi^{\frac{1}{2}} C y x^{2-\frac{n}{2}}}$$

Total washout - Instantaneous release

$$\omega = \frac{Q}{\pi C^2 (\bar{u}t)^{2-n}}$$

Total washout - Continuous release

$$\omega = \frac{Q}{(2\pi)^{\frac{1}{2}} C y \bar{u} x^{(2-n)/2}}$$

where

X	=	Concentration;	curies/meter^3
Q	=	Source strength;	curies/second
h	=	Stack height;	meters
x	=	Horizontal distance downwind from stack base;	meters

C	=	Virtual difference coefficient	Meters $^{n/2}$
d_{max}	=	Horizontal distance downwind from stack base at which maximum concentration exists;	meters
$\bar{u}$	=	Mean wind speed;	meters/second
n	=	dimensionless stability parameter	
t	=	time;	seconds
ω	=	deposited concentration;	curies/meter^2

4. Long-lived fission product concentration in river:

$$\chi = \frac{A_o}{V_w}$$

where

χ	=	Concentration;	curies/meters^3
A_o	=	Activity at origin;	curies
V_w	=	Volume of water;	meters^3

Table H-1 - Parameters

	Day	Night
Wind speed (u)	5 mps	2 mps
C_y	.22	.09
n	.25	.4
x_o correction	100 m	200 m
Cloud rise	1000 m	500 m
Cloud radius	20 m	12 m

Source strength:

Instantaneous ("Hot" cloud)

10 Mw steady power operation

11.15×10^7 Curies of mixed fission products

11.61×10^6 curies of "30 isotope" mixture

50% release:

5.6×10^7 curies of mixed fission products

5.8×10^6 curies of "30 isotope" mixture

Continuous release ("Cold" Cloud - 12 hour period)

2.58×10^3 curies/sec of mixed fission products

2.69×10^2 curies/sec of "30 isotope" mixture

River depth, 10 mile downstream average	-	4 m
River width, 10 mile downstream average	-	2800 m
River velocity	-	4.5 m/min.
Horizontal diffusion	-	0.1
Vertical diffusion	-	0.05

Activity is uniformly diffused to a depth of 0.33 m due to mechanical agitation of "washout" precipitation.

Table H-2 - External Gamma Dosage - "Hot" Cloud

	Day	Night
All distances	< 1 r	< 1 r

Note: At close distances the initial burst of gamma radiation and the physical dispersion of contaminated materials by blast would probably result in external gamma radiation in excess of the values shown above.

Table H-3 - Inhalation Dosage - "Hot" cloud (Height of rise: 1000 m - Day; 500 m - Night. 50% release of fission products "30 isotope" mixture)

Maximum Permissible Exposure: 0.24 curie sec/m^3 (25 rem to the bone)

Distance (m)	Dosage (curie sec/m^3)	
	Day	Night
100	$< 10^{-6}$	$< 10^{-6}$
500	$< 10^{-6}$	$< 10^{-6}$
1000	$< 10^{-6}$	$< 10^{-6}$
2000	--	$< 10^{-6}$
5000	$.59 \times 10^{-2}$	$< 10^{-6}$
10,000	.20	$.37 \times 10^{-3}$
20,000	--	.52
25,000	.20	--
40,000	--	2.6
50,000	$.78 \times 10^{-1}$	--
100,000	$.25 \times 10^{-1}$	1.68
Maximum:		
Distance		
15,000	.27	
48,000		2.7

Note: The inhalation dosage is very sensitive to the height of rise of the cloud. Lesser rise would increase the dosages by orders of magnitude. It should also be mentioned that vigorous large scale convection during the day may transport sufficient material downwards to greatly diminish the "skip" distance shown extending some 2000 m from the reactor.

Table H-4 - Ground Deposition by Continuous Precipitation - "Hot" Cloud

Distance (m)	Curies/m^2	
	Day	Night
100	2.5×10^3	4.5×10^3
500	3.3×10^2	9.8×10^2
1,000	1.0×10^2	3.7×10^2
5,000	5.9	2.7×10^1
10,000	1.7	8.1
25,000	.3	1.6
50,000	.082	.45
100,000	.022	.13

Table H-5 - Integrated Gamma Dosage from Deposition by Continuous Precipitation - "Hot" Cloud

Distance (m)	12 Hour Dosage (Roentgens)	
	Day	Night
100	4.5×10^4	8.0×10^4
500	5.9×10^3	1.7×10^4
1,000	1.8×10^3	6.5×10^3
5,000	100	4.6×10^2
10,000	29	132
25,000	5	25
50,000	1	6
100,000	.3	1.7

Note: Conversion to roentgens based on dosage at 1 meter above a uniformly contaminated infinite level plain. The actual radius of deposition is less than the mean free path of gamma radiation out to about 500 meters during the day and 5000 meters at night, thus the close-in dosages are quite pessimistic. A further reduction, by a factor of 10 may well result from shielding by ground irregularities, etc.

Table H-6 - Ground Deposition from Instantaneous "Total Washout" - "Hot" Cloud

Distance (m)	Curies/m^2	
	Day	Night
100	3.4×10^4	2.4×10^5
500	4.9×10^3	6.3×10^4
1,000	1.7×10^3	2.6×10^4
2,000	---	1.0×10^4
5,000	1.2×10^2	2.5×10^3
10,000	3.6×10^1	8.9×10^2
20,000	---	2.9×10^2
25,000	7.2	---
40,000	---	9.7×10^1
50,000	2.1	---
100,000	.63	2.2×10^1

Table H-7 - Integrated Gamma Dosage from Deposition by Instantaneous "Total Washout" - "Hot" Cloud

Distance (m)	12 Hour Dosage (Roentgens)	
	Day	Night
100	6.1×10^5	3.6×10^6
500	9.0×10^4	1.1×10^6
1,000	3.0×10^4	4.6×10^5
2,000	---	1.7×10^5
5,000	2.1×10^3	4.2×10^4
10,000	6.1×10^2	1.4×10^4
20,000	---	4.5×10^3
25,000	110	---
40,000	---	1.4×10^3
50,000	33	---
100,000	9.2	290

Note: Conversion to roentgens based on dosage at 1 meter above a uniformly contaminated infinite level plain. The actual radius of deposition is less than the mean free path of gamma radiation out to about 500 meters during the day and 5,000 meters at night, thus the close-in dosages are quite pessimistic. A further reduction, by a factor of 10, may well result from shielding by ground irregularities, etc.

Table H-8 - External Gamma Dosage from Continuous Release - "Cold" Cloud

Distance (m)	12 Hour Dosage (Roentgens)	
	Day	Night
100	166	828
500	32	380
1,000	19	190
5,000	3	48
10,000	.6	29
20,000	.2	6
40,000	< .1	5
50,000	< .1	3
100,000	< .01	1.4

Table H-9 - Integrated Inhalation Dosage - "Cold" Cloud

(No cloud rise, 100% release of fission products

"30 isotope" mixture at constant rate over 12 hours)

Maximum Permissible Exposure: .24 curie sec/m^3 (25 rem to the bone)

Distance (m)	Curie sec/m^3 - 12 hours	
	Day	Night
100	9.5×10^4	2.9×10^5
500	5.6×10^2	2.2×10^4
1,000	170	7.3×10^3
2,000	---	2.4×10^3
5,000	10	5.6×10^2
10,000	3	1.6×10^2
20,000	---	6.1×10^1
25,000	.6	---
40,000	---	2×10^1
50,000	.18	---
100,000	.05	4.8

Note: The long half life of the "30 isotope" mixture permits the omission of any decay correction.

Table H-10 - Ground Deposition Rate from Continuous Precipitation - "Cold" Cloud

Distance (m)	Curies/m^2 sec	
	Day	Night
100	.43	1.5
500	2.1×10^{-2}	8.2×10^{-2}
1,000	5.8×10^{-3}	2.4×10^{-2}
5,000	2.8×10^{-4}	1.3×10^{-3}
10,000	7.7×10^{-5}	3.8×10^{-4}
25,000	1.4×10^{-5}	7.2×10^{-5}
50,000	3.8×10^{-6}	2.1×10^{-5}
100,000	1.0×10^{-6}	6.0×10^{-6}

Note: It is assumed that precipitation washout begins at the time of release of the cloud and continues throughout the time required for the plume to pass each distance.

Table H-11 - Integrated Gamma Dosage from Deposition by Continuous Precipitation - "Cold" Cloud

Distance (m)	12 Hour Dosage (Roentgens)	
	Day	Night
100	3.3×10^5	1.2×10^6
500	1.6×10^4	6.3×10^4
1,000	4.4×10^3	1.8×10^4
5,000	2.1×10^2	9.9×10^2
10,000	57	2.7×10^2
25,000	9.9	47
50,000	2.6	13
100,000	.63	3.4

Note: Conversion to roentgens based on dosage at 1 meter above a uniform contaminated infinite level plain. The actual radius of deposition is less than the mean free path of gamma radiation out to about 500 meters during the day and 5000 meters at night, thus the close-in dosages are quite pessimistic. A further reduction, by a factor of 10, may well result from shielding by ground irregularities, etc.

Table H-12 - Ground Deposition from Instantaneous "Total Washout" - "Cold" Cloud

Distance (m)	Curies/m^2	
	Day	Night
100	1.7×10^{1}	1.4×10^{2}
500	4.1	4.0×10^{1}
1,000	2.2	2.3×10^{1}
5,000	.54	6.3
10,000	.30	3.6
25,000	.13	1.7
50,000	7.2×10^{-2}	1.0
100,000	3.9×10^{-2}	.57

Table H-13 - Integrated Gamma Dosage from Deposition by Instantaneous "Total Washout" - "Cold" Cloud

Distance (m)	12 Hour Dosage (Roentgens)	
	Day	Night
100	300	2.7×10^3
500	73	710
1,000	39	400
5,000	9.3	106
10,000	5.1	59
25,000	2.1	26
50,000	1.1	14
100,000	.57	7.4

Table H-14 - Activity Concentration in Potomac River

"Total Washout" - "Hot" Cloud

Distance Downstream (Meters)	Concentration $\frac{(\text{Curies})}{(\text{Meter}^3)}$
Origin	3.8×10^5
10	1.2×10^5
100	7.8×10^3
500	1.0×10^3
1,000	3.5×10^2
5,000	1.7×10^1
10,000	4.6
13,900	2.2

Note: Diffusion is limited largely by width and depth of river. At 13,900 meters (8.7 miles) downstream from the APPR-1 site this limit is reached. Concentration will then remain essentially constant until it has travelled an additional 75 miles downstream where the river width is approximately 6000 meters (4 miles). Concentration will then approximate 0.5 curie/meter^3 as it enters the Chesapeake Bay.

APPENDIX I - PRESSURE IN VAPOR CONTAINER FOLLOWING A MAXIMUM CREDIBLE ACCIDENT

The pressure-time relationship in the vapor container following a maximum credible accident has been calculated and the results shown in Chapter VIII, Figure VIII-2. The following is a summary of the basic assumptions and design characteristics and the methods of calculation used.

A. Assumptions & Design Characteristics

1. Total energy released immediately following rupture is 7.32×10^6 BTU. This release is essentially instantaneous. This value varies slightly from the value of 7.4×10^6 BTU used in the discussion of Chapter VIII because it was arrived at by entirely independent calculations by a subcontractor who used a slightly different method in the detail calculations which resulted in the curve of Figure VIII-2. Agreement is within less than 1%, however, which is considered to be good. The following values were used:

Net volume of vapor container (corrected for internal construction	37,000 ft^3
Total volume of primary circuit	200 ft^3
Total volume of secondary circuit	138 ft^3

	Wt.-Lb.	u - 10^6 BTU
Water in primary system at instant rupture (1500 psia., 596° F)	8500	5.14
Water expelled to vapor container from primary system through pressure relief valve (Av. temp. 1450° F)	431	0.26

	Wt.-Lb.	u - 10^6 BTU
Steam expelled from pressurizer	69	0.08
Water in secondary system	2900	1.75
Steam in secondary system	82	0.09

2. Afterheat released by fission product decay during 48 hours following rupture is as given in ORNL 1613. The various effects operating during this period are as follows:

   (a) Release of decay heat from fission products.

   (b) Release of heat stored in hot metal parts.

   (c) Absorption of heat by primary shield water and structure. This is accomplished by heat transfer through the walls and free water surface of the shield tank, realistic heat transfer values being used. The shield tank was assumed not to fail and release its contents into the vapor container. Heat absorption of concrete shielding outside the vapor container is ignored.

   (d) The water spray is turned on (manual emergency system) approximately two hours after the rupture and continued for 46 hours at 20 gpm.

B. Calculation Methods

1. Conservation of internal energy was used within the system under consideration.

2. The pressure in the vapor container was calculated by trial and error, assuming a final temperature and pressure, calculating volumes of steam and water and repeating until the total volume equals that available in the vapor container. Because of the rapidity of the pressure and temperature rise, the initial peak pressure is based only on energy stored in the

steam and water released.

3. The heat released by hot metal parts takes place by boiling off the water remaining in the primary system. The metal parts are assumed to be at the initial operating temperature (450° F) since the time of rise from such conditions to those at the moment of the rupture is too short to increase the temperature of this large mass of metal (46,000 lb.) appreciably. This heat release takes place in approximately one half hour and amounts to approximately 1.2×10^6 BTU.
4. The heat is absorbed by the 2 ft. concrete lining of the vapor container and is the major effect which causes the pressure to fall rapidly after the initial peak. This effect continues during the later phases of heat release from the metal parts and fission products. The heat absorbing capacity of the concrete was calculated by determining, at the end of each interval of elapsed time, the depth of penetration of the heat wave and the average temperature rise of the concrete. Density of the concrete was taken as 150 lb/ft^3 and its specific heat as 0.22 BTU/lb -°F.
5. Overall rates of heat transfer to the shield tank follow those used in previous calculations of a similar problem. They were assumed to fall no lower than 50 BTU/hr-ft^2 - ° F. When the temperature difference between the shield tank water and the surrounding vapor became small, the use of the rate equation was discontinued and only the heat balance equation was used.
6. Spray water at 75° F was assumed available for the final 46 of the 48-hour interval studied. Its heat absorption was calculated by a heat balance equation, assuming thermal equilibrium of the water and vapor.

7. Net interval energy was calculated at the end of several time intervals out to the 48-hour elapsed time. Total pressure was established at each time interval by trial and error as in the case of the initial peak.

REFERENCES

1. Boch, A.L., et al, A Conceptual Design of a Pressurized Water Package Power Reactor, ORNL 1613 and ORNL 1613 Supplement I.
2. Cooms, J.H. and Boman, E.S., Method of Fabrication of Control and Safety Element Components for the Aircraft and Homogeneous Reactor Experiments, ORNL 1463.
3. Fairbanks, F.B. and Meem, J.L., Shielding Requirements for the APPR-1, APAE-3 (in preparation).
4. Golian, S.E., et al, Transient Response of Plane Parallel Fuel Assemblies to Exponential Power Excursions, NRL 4495.
5. Dietrich, J.R., Experimental Investigation of the Self-Limitation of Power During Reactivity Transients in a Subcooled, Water-moderated Reactor, ANL 5323.
6. Holland, J.Z., Cloud Dosage Calculations, Meteorology and Atomic Energy, (to be published).
7. Sutton, O.G., The Theoretical Distribution of Airborne Polution from Factory Chimneys, Q. J. Royal Meteorological Society, Vol. 73, 1947.
8. Sutton, O.G., Micrometeorology, McGraw-Hill, New York, N.Y., 1953
9. Holland, J.Z., A Meteorological Survey of the Oak Ridge Area, ORO 99, 1953.
10. Burnett, T.J., Private Communication to J.L. Meem, 1955.
11. Chamberlain, A.C., Aspects of Travel and Deposition of Aerosol and Vapor Clouds, AERE HP/R 1261, 1953.
12. Krause, E.H., et al, Proposal for NRL Research Reactor, NRL 4129, 1953.
13. Stone, J.J., and Mann, E.R., ORNL Reactor Controls Computer, ORNL 1632.
14. Gallagher, J.G. and Winton, M.L., Derivation of the Thermal Kinetic Equations for the Package Reactor, ORNL CF 55-4-53.
15. Hurwitz, Henry, Jr., Derivation and Integration of the Pile-Kinetic Equations, Nucleonics, July 1949.

SUPPLEMENT

August 26, 1955

INTRODUCTION AND CONCLUSIONS

In order to make the APPR-1 even safer for operation; several additional safety features have been added to the reactor, over and above those described in the Hazards Summary Report (APAE No. 2). Additional calculations with regard to the hazards have also been made, and further data on population distribution and wind direction are available.

These are described in the following pages and the description is arranged according to the appropriate chapters in which the particular feature was described in the original report.

The conclusion is even more positive that the maximum credible accident can be properly contained and will not endanger the population of the surrounding area. The add itional safety features and further calculations show that the possibility of a nuclear runaway is completely incredible.

Chapter I

C. Site

The population distribution and percentage frequency of wind direction near the site are shown in Figures I - 4, 5 and 6. The figures are self explanatory. Populations are based on the 1950 census, and the wind directions are based on Washington National Airport hourly observations from January 1945 through December 1952. Fig. I - 4 illustrates the above relationship for all wind conditions; Fig. I - 5 when precipitation is falling (washout); and Fig. I - 6 when the inversion base is below 500 feet (night time condition). Data for the latter figure are from daily readings taken at 0300 GCT.

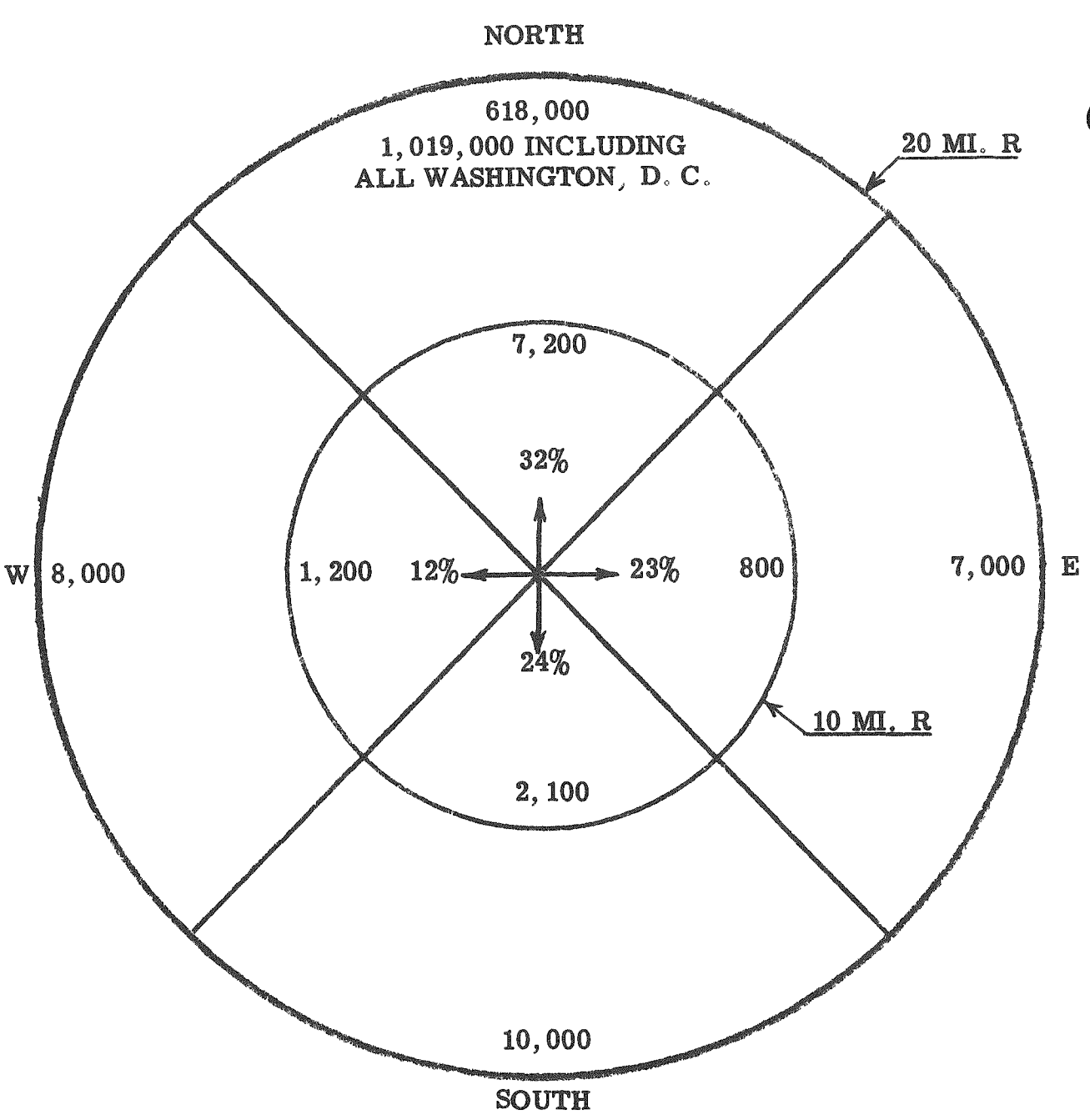

CALM - 9.2%

POPULATION DISTRIBUTION AND PERCENTAGE FREQUENCY OF WIND DIRECTION

FIG. I - 4

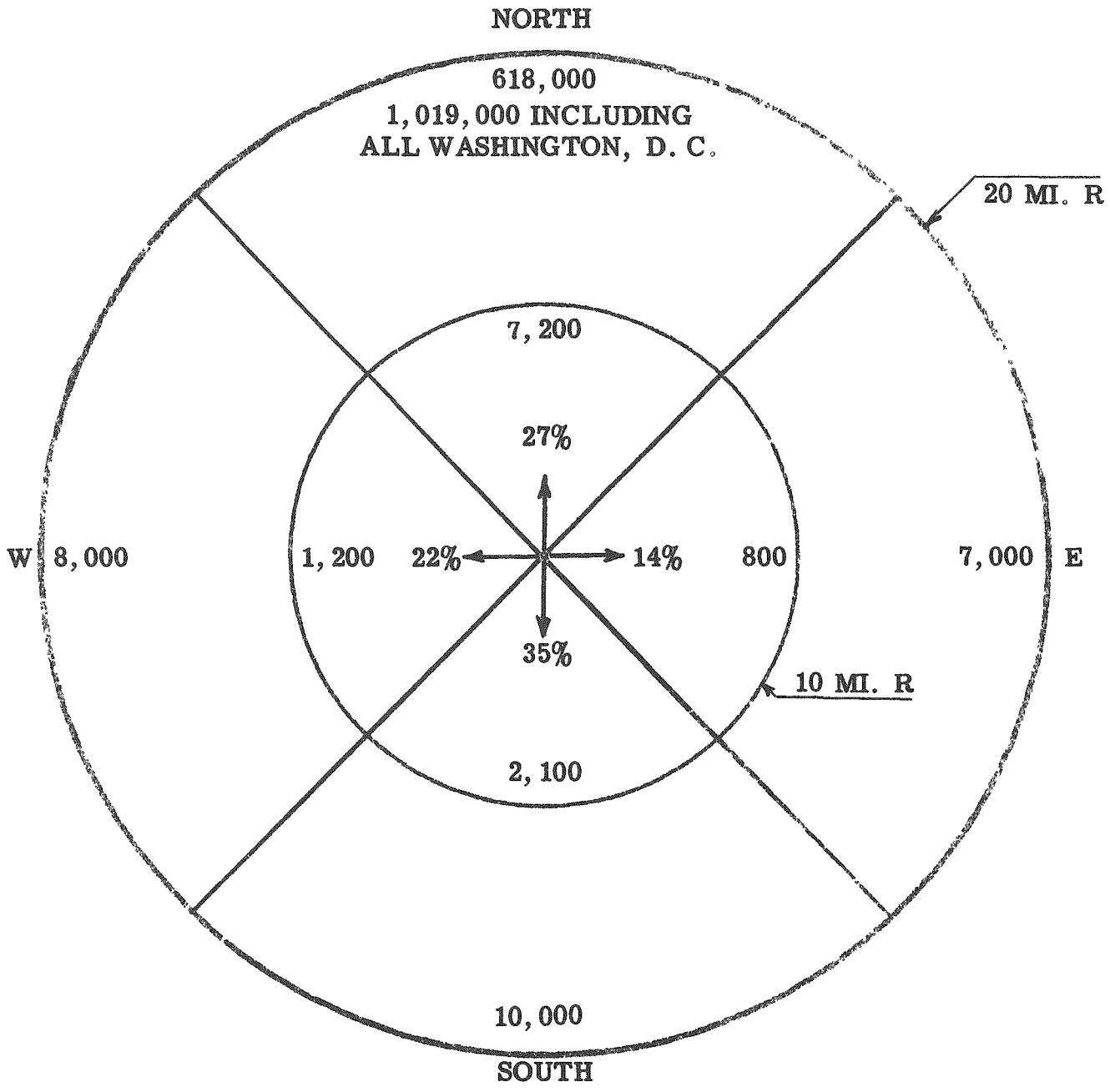

CALM 3.5%
DURING 1953 THERE WERE 153 DAYS HAVING SIGNIFICANT PRECIPITATION.

POPULATION DISTRIBUTION AND PERCENTAGE FREQUENCY
OF WIND DIRECTION DURING PRECIPITATION

FIG. I - 5

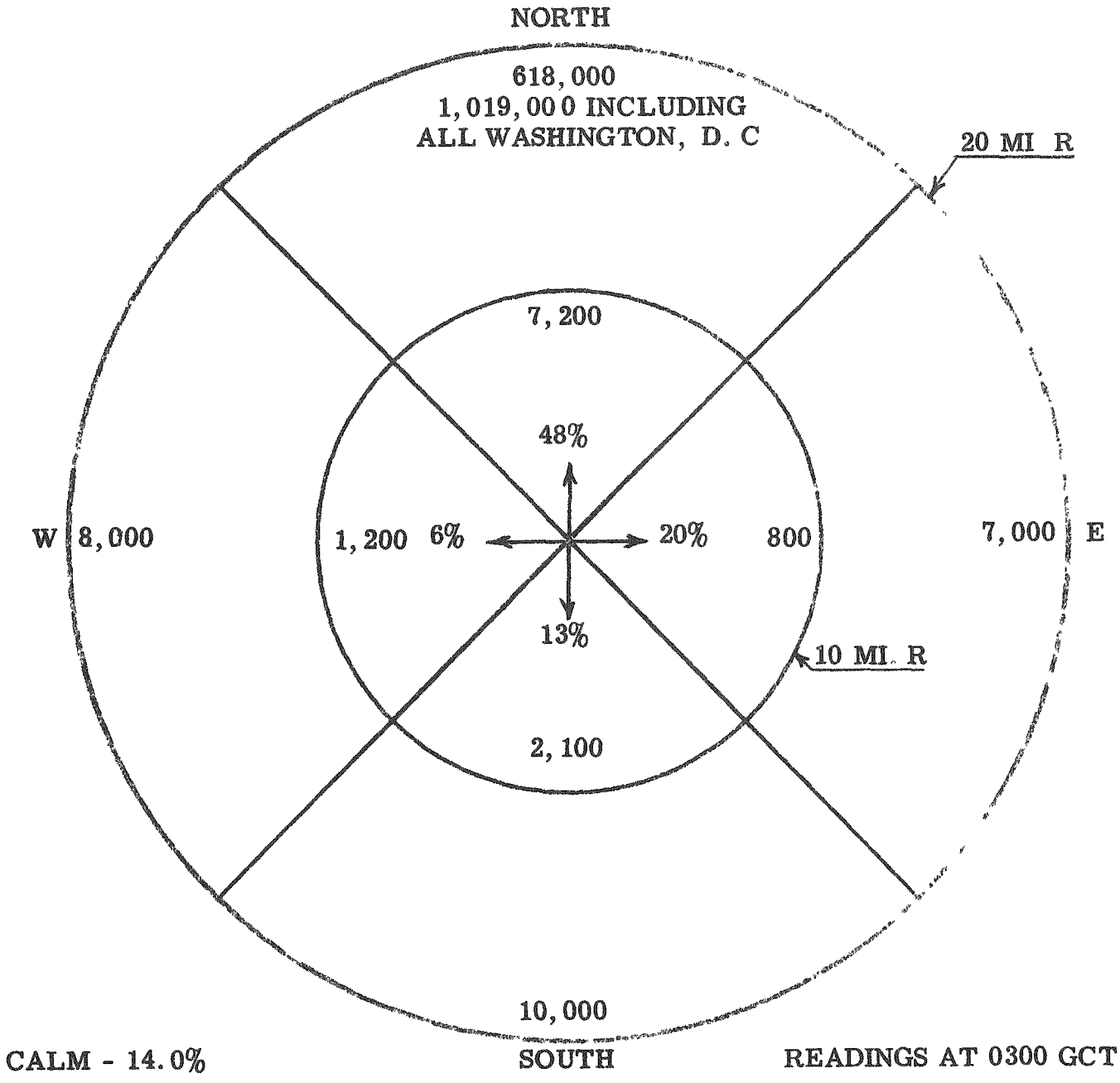

POPULATION DISTRIBUTION AND PERCENTAGE FREQUENCY
OF WIND DIRECTION WHEN INVERSION BASE IS BELOW 500 FEET.

FIG. I - 6

CHAPTER III

C. Primary Makeup and Blowdown

A revised flow sheet is included in this supplement which replaces Fig. III - 1 in tne original report. Changes are in the primary makeup and blowdown which is now essentially a closed system. A portion of the circulated primary water is, however, passed through a demineralizer to maintain the concentration of corrosion products below 2 ppm. This blowdown will be approximately 365 lb/hour. The water will pass through a blowdown cooler, throttling valve, and through a 1 cu ft hold-up to allow monitoring. If a fuel rupture is detected the blowdown water is diverted to an underground hot waste tank. Otherwise, the water is passed through a demineralizer into the makeup water tank, and finally pumped back into the primary circuit. The effluent from the demineralizers will contain less than 0.5 ppm of solids. A filter is installed in the downstream side of a demineralizer to catch any resins that may break through the demineralizer.

A cartridge type resin bed will be employed. After the resin bed has been exhausted it will be placed in a lead cask and shipped to the proper installation for disposal.

Hydrogen gas will be used as a corrosion inhibitor in the primary water. The hydrogen will be introduced into the makeup water tank so as to maintain a concentration of approximately 10 - 20 cc/liter. The hydrogen will be supplied from 220 cu ft bottles.

The makeup and blowdown of the primary system will be metered continuously to determine conductivity. Daily chemical analysis of the water will be made until such time as the curves are established. The service water used for the blowdown cooler will be monitored prior to discharge to the river. If activity develops as a result of a leak in this system, the service water will be diverted to the hot waste tank.

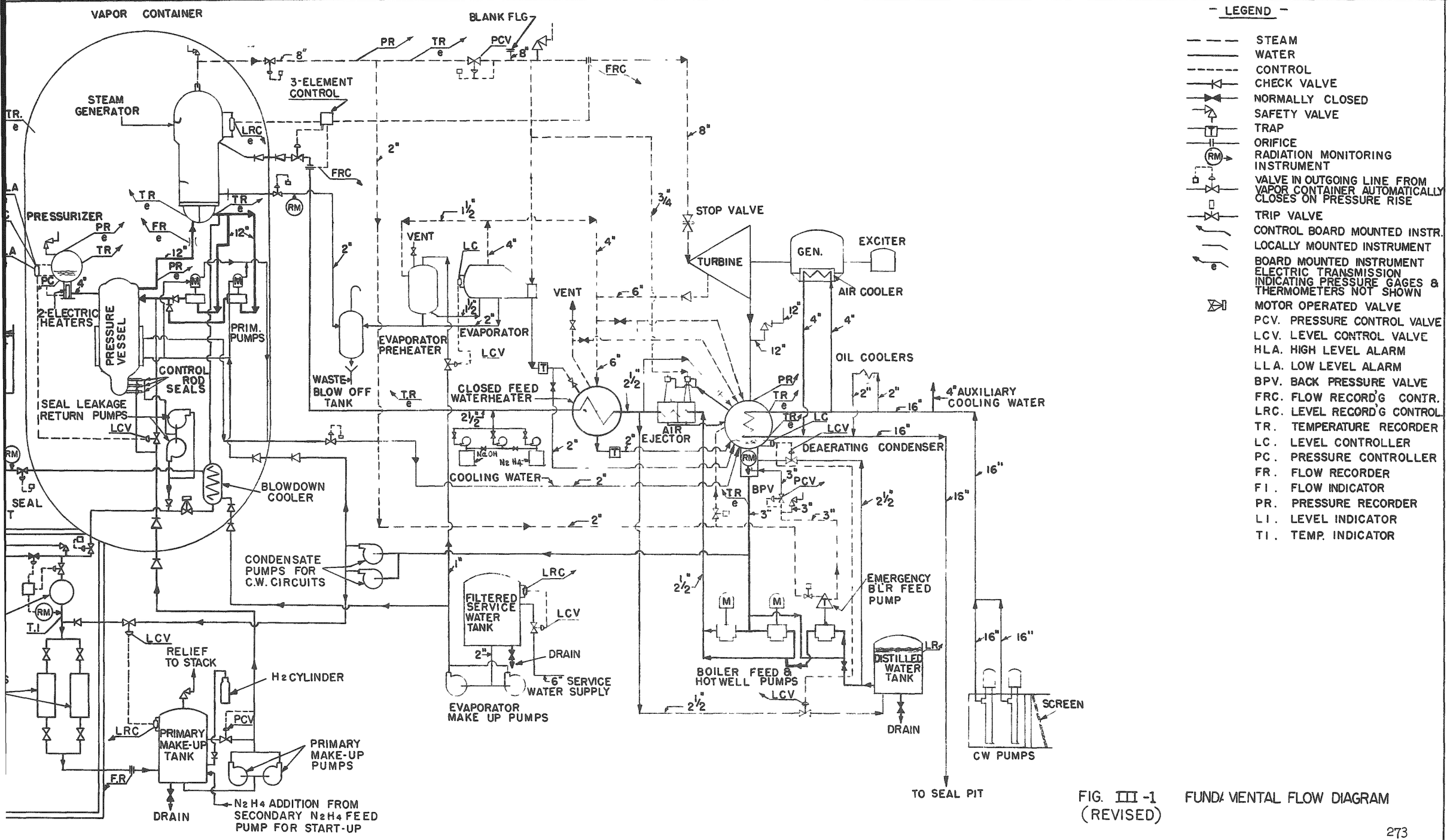

FIG. III-1 (REVISED) FUNDAMENTAL FLOW DIAGRAM

C. Penetrations

Reference was made in Chapter III, P. 52, to check valves used in all incoming piping to the vapor container, and to power operated valves in the outgoing lines. The following discussion is intended to amplify this reference and to show in more detail the purpose of these valves and the means used to assure their proper function in case of emergency.

There are five check valves, all in water lines. Only one of these is in direct communication with the primary system, and is in the make-up line. All check valves are paired with a manually operated shut-off valve (not shown on the flow diagram, Fig. III-1 (Revised) in all cases) between it and the vapor container. The manual valve serves as a final shut-off to assure zero leakage, the check valve thus serving essentially as a first line automatic device to hold until final closure can be made after a reasonable period of time.

A pressure connection is provided between each check valve and its corresponding shut-off valve. A leakage check will be made periodically by closing the manual valve and pressurizing the volume between it and the check valve. Leakage will be detectable by drop in pressure and repairs made as required.

There are six power operated valves in outgoing lines of which one is in the main steam line, one in the primary blow-down line, and the rest in coolant lines, etc. All of these valves are operated pneumatically and derive their operating energy from bottled nitrogen. They are thus independent of building air.

Sensing elements to actuate these valves are electrical pressure sensitive devices located in the vapor container and protected from possible missile damage. They are connected to solenoid operated pilot valves which control the main valve actuating cylinders. Electric power comes from the emergency DC system,

and all valves are normally closed without power so as to fail safe in case of system failure. Manually operated shut-off valves are used as back-up and test devices in the same manner as with the check valves.

CHAPTER VI

B. General Description of Instrumentation and Controls

In the original report it was stated that below 100 KW the reactor may be operated without flow. This has been revised so that the rods can not be raised without first starting the primary coolant pump. During routine operation the reactor can not be brought critical until at least 60% of the design coolant flow rate of 4000 gpm is achieved.

During the initial critical experiment and zero power experiments it will be necessary to withdraw the control rods without flow. A lock switch will be provided on the console so that power can be supplied to the rod motors for these experiments. When this switch is on, an interlock will be energized so that if the reactor power reaches 1 KW a scram will be initiated. The key to the lock switch will be in the possession of the plant supervisor at all times.

G. Temperature Transients Following Pump Failure - (New Section)

An investigation of the possibility of reactor damage due to boiling and burnout following a failure of the power supply to the primary circulating pumps has been carried out. The question naturally presents itself whether there might not be serious overheating in the reactor if the electrically-driven primary coolant circulating pumps suffered either mechanical or electrical failure, even though the automatic safety devices initiated a scram within a fraction of a second of the occurrence of the failure. This problem was treated in ORNL 1613, but the present study relates it to the exact control sequence planned for APPR-1.

Calculations have been performed which indicate conclusively that there is no danger in this case. These are based on a conservative estimate of the residual rate of coolant flow due to pump and liquid inertia, combined with the reactor power decay curve. Using the analysis and formulae given in ORNL 1613 and ORNL CF-53-4-284, curves were developed giving equilibrium values of the maximum surface temperature for various combinations of coolant flow and heat generation rates. Since these are equilibrium values which do not take credit for the thermal inertia of the plate and adjacent water and are therefore conservative to an extreme. An evaluation of the transient condition is given later on. Reading the curves described above at the conditions expected for the first three seconds and plotting surface temperature versus time, the curve rises above the saturation temperature of the primary system only between 0.06 and 0.36 seconds after power failure. The maximum excess indicated is 38° F.

Transition to nucleate or local boiling occurs when the heat dissipation rate (q/A) due to this process exceeds that due to non-boiling convection. With nucleate boiling the rise in heat dissipation capacity per degree of excess temperature ($t_{wall} - t_{satur.}$) is so great that very little further rise in metal temperature could occur with the ratio of heat generating and dissipating capacities existing in the reactor. Thus film boiling, which would cause burn-out, cannot occur, even with this conservative model for calculation.

The foregoing analysis is based on equilibrium values, as noted above, but for such a short surge in the ratio of heat generation to heat removal the actual transient values would be much lower. A more realistic evaluation of maximum surface temperature has been made taking into account the combined heat masses of plate and water per unit area of surface. Applying an approximate value of the mean excess of heat generated over heat removed at the initial temperatures, the result is a temperature rise in this period at the rate of 20° F. per second.

During the 0.42-second period that the heat generated exceeds the heat dissipation capacity of the plate with its original maximum surface temperature, this could only produce 8° F. temperature rise of the metal surface. Thus the hottest spot, initially 16° F. below saturation temperature of the water, would experience a transient peak 8° below this level.

CHAPTER VII

D. Fuel Plate Melting and Void Fraction

A more accurate figure showing the total energy release as a function of excess multiplication is given in this supplement. This figure replaces Fig. VII - 4, page 100, in the original report. Table VII - 1, page 105, in the report has been revised accordingly and is also given in this supplement. The results are not significantly different from those in the report.

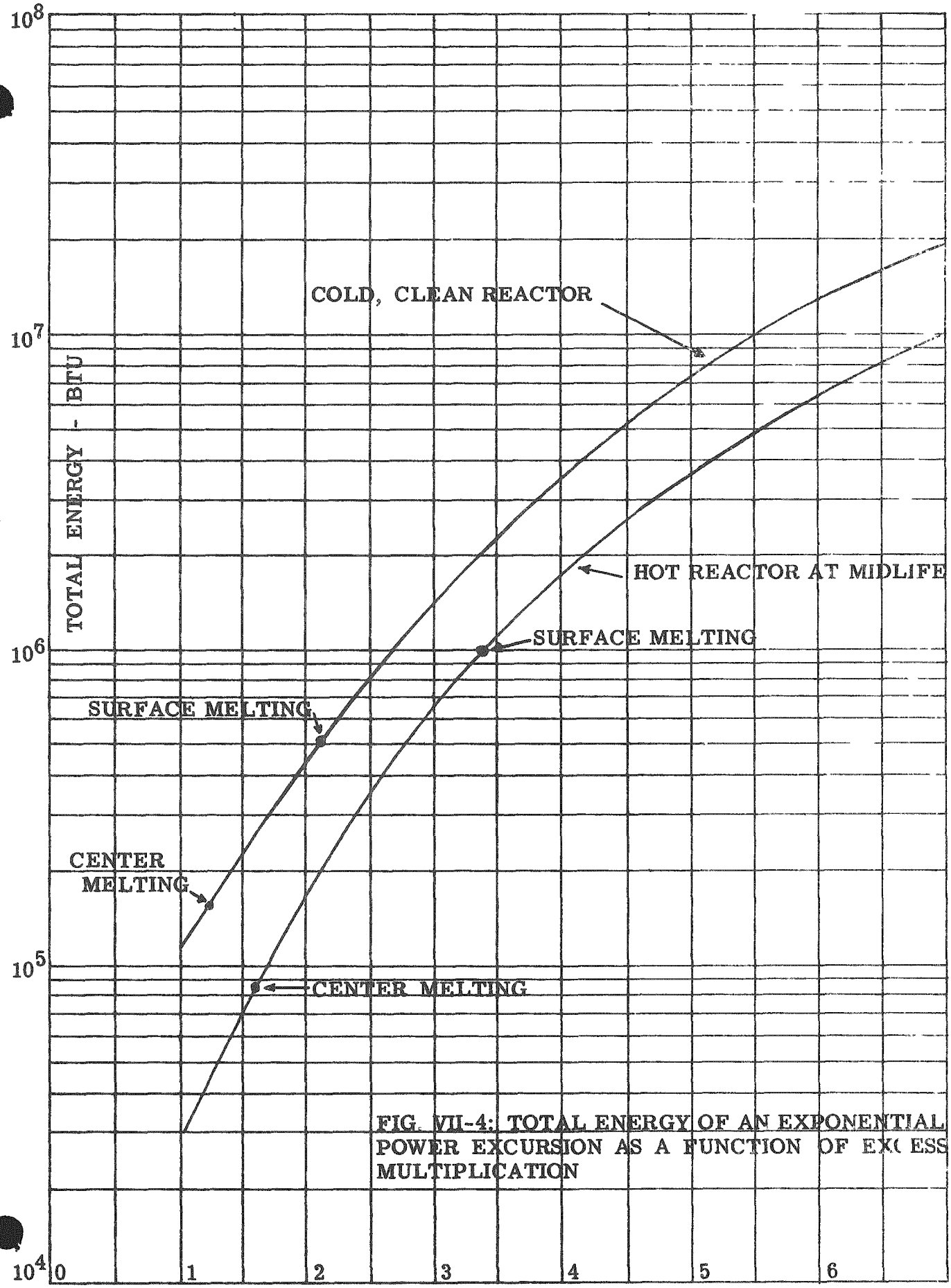

FIG. VII-4: TOTAL ENERGY OF AN EXPONENTIAL POWER EXCURSION AS A FUNCTION OF EXCESS MULTIPLICATION

Table VII-1

FUEL ELEMENT TEMPERATURES AND ENERGY RELEASES AT TERMINATION OF STEP REACTIVITY ADDITIONS

Reactor Condition	Excess Multiplication (Percent)	Reactor Period (Milliseconds)	Fuel Plate Temperature at Shutoff, (^{o}F)		Peak Power (Megawatts)	Energy Release to Shutoff (BTU)
			Center	Surface		
Cold, clean, no power	1.2	4.0	2590	990	4.08×10^{4}	155,000
	2.1	1.5	--	2590	3.59×10^{5}	510,000
Hot, mid-life, full power	1.6	2.2	2590	900	4.14×10^{4}	86,000
	3.4	0.72	--	2590	1.47×10^{6}	1,000,000

F. Possibility of Rod Ejection

As discussed in the report, if a system rupture occurs that will eject the rods from the reactor, the reactor is immediately made subcritical by void formation. Further calculations have shown that after the steam-water mixture has been expelled from the primary system, a maximum of 4 cubic feet of water will remain in the system. The volume in the pressure vessel below the bottom of the core is 14 cubic feet. Accordingly, the reactor will not fill with water and become critical. The shield water contains 1/4% by weight of boron as does the spray water for cooling the vapor container after the maximum credible accident. If either of these sources of moderation enter the core, the reactor will be poisoned and will not become critical.

Calculations have been made to ascertain if the core melts in the event it is suddenly deprived of all coolant. Data from the experiments at the LITR in 1953 have been used. In those experiments the cooling water was dropped out of the LITR core from powers up to 1500 KW and the maximum fuel plate surface temperatures were measured. The surface temperature is governed by the following equation:

$$W\,Cp\,\frac{dT_s}{dt} = Q_{FP}(t) - Q_{lost}(T_s)$$

where: W = weight of fuel element (lbs.)

Cp = specific heat (Btu/lb. - °F.)

$Q_{FP}(t)$ = fission product decay power (function of time) (Btu/sec.)

$Q_{lost}(T_s)$ = power lost by convection (function of surface temperature and ambient temperature) (Btu/sec.)

Calculations using this relationship checked the experimental results from the LITR very closely.

Using the same method, the maximum fuel plate temperature in the APPR was calculated after complete loss of coolant at 10 megawatts power. The ambient temperature was assumed to be 312° F. corresponding to the saturation temperature of

water at 81 psia (highest pressure after the maximum credible accident), and it was assumed that the heat release in the center element was four times that in the average element. Even with these very pessimistic assumptions the maximum surface temperature attained is 1910° F., which is well below the melting temperature of 2590° F. The conclusion is that the core of the APPR does not melt after the maximum credible accident.

CHAPTER VIII

C. Sequence of Failures

Mention is made in the original report of a rupture disc which yields at 2000 psi. This rupture disc is located in the inlet line to the pressure vessel from the steam generator.

APPENDIX B-1 - LEAK TESTING

The maximum allowable leakage rate from the vapor container is specified as 0.075 cu. ft./hr. Even though the core of the APPR does not melt after the maximum credible accident it is assumed that one percent of the total fission product activity is released within the vapor container. With an inversion period of 12 hours the integrated inhalation dosage at 800 meters (the nearest residence) will be 2.4×10^{-3} curie-seconds/cubic meter corresponding to a total dose of 250 millirems which is less than the weekly laboratory tolerance of 300 millirems.

Following a careful bubble test for leakage, but prior to application of any protective coatings, a gas leak-rate test will be given the vapor container, including all penetrations and closures. This test replaces the liquid leak test referred to on page 152 of the report.

The test consists of inflating the vapor container with air to a pressure of 30 psig, and measuring the pressure drop resulting from leakage over a period of

at least one hundred hours. In order to meet the requirements of 0.075 cu. ft./hr. average leakage rate, (corrected for integrated mean pressures for 48 hours following the maximum credible accident), the allowable pressure drop during this test may not exceed 0.055 in. H_2O in 100 hours. This small pressure drop will be measured on a sensitive inclined manometer having one leg connected to the vapor container volume, and the other connected to a constant temperature reference volume. The reference temperature will be maintained by a blanket of melting ice.

Temperatures will be measured by means of bridge type resistance thermometers at approximately 50 locations throughout the vapor container volume and on the walls. These temperatures will be recorded at frequent intervals and their values integrated to arrive at a true weighted mean temperature plot so that temperature variations in the vapor container during test can be accurately accounted for in arriving at the final leakage rate. The number of observations and accuracy of instrumentation will be sufficient to obtain high statistical accuracy. Temperature variations during test will be minimized by maintaining a running river-water blanket over the outside of the vapor container shell at such a rate that the shell will be maintained very nearly at river water temperature.

APPENDIX B-2 - MISSILE PENETRATION

In the original calculations for missiles within the vapor container it was found that most missiles reached a velocity in the neighborhood of 500 ft. per second. The maximum velocity was attained with a 2" valve, which was found to reach a terminal velocity of 700 feet per second at the point of impact. Since this work was being done at the preliminary stage, our calculations were done on a conservative basis so that penetrations were calculated for all the missiles at both 500 and 700 feet per second. Thus despite the fact that most penetrating missiles could not reach a velocity of 700 feet per second, the maximum value of effective penetration in the report was based upon this high missile velocity. Because of this

conservatism the calculations are both pessimistic and unreal.

In the calculations reported in the supplement, missiles under consideration are restricted to two physical pieces of equipment, which could become possible missiles. These are the 2" diameter 1500-pound test valve and a four-foot length of two inch schedule 160 stainless steel pipe. The water within the system at the time of rupture is assumed to be the 1500 psi saturated water established with a maximum credible accident. The calculations develop the actual velocities for the two missiles, using conservative assumptions for such factors as jet efficiency and expansion angles.

The selection of these two missiles restricts our attention to those real missiles which have been shown by previous work to have the greatest penetrating power. Hence calculation of the effective penetration for these two missiles establishes an upper limit as a basis for design of the vapor container concrete thickness.

The calculations for the two missiles are as follows: -

MISSILE #1 - 2" VALVE

This valve weighs 50 lbs. and the complete projected area is 30 sq. in. in the bottom-on position. The projected area in the end-on position is approximately 7 sq. in., but after initial impact this would be increased to 18 sq. in.

This missile is propelled by the jet stream issuing from a 3 in. opening in the primary system until it contacts the vapor container, a total distance of 40 ft.

The propelling jet is provided by the primary coolant flowing through the 3" orifice opening and expanding isotropically at an angle of 12 deg. to atmospheric pressure. The coolant flows through the orifice at a rate of 1070 lb./sec. and a velocity 513 fps, and attains a maximum velocity of 2200 fps at 15 psia - 10 ft. from the orifice.

The force of the jet acting on the missile: -

$$F = \frac{Wf}{g} (V_f - V_m)$$

This force is maximum when $V_m = 0$ at the start and becomes o when $V_m = V_f$ (V_m never reaches V_f in the available distance traveled).

The force is obtained by trial and error assuming a value for V_m. Knowing the force the acceleration is computed from $A_m = \frac{g}{W_m} \times F$.

From the acceleration the final V_m is computed:

$$V_m = \sqrt{2 as + V_o^2}$$

where s = distance traveled

The missile reaches a velocity of 420 fps at s = 10 ft. (point at which propelling jet reaches 15 psia), and a final velocity of 540 fps at wall of vapor container.

MISSILE #2 - 2" 160 SCHEDULE PIPE

This pipe is 4' long, weighs 36 lbs., and has an actual cross-section area of 2.65 sq. in.

This missile is self propelled by virtue of the utilization of the kinetic energy stored within the fluid contained in the hollow pipe.

This fluid at 1500 psia sat. on expansion to 15 psia (worst condition) releases a maximum of 98.2 Btu/lb. The internal volume or capacity of this pipe 4 ft. long is .0496 cu. ft. or 2.11 lbs. of fluid.

The total kinetic energy is 161,000 ft./lb. A reasonable value for the available K.E. is 50% of the total or 80,500 ft./lb.

The maximum attainable velocity of the missile is found by

$$V = \sqrt{\frac{2\,KE}{m}}$$

or velocity = 378 fps

MISSILE PENETRATION

Using the accepted BRL formulations for penetration of concrete and steel:

$$P = \frac{6\ Wd^{1/5}}{d^2} \left(\frac{V}{1000} \right)^{4/3}$$

where:

P = penetration, in. of concrete

W = weight of missile, lbs.

d = equivalent dia., in.

V = velocity, fps

Using this formula BRL recommends multiplying the penetration by a factor of 1.3 to indicate the maximum depth of cracking which extends ahead of the penetration.

MISSILE #1

Data: W = 50 lbs.

d = 4.8 in. from A_m = 18 sq. in.

V = 540 fps

then for concrete: P = 7.88 in.

1/3 x P = 10.2 in.

for steel:

$$t^{3/2}\ (\text{penetration}) = \frac{1/2\ \text{in.}\ V^2}{K^2\ 17{,}400\ d^{3/2}}$$

K = 1 for good grade steel

t = 1.145 in.

MISSIIE #2

Data: W = 36 lbs.

V = 378 fps

d = 1.83 in. from A_m = 2.65 sq. in. -

however, since there is an increased resistance to penetration due to coring (concrete is forced through the center of the pipe which presents an additional drag surface and restricted expansion of the concrete) of the concrete by the missile, the equivalent diameter is multiplied by a factor of 1.2, therefore, d = 2.16 in. (this is conservative since for pipe missiles the total cross section dia. is used; in this case that would be 2.375 in.).

for concrete: $P = 14.75$ in.

$1/3 \times P = 19.2$ in.

for steel:

$$t^{3/2} = \frac{1/2 \text{ in. } V^2}{K^2\ 17{,}400\ d^{3/2}}$$

$$= \frac{1/2\ \frac{36}{32.2} \times (378)^2}{(1)^2 \times 17{,}400 \times (2.16)^{3/2}}$$

$$= 1.45$$

$$t = 1.28 \text{ in.}$$

LARGE VESSELS AS MISSILES

Upon further investigation it has been determined that the larger vessels in the primary system might become missiles in the event of a credible accident. These vessels include the pressurizer, reactor vessel, and steam generator.

MISSILE #1 - PRESSURIZER

The pressurizer is considered to be full of water at 1500 psia sat. Total weight of the water in the vessel would be 1550 lbs., and the maximum available energy would be 98.2 Btu/lb. It is assumed that the bottom flange is blown off.

Therefore: $KE_t = WJ\Delta h$

$= 11.8 \times 10^7$ ft./lb.

at 50% of the KE available:

$$KE = 5.9 \times 10^7 \text{ ft./lb.}$$

$$\text{Vel. of missile} = \frac{2\,KE}{w/g}$$

or: $\underline{\text{Vel.} = 1330 \text{ fps (max.)}}$

The BRL formulation for penetration can not be used for these missiles because of the large area involved, but it is apparent that missiles #3 and #4 could cause damage to the vapor container at their respective velocities. To eliminate this possibility these vessels will be tied down sufficiently to resist the forces applied.

MISSILE #4 - REACTOR VESSEL

It is assumed that this vessel becomes a self propelled missile when the bottom cap breaks off at the weld. The vessel weighs 14,500 lbs. and contains 3100 lbs. of coolant at 1500 psia. Above the vessel is 12 ft. of water which will oppose acceleration of the vessel by virtue of its mass and shearing resistance (taken as zero). Therefore, the total weight to be accelerated will be the weight of the vessel plus the weight of this 12 ft. column of water, a total of 25,800 lbs.

$$KE = WJ\Delta h$$

$$KE = 23.6 \times 10^7 \text{ ft./lbs.}$$

at 50% of KE available:

$$KE = 11.8 \times 10^7 \text{ ft./lbs.}$$

$$V = \sqrt{\frac{2\,KE}{w/g}}$$

$$\underline{V = 542 \text{ fps}}$$

MISSILE #5 - STEAM GENERATOR

The effective utilization of the primary coolant as a propellant in this vessel differs from that of the other two vessels in that the coolant is contained as follows:

The inlet and outlet box at the bottom of the steam generator contains approximately two-thirds of the coolant in the vessel and would be open to atmospheric pressure over a large area, this volume is 9.9 cu. ft. It is assumed that the coolant expands from 1500 psia to 15 psia isotropically. Equal force will be asserted on both vessel and coolant at the tube sheet.

$$\text{Force} = M_m A_m = M_f A_f = \frac{Q_f}{g} V_f$$

Q = flow rate of coolant from steam generator

V_c = vel. of coolant through opening

$$= C_v \sqrt{2g \frac{\Delta P}{\rho}}$$

$$= 474 \text{ fps}$$

$$Q_f = \rho VA$$

$$Q_f = 1200 \text{ lb./sec.}$$

$$A_m = \frac{V_f Q_f/g}{M_m/g}$$

$$= 176 \text{ ft./sec.}^2$$

minus the force of gravity:

$$A_m - g = 144 \text{ ft./sec.}^2$$

Therefore: $V_m = 50.7$ ft./sec.

Influence of the expansion of coolant in tubes to 15 psia.

There are 370 - 3/4 in. tubes, 6-1/2 ft. long.

Tube vol. = 5.2 cu. ft.

W_f = vol. x

= 222#

KE = $WJ\Delta h$

KE = 17×10^6 ft./#

at 50% of KE available:

$$V_m^1 = \sqrt{\frac{2\ KE}{w/g}}$$

$$V_m^1 = 18.8 \text{ fps}$$

This is the vel. attained by the missile due to the expansion of coolant in tubes.

$$Q_f = V_f A$$

$$= 42.6 \times 474 \times .785$$

$$= 1590 \text{ \#/sec.}$$

$$F = \frac{Q_f}{g} (V_f - V_m)$$

$$F = 107{,}500\#$$

$$A_m = \frac{g}{W_m} F$$

$$A_m = 230 \text{ ft./sec.}^2$$

$$A(net) = A_m - g$$

$$A(net) = 198 \text{ ft./sec.}^2$$

The actual acceleration of the missile is:

$$A = A_m + A(net)$$

$$A = 342 \text{ ft./sec.}^2$$

Therefore, actual vel. of the missile upward is:

$$\underline{V_m = 67.0 \text{ ft./sec.}}$$

This vessel can be tied down, too. However, the restraining force of the vessel weight and piping connections should be sufficient to overcome the propelling force.

APPENDIX E-2 - CONTROL ROD WITHDRAWAL AT ROOM TEMPERATURE

As was discussed in Appendix E-2 of the report, withdrawal of the control rods by the drive motors, assuming all scrams fail, will give an initial transient with a period of 10 milliseconds. (The calculations were based on the very pessimistic assumption that the rate of introduction of reactivity was four times that specified). It was then mentioned that the qualitative behaviour of the reactor power after the initial transient would follow that resulting from rod withdrawal at operating temperature and power (Appendix E-3). Additional corroboration of this behaviour results from a comparison with the 1954 Borax Experiments. Fig. 7 (page 47) of ANL 5323 is reproduced in this addendum. From the figure it can be seen that in that experiment the Borax reactor reached a 14 millisecond period on the initial transient with a peak power of 7000 megawatts. Succeeding oscillations in power were of much lower amplitude and the reactor leveled off at an average power of 7 megawatts.

In the case of the 10 millisecond transient with the APPR the peak power reached 50,000 megawatts with a total energy release of 50,000 BTU's and a maximum fuel plate temperature of 1200 deg. F. which is far below the melting temperature of 2590° F.

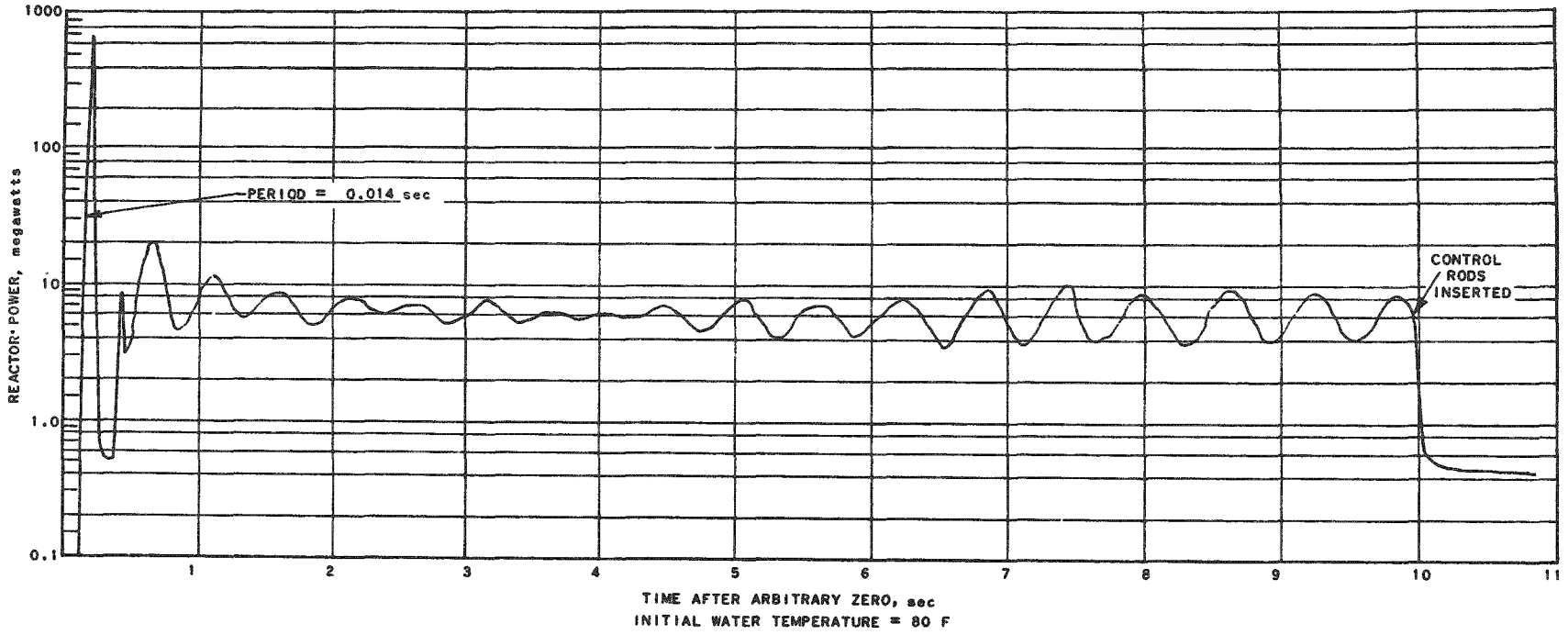

FIG. 7
REACTOR POWER VARIATION DURING 10 SECOND RUN
FOLLOWING INITIAL EXCURSION OF 14 MILLISECOND PERIOD

FROM ANL 5323 BORAX - I EXPERIMENTS, 1954